

A photograph of a wooden mine tunnel. The tunnel is supported by numerous wooden beams and posts. On the right side, there is a large wooden barrel. The floor is dark and appears to be made of stone or concrete. The walls are also made of wood and stone.

Mines of the Mojave

David M. Miller & Stephen M. Rowland, editors

2023 Desert Symposium Field Guide and Proceedings
April 2023

Founders Circle of the Desert Symposium Inc.

The Desert Symposium Inc., incorporated as a nonprofit 501c3 institution February 2018, is dedicated to perpetuating the Desert Symposium meetings and related scientific and educational endeavors. This institution evolved directly from the Desert Symposium and its predecessor, the Mojave Desert Quaternary Research Center (MDQRC), whose originators and sustainers are listed below as “Emeritus Founders”. Without their hard work and vision the current institution would not exist.

The Founders Circle provided initial financial footing. Join us in thanking the following for donations toward, and fellowship in, the Founders Circle.

EMERITUS FOUNDERS

Bob Adams
George Jefferson
Jennifer Reynolds

Fred Budinger
Jeff Lovich
Robert Reynolds

Jim Cornett
Norman Meek
Thomas Schweich

5-YEAR FELLOW

Bruce Hamilton
Tanya Henderson
Steve Finney
Pat Flanagan
Keith Howard
Sherry Keesey
Ed LaRue
Jane E. Rodgers
Steve Rowland
Cheryl Schweich
Carole Zeigler

10-YEAR FELLOW

Ernie Anderson
Vera Rose Anderson
Hal Beesley
James Bishop
Bruce Bridenbecker
Anna Garcia
Gregor Losson
David Lynch
Dave Miller
Thomas Schweich
Joann Stock

25-YEAR FELLOW

Catherine Badgley
Victoria Langenheim
Kevin Schmidt
Gerald Smith
Geoffrey Spaulding
Gregg Wilkerson

Friends of Desert Symposium

In order to continue to develop the General Fund for DSI, Friends of Desert Symposium was initiated in 2023. As with the Founders Circle, donations will go to operational needs and will enable continued meetings and associated field trips. Visit www.desertsymposium.org for information.

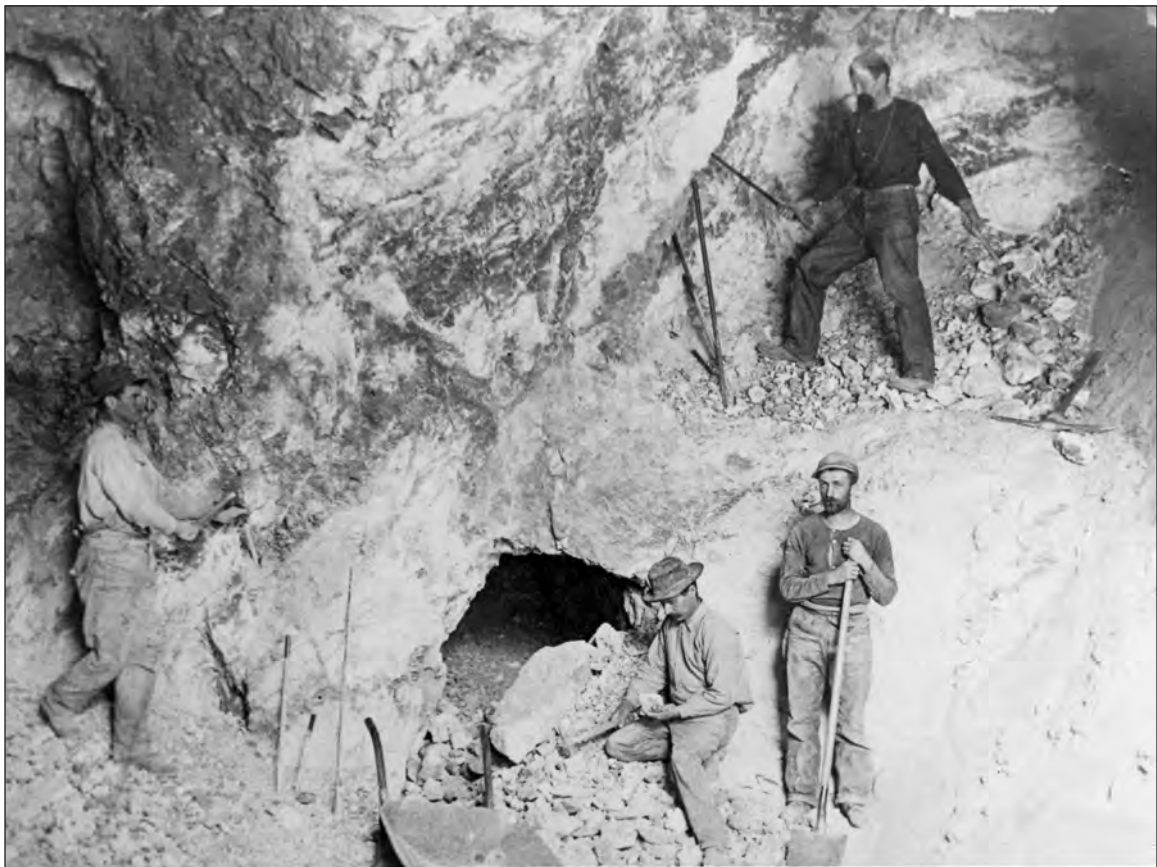


The 1989 MDQRC field trip. *Photographs by Robert E. Reynolds*



Mines of the Mojave

David M. Miller and Stephen M. Rowland, editors



2023 Desert Symposium Field Guide and Proceedings
April 2023

Captions

Front cover: *Golden Queen mine, Mojave, California, 1997. Bob Reynolds photo.*

Title page: *Miners at the west end of Mammoth stope, 60 feet wide, Red Cloud mine, Calico, California. James Mulcahy drilling a lower hole; Matt Phillips sorting ore; Steve Rowe with shovel; Harry Livingston drilling an upper hole. San Bernardino County Museum collection.*

© 2023 Desert Symposium, Inc., a non-profit 501(c)3 organization.

Terms of use: copies may be made for academic purposes only.

The Desert Symposium is a gathering of scientists and lay people interested in the natural and cultural history of arid lands. The meeting comprises scientific presentations followed by a field trip. The Desert Symposium and its field trip take place annually, usually in April. The Desert Symposium publishes a volume of papers and a field trip road log. Safety, courtesy, desert awareness, and self-reliance are expected of all participants.

A color version of this and past volumes may be viewed at <http://www.desertsymposium.org/Publications.html>

Table of contents

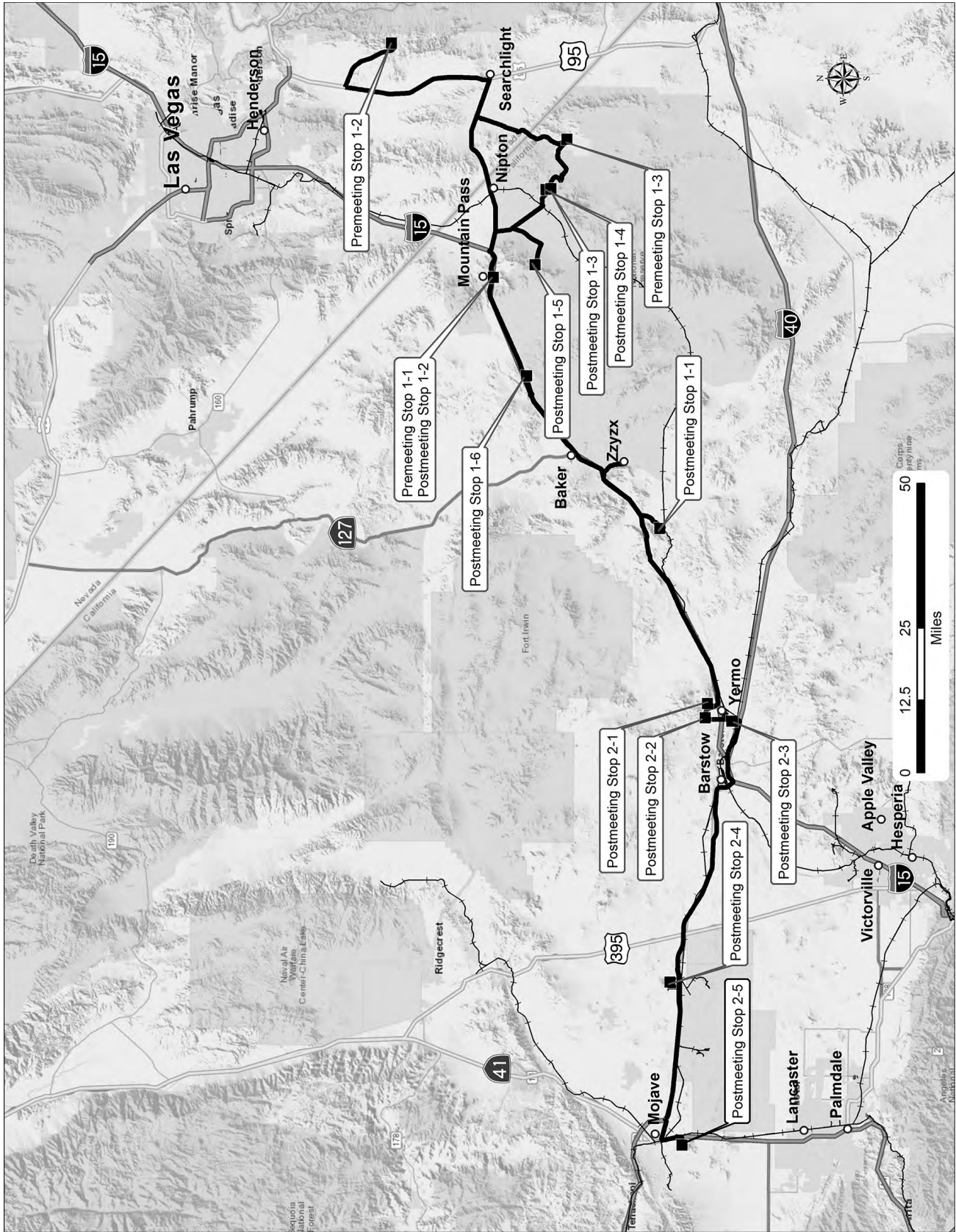
Mines of the Mojave: the road log	7
<i>Larry M. Vredenburg and Gregg Wilkerson</i>	
Into the mines: the road log for the pre-meeting field trip	40
<i>Larry M. Vredenburg and Gregg Wilkerson</i>	
Carbide lamps and hard hats: snapshots of mines in the Mojave	54
<i>Jennifer Flesher Reynolds</i>	
Illuminating the Waterloo silver deposit in three-dimensions using multi-element data	81
<i>C.E. Fitzgerald, C.S. Gallagher, and W.T. Pratt</i>	
Memories of Old Borate	92
<i>Wm. H. Smitheram</i>	
ἱστορία: Hunting for Old Calico's silver output	101
<i>Douglas Steeples</i>	
A review of geology and mining in the Marble Mountains, southeastern California	111
<i>David C. Buesch and Bruce W. Bridenbecker</i>	
Early Miocene volcanism, sedimentation, and extensional faulting in the Van Winkle hills, Mojave National Preserve, southeastern California	122
<i>Phillip B. Gans, Elizabeth OBlack Gans, and Andrew Kylander-Clark</i>	
Plant rings in the Colorado River Delta: clones, ghosts, and zombies	137
<i>David K. Lynch, Steven M. Nelson, and Tomás E. Rivas Salcedo</i>	
The Colorado River (Mexico) tidal bore: persistent phenomenon in a changing estuary	144
<i>Steven M. Nelson, David K. Lynch, and Tomás E. Rivas Salcedo</i>	
Curtis Howe Springer and Zzyzx	155
<i>Larry M. Vredenburg</i>	
Abstracts from proceedings: the 2023 Desert Symposium	161
Lithium enrichment in claystones of the mid-Miocene Barstow Formation, Mojave Desert, California	
<i>Thomas R. Benson</i>	161
Formation of gas-escape sedimentary structures in ephemeral ponds (Ubehebe Crater, Death Valley NP): relevance to Mars	
<i>R. Bonaccorsi, D. Willson, L. Baker, and C.P. McKay</i>	161
Bagdad-Chase mine, San Bernardino County, California	
<i>Tara Bonas and Jake Anderson</i>	162
Origin of borate deposits in the Furnace Creek Formation, Death Valley, CA	
<i>J.P. Calzia</i>	163
Paul VanderEike and the California Federation of Mineralogical Societies	
<i>Stephen Collett</i>	163
Freshwater turtles in the Mojave Desert: what could go wrong?	
<i>Kristy Cummings, Jeffrey E. Lovich, Shellie R. Puffer, and Sara Greely</i>	163

New surficial geologic mapping of Leuhman Ridge and the surrounding area, northeastern Edwards Air Force Base, Kern and San Bernardino Counties, California in support of Quaternary fault and hydrologic evaluations <i>Andrew J. Cyr and David M. Miller</i>	164
Finally, the Paleontological Resources Preservation Act final regulations— what changed in the 66 months that passed since the draft rule was published, and why <i>Chris Dalu</i>	164
Tephrochronology of the Miocene Barstow Formation, western Mojave, CA <i>Ryan Eden, Phil Gans, and John Cottle</i>	168
Geologic framework of the Rio Tinto boron deposit, Mojave Desert, California <i>Phillip B. Gans</i>	169
Wetland dynamics at the Salton Sea <i>Krishangi Groover and Alexandra Lutz</i>	170
The cosmogenic origin of boron <i>Ted A. Hadley</i>	170
The ecological impacts of solar energy development in the southwestern U.S. <i>Claire Karban, Jeffrey E. Lovich, Seth M. Munson, Josh R. Ennen, and Steven M. Grodsky</i>	171
Anthropogenic impacts on Bonanza Spring: Clipper Mountains, Mojave Desert <i>Miles Kenney</i>	171
Pleistocene porcupine (Erethizontidae) records in arid southwestern North America and comparisons with their modern distribution in southern California and Arizona <i>Jeffrey E. Lovich and George T. Jefferson</i>	172
Phil Swing and the path to Hoover Dam: a river, a canal, an empire <i>Brian McNece</i>	173
The Vanderbilt mine, San Bernardino County, California <i>Leonardo Menchaca</i>	173
Structural framework for the Mountain Pass rare earth metals mine, Clark Mountain Range, California <i>David M. Miller and Joseph L. Wooden</i>	174
Early Miocene volcanism, sedimentation, and faulting in the western Lava Hills, California <i>Alexander S. Noorzad, Cole B. Jacobs, Phillip B. Gans, and Andrew Kylander-Clark</i>	174
Telegraph mine, Halloran Springs District, San Bernardino County, California <i>Michelle Nop</i>	175
Isotopic constraints on the origin of the igneous hosts of the Mountain Pass REE deposit, San Bernardino County, California <i>O. Tapani Rämö and James P. Calzia</i>	176
Evidence of Miocene earthquakes recorded in sedimentary structures within the Horse Spring Formation, southern Nevada, including paleoliquefaction evidence of a very large earthquake on the Las Vegas Valley shear zone or Lake Mead fault system at approximately 13.7 Ma <i>Stephen M. Rowland and Jerry King</i>	176
The Frenchman Mountain Dolostone: a new Cambrian formation in southern Nevada and the Grand Canyon <i>Stephen M. Rowland, Slava Korolev, and James W. Hagadorn</i>	177
A vascular flora of the Sacatar Trail Wilderness <i>Kimberly Schaefer</i>	177
Ediacaran test tubes: constraining the taxonomy of Ediacaran nonmineralized tubular taxa to elucidate Earth's earliest experiments in multicellularity <i>Rachel Surprenant</i>	178
The Morning Star mine, San Bernardino County, California <i>Ryan Tengelsen</i>	178

Bureau of Land Management’s mineral investigation of Viceroy Gold Corporation’s mineral patent applications at the Castle Mountain mine during the period from 1992 through 2001 <i>Robert Waiwood</i>	179
Stromatolites in spring-fed streams of Death Valley National Park: past, present, and future <i>Kenneth L. Wright Jr., Torrey Nyborg, Kevin E. Nick</i>	180
Billie borate mine, Inyo County, California <i>Gregg Wilkerson</i>	181
Briggs mine, Inyo County, California <i>Gregg Wilkerson</i>	182
Bristol Lake salt plant, Amboy Crater area, San Bernardino County, California <i>Gregg Wilkerson</i>	182
Geology and history Cerro Gordo Mining District, Inyo County, California <i>Gregg Wilkerson</i>	183
Fort Cady borate solution mine, San Bernardino County, California <i>Gregg Wilkerson</i>	183
Hectorite from Hector, San Bernardino County, California <i>Gregg Wilkerson</i>	184
War Eagle mine, San Bernardino County, California <i>Gregg Wilkerson</i>	184
The Brubaker-Mann Quarries, San Bernardino County, California <i>Gregg Wilkerson and Alyssa Kaess</i>	185



Calico adventures with friends and family. San Bernardino County Museum collection.



Mines of the Mojave: the road log

Larry M. Vredenburg and Gregg Wilkerson

Day 1

Convene at the Desert Studies Center. Make sure vehicles are packed with all your personal gear and have a full tank of gas. Check your spare tires. Carry water and snacks, plan your clothing for the conditions. Wear sturdy shoes. Bring hats and sunscreen. Watch for harmful plants and animals. Note that some stops are on Federal lands managed by the Bureau of Land Management and National Park Service. Respect the land and leave it as you found it: no rock or artifact collecting, digging, or harming plants and wildlife is allowed. Part of this day's route is within the Mojave National Preserve where special use permits are required for field trips with more than a limited number of vehicles or visitors.

Carpooling is mandatory today. Make carpool arrangements at the symposium on Friday or Saturday. At one stop the trip requires high clearance – 4WD due to soft sand. Please leave less road-worthy vehicles at Zzyzx. We will return to Zzyzx Sunday night.

Introduction

The 2023 Desert Symposium field trip will highlight several mines in the Mojave Desert. This year's theme was inspired by the South Coast Geological Society's 1980 publication "Geology and Mineral Wealth of the California Desert" (Fife and Brown, 1980), which included a field trip guide. The geographic scope of that work was the California Desert Conservation Area, which extends from northeast of Bishop to the Mexican border. The scope of "Mines of the Mojave" is the Mojave Desert geomorphic region within California. Strictly speaking, this region extends from the Garlock fault on the north to the San Andreas fault on the southwest, and on the south and east by the state and international boundaries. We will not visit the southern part of this area; the field trip will be entirely within the desert parts of San Bernardino and Kern counties. Within this area the U.S. Geological Survey's Mineral Resources Data System (MRDS) indicates there are 1,788 past and present mineral producers.

Currently this area boasts two active world-class mineral deposits, the rare earths mine at Mountain Pass and the borate mine at Boron. In addition, there are active gold, limestone, clay, saline, and iron mines, to name a few. The feasibility of mining a massive silver deposit at the Calico Mountains (Fitzgerald and others, this volume) and borates at the Fort Cady deposit is currently being explored. New models for mineral deposits, new methods of mining and beneficiation, and renewed exploration are leading to continued development of mineral resources

in the Mojave Desert. An ongoing question is how many more of these deposits may be hidden below the surface.

With the passage of the Federal Land Policy and Management Act of October 21, 1976, Congress established the California Desert Conservation Area and directed the Secretary of Interior to "... prepare and maintain on continuing basis an inventory of all national resource lands, and their resource and other values." The California Desert Plan was completed on September 30, 1980, and just days later the South Coast Geological Society conducted their field trip. An extensive inventory of known and prospective mineral resources was conducted by the Bureau of Land Management during the short time allotted by Congress (U.S. Bureau of Land Management, 1982; Vredenburg, 2017).

Inventory of mineral resources of the United States will never end because technology and methodology are ever changing. As recently as 2017 the U.S. Geological Survey announced the Earth Mapping Resources Initiative (Earth MRI) "in response to a Federal directive calling on various Federal agencies to address potential vulnerabilities in the Nation's supply of critical mineral resources" (U.S. Geological Survey, 2023). This initiative's database, accessible at <https://usgs.gov/earthmri>, hosts a vast array of publicly available mineral data.

Mining in the desert region of California has played, and continues to play, an important role in the development of the state. The Cerro Gordo 1868–1876 and Calico 1881–1892 silver mines stimulated the Los Angeles region, Calico being the most productive silver district in the state (Steeple, this volume). Many minerals first mined over a hundred years ago are still being produced. Gold mines and prospects are widely distributed across the area.

During this field trip you will have a chance to see a few historic mines and few active mines. We will stop and view the two world class deposits mentioned above at Mountain Pass and Boron. In this field guide and proceedings, we have made an effort to describe these mines, along with their history, geology, and mineralization. It is our goal that this year's Desert Symposium and Field Trip will give you an introduction to the story of the mineral wealth of the California Desert.

Today we will examine eastern Mojave Desert mines. We will begin by heading west to the Cave Mountain / Baxter iron mine. Following that stop we will drive east to the Mountain Pass rare earth mine. We won't tour the mine; however, we will stop south of I-15 and discuss it. Those who attended the Pre-conference Field Trip and toured the mine will share their observations. After this

we will head to the Vanderbilt mine in the New York Mountains, the Morning Star mine on the east side of the Mescal Range, and on the way back stop at the Telegraph mine near Halloran Springs. We will travel 180 miles and return to the Desert Studies Center this evening. This tour will provide a sampling of the wide variety of mines and minerals in this part of the desert, as well as a variety of mining methods that changed with time.

Curtis Howe Springer's mining claims

On October 9, 1944, Curtis Howe Springer, the founder of the Zzyzx health resort, staked eighty 160-acre placer mining claims and one lode mining claim on Soda Lake and the surrounding area. Over time Springer's health resort that he named Zzyzx took shape. Operating a health resort on a mining claim was clearly not the intention of the mining law. However, he tried to legitimize his unauthorized occupancy of public lands by attempting to acquire the land under the authority of other laws. Each application was rejected. Finally on November 6, 1968, the Bureau of Land Management contested the validity of the mining claims.

Edward F. Cruskie, the Bureau of Land Management Mining Engineer assigned to evaluate these claims concluded:

There is no apparent significant mineralization, veins or structures, in the rock in place portions of these claims that could have contributed any gold or other placer values to the predominant covering of the lake silt beds. The claims are essentially non mineral in character.”

The mining claims were declared null and void on November 14, 1972, by the Interior Board of Land Appeals (IBLA). Following this decision, the case was heard by the District Court. On March 6, 1973, the court permanently enjoined Springer and the other appellants from trespassing on or occupying the federal land. Following this decision Springer appealed to the 9th Circuit Court of Appeals, which upheld the District Court decision. In 1974, the U.S. Supreme Court refused to review the lower court decisions.

Today the facility is managed by the California State University under an agreement with the National Park Service (Vredenburg, this volume).

Salt and soda from Soda Lake

With the 1906 construction of the Tonopah and Tidewater Railroad along the west side of Soda Lake and directly through Soda Springs, a long-standing watering hole on Mojave Desert routes, the salts of Soda Lake drew commercial interest. Shortly after the railroad was built two separate companies began building plants to extract saline minerals from the brines of Soda Lake.

The Pacific Coast Soda Company was incorporated in January 1907 by men from Santa Ana. Shortly later the company began running full-page ads in the Los Angeles

Times (April 7, 1907) and other newspapers promoting “the greatest natural deposit of all the many rich treasures of the Death Valley section,” and inviting the public to buy stocks. By May 1907, the Pacific Coast Soda Company began construction of solar evaporation ponds, a narrow-gauge railroad, and a plant to process the salt crust mined from the surface of the lakebed. The material was dried in a 40-foot-long horizontal revolving kiln that was erected south of the hill behind the remains of “Fort Soda.” The company intended to produce salt and sodium sulphate. Product from the Soda Lake plant was to be shipped to another plant in Santa Ana that was to convert the sodium sulphate into sodium carbonate, bicarbonate, and caustic soda. The plant at Soda Lake cost over \$25,000 and the plant at Santa Ana that was to be completed in the fall of 1908 was estimated to cost \$75,000. However, it appears that the entire project was a failure from the start. The Los Angeles Express (12 November 1909, p. 17) reported: “the directors of the Pacific Coast Soda Company today decided to dispose of all surplus machinery owned by the corporation and use any surplus funds for conducting further experiments at Soda Lake on the desert. The method for precipitating sulphates of soda from soda crusts found on the company's property has proven a failure and the directors now are endeavoring to find a solution to the problem.”

In June 1910 the shareholders refused to invest additional funds in the project and filed a suit against the board of directors (Los Angeles Times, 16 June 1910, p. 30). A July 1912 newspaper article stated the plants were sold at a loss of \$100,000 for scrap (Anaheim Gazette, 16 May 1912; Pomona Morning Times, 12 Jul 1912, p. 3; Fulton, 2005)

About the same time a second company, Pacific Salt and Soda Company (Figure 1), was incorporated by Los Angeles men to extract salt from Soda Lake. By June 1907 the company had a crew at work at the site building evaporation ponds and erecting a plant to dry salt. This operation was located about a half mile north of the works of the Pacific Coast Soda Company (Los Angeles Times, January 26, 1908). It was reported by the San Bernardino Sun (August 11, 1907) that “splendid stone buildings are being constructed on the site of the old fort.” Nothing more is heard about this operation until the Barstow Printer (January 5, 1912) stated that the company elected new officers, and that “. . . new blood has been interested in the company and more activity is expected soon.” By this time most of the news regarding the company was allegations of fraud, Stock Assessment notices and Delinquent Stock Sale notices. In the Sacramento Bee (April 3, 1916) the company was listed as delinquent paying corporation taxes and its right to do business had been forfeited.

Soda Lake gold (?)

During the 1970–1980s, “mining” companies promoted the recovery of gold from sand and silt located in Soda



Figure 1. Soda Lake view to north, showing the Pacific Coast Salt and Soda Company plant. Photo by D. G. Thompson, December 7, 1919. U.S. Geological Survey photo tdg00433.

Lake, Silver Lake, and Shadow Valley. According to the promoters the ore was water soluble and was leached from the surrounding mountains and washed into these centrally located dry lakes.

On Silver Lake gold assays increased in value toward the roadbed of the Tonopah and Tidewater railroad, which happened to have been constructed with gold bearing andesite from the Bagdad-Chase mine located south of Ludlow (Reynolds and Weasma, 2005, p. 12).

Assemble at the Desert Studies Center main gate.

Proceed north on Zzyzx Road 4.7 miles to I-15.

0.0 (0.0) **RESET ODOMETER to zero. Turn left** to merge onto I-15 south (west).

Pink Lady Bentonite

From this overpass, the Pink Lady Bentonite mine is located about 0.4 mile north and a little east up the dry wash. Bentonite at this mine has a distinctive pink color on freshly exposed surfaces. It was developed by a 600-foot-long dozer cut and a 40-foot-long adit driven west into the hill. About 80 tons were shipped to Los Angeles for testing as drilling mud. Reportedly it has also been used for cosmetics. The bentonite is exposed in 3- to 4-foot-thick beds which are overlain by alluvium. The bentonite is composed of high-quality montmorillonite, which is a highly swelling and highly thixotropic clay (Henderson, 1980).

The Blue Bell mine

Also from this overpass, if you were to follow the dirt track northwest about 5 miles you would come to the Blue Bell mine. This mine has produced specimens of more than 97 different mineral species and is the type locality for 5 mineral species. The primary ore minerals were emplaced largely as replacement veins, controlled by faults and fractures in Pennsylvanian limestone beds during

intrusion by Cretaceous quartz diorite. Fluids from the intrusion converted limestone to skarn, composed mostly of garnet and diopside (Wise, 1996; www.mindat.org). Adams and Housley (2019) describe recent findings in the mine. The mine was first worked in the 1880s when exceptionally high silver assays were reported. At this time the location was known as Joe Dandy Hill. The May Queen claim located January 1885 was patented. Mining continued until the early 1890s (Vredenburg, 1994). The mines were reactivated in 1949 as the Blue Bell, Little Mike, and Hard Luck. Forty tons of ore containing lead, copper, and silver was shipped from the Little Mike and 80 tons from the Blue Bell. Ore was also shipped from the Hard Luck in 1951 and 1952 (Maynard and others, 1984).

9.7 (9.7) **EXIT Basin Road.** Turn left, cross over I-15 and head south on Basin Road.

11.9 (2.2) **Keep right** at the fork in the road.

14.0 (2.1) Arrive at the Baxter Iron Mine

Stop 1-1: Baxter (Cave Canyon) iron and limestone mines

UTM 11S 563593 3879365; 35.0550, -116.3026

Little has been published about the pre-1917 mining here; however, most of the mining claims were patented between 1906 and 1908. The Cave Canyon deposit is described in Cloudman (1919, p. 872-876), Logan (1947, p. 281), Tucker and Sampson (1930, p. 308), Tucker and Sampson (1931, p. 383), Tucker and Sampson (1943, p. 516), Collier and Danehy (1958), Brown and Monroe (2000), Bishop (2013), and Wilkerson (2015). Wright and others (1953, p. 93) mentioned that the deposits had been mined intermittently since 1930 as a source of iron used in the manufacture of cement. The geologic map of Bishop (2013) is shown in Figure 2. In 1952 the deposit was developed by an 800 x 200 x 70-foot open cut as well as shafts, adits, and trenches. At that time mining operations occurred during a period of a few weeks spaced by two-year intervals. The patented (private) land is owned by CalPortland. Active mining continues at this deposit (Figure 3).

In the 2013 Desert Symposium Proceedings and Field Guide, Bishop (2013) described the geology and mineralization at this mine:

... iron deposits mined at the Baxter Mine occur in two variably brecciated landslide deposits interpreted to be rock avalanche deposits interbedded with sandstone and conglomerate. The stratigraphically

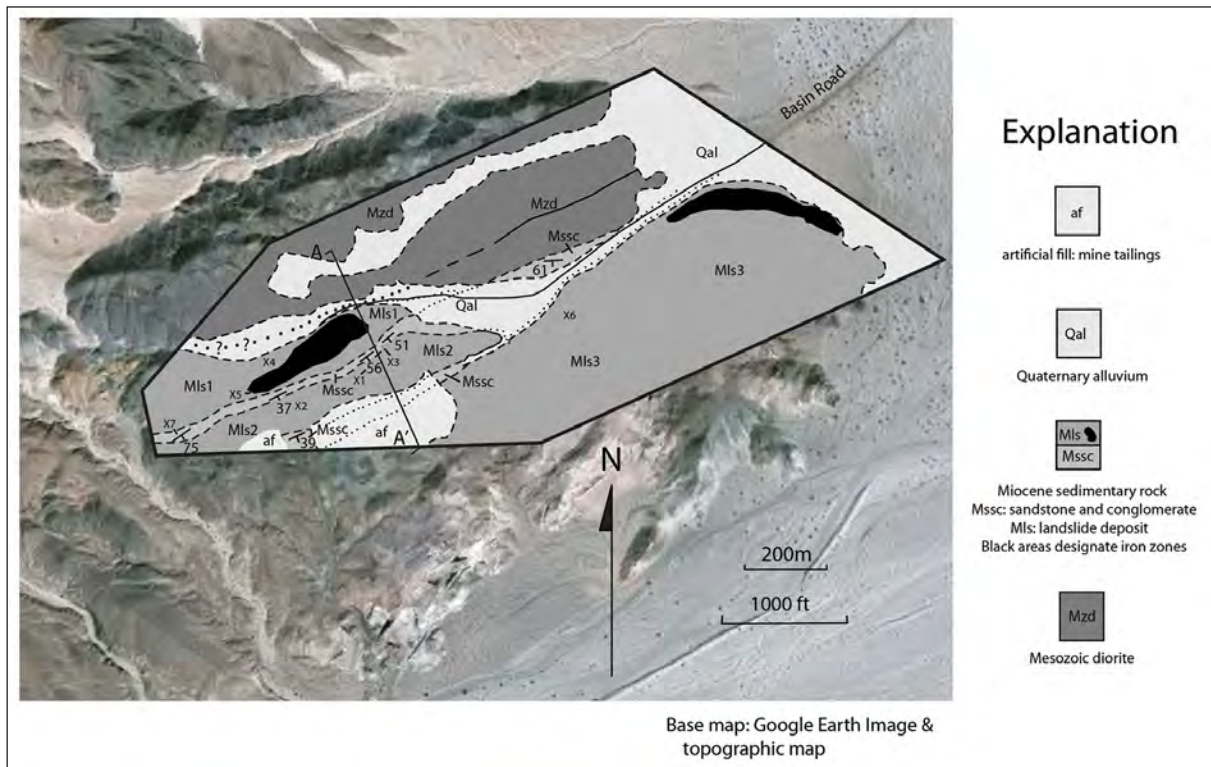
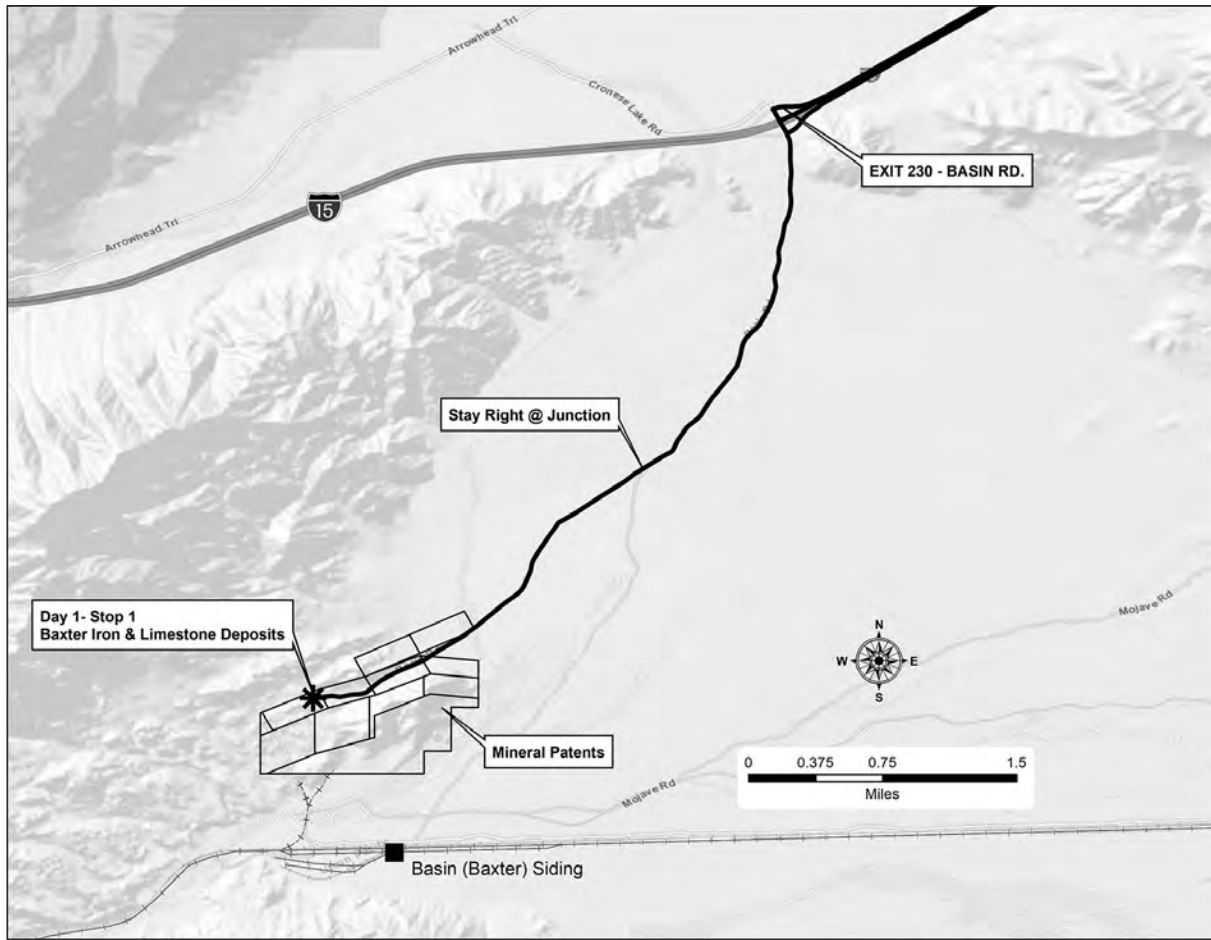


Figure 2. Geological map of the Baxter mine, iron deposits (Bishop, 2013, p. 108, Figure 2).



Figure 3. View of the Baxter iron mine (Photo by Gregg Wilkerson, Dec. 2014)



Figure 4. The Baxter limestone quarry (Photo by Gregg Wilkerson, Dec. 2014).

lower landslide consists mainly of metamorphosed rock derived from Mesozoic volcanic and quartzose deposits and the higher landslide mainly consists of Paleozoic limestone and mafic intrusive rock. A third landslide unit, thoroughly brecciated and barren of exposed iron mineralization, lies stratigraphically between the other two landslides. Separating the landslides are non-metamorphosed fluvial arkosic sandstone and conglomeratic deposits. The entire sequence of fluvial and landslide units dips southward at 37 to 75 degrees. The sequence appears to form the base for the Miocene terrestrial sedimentary and volcanic deposits exposed in Afton Canyon to the west and in the Cady Mountains to the south. If correct, then the fluvial and landslide sequence is also Miocene.

Iron mineralization within the rock avalanches occurs within the metavolcanic

rocks in the stratigraphically lowest landslide and in mafic plutonic rocks that invaded Paleozoic limestone in the highest landslide. The mineralization occurred within the source rock for the landslides, although the location for the source rock is not known. The geologic setting for the iron deposits at Cave Mountain is quite similar to those in the Silver Lake area of the southern Avawatz Mountains, 40 km to the north.”

Limestone outcrops immediately adjacent to and south of the iron deposit (Figures 4, 5) were mined from 1906 until the early 1920s for use in the manufacture of sugar (Cloudman, 1919, p. 872-876). Claims were patented in 1908, 1923, and 1960 totaling 309.99 acres. When operations ceased in the 1920s most of the equipment, including two vertical kilns, were purchased for use at the Chubbuck limestone operation, located about 16 miles south of Cadiz siding (Vredenburg, 2014, p. 57-59). In 1930 the land was acquired by California Portland Cement Company, now CalPortland (Wright, and others, 1953, p. 172; Lamey, 1948; Southern Pacific Company, 1964; Brown and Monroe, 2000).

These high purity limestone deposits occur in the Crystal Pass Member of the Sultan Limestone of Devonian age and

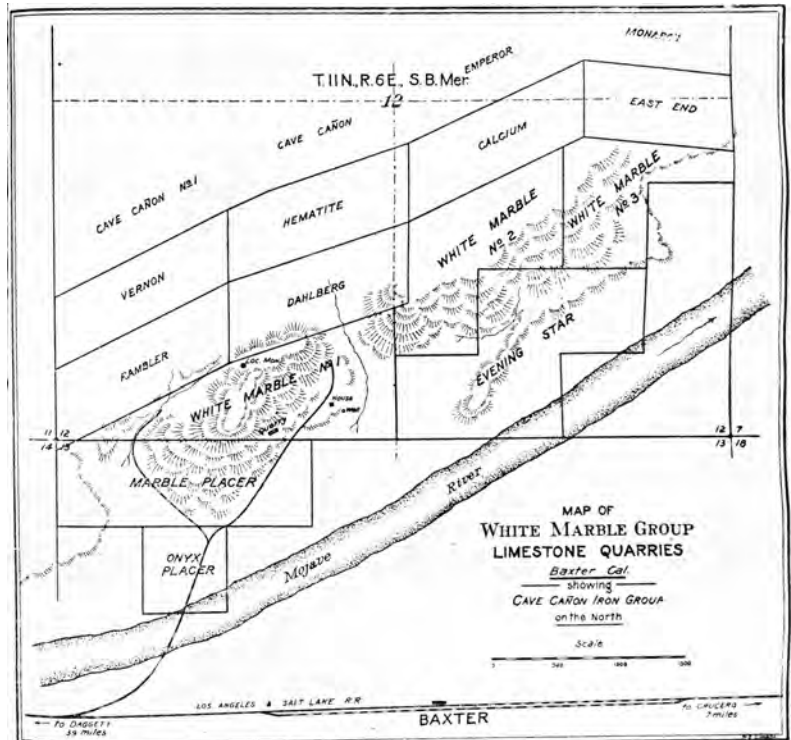


Figure 5. Geologic map of the White Marble Group, Cloudman (1919, p. 873).

in the Bullion Member of the Monte Cristo Limestone of Mississippian age. The Crystal Pass forms variably pure white calcite marble, and the Bullion forms quite pure calcite marble, both of which have been bleached white by metamorphism (Brown and Monroe, 2000, p. 44).

18.1 (4.1) Retrace Basin Road north to I-15.

0.0 (0.0) RESET ODOMETER. Enter north (east) bound onramp.

3.8 (3.8) Pass Razor Road. Here we cross a contact with volcanic rocks to the northeast and Quaternary gravels to the southwest.

9.7 (5.9) Pass Zzyzx Road.

16.1 (6.4) Pass Baker and Death Valley Road, State Highway 127.

Baker was founded as a station on the Tonopah and Tidewater (T&T) Railroad in 1908 and was named for Richard C. Baker, business partner of Francis Marion Smith in building the railroad. Baker later became president of the T&T. The town of Baker was established in 1929 by Ralph Jacobus Fairbanks (1857–1942), who was an American prospector, entrepreneur, and pioneer who established several towns in the Death Valley area of California, including Fairbanks Springs (1904–05) and Shoshone (1910) (Wikipedia, 2023).

Otto Mountain is located about 1.5 miles northwest of Baker. The Aga mine, a lead, silver, copper, and gold prospect, which is located here, is a world-class mineral locality. Several previously undescribed minerals have been found (Wright and others, 1953, tabulated list, p. 71; Mills and others, 2014).

Hanks Mountain is located 2.4 miles south of Baker. The eastern part of this hill is Paleozoic carbonate rocks and the western part is Cretaceous-Jurassic granitoid rocks. Part of Hanks Mountain is underlain by rock avalanche deposits (Frank Jordan, personal communication, 2022). Two small workings are found at this location, the Preema Gold prospect and the Rat Hole Gold-Tungsten prospect. The Preema prospect exposes a shear zone that strikes N 25° W. and dips 70° NE in phyllitic and gneissic metasediments. The zone contains quartz lenses stained with hematite. The Rat Hole prospect exposes a 6.5-ft wide shear zone in limestone that strikes N 15° W and dips 70° E. The iron oxide-stained and bleached shear zone is in contact with a thrust fault dipping 25° SW. Minor secondary copper mineral staining occurs along fractures in limestone in the upper pit (U.S. Bureau of Mines, 1990a, p. 134).

29.0 (12.9) Pass Halloran Springs Road. Rocks on either side of the freeway are Cretaceous Teutonia Granite. To the northeast are lava-capped tablelands. The lava is basalt of the Cima volcanic field. This volcanic field covers an area of about 200 square miles. The oldest flows are ~7.6 Ma, and the youngest are between 40,000

and 12,000 (Gans, 2022a). We will explore Telegraph mine just south of the freeway and about 3 miles east of here on our return trip.

Turquoise Mines: During the 2005 Desert Symposium field trip we visited the turquoise mines situated just north of Halloran Spring. According to Reynolds (2005, p. 63) turquoise was probably deposited in the Halloran Hills after 5 Ma. Ground water leached phosphate from basalt, picked up copper sulfate solutions from the gravels, and traveled laterally through the porous, weathered granite until it reached alunitized quartz monzonite. Although generally botryoidal, turquoise also fills voids and replaces original minerals in miarolitic cavities in the Teutonia granite pluton. Turquoise mining in the Halloran Hills has continued from about 500 CE to the present: over one thousand years of mining (Reynolds, 2005).

Turquoise is found at several mines situated from about 6 miles northeast to 6 miles northwest of the Halloran Springs overpass. Many of these mines were patented.

34.9 (5.9) Pass under Halloran Summit Road overpass.

The rocks on either side of the freeway are Tertiary gravels. View northeast of Clark Mountain, Mohawk Ridge, and the Mescal Range. View to southeast of Cima Dome.

40.5 (5.6) Pass Valley Wells Rest Area. Rocks in the hills to the north are Cretaceous Teutonia Granite. Rocks to the south at 1,249 Hill are Tertiary gravel.

42.1 (1.6) Pass Valley Wells Exit. Cima Road is to the south and the Excelsior Mine Road is to the north.

Light colored bluffs on both sides of the freeway are Pleistocene wetland (groundwater discharge) deposits.

Valley Wells smelter site

The site of the Valley Wells smelter (Figs. 6, 7) is 1.6 miles north of I-15 and just east of the Excelsior Mine Road. The smelter processed copper ore from the Copper World mine. A large slag deposit still exists at the site.

Copper World and Mohawk mines

The Copper World mine is located on the southwestern flank of Clark Mountain 2.5 miles due north of Interstate 15. The Mohawk mine (Fig. 8) is located near the western end of Mohawk Hill 1.0 miles north of Interstate 15 and about 1.75 miles southeast of the Copper World Mine. Both mines are accessible from the Cima Road exit on Interstate 15.

History: Hewett (1956, p. 136, 145) discusses both mines, as did Paul Adams (2020) in an extensive article that covered the history, geology, and mineralization of these deposits. The Copper World mine was discovered in 1868 by Johnny Moss after an Indian brought him a sample of metallic copper (Vredenburg and others, 1981). Two years later a few tons of high-grade ore was mined and shipped to San Francisco. The claims changed hands repeatedly until the early 1890s. In 1898 the Ivanpah



Figure 6. Copper World Smelter. San Bernardino County Museum collection.



Figure 7. Copper World smelter crew. Riley Bemby collection.



Figure 8. Ore-loading platform, burro ore train, and ore wagons at Mohawk mine. Photo by D.G. Thompson, October 27, 1917. U.S. Geological Survey photo: tdg00120

Smelting Company was incorporated and in December construction began on a smelter capable of processing 50 tons a day at Valley Wells (or Rosalie Wells, or simply Rosalie). The smelter began operations on March 10, 1899. Up to June 1900 it was reported that 11,000 tons of 13.5% ore had been produced. However, during its short existence, the Ivanpah Smelting Company was entangled in complicated legal problems. In May 1903, a sheriff's sale of the property was held for failure to pay back debts.

Dr. L. D. Godshall acquired the title to the property in 1906 and organized the Cocopah Mining Company. This company operated the mine from August 1906 until 1908. Between 1902 and 1906 the smelter fell into disrepair and the new owners were forced to haul unprocessed ore to the railhead at Ivanpah and then to the Needles smelter. The "Panic of 1907" and the fall in the price of copper closed the mine.

With higher copper prices during World War I, Dr. Godshall entered into a 10-year lease of the Copper World and Mohawk mines from the Cocopah Copper Company, of which he was vice president and general manager. Beginning in November 1917 high-grade ore from the Copper World was processed at the newly repaired Rosalie smelter, which had a 100-ton blast furnace. About 100 tons of ore a day was hauled to the smelter by tractor, while 13,000 tons of slag was re-smelted. Copper matte was hauled 25 miles to the Salt Lake Railroad at Cima and shipped to the smelter at Garfield Utah. Between 1916 to 1918 about 1,735 tons of ore that contained about 4% copper and 1,353 tons of matte containing 25–28% copper was shipped. In 1944 3,743 tons of tailings from the Rosalie slag dump were treated and shipped to the Garfield, Utah smelter. Between 1977 and 1981 the Copper World was leased to Philip Rivera. Azurite and malachite were mined and marketed as "Royal Gem Azurite."

Early history of the Mohawk mine mirrors that of the Copper World since they were owned by the same

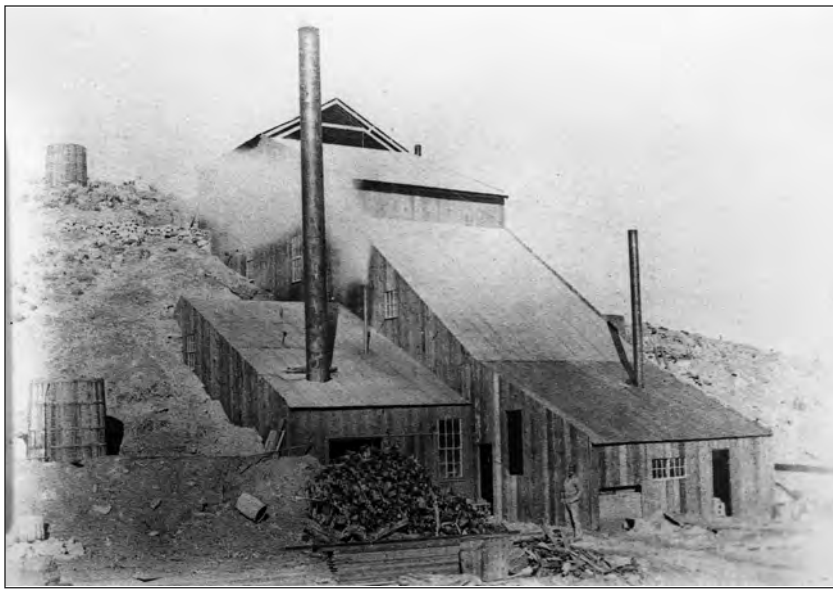


Figure 9. Mescal Mill c. 1880. E.L. MacFarland collection.

companies. Both mines were acquired by the Cocopah Copper Company in 1906. During World War I 2,893 tons of ore were shipped. During World War II the mine was marginally economical. Between 1942 and 1952 16,723 tons of ore were mined (Wright and others, 1953, p. 110-111).

Geology

The Copper World mine is situated in Cambrian to Devonian Goodsprings dolomite that has been intruded by several sill-like bodies of quartz monzonite. The mine yielded copper and lead-silver-zinc. Ore minerals include azurite, malachite, and chrysocolla. The Mohawk mine workings are bounded on the east by the Mesquite Pass thrust and on the west by the Pachalka/Winters Pass thrust. All the mine workings are located within carbonate rocks of the Cambrian Bonanza King Formation, near contacts with quartz monzonite. The contacts between the carbonate and intrusive rocks show no sign of thermal metamorphism

which suggests the contacts are faults (Adams, 2020).

In the Mohawk mine, none of the mine workings reached unoxidized ore. Secondary minerals are dominated by arsenates of lead, zinc, and copper. Mineral identifications were made by Wise (1990, 1993), who performed the first detailed study of the Mohawk mine. Adams (2020) identified 62 different mineral species at this mine.

Geologic reports for the Mohawk mine are found in Jessey (1988) and Jessey and Fallis (1989), as well as U.S. Bureau of Mines (1990a, p. 74).

45.6 (3.5) View to north and slightly east at the Mohawk Mine workings and ore bin high on the south side of Mohawk Hill.

STOP 1-2: Mountain Pass Rare Earths mine

UTM 11S 633510 3925680; 35.465662, -115.528572

51.0 (5.4) **TAKE EXIT 281:** Bailey Road, Mountain Pass Mine exit. Stop sign at intersection. **TURN RIGHT, THEN** straight onto a dirt road heading south about .1 mile. Pull out in a wide area. The outcrop to the west contains clasts of maroon syenite and garnet augen gneiss, two of the rock types in late Tertiary fanglomerate deposits in Shadow Valley basin.

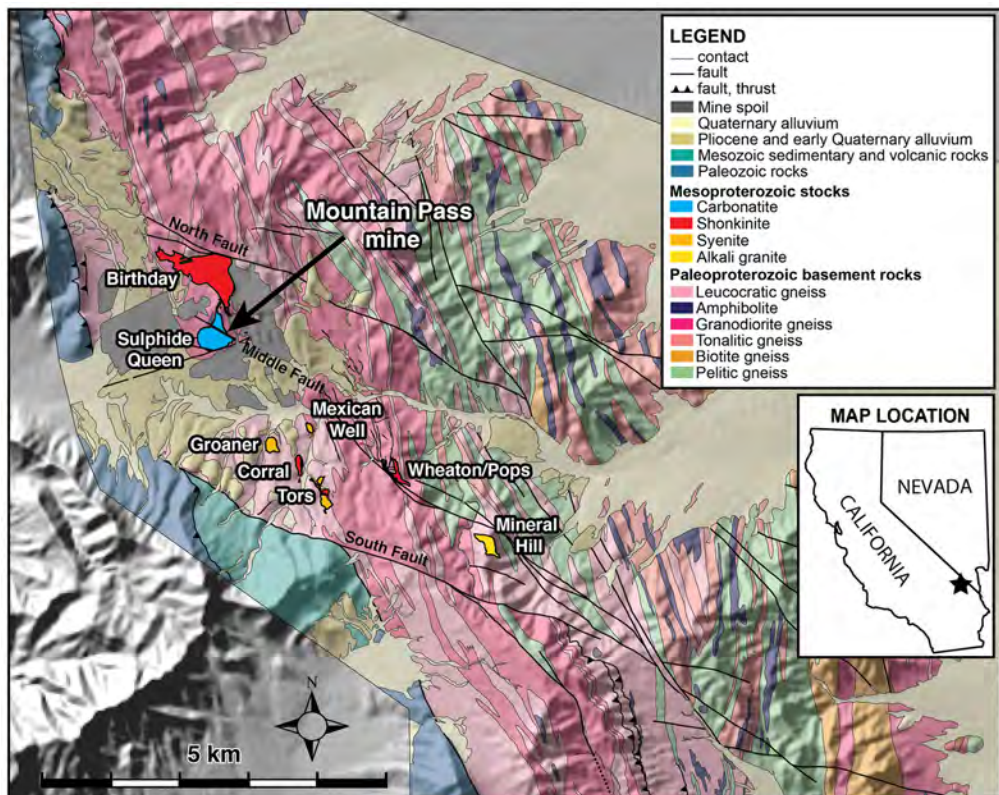


Figure 10. Mountain Pass area geologic map (Watts and others, 2022).

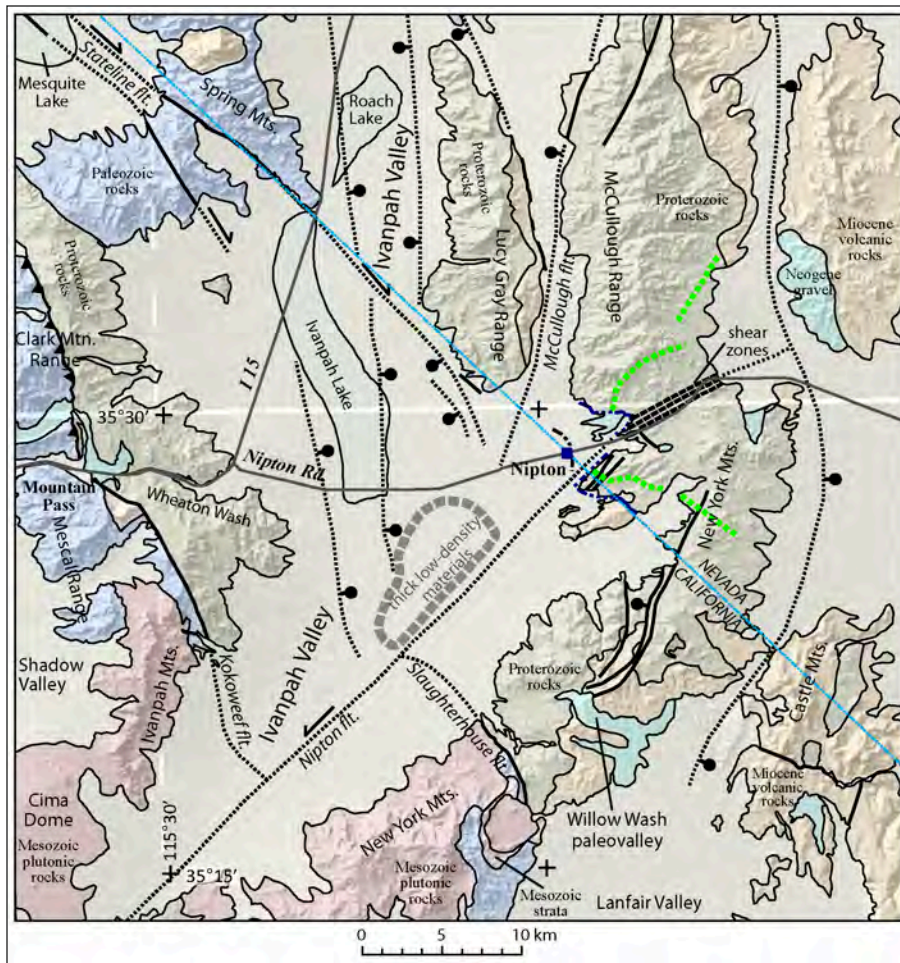


Figure 11. Geology and physiography of the Ivanpah Valley area (Miller and others, 2019, p. 13). Major Cenozoic faults are shown as well as a few important Mesozoic faults. Most thrust faults of the Mescal and Clark Mountain ranges are omitted for simplicity. The 1.4 Ga ultrapotassic intrusive suite of the Mountain Pass area straddles I-15; Bar-and-Ball – on downthrown side of normal fault; Arrow shows sense of offset on strike-slip fault. Green dashed lines show transects along which apatite was sampled.

The Mollusk (Mescal or Cambria) mine (Figure 9) is high on the ridge to the southwest. It was discovered in 1879 and produced silver until 1890. The mill was located at a spring about a half mile south of where we parked. It is estimated the mine produced \$250,000 in gold and silver (Vredenburg, 1996, p. 70). We have stopped across from the active workings of the Mountain Pass mine, a major producer of rare-earth elements. At this stop we will discuss the geology and mineralization at this important mine (Figure 10). Please see the Road Log for the Premeeting Field Trip for more information on the Mountain Pass mine.

0.0 (0.0) **RESET YOUR ODOMETER. RETRACE** the route back to Interstate 15. **TURN RIGHT** (east) on I-15 toward Las Vegas.

Caution: Maintain speed and be aware of closing traffic going down-grade here on the interstate. High-speed, truck heavy traffic makes this stretch of highway more dangerous than others.

5.0 (5.0) **EXIT** 286 Nipton Road. **TURN RIGHT** onto Nipton Rd. Nipton Road was built in the 1930s to support the construction of Hoover Dam. Consult Figure 11 for roads and an overview of geology of the Ivanpah Valley area.

8.4 (3.4) **TURN RIGHT** on Ivanpah Road. Buildings on the right after we turn are part of the water supply for an earlier iteration of the Mountain Pass mine. Enter Mojave National Preserve after a short distance.

11.6 (3.2) Continue straight on Ivanpah Road, pass the Morning Star Mine Road. This intersection is near the railroad siding and town site of Ivanpah, the second of three locations with this name. In early 1902, the California Eastern Railroad extended the line from (Manvel) Barnwell to this location to haul coal to the Copper World mine and copper ingots for final smelting. Two years later, in 1904 Francis Marion “Borax” Smith graded a 104-mile road at a cost of around \$100,000 from here to the Lila C borax mine located southwest of Death Valley Junction. The steam tractor Dinah only made it 14 miles before it bogged down in sand and the engine seized completely. With this failure he

decided to build the Tonopah and Tidewater Railroad to haul borax ore from the Lila C mine to Ludlow (Myrick, 1964, p. 545; Serpico, 2013, p. 28).

STOP 1-3 The Vanderbilt mine

UTM 11S 657156 3910690; 35.327104, -115.270951

20.8 (9.2) **TURN LEFT** onto the unmarked road to the Vanderbilt mill. **Stop here: do not pull forward beyond the road cut.**

We were not able to obtain permission to access the millsite. We will have to view it from a distance after a short level walk. The road cut was constructed by the California Eastern Railroad in 1902 to access the railhead at Ivanpah. The railroad changed hands (and names) at least twice after being built. The cut passes through Cambrian silicified limestone. About 550 feet northeast of the cut the limestone is in fault contact with Proterozoic



Figure 14. Vanderbilt ball mill. Jan. 21, 2023. Photo: Larry M. Vredenburg.

Menchaca, 2023). In 1965 Heavy Metals Corporation drilled the property and satisfied with the results, began developing the mine and erected a 500 ton per day capacity mill. Between 1969–1970 and 1974–1975 about 100,000 tons of ore were milled (Vredenburg and others, 1981, p. 119). Gold resources at the mine were estimated in 1972 as 383,000 tons of ore, containing 224,000 oz gold, 1.1 million oz silver, 1.9 million lb. copper, and 2.6 million lb. lead (U.S. Bureau of Mines, 1990a, p. 115).

In May 1982, Vanderbilt Gold Corporation was in the process of converting their bulk-flotation mill to an



Figure 15. Vanderbilt Saloon. Huntington Library.

agitated-leach operation (John Jordan Jr., Heavy Metals Development; Miller and others, 1986).

Proterozoic granite gneiss and mica schist are cut by two mineralized fault zones that strike N 55°–63° W and dip 65°–80° NE (Fig. 16). Many branch veins and/or cross veins are between the two main veins. Mineralized fault zones are accompanied by heavily argillic altered, gray dike rocks that are highly fractured. Ore shoots occur along dike-schist contacts and as lenticular bodies within the fractured, light gray dikes. Gold is associated with pyrite. Sulfide ore consists of quartz with major pyrite and minor chalcopyrite, galena, sphalerite, marcasite, cubanite, and traces of arsenopyrite, magnetite, tennantite, tetrahedrite, bornite, and pyrrhotite. Veinlets of hematite up to 5 in. wide were noted (U.S. Bureau of Mines, 1990a, p. 115).

21.7 (0.9) **TURN LEFT** (south) on Ivanpah Road, continue .9 mile

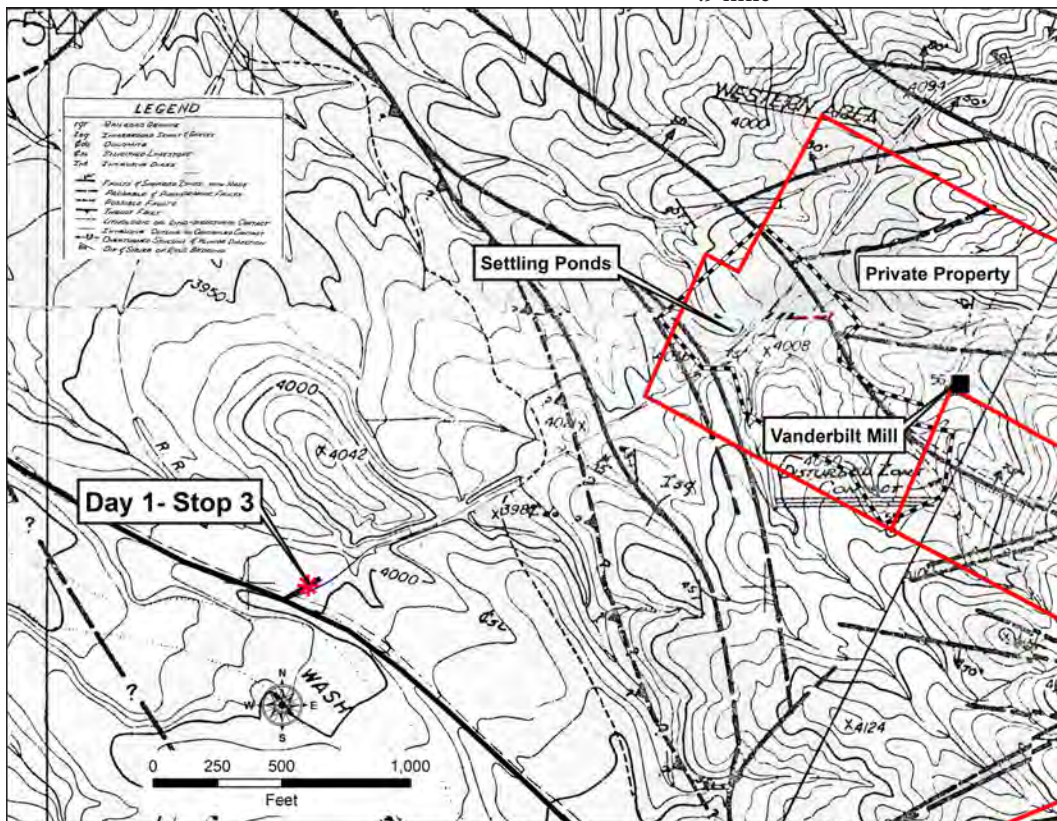


Figure 16. Geologic map of the Vanderbilt mine area.

**Stop 1-4:
The historic
Boomerang
millsite**

UTM 11S
658073 3909650;
35.317585,
-115.261069

Look for the stone foundation of the Boomerang millsite against the hill on your left. Compare the circa 1917 photo (Figure 17) and the 1984 photo (Figure 18) with what you see today.

**RESET YOUR
ODOMETER.**

U-turn and
continue



Figure 17. Vanderbilt Boomerang Mill. Source: "A Historical Review of the Vanderbilt District." The 6 page document reproduces historical documents. There is no author or date - probably Vanderbilt Gold Corp. c. 1970.



Figure 18. Boomerang Millsite. 1984. Larry M. Vredenburg photo.

northwest on Ivanpah Road to the Morning Star Mine Road.

10.0 (10.0) **TURN LEFT** (south) at Morning Star Mine Road. Go west-southwest on the Morning Star Mine Road.

15.7 (5.7) **STOP AT JUNCTION** with the unsigned Morning Star mine cutoff road (35.3434, -115.4294). At this point low clearance and 2-wheel drive vehicles must be parked and you will need to grab a ride in a 4X4 vehicle – the first portion of this road is VERY sandy and rough.

19.5 (3.8) **ARRIVE** at Morning Star open pit mine

Stop 1-5 MORNING STAR MINE

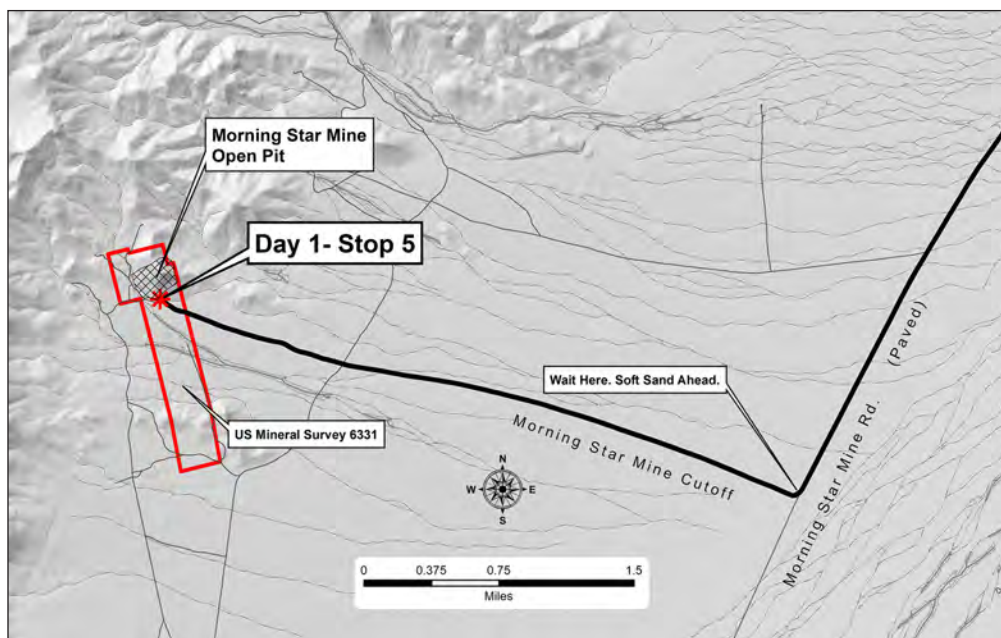
UTM 11S 637025 3914040; 35.360264, -115.491801

At this stop you will see the abandoned Morning Star mine, an open pit mine with heap leach pads (Tengelsen, 2023).

The Morning Star mine, situated on the east slope of the Ivanpah Mountains, was first active in 1907. Between 1927 and 1933 the deposit was extensively explored. Between 1937 and 1938 Richard W. Malik of Los Angeles optioned the property from the claim owners, J. B. Mighton and H. T. Brown. During Malik's operations 17,000 feet of crosscut drifts were driven and winzes were sunk on the tunnel level. In April 1939, E. P. Halliburton, owner of the Halliburton oil service company, began operations. Halliburton employed ten men until the property was shut down in 1942 by War Production Board's Order L-208,

closing gold mines (Vredenburg, 1996b, p. 75, 76). Before shutting down, underground developments consisted of a 600-foot tunnel with over 1,300 feet of drifts and two winzes, 240 and 420 feet deep (Tucker and Sampson, 1943, p. 304). The claims were surveyed in 1945 but not patented (Figure 19). As seen in 1947, small dumps and a few buildings existed (Figure 20).

The Vanderbilt Gold Corporation acquired the property in 1964



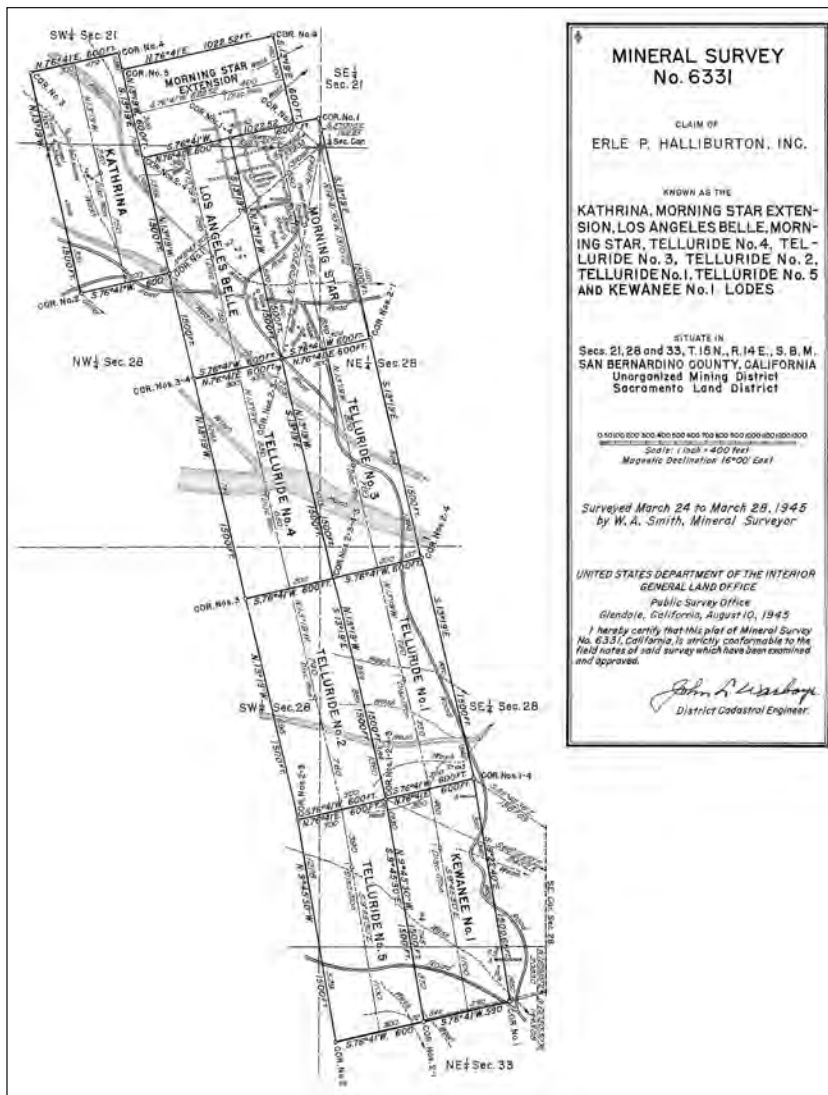


Figure 19. Morning Star mine claim survey map, U.S. Mineral Survey 6331



Figure 20. Morning Star Mine 1947. J. Riley Bemby collection.

following the death of Halliburton in 1957. The company drilled and sampled the property. In late 1979 they had raised sufficient capital to begin development. In the early 1980s the Morning Star was reactivated as an underground mine using trackless mining equipment. Ore was processed at Vanderbilt's mill at the site of the 1890s town of Vanderbilt, seventeen miles away. The ore was processed by flotation with concentrates shipped for smelting. With the drop in the price of gold, mining ceased in 1982, but exploration by underground long-hole drilling continued. In 1983 the mill circuit was converted to cyanide carbon-in-leach. This allowed doré bullion to be produced at the mill, eliminating the expense of having concentrates smelted. Drilling during this period established an 8-million-ton ore reserve averaging 0.062 ounces of gold. In the fall of 1984 one million tons of overburden was moved and a \$500,000 heap leach facility was constructed. Full-scale leaching began October 1987, and by year end 10,000 ounces of gold and 15,000 ounces of silver had been recovered. Production of ore was 75,000 tons per month. The operation was initially plagued by inadequate water supply, and lower than expected recoveries. This dilemma was solved by changing the spray leaching to drip — this doubled the amount of solution leaching through the heap and used less water. Two heaps were ultimately constructed. The operation suffered from environmental violations including bird and animal deaths in the cyanide ponds, and cyanide solution leaking from the heaps into the adjacent drainage (Ely, 1990). Mining had ceased by 1993 (Vredenburg, 1996b, p. 75,76).

Wise (1990, p. 27) observed "the Mohawk Mine, the Evening Star Mine, and the Morning Star gold mine have several similarities, especially the geologic setting and mineralogy. At the Morning Star Mine, pyrite, chalcopryrite, galena, sphalerite, covellite, and silver-gold occur in calcite and quartz veins. The veins are located along faults and fractures in the hanging wall block above the Morning Star Thrust Fault. The Ivanpah Granite phase of the

Teutonia Batholith forms both the foot and hanging walls of the fault; no carbonate rocks were involved in the mineralization.”

Burton (1987, p. 4, 5) also noted: “The granite was intruded by lamprophyre dikes which represent the magmatic differentiate phase of the Ivanpah Granite. The dikes acted as conduits for later mineralized fluids, creating a gold and silver rich, porphyry-style deposit. Subsequent tectonic activity related to the Sevier thrust belt decapitated the deposit, moving the upper plate to the east. The thrust faulting was so intense that a ten-foot gouge zone formed at the contact of the Ivanpah Granite (hanging wall) and the lamprophyre (footwall), setting up an impermeable layer which prevented the pass-through of any mineralized fluids. The thrust faulting generated enough heat to boil the ground waters which in turn remobilized the gold and silver and precipitated it down near the fault contact, creating a supergene enriched zone.”

The Ivanpah Granite is a striking rock, containing conspicuous large potassium feldspar (ksp) phenocrysts set in a quartz-plagioclase-ksp matrix, along with minor amounts of biotite. It was dated as ~150 Ma by Walker and others (1995). Geologic mapping by D.M. Miller reveals that the thrust fault exhibits brittle-ductile behavior consistent with elevated temperatures. Furthermore, several parallel shear zones exist in the footwall and hangingwall rocks; these typically are mylonite to ultramylonite zones and cut both mafic dikes and the

Ivanpah Granite. Lineations in the mylonite zones are nearly down dip, plunging moderately to the west. Shear sense as given by rotated porphyroblasts gives top to the east or thrust sense. These observations are consistent with a model of several shear zones cutting the granite body shortly after intrusion at about 150 Ma.

23.3 (3.8) **RETRACE** route to Morning Star Mine Road and recover cars parked there.

29.0 (5.7) **TURN LEFT** (north) on the Morning Star Mine Road.

32.2 (3.2) **TURN LEFT** (northwest) on Ivanpah Road

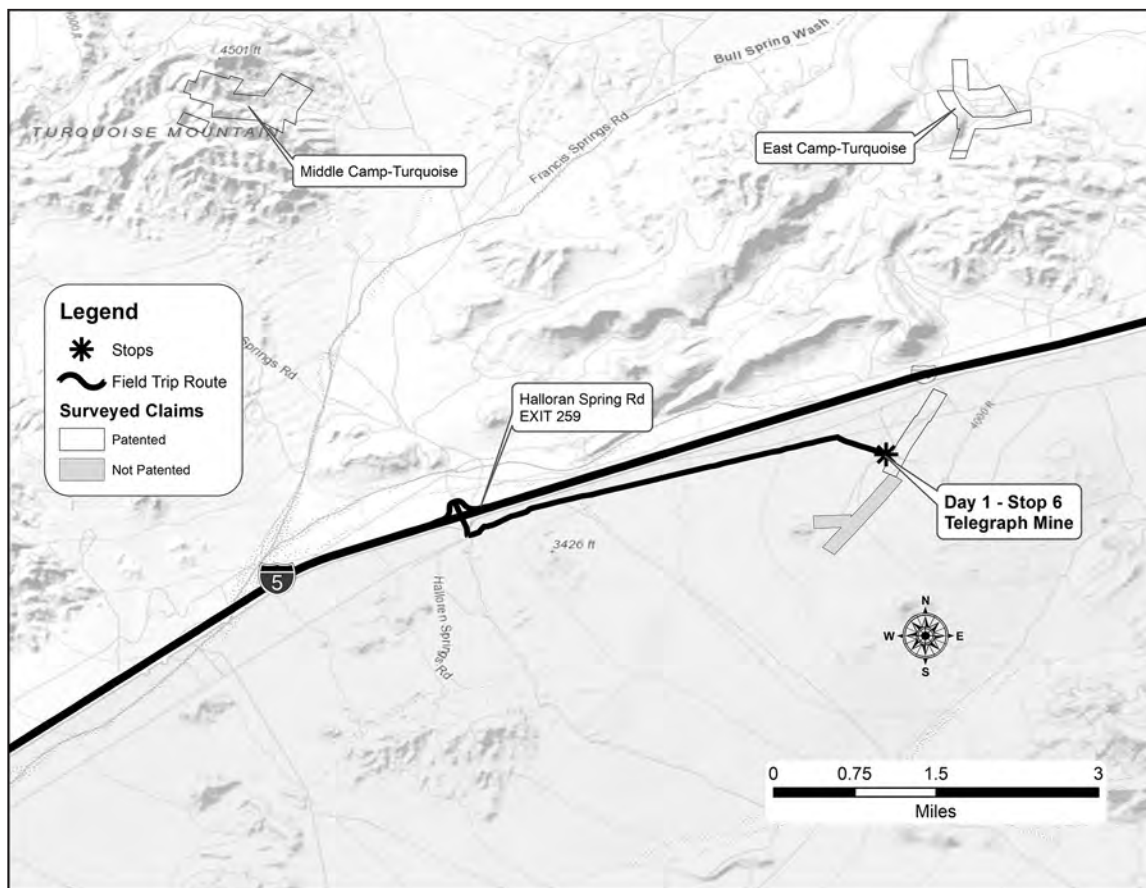
30.4 (3.9) **TURN LEFT** (northwest) on Nipton road, cross I-15 and turn left and enter the south (west) bound onramp.

57.0 (26.6) **TAKE EXIT 259**: Halloran Springs Road. At the stop sign at Halloran Springs road, turn left (south) and cross over the freeway.

57.3 (0.3) After crossing the highway continue south. About 400 feet beyond the end of pavement, Halloran Springs Road makes a sharp left (east) turn and parallels the highway.

60.2 (2.9) **TURN RIGHT** (south) on a dirt road. Mine operations are visible ahead.

66.6 (0.4) Arrive at Telegraph mine heap leach pad.



Stop 1- 6: Telegraph mine

UTM 11S 605874 3916113; 35.382744, -115.834334

The Telegraph mine was discovered November 9, 1930, by A. A. Brown and Ralph Brown of Salina, Utah. One sample showed free gold in calcite and quartz and assayed up to \$800 per ton in gold. They returned to Utah and interested Vivian and Robert Burns, who located a large number of claims. O. Perry Riker, of Long Beach, California leased the property from December 1932 to 1935. During this period, 220 tons of ore was milled at a mill at Yucca Grove, three miles northeast of the mine. Also, 990 tons of ore was shipped for smelting. Total production was \$35,200. The mine was idle in 1943 and by 1953 all equipment had been removed (Nop, 2023). In 1973 the Bureau of Land Management surveyed 7 mining claims. Two full claims encompassing 139.195 acres were patented on September 30, 1980. Part of one additional claim totaling 17.908 acres was patented on June 10, 1982. All claims were patented by Perry B. and Morgan McGlivray. An additional four claims that were surveyed were not patented. The heap leach pad is situated on land administered by the National Park Service.

The U.S. Bureau of Mines (1990a, 1990b) reported that the Telegraph Mine had apparent resources of 73,000 tons that would yield 0.51 ounces of gold per ton and 1.16 ounces of silver per ton (Vredenburg, 1996c; U.S. Bureau of Mines, 1990a, p. 79, 225).

The Telegraph deposit consists of two five feet thick parallel stockworks of intensely silicified Cretaceous Teutonia granite. The silicified zones are N 38 E strike and 55° northwest dip. Outcrops can be traced for several thousand feet. The stockworks consist of systems of closely spaced 1/4" to 1/2" thick quartz veins in sheeted, porous granite containing large and abundant cavities. The quartz veins are brecciated, cemented and encrusted with calcium carbonate and silica, indicating multiple vents of shearing and associated mineralization. Feeble pyritization (hematite after pyrite), chalcopyrite, manganese oxide, and malachite absorbed in kaolin are present, with bornite and free gold and silver reported (Ito and Morgan, 1980). The intervening ground between the two silicified zones is approximately 10 to 20 feet thick. This intervening ground and a hanging wall and foot wall thickness of at least 30 feet are intensely kaolinized or chloritized. The ground adjacent to the two silicified zones is also feebly but consistently pyritized (hematite after pyrite) (Greenwood, 1985, p. 52).

There is a heap of rock at the mine site that appears to have been a heap leach operation. It is unknown when this operation occurred.

64.3 (3.7) **Retrace route to I-15.** Cross over the freeway, turn left, and enter the ramp southbound (west).

83.6 (19.3) **TAKE EXIT 239:** Zzyzx Road

88.4 (4.8) **TURN LEFT** toward Zzyzx Road, cross the freeway, arrive at the Desert Studies Center.

Day 2

Convene at the Desert Studies Center. Make sure vehicles are packed with all your personal gear and a full tank of gas. Check spare tires. Carry water and snacks, plan your clothing for the conditions. Wear sturdy shoes. Bring hats and sunscreen. Watch for harmful plants and animals. Note that some stops are on Federal lands managed by the Bureau of Land Management. Respect the land and leave it as you found it: no artifact collecting or harming plants and wildlife is allowed.

Today we head west primarily by travelling on paved roads. There will be three stops at the Calico Mountains, a stop at the borax mine at Boron, and the Soledad Mountain (Golden Queen) gold mine south of Mojave. Low clearance vehicles are not recommended for our stop at Apollo Silver's Waterloo project and must remain on Ghost Town Road. We will be travelling about 150 miles. The field trip will conclude south of Mojave at Soledad Mountain.

Drive north on Zzyzx Road from the Desert Studies Center.

0.0 (0.0) At the I-15 Zzyzx Road overpass **cross over I-15, turn left and enter the south (west) bound onramp. RESET YOUR ODOMETER**

5.9 (5.9) Pass Razor Road.

9.7 (3.8) Pass Basin Road.

17.3 (7.6) Pass through faulted Miocene sediments in road cut (Miller and others, 2017).

18.5 (1.2) Pass Afton Road. View south to Manix Lake sediments (Jefferson and others, 2020).

22.7 (4.2) Pass the rest stop.

26.5 (3.8) Pass Field Road and the anticlinally folded Plio-Pleistocene gravels.

30.6 (4.1) Pass Alvord Mountain Road that traverses beneath the freeway (no exit).

32.4 (1.8) Continue past the southeast arm of Lime Hill, with east-dipping Pliocene gravels exposed in the road cut; these overlie the Miocene Barstow Formation (Miller and others, 2011).

33.6 (1.2) Pass Harvard road.

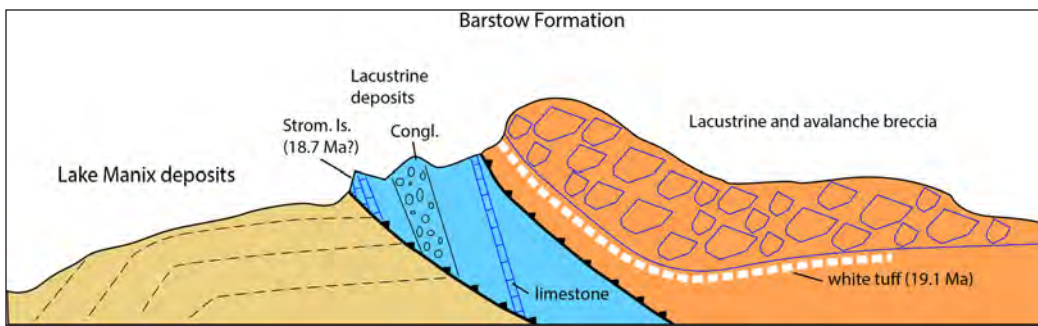


Figure 21. Cross section through southern part of Harvard Hill showing thrust faults adjacent to the Manix fault. Lower fault cuts Pleistocene beds of the Manix Formation.

Harvard Hill

Harvard Hill is 1.7 miles west of Harvard Road, and just to the south of I-15. The stratigraphic section contains early Miocene marker beds that can be traced westward through Daggett Ridge and eastward to the Calico Mountains to the type section of the Barstow Formation (Reynolds, 2002; Reynolds and Woodburne, 2002; Leslie and others, 2010).

The southern margin of Harvard Hill has interesting geology. A Pleistocene thrust fault places Miocene limestone of the Barstow Formation over Pleistocene Lake Manix sediments. Lake Manix sand, beach gravel,

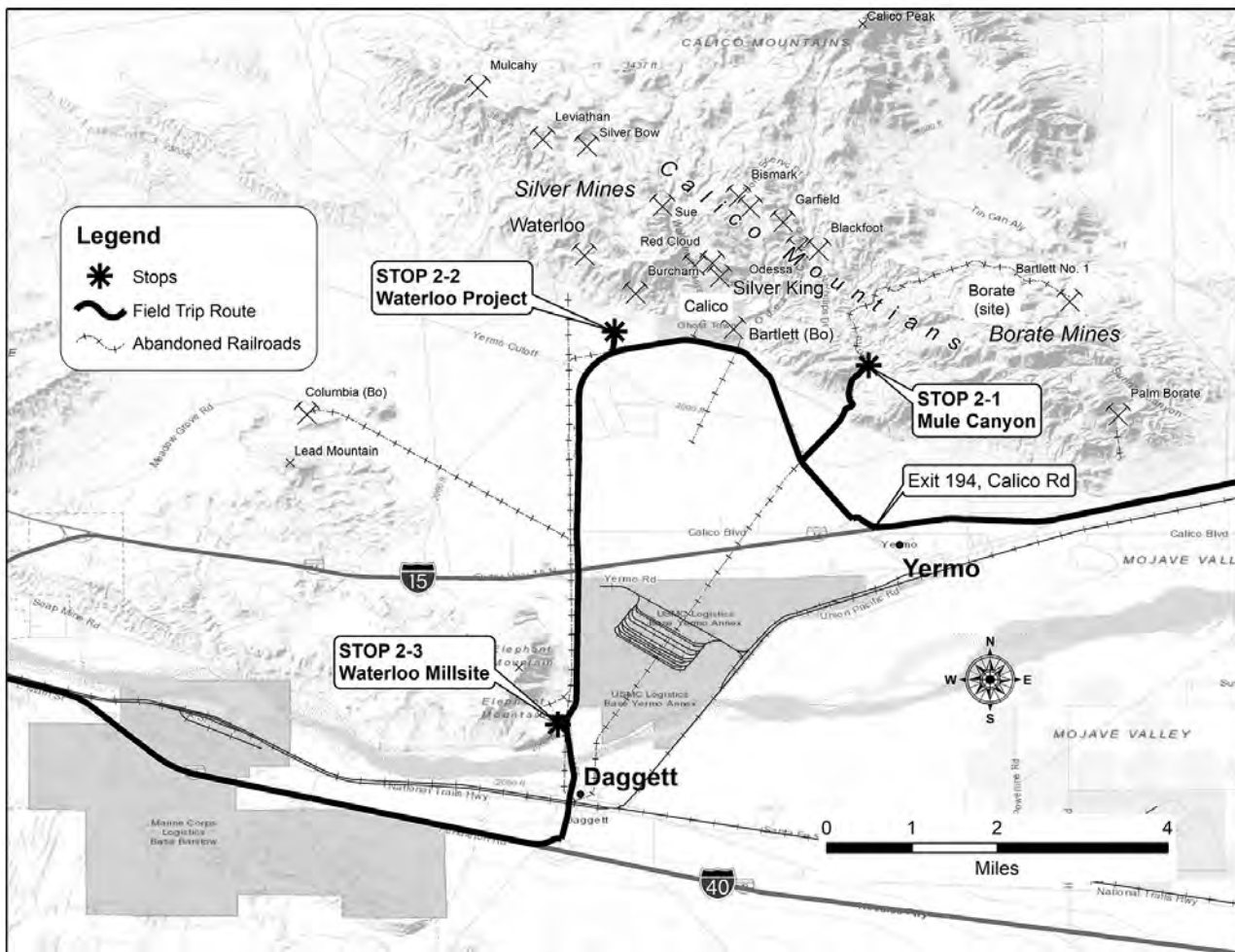
and minor muds are exposed in the pale badlands to the west. They represent folded sets of beach gravels interbedded with sands of a fluvial delta. These beds at their highest point lie at least 50 m above their original level, representing significant uplift in the late Pleistocene

and Holocene. Strands of the Manix fault lie to the north and south of the outcrops, and probably intersect with the Dolores Lake fault on the west side of Harvard Hill to cause local compression. The thrust fault over the lake beds probably represents a more impressive manifestation of this same compression (Reynolds and Miller, 2010).

38.2 (4.6) Pass Coyote Lake Road.

41.5 (3.3) Pass Minneola Road.

43.6 (2.1) Pass Yermo Road.



- 45.1 (1.5) **TAKE EXIT 194** Calico Road.
- 45.5 (0.4) **TURN RIGHT** at Calico Road.
- 46.3 (0.8) **TURN RIGHT** at Mule Canyon Road. Pull a short distance along Mule Canyon Road. Stop and wait for the group to regather.
- 47.7 (1.4) Continue up Mule Canyon a short distance and stop on the right.

STOP 2-1 Calico Member of the Barstow Formation

UTM 11S 514855 3866110; 34.937372, -116.837332

At this stop we will walk through part of the Calico Member of the Barstow Formation (Singleton and Gans, 2008); Figures 22, 23. The beds are mainly composed of fine sandstone and mudstone, and evidently are of fluvial to lacustrine depositional environment. Note the wild folding in places.

We will walk to an area that was explored for borate minerals. A white bed with carbonate minerals is also present. We will discuss lithium enrichment in mudstones like those we walk through.

Lithium clays of Hector Basin

The U.S. Borax mine at Boron, as well as the Fort Cady deposit and the Hector Clay mine just west of Pisgah Crater, are all known to contain lithium-rich clay. U.S. Borax is experimenting with the recovery of lithium at their mine at Kramer. Due to the unique

properties of hectorite it demands a high price and is not considered as a source of lithium. Tom Benson (personal communication) reported: “Recently, Lithium Americas Corp. discovered that clay-rich lacustrine sediments within the Calico Member of the Barstow Formation contain high concentrations of lithium up to 2,500 ppm Li (whole-rock). Other clay-rich outcrops of the Barstow Formation in the area also contain high concentrations of lithium and are areas of ongoing exploration by Lithium Americas Corp. in conjunction with academic collaborators.”

Borates and associated minerals of the central Mojave Desert: History

Water soluble sodium borates were first recovered in California from Clear Lake, located north of San Francisco, during the 1860s. By the 1870s borates were recovered from evaporite crusts on dry lake beds at Teel’s, Columbus, and Rhodes Marshes, Nevada. In 1881 a similar borate deposit was discovered and mined in Death Valley. In October 1882 outcrops of a newly identified calcium borate mineral, colemanite, were discovered east of Death Valley. A year later Hugh Stevens, a Calico silver prospector, discovered colemanite in the Calico Mountains. The new mine was named Borate and operated by the Pacific Coast Borax Company, starting production in 1888. In time, borax was discovered and mined throughout the Calico–Daggett area. These mines include Palm Borate about 1.5 miles due south of the Pacific Coast Borax Company’s Borate mine; Western

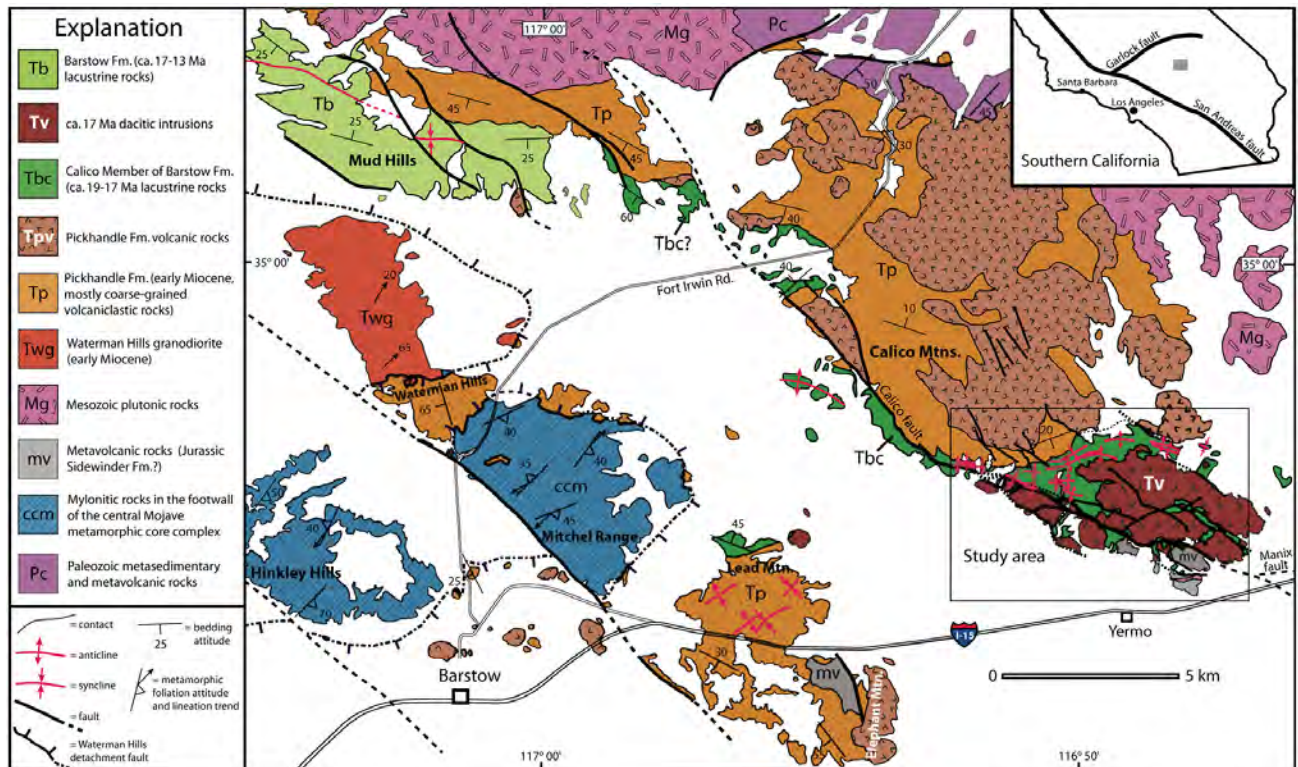


Figure 22. Geologic map of the central Mojave Desert region near Barstow, California, (Figure 1 of Singleton and Gans, 2008; see that paper for details about sources for map).

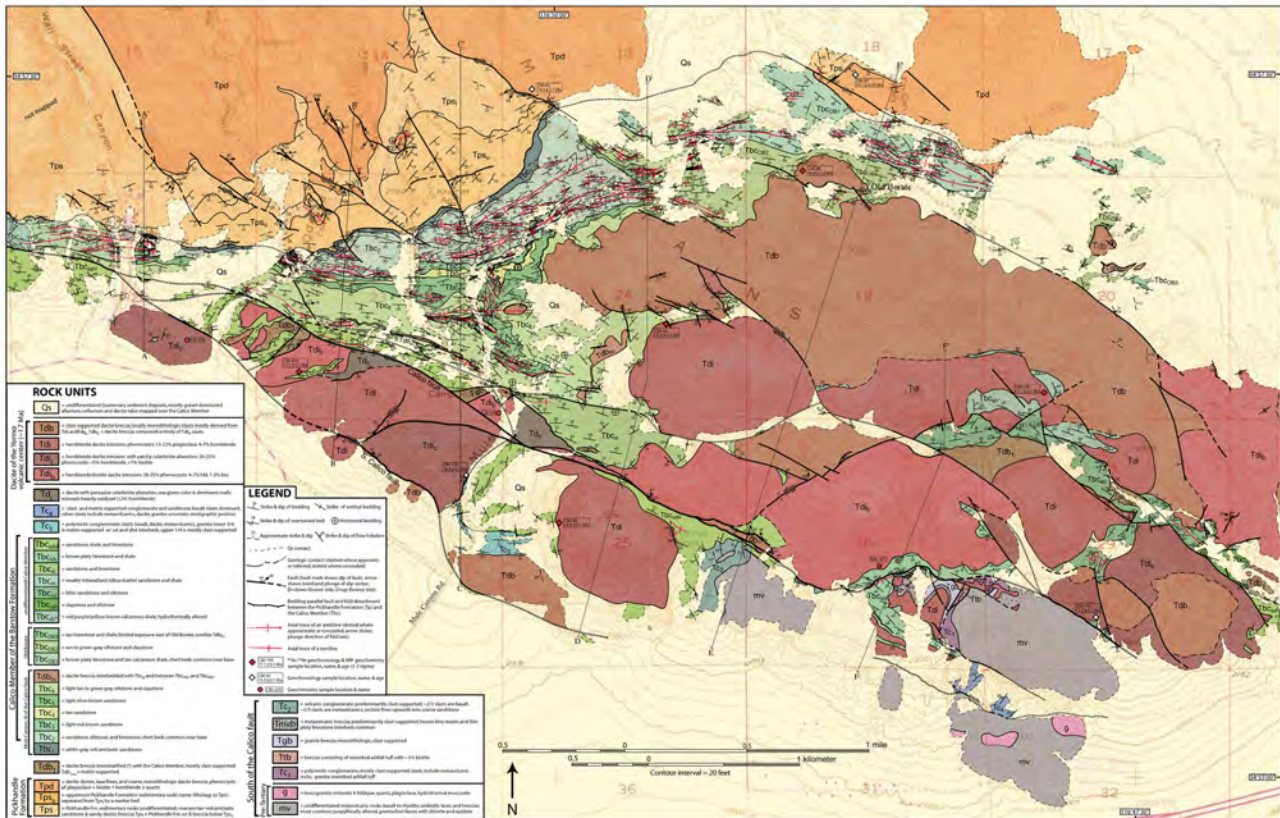


Figure 23. Plate 1 of Singleton and Gans (2008). Geologic map of the southern Calico Mountains, Yermo Quadrangle, central Mojave Desert, California.

Mineral Company's Bartlett mine, just southeast of Calico (see images on back cover); American Borax Company's Columbia mine northwest of Lead Mountain and the Columbus Borax Company's Gem mine south of Daggett. At one time this area was one of the most important sources of borates in the world, but by 1908 the Calico mines were exhausted and the Lila C mine located east of Death Valley began producing borax that was shipped via Smith's newly completed Tonopah and Tidewater Railroad (Travis and Cocks, 1984).

Kramer

In 1913 Dr. John Suckow struck colemanite at the depth of 370 feet while drilling for water on his homestead claim near Kramer. A short time later Pacific Coast Borax Company purchased his homestead claim and refiled mining claims (see more below) (Dibblee, 1967, p. 124-125).

Borates of Hector Basin

Another significant borate find in the central Mojave Desert is the Fort Cady deposit located 2 miles west of Pisgah Crater. It is not known if this deposit is hosted by the Barstow or Hector Formation. In 1964 colemanite was discovered in an exploratory hole drilled by Congdon and Carey Minerals Exploration Company (Madsen, 1970). Colemanite occurs in thinly laminated silt clay and gypsum beds which range in thickness from 70 to 225

feet. Subsequent drilling has outlined a borate deposit that is from 1,000 and 2,000 ft below the surface. The deposit, which is greater than 5% B₂O₃ trends N 40-50 W and is approximately 2,000 feet wide and 8,200 feet long. The deposit is owned by American Pacific Minerals. Presently they are constructing a processing plant and drilling production wells. They will be extracting borates by in-situ solution mining. The Fort Cady project has proven reserves of 27 Mt, grading 6.70% B₂O₃, 11.91% H₃BO₃, and 379 ppm Li as of December 2018. The probable reserves are estimated at 13.80 Mt grading 6.40% B₂O₃, 11.36% H₃BO₃, and 343 ppm Li (Fourie, 2018).

The Hector clay mine, located about 16 miles east of Newberry Springs, lies a short distance west of the Fort Cady deposit. The clay deposit at Hector has been mined continuously since 1931. Presently hectorite is mined from an open pit. The deposit is underlain by an andesite lava flow. Hectorite, a magnesium, lithium smectite, is associated with a north-trending travertine ridge. It has been proposed that hectorite resulted from the alteration of lakebed tuffs by lithium and fluorine bearing hydrothermal activity, reacting with magnesium-rich lake waters within a shallow lagoon. The travertine ridge is evidence of a buildup of calcium carbonate from nearby hot springs. Within these sediments are numerous thin tuff beds not greater than two feet in thickness, many of which have been altered to zeolite. Hectorite is utilized in numerous products, such as paints, paper, and cosmetics

(Monroe, 2002). The mine is presently operated by Elementis.

Geology of central Mojave Desert borate and lithium occurrences

The lower Barstow Formation contains a series of marker beds including one named the Strontium-Borate horizon. Borate and strontium minerals contained in this bed have been mined from sediments in the Mud Hills, Lead Mountain, Calico Mountains, Daggett Ridge, the Fort Cady deposit, and at the southwestern edge of the Cady Mountains northwest of Ludlow; they also occur at Agate Hill (north of Harvard Hill) and in hills west of the Fort Irwin cantonment. Minerals are found as nodules or geodes in limestone layers, and economic quantities were mined from lenticular pods up to 9 feet thick consisting of colemanite. Colemanite, howlite, celestine, calcite, and quartz occur in cavities within petroleum bearing, siliceous lacustrine limestone. Borate minerals appear to be restricted to lacustrine limestone and lacustrine siltstone. Original borate minerals in the lacustrine deposits were probably sodium and sodium/calcium borates (borax and ulexite). These soluble borates have been altered by ground water to the more stable calcium borate (colemanite) and calcium borosilicate (howlite), the calcium ion being obtained during ground water leaching of the lacustrine limestone.

The Strontium-Borate horizon contains sulfate and carbonates of strontium in addition to borate minerals. Celestine (strontium sulfate) is often associated with the borate minerals, but is not confined to borate localities, and appears to have a much wider distribution. Boron is believed to have been sourced from thermal waters that flowed from hot springs in the region during times of active volcanism. (Miller and others, 2010, p. 148-161).

0.0 (0.0) **RESET YOUR ODOMETER.**

1.4 (1.4) **Retrace** your route down Mule Canyon Road to Calico Road, **TURN RIGHT.**

3.3 (1.9) Pass the entrance to Calico Ghost Town. **Continue straight** on the paved road. The road changes its name from Calico Road to Ghost Town Road here.

4.1 (0.8) **Turn onto dirt road** toward the Apollo Silver Company's Waterloo Project Road. **High clearance vehicles only!!** Others, please **park** along Ghost Town Road. At the entrance

to this dirt road will be several signs warning the public not to trespass on the property and warning about the dangers of open or unsecured workings and unknown hazards. Please do not enter the private lands without prior authorization from a representative of the company. For the 2023 Desert Symposium field trip visit to Waterloo Project, access will be granted by a company representative who will be participating in the Symposium. Always stay with a company representative. Stay on roads, and do not disturb shrubs, soils, or rocks.

4.4 (0.3) Proceed to assembly area where three roads meet.

STOP 2-2: Apollo Silver Company's Waterloo Project

UTM 11S 510912 3866741; 34.943115, -116.880496

Calico Mountains silver

In 1875 George G. Lee discovered what he thought was cinnabar 4 miles north of the present location of Barstow. Lee died near Old Woman Springs in the fall of 1879 (San Bernardino Index 8 Sept 1881, p. 1). A few months later, in June 1880, Robert W. Waterman and John L. Porter examined Lee's prospect, took samples, and found they had discovered a rich silver deposit. Within a year they had erected a 10-stamp mill. News spread quickly and soon prospectors had staked hundreds of claims. On April 6th the Silver King was staked by San Bernardino residents, Frank Mecham, George Yager, Mecham's uncle; and Tom Warden and Huse Thomas, sheriff's deputies. They were grubstaked by San Bernardino County Sheriff John C. King (an uncle to Walter Knott) and Ellis Miller. The Silver King was one of the first and most productive mines in the district (Figures 24, 25). Between 1883 and 1886 the mine yielded 37,000 tons of ore with a gross value of \$1,355,000 or \$36.61 per ton.



Figure 24. Calico townsite. C. late 1880s. O.A. Russell collection.

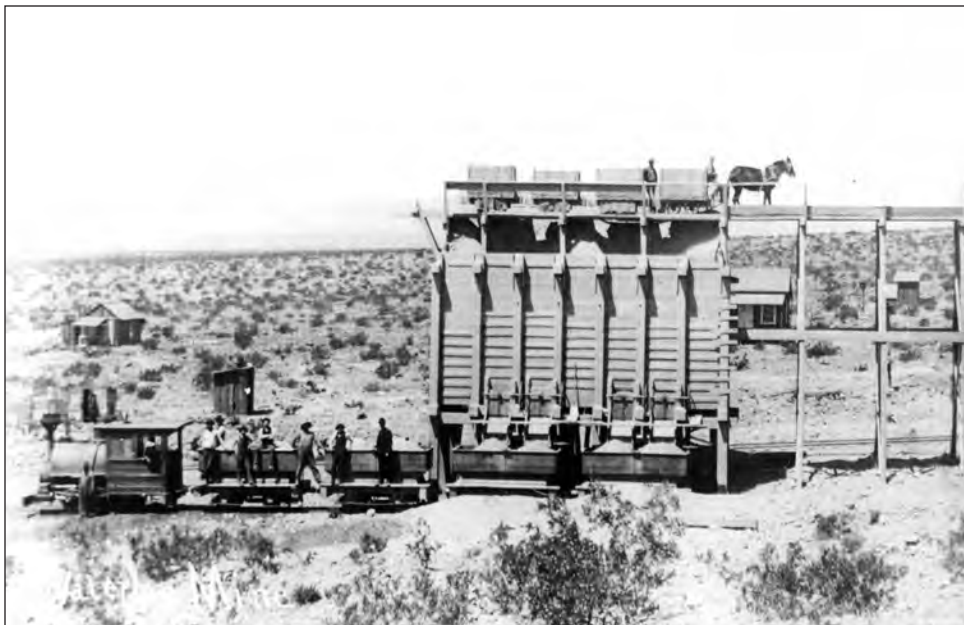


Figure 25. Loading ore cars at the Waterloo Mine. Taken after 1888. O.A. Russell Collection

All the mines had closed by 1896 due to the fall in the price of silver. According to Steeples (this volume) an estimated \$15,356,339 was produced during the period of 1882 to 1900. A total of approximately 18,700,000 ounces were produced. The average value of Calico ore has been estimated at 10 to 20 ounces per ton.

The Calico District lies near the eastern edge of a rectangular shaped area of silver-barite mineralization which is roughly 18 miles long in an east-west direction and 9 miles wide. The mines have been aggregated into three types based on location and differences in character: Calico, East Calico, and West Calico. There are more than 50 past producers in the district. The Waterloo mine is in the West Calico area. It is also the site of brecciated, disseminated silver bearing deposits of moderately to intensely silicified and baritized siltstone, sandstone, and conglomeratic sandstone of the Barstow Formation (Weber, 1976, p. 85). ASARCO acquired the property in 1964 and drilled the Waterloo mine, revealing disseminated silver mineralization. In 1982 they announced that they had outlined resources of about 30 million tons which averaged 3 ounces of silver a ton and from 7 to 15 percent barite (Harthrong, 1982). From 1980 until the mid-1980s Dusty Mac (perhaps under a lease) began

a drilling program. In 1984 they announced, “Reserves in all categories presently stand at 35 million tons, which includes three million tons grading 3.0 ounces of silver per ton,” (“Drilling gets underway on Dusty Mac site,” North American Gold Mining Industry News, Dec. 7, 1984 p. 22).

Apollo Silver Corporation

Fitzgerald, C.E.¹, and Gallagher, C.S.²

¹Apollo Silver Corporation, Vancouver, B.C., Canada. Email: cathy@apollosilver.com and ²Rogue

Geoscience Inc., Kimberley, B.C., Canada

To the north of the field trip stop there is a broad view of the Waterloo silver-gold deposit with the historic Burcham mine visible to the northeast (Figure 26). The highest topographic point on the property directly north (showing rings of roads built by previous operators for drilling activities) is underlain by dip slope brecciated silicified sediments (fine to medium grained sandstones and siltstones). These rocks host stratiform replacement style and stockwork (fine veins) silver mineralization and

The Calico District lies near the eastern edge of a rectangular shaped area of silver-barite mineralization which is roughly 18 miles long in an east-west direction and 9 miles wide. The mines have been aggregated into three types based on location and differences in character: Calico, East Calico, and West Calico. There are more than 50 past producers in the district. The Waterloo mine is in the West Calico area. It is also the site of brecciated, disseminated silver bearing deposits of moderately to intensely silicified and baritized siltstone, sandstone, and conglomeratic sandstone of the Barstow Formation (Weber, 1976, p. 85). ASARCO acquired the property in 1964 and drilled the Waterloo mine, revealing disseminated silver mineralization. In 1982 they announced that they had outlined resources of about 30 million tons which averaged 3 ounces of silver a ton and from 7 to 15 percent barite (Harthrong, 1982). From 1980 until the mid-1980s Dusty Mac (perhaps under a lease) began

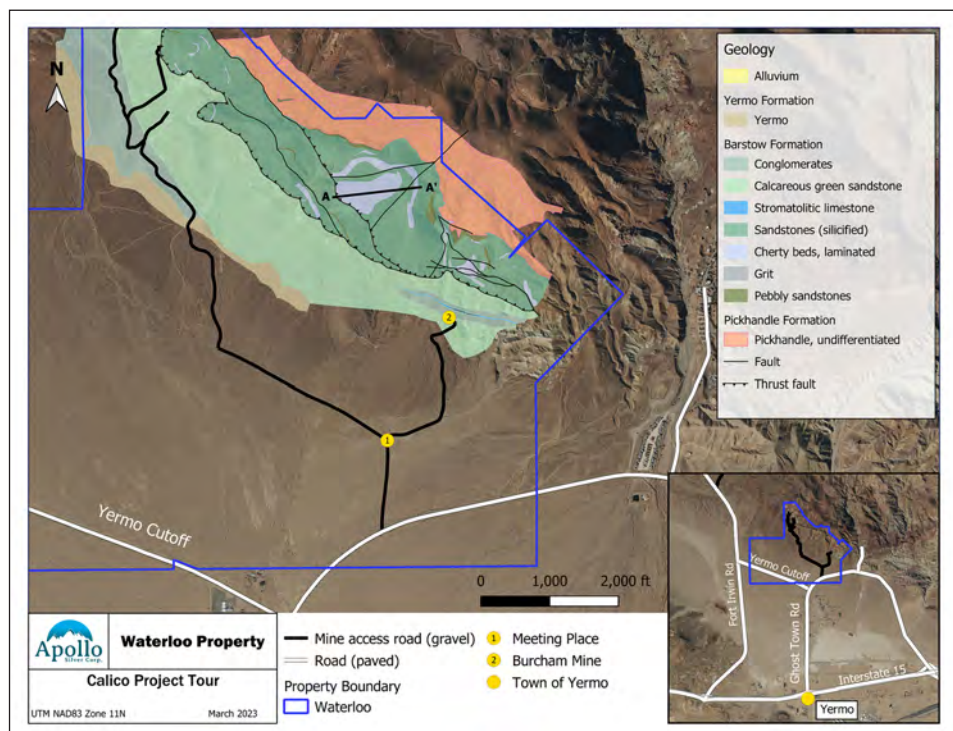


Figure 26. Waterloo property stop location and 2022 geological mapping.

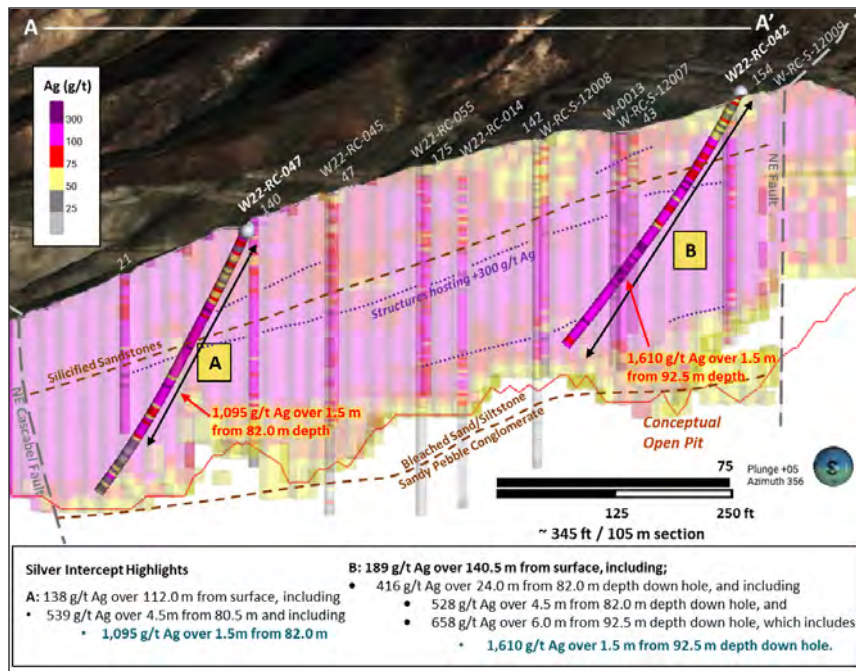


Figure 27. Cross section of silver mineralization (resource block model) and selected drill holes.

show some of the highest disseminated silver grades on the property (average 100 to +400 g/t Ag (2.9 – 11.7 opt)). Based on historic drill data collected by previous operators between 1989 and 2013 Apollo reported a mineral resource estimate for the Waterloo silver deposit of 116 million troy ounces of silver (3,608 metric tonnes, or 3,977 short tons of silver) in 38.9 million tonnes (42.8 million short tons) at a 93 gram per metric tonne (2.7 opt) cutoff grade in early 2022 (Figure 27). In 2022, Apollo completed extensive surface technical work across Waterloo including surface mapping (see Figure 1) and sampling (see examples of rock types in Figure 28), magnetic and 3D induced polarization geophysical surveys, geotechnical mapping and drone hyperspectral surveying. Geophysical results assisted with defining structure features and

the hyperspectral work assisted in preliminary characterization of difference in alteration assemblages at surface. Geological mapping built upon and refined interpretations of major lithologies, faults and lithologic contacts from work completed by Fletcher (1986) and identified north trending high-grade structures that host more than 1,000 g/t (29.1 opt) Ag (intersected by drilling). This work collected detailed information on bedding of the Barstow stratigraphy, orientations of faults and contacts and provided a better understanding of the spatial distribution of silver and gold mineralization. The mineral resource work and comprehensive surface program formed a solid foundation of information on which to design a 10,000 meter (32,800 feet) (88 holes)

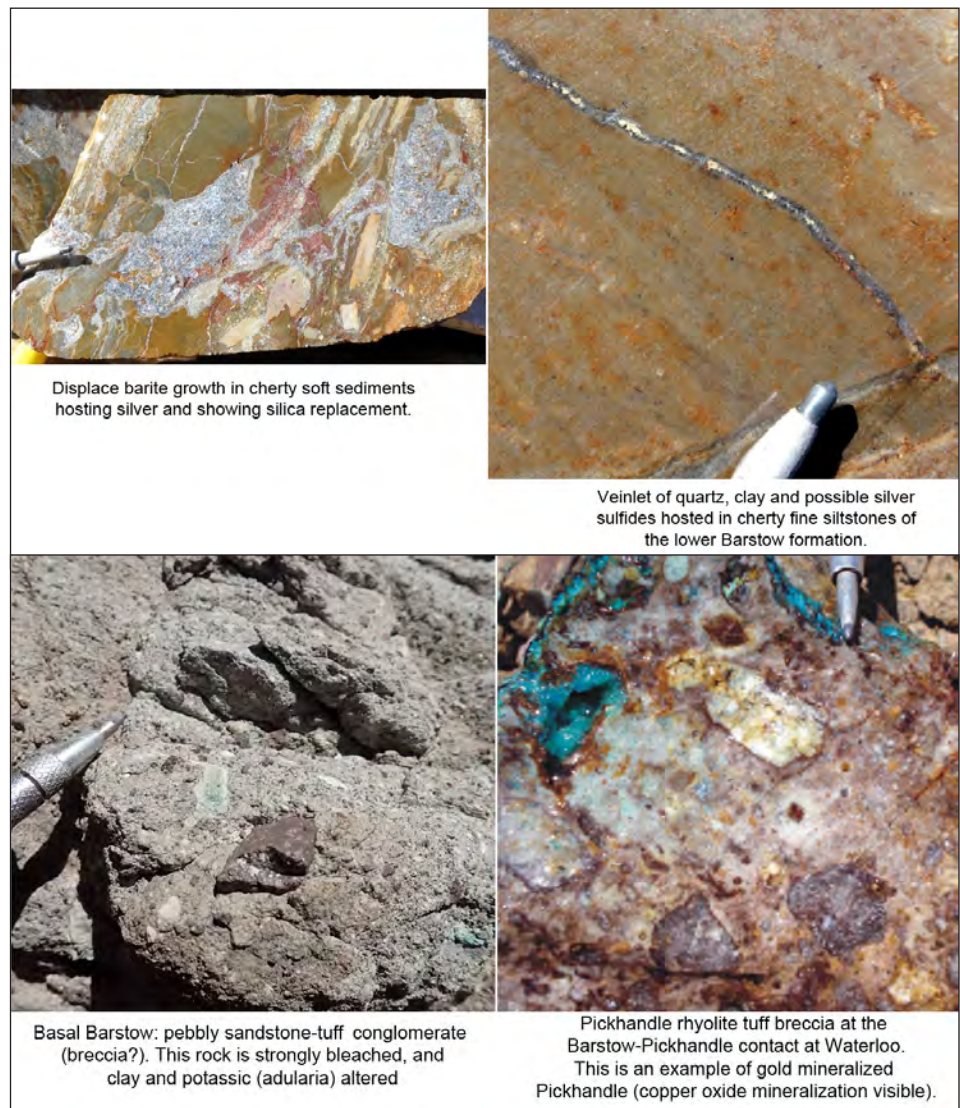


Figure 28. Surface rock samples from Waterloo. A. Mineralization details. B. Outcrop examples.

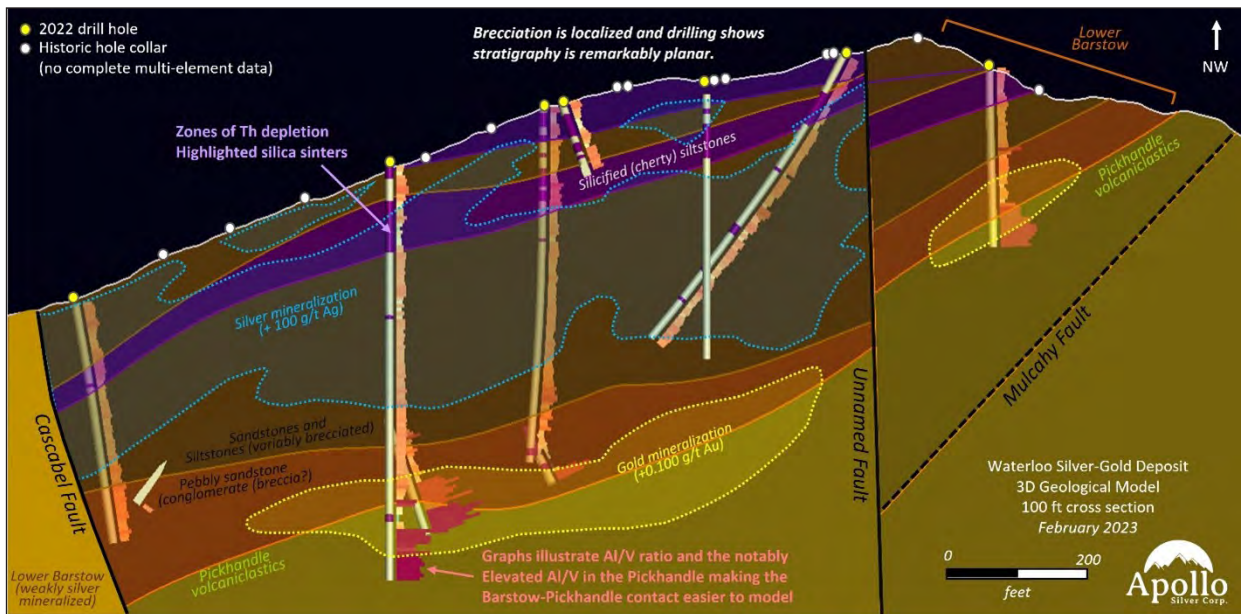


Figure 29. Cross section of the 2023 Waterloo geological model showing refinement of stratigraphy and mineralized horizons using multi-element data.

reverse circulation drill program that was completed between April and November 2022. The goal of this work is to update the size and confidence of the 2022 mineral resource estimate for Waterloo, using multi-element data from the drilling and the robust geological information it and surface work provided. All this information was critical in allowing Apollo to produce a robust three-dimensional geological model for the Waterloo deposit for the first time (Figure 29).

Limited diamond drilling has been completed at Waterloo and due to extremely difficult drilling conditions RC methods were the preferable choice for resource estimation work. However, with traditional chip logging it is difficult to determine stratigraphic relationships, and even fully characterize lithology, mineralization, and alteration. Apollo completed RC chip logging however this information was supplemental to the comprehensive multi-element data that has been collected across the entirety of the deposit via both traditional laboratory and handheld analysis methods.

Apollo completed whole rock major element XRF analysis on three diamond drill holes completed by a previous operator in 2012 and used that to validate and fine-tune ICP multi-element (4-acid digestion) interpretations. A near total digestion for 4-acid ICP analysis allows one to use immobile elements to characterize primary lithologies and quantify alteration. For example, the ratio of Al to V highlighted very well the boundary in the subsurface between Barstow sedimentary rocks and Pickhandle volcaniclastics: V was significantly elevated in Barstow sediments relative to Pickhandle volcaniclastics (see Figure 29). Other element relationships were used to identify silica-rich, immobile element depleted (Al, Ti and Th) sinter caps, gold mineralized horizons (elevated Pb concentrations where no Au data

was available) and pinpoint the Calico fault which forms the contact between the silver mineralized lower Barstow rocks and the calcareous green sandstones (generally unmineralized) of the upper Barstow (distinct elevated Ca, Li). Gaussian mixture modeling was also performed on the multi-element data to look for geochemical and spatial trends. Elements typically associated with hydrothermal activity were selected (Ag, Au, Bi, Cu, Fe, Mn, S, Sb, W, As, Mo, Pb and Zn) for this modeling, with clustering of certain elements highlighting distinct geochemical domains that could be then modeled in three dimensions. Amazingly the element clusters defined three zones within the Barstow that correlate in a broad sense very well with three stratigraphic horizons that had been mapped out in the subsurface by Fletcher (1986) using detailed surface mapping and limited drilling information. The chemical modeling culminated in the refinement of the 3D model for Waterloo, a better understanding on the distribution and controls on silver mineralization and illustrated the extent of gold mineralization here which is far broader (over 1,000 m strike length) than previously known.

We will not visit the Burcham mine today; as already mentioned, it is visible to the northeast from this location. At this mine two northwest trending high-angle structures (veins?) were developed using underground drifts in the 1940s (the amount of gold extracted is unknown). In the late 1980s ASARCO (the project owner at the time) completed 10 short rotary holes, three diamond drill holes and underground and surface sampling and determined that the basal Barstow sediments in this area also host disseminated gold. In 2022, as part of a 10,000 m (32,808 ft) reverse circulation drill program across the property, Apollo completed some drilling and surface sampling in this area to follow

up on this historic work. Recent results show that the disseminated gold averages approximately 0.1-2 g/t (.0029 - .058 opt) Au with high angle structures hosting up to 10 g/t (.29 opt) Au. Major structural intersections host more than 200 g/t (5.8 opt) Au. The gold mineralization in the Burcham area is hosted by bleached and possibly brecciated pebbly sandstone-tuffaceous conglomeratic rock of the lowermost Barstow formation, and by the underlying tuffs and tuff breccias of the Pickhandle formation. The contact in this area appears to be conformable. This gold mineralized package extends northwestwards underneath the topographic high (and underneath the silver mineralized portion of the package). The stratigraphy of the entire lower Barstow package here dips northwestwards in an anticlinorium. At the Burcham area we interpret that the silver mineralized package has been eroded off.

Refer to Fitzgerald and others (this volume) and Steeples (this volume) for more information about silver mining in the Calico Mountains.

4.7 (0.3) **Retrace route to Ghost Town Road. TURN RIGHT, CONTINUE STRAIGHT.**



Figure 31. Waterloo Mine Railroad. O.A. Russell collection.



Figure 30. Waterloo 15 Stamp mill. San Bernardino County Museum collection.

7.4 (2.7) Pass under I-15. The road changes name here to the Daggett-Yermo Road.

9.1 (1.7) **TURN RIGHT** onto a nondescript dirt road across from a sewage treatment plant (?). Note the two stone mill foundations. The 60-stamp mill stood about 700 feet to the north of the 15-stamp mill.

STOP 2-3: The Waterloo millsite

UTM 11S 510041 3859341; 34.876396, -116.890124

The Silver King Mine—the most productive in the Calico District—was discovered April 6, 1881. But to recover the values from this fabulously rich ore you need an expensive mill. At the same time, In May 1881, a mill a relatively short distance to the south sat idle, in need of

ore. The Oro Grande Mill and Mining Company had built a water-powered 10-stamp mill in Oro Grande, some 25 miles from Calico. However, the mill couldn't recover gold and silver from their mine's ore (Vredenburg, 2015). The Oro Grande Company leased the Silver King mine in October 1882 and by March 1883 thirty tons of ore was being hauled to their mill each day.

During this time several small mills had been erected in the vicinity of Calico. The Southern Pacific Railroad was completed westward to Daggett on November 13, 1882. Shortly afterward a new 10-stamp mill arrived to run ore from the



Figure 32. Waterloo mills. 15 stamp mill on left 60 stamp mill on right. Orange County Archives collection.



Figure 33. Waterloo 60 Stamp Mill & Railroad. O.A. Russell Collection



Figure 34. Waterloo 60 stamp Mill. May 12, 1894. Mining and Scientific Press

Oriental Mine. The mill was erected north of Daggett on the southeast side of the Elephant Mountain and was finally up and running on April 26, 1883. In December 1883 it was announced that the Oro Grande Company had purchased the Oriental mill and that they intended to add another 5 stamps. By January 1884 the Oriental mill began milling ore from the Silver King mine, and it appears that the additional 5-stamp battery had been added within a month (Figure 30).

By May 1886 the Silver King mine output had been severely reduced because all the mill capacity was entirely taken up by ore from the Waterloo mine (also owned by the Oro Grande Company). Soon afterward the mill, now known as the Waterloo, was renovated – the old amalgamation pans were replaced. But that still wasn't enough. The superintendent mentioned that they were planning to add another 15 stamps. But instead, they erected a new mill. On March 17, 1887, the San Bernardino Daily Courier ran an article stating the new 60-stamp mill would cost \$250,000 and take 6 months to complete.

The mill was nearly complete when on August 14, 1887, at 6 pm it burned to the ground. Not to be deterred, reconstruction began immediately. The new mill was completed in May 1888 for a reported cost \$175,000, it was located just north of the 15-stamp mill. At the same time a new narrow-gauge mine railroad was laid from the Waterloo mine to the mill (Figure 31). In February 1889 the Oro Grande Company was reorganized as the Waterloo Mining Company. With the fall in the price of silver the Waterloo Company closed its

mines and mills in March 1892; 120 to 150 were out of jobs. (Vredenburg, 2013).

At the 60-stamp mill (Figure 32), each stamp weighed 850 pounds, and dropped 6 1/2 inches 100 times per minute. This and the 15-stamp mill had the capacity of 225 tons per 24-hour day (“Waterloo Mills and Mines,” Mining and Scientific Press, May 12, 1894, p. 289).

In 1908 the Waterloo mill building was dismantled and moved a few miles to the east to the Borax Properties Limited millsite. The machinery was sold to a Los Angeles junk dealer. The engine which had been built by the Union Iron Works of San Francisco was gigantic – about forty feet long and six feet wide. The flywheel was 30 feet in diameter, and “a good-sized child can easily stand up in the cylinder” (“Waterloo silver mill a thing of the past,” Los Angeles Herald, 15 Jun 1908, Mon. Page 12).

The Waterloo mill and Elephant Mountain geology

The Waterloo mill is on the northeast flank of Elephant Mountain and is part of the Calico Mining District (Jessey, 2010). Dibblee and Minch (2008) mapped Elephant Mountain as underlain mostly by andesite intrusive with smaller bodies of andesite breccia, . . . and tan felsite at its north end. The largest dome, Elephant Mountain (0.55 km²), is a composite of several hornblende dacite domes intruding the Pickhandle Formation and was dated (40Ar/39Ar; plagioclase) as 18.29 ± 0.10 Ma. The composite dome is mantled by breccia in the north. Two smaller domes (~0.35 km² each) lie north and

south of the domes of Elephant Mountain. The northern dome contains quartz and biotite as well as hornblende and yielded an age of 18.17 ± 0.12 Ma. A southeastern dome (0.25 km²) near Elephant Mountain was studied by Glazner (1990), who described a plagioclase-biotite-hornblende assemblage. This dome is higher in silica, bordering on rhyolite, than those in the Yermo volcanic field. A small dome is to the southwest and consists of reddish-brown plagioclase-sanidine-quartz-biotite rhyolite with platy structure (Miller and others, 2022, p. 127).

0.0 (0.0) **RESET YOUR ODOMETER.** After viewing the Waterloo mill foundations, **TURN RIGHT** and continue south on Daggett-Yermo Road

1.0 (1.0) Cross the railroad

1.5 (0.5) Make a **RIGHT TURN** onto the I-40 west bound onramp.

1.8 (0.3) Merge onto I-40

9.0 (7.2) Merge onto I-15. **NOTE: YOU WILL EXIT THE FREEWAY** in 3.5 miles. Trucks are slow; this is a steep grade from the Mojave River to Barstow Road.

12.5 (3.5) **TAKE EXIT 179** - State Route 58 West. Use the right two lanes.

30.1 (17.6) Pass U.S. 395.



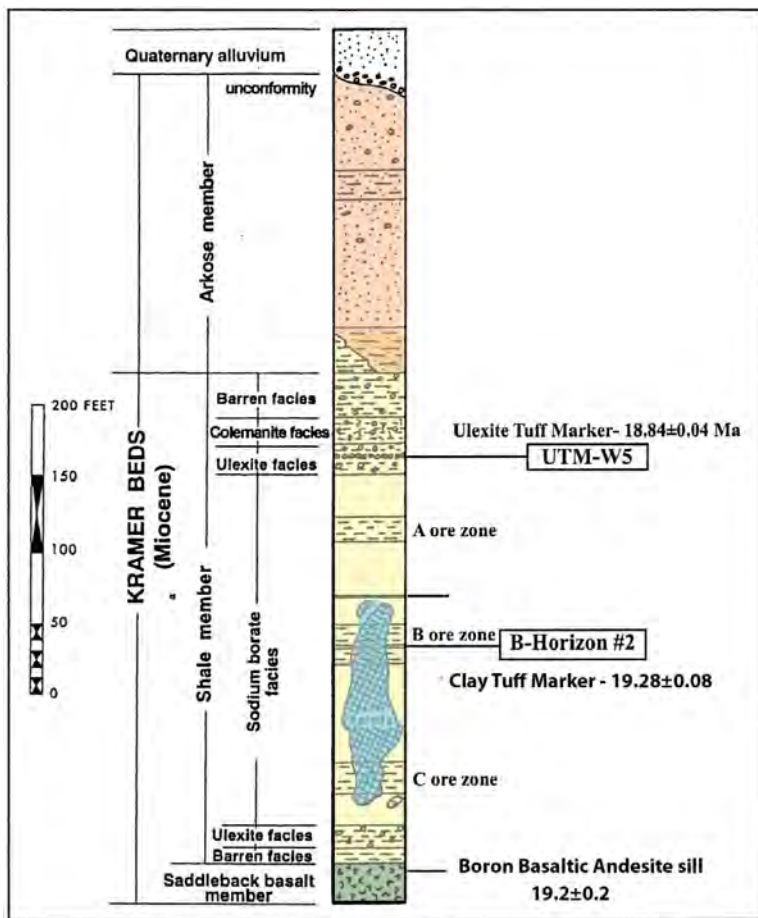


Figure 35. Generalized stratigraphic column for the upper Kramer beds in the Tropic Group. From Gans (2022a), figure 3.

Boron open pit mine shows black basaltic andesite sill rock (19.2 Ma, Gans, 2022b) at the base of the section (Figure 35), overlain by the Shale member, greenish sediments that contain white borate minerals. The overlying Arkose member contains 17 taxa of mid-Hemingfordian age vertebrates that comprise the Boron Local Fauna (Whistler, 1984). Exhibits and videos can be seen inside the museum. Twenty-mule team wagons, a headframe, and mineral stockpiles for young and old collectors are outside (Reynolds, 2002, p. 7). Phillip Gans will give a talk at the pit overlook.

The Kramer borate deposit

In 1913 Dr. John Suckow filed a homestead claim on land near Kramer in eastern Kern County and contracted with Les Griffin to drill a water well. Instead of water the crew struck colemanite at the depth of 370 feet. John Ryan, General Manager of the Pacific Coast Borax company, heard of the discovery and soon the company purchased Dr. Suckow's claim and refiled the mining claims. Exploratory drilling during the mid-1920s revealed this deposit primarily consisted of colemanite but later drilling found the deposit was mostly sodium borates (Dibblee, 1967, p. 124-125).

Sodium borates are much easier to process. An exploratory shaft was sunk in August 1926. Excavation for the open pit began in January 1956 (Ver Planck, 1962, p. 39-41). Figures 36 and 37 show the evolution of the pit over 30 years.

The ore from the Kramer deposit was easier to mine, mill, and ship than other mines. As a mineral compound,

- 34.5 (4.4) Pass Boron Ave.
- 37.3 (2.8) TAKE EXIT 196: Borax Road.
- 37.6 (0.3) TURN RIGHT (north) on Borax Road.
- 39 (1.4) The road name changes to Suckow Road. The road is name after Dr. John Suckow, the original claimant of this land, and discoverer of this enormous borate deposit.
- 39.5 (0.5) Cross railroad tracks, stay to right to continue on Suckow Road up the hill on your right.
- 40.4 (0.9) ARRIVE at the visitors' center.

STOP 2-4: U.S. Borax, Baker Pit

UTM 11S 437313 3876548;
35.02966, -117.687209

PARK at the Visitors' Center. The view north into the



Figure 36. The Boron pit c. 1962, from a postcard.



Figure 37. Boron pit. January 1992, Larry Vredenburg photo.

borax hardness is lower and its solubility is higher than that of colemanite. These factors make borax a superior raw material in the mining, crushing, and dissolving processes. Milling costs were far less for processing borax ore from Kramer than with the colemanite ore from the Death Valley region. In the milling process at Kramer, treating the raw borax to make refined borax required less energy than converting colemanite, a calcium borate mineral, into refined borax, a sodium borate product (Mulqueen, 2002, p. 23)

Geology

The geology of Kramer deposit has been investigated in detail by several authors (Gale, 1946; Barnard and Kistler, 1965; Dibblee, 1967; Siefke, 1991; Gans, 2022b).

The borate deposit at Kramer deposit formed in a sedimentary basin hosted by the Tropic Group, a sequence of Miocene volcanoclastic, lacustrine and alluvial/fluvial sedimentary rocks. The Kramer deposit consistently lies stratigraphically above a basaltic andesite sill in the middle member of the Tropic Group and is enclosed within lacustrine shales.

The Kramer borate deposit is distinct from the deposits in the vicinity of the Calico Mountains. It consists primarily of sodium borates, whereas the borate deposits hosted by the Barstow Formation are almost entirely calcium borates. Recently Gans (2022b) published the results of a detailed study

of the age and composition of basalts in the vicinity of the deposit that had all previously been lumped together as Saddleback Basalt. He distinguished three different mafic volcanic units: the Saddleback Basalt (20.5 ± 0.3 Ma), the Stonehouse Andesite (19.4 to $19.7 (\pm 0.2)$) and the Boron Basaltic Andesite ($\sim 19.2 \pm 0.2$ Ma). He concluded that: "Observations from the mine and drill holes east of the mine suggest that much of the fine-grained lacustrine sedimentation in the Boron basin is bracketed between ~ 19.5 Ma and 18.8 Ma. The

precipitation of borate ores at $\sim 19.28 \pm 0.08$ is closely associated in time and space with the emplacement of the underlying 19.2 ± 0.2 Ma Boron basaltic andesite sill in the mine area, suggesting that this magmatic event may have played an important role in borate mineralization."

43.2 (2.8) **RETRACE** back to SR58. **WATCH OUT!** The westbound onramp is on the left, north of SR 58, and immediately south of the westbound offramp.

43.4 (0.2) Merge onto SR 58 west

45.4 (2.0) Pass Gephart Road, formerly Rich Road. This road continues south to Leuhman Ridge which is within Edwards Air Force Base. The Air Force and Jet Propulsion Labs test rocket engines here.

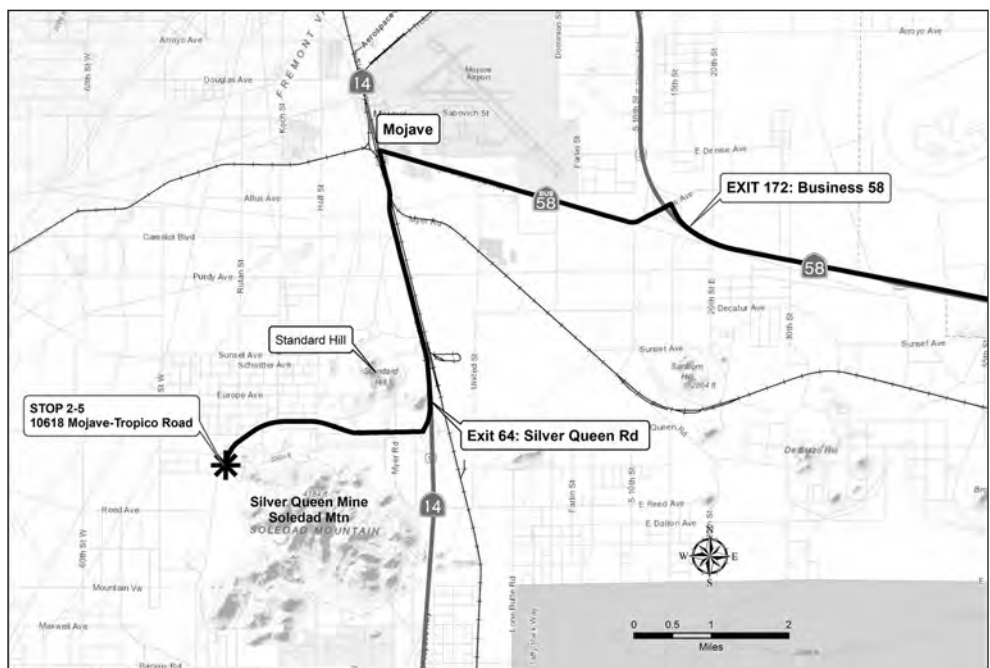




Figure 38. Elephant Eagle mine (now part of the open pit) shown by red arrow. Soledad Mountain on the left, Tehachapi Mountains in the distance to the northwest. Photo by Burton Frasher, 1935.

55.5 (10.1) Pass California City Blvd. Use caution. This portion of SR 58 is no longer freeway. Many cars enter SR 58 from your right.

66.1 (10.6) EXIT FREEWAY. **TAKE EXIT 172** toward Mojave / SR 58 Business West (Mojave-Barstow Highway).

66.5 (0.4) **TURN LEFT** onto SR 58 Business West.

Mojave

The town of Mojave began in 1876 as a construction camp on the Southern Pacific Railroad. From 1884 to 1889, the town was the western terminus of the 165-mile (266 km), twenty-mule team at Harmony Borax Works in Death Valley. It later served as headquarters for construction of the Los Angeles Aqueduct (Duram, 1998).

70.4 (3.9) **TURN LEFT** (south) at T-Intersection with SR 14 – continue south on SR 14.

As you approach the Silver Queen Road offramp, Standard Hill is on your right (west). The hill is dominated by Gem Hill Formation felsite. This was the site of several old mines and was the first heap-leach operation in the Mojave Mining District. The felsite forms dikes in Jurassic or Cretaceous quartz monzonite on the southwest side of Standard Hill.

73.8 (3.4) EXIT FREEWAY. **Take exit # 64** for Silver Queen Road.

74.1 (0.3) **TURN RIGHT** on Silver Queen Road.

75.3 (1.2) Pass the Soledad Mining Company offices. Continue on Silver Queen Road.

76.7 (1.4) At this point the road name changes to Mojave-Tropico Road.

76.9 (0.2) **TURN LEFT** into the Golden Queen parking lot. Immediately on the left you will see a mine facility and parking lot. The address for the parking lot is

10618 Mojave-Tropico Road. There is a Golden Queen sign immediately before the dirt parking lot. Left turn into the parking lot. If you see a sign for MRC, you have gone too far.

STOP 2-5: The Golden Queen mine

UTM 11S 389890 3872453;
34.988684, -118.206463

Mining history

Gold was first discovered at Standard Hill in 1894, and soon gold was also discovered at nearby Soledad Mountain, Tropico Hill, and Middle Buttes. Numerous mines were developed quickly, and several stamp mills erected. Most of the high-grade ore was exhausted by 1910, but there was still plenty of



Figure 39. Gibson crusher, used at the Elephant Eagle mine (now part of the open pit) in the 1930s. Richard Graeme, geologist with Golden Queen Mining Company, worked to donate this rare Gibson Gyratory Crusher to the Mojave Desert Heritage and Cultural Association (MDHCA) at Goffs, California in 1999. It was restored and now operates. Photo by Bill Fullerton, MDHCA



Figure 40. Golden Queen Mine c. 1940.

gold to be had. During the 1930s the district experienced a significant revival; old mines were subleased, miners were grubstaked, and their ore was custom milled at the Tropico mill. Figure 38 shows one of the early mines, the Elephant Eagle mine; that mine employed the Gibson crusher (Fig. 39).

On September 17, 1933, George Holmes, who was leasing claims on Elephant Hill, discovered promising float on Soledad Mountain that assayed phenomenal gold and silver values. George and his father Marvin named their claim the Silver Queen. Over the next year the Holmes and a crew of 50 men developed the discovery, and on January 10, 1935, they sold the property to Gold

Fields American Development Company for \$3,170,000, (about \$68,200,000 today) plus a retained royalty interest.

The new owners renamed the mine the Golden Queen (Figure 40), conducted extensive exploration and erected a 300-ton per day capacity mill. Their operation was shut down in 1942 by War Production Board's Order L-208, closing gold mines. It is estimated that the mine produced about \$9,000,000 in gold.

In the 1980s Golden Queen Mining Company began exploring the potential of reactivating the mine. The proposal was approved by Kern County and the Bureau of Land Management in 1997. A modified Environmental Impact Report was approved in 2010. At that time, it was estimated the mine would be active for 12 years, that 51.2 million tons would be heap leached, and up

to 225 million tons of overburden mined. It was projected that gold and silver production would be 1,067,000 oz of gold and 12,039,000 oz of silver over a period of 15 years. Mining began in 2015 and the first pour of gold occurred in March 2016. Currently 75,000 tons of material is moved every 24 hours. The average grade is 0.023 ounces of gold per ton. The mine is projected to continue until 2029. Presently there are 235 full-time employees (Barkha Singh, personal communication). Photographs of the current mine configuration are in Figure 41.



Figure 41. Photos in 2023 of the Golden Queen Mine. Top: Golden Queen Mine 2023 Feb 9. Lower left, Feb 9, 2023. View to west L. Vredenburg. Lower right: 2020-05-24 G. Wilkerson photo.

Geology

Soledad Mountain is an eroded silicic volcanic dome complex which was the site of many eruptions of early Miocene age (16.9 to 21.5 million years). McCusker (1982) mapped seven coalescing volcanic domes as well as lava flows, dikes, and pyroclastic deposits that were erupted during at least three episodes. McCusker (1982) mapped from oldest to youngest, the following main units: (1) quartz latite, middle pyroclastic unit, and aphanitic rhyolite, all dated at about 21.5 Ma; (2) a minor sequence of lacustrine sediments and andesite flows; and (3) an upper unit of pyroclastic material and porphyritic rhyolite, dated at about 17 Ma. Initial widespread sheet flows and pyroclastic deposits of quartz latite were followed by restricted centers of rhyolitic flows and rhyolite porphyry intrusives.

Within the Tropic Group, Dibblee (1963, 1967) mapped a volcanic unit, the Gem Hill Formation, which includes a subunit at Soledad Mountain called the Bobtail quartz latite member. He placed the pyroclastic phases at Soledad Mountain in the Gem Hill and the hypabyssal and lava phases in the Bobtail member. McCusker (1982) interpreted his aphanitic rhyolite unit and porphyritic rhyolite units to be the same as the porphyritic felsite of Dibblee's (1963) Bobtail quartz latite member.

The Soledad Mountain deposit consists of precious metal epithermal quartz veins superimposed on this the Miocene silicic volcanic complex which consists of a volcanic sequence of rhyolite porphyries, quartz latites, and bedded pyroclastic rocks of the Gem Hill Formation. All volcanic units of the Soledad Mountain complex have been affected by hydrothermal alteration, which is most extensive adjacent to veins. The most productive of the veins appear temporally and spatially related to the porphyritic rhyolite unit on the north side of Soledad Mountain.

At the Golden Queen Mine, gold is present as electrum and native gold; and silver as acanthite, pyrrargyrite, polybasite, and native silver. Gangue and alteration minerals include quartz, pyrite, alunite, sanidine, goethite, jarosite, hematite, pseudomorphic calcite, epidote, chlorite, illite, smectite, kaolinite, muscovite, biotite, and rutile (Barkha Singh, personal communication, 2023).

Several silicic eruptive centers of Tertiary age in the western Mojave Desert have been the site of epithermal precious-metal mineralization. Besides Soledad Mountain, other deposits of a similar epithermal nature within these volcanic centers include Standard Hill, Middle Buttes, and Tropic Hill (USGS MRDS id=10310681).

END OF TRIP. Return to SR 14, which leads south to Los Angeles or north to Mojave and points beyond.

References cited

Adams, P.M., 2020, The Copper World and Mohawk Mines: *The Mineralogical Record*, 51 (2), pp. 309-352.

- Adams, P.M., and Housley, R.M., 2019, Additional notes on the mineralogy of the Blue Bell mine, San Bernardino County, California, in D.M. Miller (ed.), *Exploring ends of eras in the eastern Mojave Desert: Desert Symposium Inc.*, p. 49-52. <https://www.desertsymposium.org/>
- Barnard, R.M. and Kistler, R.B., 1965, Stratigraphic and structural evolution of the Kramer sodium borate ore body. In *Boron, California: Paper presented at Second Symposium on Salt*, Northern Ohio Geol. Soc., Cleveland.
- Bishop, K.M., 2013, Rock avalanche setting of the Cave Mountain (Baxter Mine) iron deposits, Afton Canyon, California, in R.E. Reynolds (ed.), *Raising Questions in the Central Mojave Desert: California, State University Desert Studies Center, Desert Symposium.*, p. 107-113. <https://www.desertsymposium.org/>
- Brown, H.J. and Monroe, L., 2000, Geology and Mineral Deposits in the Baxter-Basin Area South of Cave Mountain, San Bernardino County, California, in R.E. Reynolds (ed.), *Empty Basins, Vanished Lakes: San Bernardino County Museum Association, Quarterly*, 47 (2), p. 42-46.
- Burton, V., 1987, Bright Future Projected for Vanderbilt's Morning Star Mine: *California Mining Journal*, 56 (7), p. 4-6.
- Cloudman, H.E., Huguenin, E., and Merrill, F.J.H., 1919, San Bernardino County: California Mining Bureau Report 15.
- Collier, J.T. and Danehy, E.A., 1958, Geology and mineral resources of Township 11 North Ranges 5 and 6 East, San Bernardino Meridian, San Bernardino, California: Southern Pacific Company, unpublished report and map.
- Dibblee, T.W., Jr., 1963, Geology of the Willow Springs and Rosamond quadrangles, California: U.S. Geological Survey Bull. 1089-C, p. 141- 253, scale 1:62,500..
- Dibblee, T.W., Jr., 1967, Areal geology of the Western Mojave Desert, California: US Geological Survey Professional Paper 522, 153 pp.
- Dibblee, T.W., and Minch, J.A., 2008, Geologic map of the Rodman Mountains & Lavic 15 minute quadrangles, San Bernardino County, California: Dibblee Geological Foundation, Dibblee Foundation Map DF-378, scale 1:62,500.
- Durham, D.L., 1998, *California's Geographic Names: A Gazetteer of Historic and Modern Names of the State*. Clovis, Calif.: Word Dancer Press. p. 1074.
- Ely, M.F., II, 1990, Inside Story, The Morning Star Mine, *Sentinels in the West, Headframe*, 1 (1) p. 3 – 9 <https://archive.org/details/headframe-sep-oct-1990-vol-1-no-1>.
- Fife, D.L., and Brown, A.R., 1980, Geology and Mineral Wealth of the California Desert – Dibblee Volume, (South Coast Geological Society: Santa Ana), 555 pp.
- Fitzgerald, C.E., Gallagher, C.S., and Pratt, W.T., Illuminating the Waterloo silver deposit in three dimensions using multi-element data: this volume.
- Fletcher, I.D., 1986. Geology and Genesis of the Waterloo and Langtry Silver-Barite Deposits, California: M.Sc. Thesis Stanford University, Ph.D., 158 p.
- Fourie, L., 2018, Resource Estimation for the Fort Cady Project San Bernardino County California, Prepared for American Pacific Borate and Lithium Limited, Terra

- Modelling Services Inc. https://downloads.regulations.gov/EPA-R09-OW-2020-0318-0015/attachment_6.pdf.
- Fulton, R., 2005, Evaporative salt production on Soda Dry Lake, *in* R. E. Reynolds (ed.), *Old Ores, Mining History in the Eastern Mojave Desert*: California State University Desert Studies Consortium and LSA Associates, Inc., pp. 55-60.
- Gale, H.S., 1946, *Geology of the Kramer Borate District, Kern County, California*: Calif Div. of Mines, California Journal of Mines and Geology, Vol. 42, No. 4, p. 325-378.
- Gans, P.B., 2022a, Monogenetic and polygenetic basaltic cinder cones and lava fields in the Cima Volcanic Field, Eastern Mojave Desert, *in* D.M. Miller (ed.), *Volcanoes in the Mojave: The Desert Symposium Inc.*, p. 51-73.
- Gans, P.B., 2022b, Age(s) and characteristics of Saddleback Basalt: Implications for the Miocene stratigraphy and origin of the Boron deposit, Mojave Desert, California, *in* D.M. Miller, (ed.), *Volcanoes in the Mojave: The Desert Symposium Inc.*, p. 160-171
- Geomorphc Regions of California
<https://www.csun.edu/science/sierras/geomorphc-regions/index.html>
- Greenwood, R. B., 1985, Mineral land classification of the Mid Hills 15' quadrangle, San Bernardino County, California: California Department of Conservation, Division of Mines and Geology Open-File Report 85-8 LA, 110 pp.
- Harthrong, D.S., 1982, Renewed Mining Activity in the Calico Mountains, A Report of the ASARCO-Waterloo Project: California Geology, V.36, No. 10, pp. 216 – 225.
- Henderson, G.V., 1980, Geology of the Pink Lady Bentonite Mine, Zzyzx, California, *in* D.L. Fife and A.R. Brown (eds.), *Geology and Mineral Wealth of the California Desert – Dibblee Volume*: South Coast Geological Society, Santa Ana, p. 278.
- Hensher, A., 2005, The historical mining towns of the eastern Mojave Desert *in* R. E. Reynolds, and T. Weasma (eds.), *Old Ores: mines and mineral marketing in the east Mojave Desert—a field trip guide*: California State University Desert Studies Consortium and LSA Associates, Inc., p. 28-40.
- Hensher, A. and Vredenburg, L.M., 1986, Ghost Towns of the Upper Mojave Desert, Vol. 1 San Bernardino County. Unpublished typescript., 127 pp. <https://archive.org/details/UpperMojaveDesertHensher1986>
- Hewett, D. F., 1956, *Geology and mineral resources of the Ivanpah Quadrangle California and Nevada*: U.S. Geological Survey Professional Paper 275, 170 pp.
- Ito, T., and Morgan, G. J., 1980, The Telegraph gold mine, Halloran Spring quadrangle, San Bernardino County, California, *in* D.L. Fife and A.R. Brown (eds.), *Geology and mineral wealth of the California Desert*: South Coast Geological Society, p. 336-338.
- Jefferson, G.T., Reheis, M.C., Miller, D.M., 2020, A compilation of Lake Manix basin geological and paleontological data and references, *in* D.M. Miller, (ed.), *Changing Facies, The 2020 Desert Symposium Field Guide and Proceedings*: Desert Symposium Inc., p. 34 – 50.
- Jessey, D.R., 1988, A geologic evaluation of the Mohawk mine, San Bernardino County, California: California Polytechnic University, 18 pp.
- Jessey, D.R., 2010, Geology and ore genesis of epithermal silver–barite mineralization in the central Mojave Desert, California, *in* R.E. Reynolds and D.M. Miller, (eds), *Overboard in the Mojave: 20 million years of lakes and wetlands: Desert Symposium Proceedings*, Desert Studies Consortium, p. 213-223.
- Jessey, D. R., and Fallis, C. N., 1989, The Mohawk mine; a base metal-silver deposit related to possible Late Cretaceous normal-slip movement within the Clark Mountain thrust complex, San Bernardino County, California, *in* The California desert mineral symposium, compendium: U.S. Bureau of Land Management, Sacramento, CA, pp. 163-176.
- Lamey, C.A., 1948, Cave Canyon iron-ore deposits, San Bernardino, California: California Division of Mines Bulletin, 129, p.69-83.
- Leslie, S.R., Miller, D.M., Wooden, J.L., and Vazquez, J.A., 2010, Stratigraphy, age, and depositional setting of the Miocene Barstow Formation at Harvard Hill, central Mojave Desert, California, *in* Reynolds, R.E., and Miller, D.M., ed., *Overboard in the Mojave: Desert Studies Consortium, California State University, Fullerton*, p. 85-104.
- Logan, C. A., 1947, Limestone in California: California Jour: Mines and Geology, Vol. 43, pp. 175-357.
- Longwell, C.R., Pampeyan, E.H., Bowyer, B and Roberts, R.J., 1965, Geology and mineral deposits of Clark County, Nevada: Nevada Bureau of Mines and Geology, Bulletin 62, 218 pp.
- Madsen, B., 1970, Core logs of three test holes in Cenozoic lake deposits near Hector, California: U.S. Geological Survey Bulletin 1296, 43 p.
- Maynard, M.F., and others, 1984, The Blue Bell Claims, San Bernardino County, California: San Bernardino County Museum, Department of Earth Sciences, 61 p.
- McCusker, R.T., 1982, Geology of the Soledad Mountain volcanic complex, Mojave Desert, California: San Jose State University, M.S. thesis, 113 p.
- Menchaca, Leonardo, 2023, The Vanderbilt mine, San Bernardino County, California (this volume)
- Miller, D.A., Frisken, J.G., Jachens, R.C., Gese, D.D., 1986, Mineral Resources of the Castle Peaks Wilderness Study area, San Bernardino County, California: U.S. Geological Survey Bulletin 1713-A, 19 pp.
- Miller, D.A., and Wooden, J.L., 1993, Geologic map of the New York Mountains area, California and Nevada: U.S. Geological Survey Open-File Report 93-198, 10 pp.
- Miller, D.M., Leslie, S.R., Hillhouse, J.W., Wooden, J.L., Vazquez, J.A., and Reynolds, R.E., 2010, Reconnaissance geochronology of tuffs in the Miocene Barstow Formation: implications for basin evolution and tectonics in the central Mojave Desert, *in* Reynolds, R.E., and Miller, D.M., ed., *Overboard in the Mojave: Desert Studies Consortium, California State University, Fullerton*, p. 70-84.
- Miller, D.M., Reheis, M.C., Wan, E., Wahl, D.B., Olson, H., 2011, Pliocene and early Pleistocene paleogeography of the Coyote

- Lake and Alvord Mountain area, Mojave Desert, California, *in* Reynolds, R.E., ed., *The incredible shrinking Pliocene: Desert Studies Consortium, California State University, Fullerton*, p. 53-67.
- Miller, D.M., Reynolds, R.E., Phelps, G.A., Honke, J., Cyr, A.J., Buesch, D.C., Schmidt, K.M., Losson, G., 2017, Active tectonics of the northern Mojave Desert: the 2017 Desert Symposium field trip road log, *in* Reynolds, R.E., ed., *Revisiting the Eastern California Shear Zone: California State University, Fullerton, Desert Studies Consortium*, p. 7-44.
- Miller, D.M., (ed.), 2022, *Volcanoes in the Mojave, 2022 Desert Symposium Field Guide and Proceedings*, 252 pp. <https://www.desertsymposium.org/>
- Mills, S.J., and others, 2014, Mojaveite and bluebellite, two new minerals from the central Mojave Desert, *in* Reynolds, R.E., (ed.), *Not a drop left to drink: California State University Desert Studies Center, 2014 Desert Symposium*. p. 165 – 167. <https://www.desertsymposium.org/>
- Monroe, L. W., 2002, Geology and minerals in the area of Pisgah Volcanic cone, *in* R. E. Reynolds (ed.), *Between the Basins: Exploring the Western Mojave and Southern Basin and Range Province: California State University, Desert Studies Consortium and LSA Associates, Inc.*, p. 26 – 28.
- Mulqueen, Steve, 2002, Borax Smith and the Tonopah & Tidewater Railroad, *in* R. E. Reynolds, (ed), *Between the Basins: Exploring the Western Mojave and Southern Basin and Range Province: California State University, Desert Studies Consortium*, April 2002, p. 23.
- Myrick, D. F., 1964, *Railroads of Nevada and Eastern California, Vol 2* (Howell-North Books: Berkeley, California) p. 845.
- Nop, Michelle, 2023 *Telegraph mine, Halloran Springs district, San Bernardino County, California* (this volume)
- Reynolds, R.E. 2002, *Between the Basins: Field Guide*, *in* R. E. Reynolds (ed.), *Exploring the Western Mojave and Southern Basin and Range Province: California State University, Desert Studies Consortium, LSA Associates, Inc.*, p. 3, 10. <https://www.desertsymposium.org/>
- Reynolds, R.E., 2005, *Halloran turquoise: a thousand years of mining history*, *in* R. E. Reynolds, (ed.), *Old Ores. Mining History in the Eastern Mojave Desert: California State University, Desert Studies Consortium and LSA Associates, Inc.* p. 63-67. <https://www.desertsymposium.org/>
- Reynolds, R.E., and Miller, D.M., 2010, *Overboard in the Mojave: the field guide: Desert Studies Consortium, California State University, Fullerton*, p. 7-23.
- Reynolds, R. E., and Weasma, Ted, 2005, *Old ores: mines and mineral marketing in the east Mojave, Desert—a field trip guide* *in* R.E. Reynolds (ed.), *Old Ores Mining History in the Eastern Mojave Desert: California State University, Desert Studies Consortium and LSA Associates, Inc.*, pp. 13-14. <https://www.desertsymposium.org/>
- Reynolds, R.E., and Woodburne, M.O., 2002, *Marker bed correlations between the Mud Hills, Calico Mountains and Daggett Ridge, central Mojave Desert, California*, *in* Reynolds, R.E. (ed.), *Between the Basins: Exploring the Western Mojave and Southern Basin and Range Province*, Abstracts from the 2002 Desert Symposium California State University, Desert Studies Consortium and LSA Associates, Inc., p. 82.
- Serpico, P., 2013, *Tonopah and Tidewater Railroad, the Nevada short line*, (Omni Publications: Palmdale, California) 296 p.
- Siefke, J.W., 1991, “The Boron Open Pit Mine at the Kramer Borate Deposit,” *in* M.A. McKibben, (ed), *The Diversity of Mineral and Energy Resources of Southern California: SEG Guidebook Series, Vol. 12*, p. 415.
- Singleton, J.S., Gans, P.B., 2008, *Structural and stratigraphic evolution of the Calico Mountains: Implications for early Miocene extension and Neogene transpression in the central Mojave Desert, California: Geological Society of America*, 4 (3) p. 459–479.
- Southern Pacific Company, 1964, *Minerals for Industry, Southern California, Volume III*, p. 132.
- Steeple, Douglas, *Hunting for old Calico’s silver: this volume*.
- Tengelsen, Ryan, 2023, *The Morning Star mine, San Bernardino County, California* (this volume)
- Travis, N. J. and Cocks, E. J., 1984, *The Tincal Trail*, (Harrap Limited: London), 311 pp.
- Tucker, W. B., and Sampson, R. J., 1930, *Los Angeles Field Division, San Bernardino County: California Division of Mines, Report of the State Mineralogist, Vol. 23 No. 3*, p. 202-325.
- Tucker, W. B., and Sampson, R. J., 1931, *Los Angeles Field Division, San Bernardino County: California Division of Mines, Report of the State Mineralogist, Vol. 27 No. 3*, p. 262-401.
- Tucker, W.B. and Samson, R.J., 1943, *Los Angeles Field District, Mineral Resources of San Bernardino County: California Division of Mines, Report of the State Mineralogist, Vol. 39, No. 4*, p. 427-549.
- U.S. Bureau of Land Management, 1982, *Final Environmental Impact Statement and Proposed Plan (Revised January 1982) Appendix G, Appendix XIV, Geology – Energy – Minerals*, pp 1 – 184. https://archive.org/download/californiadesert00unse_2/californiadesert00unse_2.pdf.
- U.S. Bureau of Mines Staff, 1990a, *Minerals in the East Mojave National Scenic Area, California: A Minerals Investigation, U. S. Bureau of Mines, MLA 6-90. Volume 1*, 356 p. <https://archive.org/details/MineralsInTheEastMojaveBOM1990Vol1/>.
- U.S. Bureau of Mines Staff, 1990b, *Minerals in the East Mojave National Scenic Area, California: A Minerals Investigation, U. S. Bureau of Mines, MLA 6-90. Volume 2*. 52 p. <https://archive.org/details/MineralsInTheEastMojaveBOM1990Vol2/>
- U.S. Geological Survey, 2023, *Earth Mapping Resources Initiative (Earth MRI)*, <https://usgs.gov/earthmri>.
- Ver Planck, W.E., 1962, *Kramer Borate District* *in* Troxel, B. W. and Morton, P. K., *Mines and Mineral Resources of Kern County, California: California Division of Mines and Geology, County Report 1*.
- Vredenburg, L.M., Shumway, G.L., and Hartill, R.D., 1981, *Desert Fever, An overview of mining in the California desert: (Living West Press: Canoga Park, California) 323 p.* For Vanderbilt, see p. 119.

- Vredenburg, L.M., 1994, Fort Irwin and Vicinity: History of Mining Development *in* R. E. Reynolds (ed.), Off Limits in the Mojave, San Bernardino County Museum Association Special Publication 94 (1), pp. 61 – 90. <https://www.desertsymposium.org/>
- Vredenburg, L.M., 1996b, Later Mining History in the Mescal Range, Ivanpah Mountains and South Clark Mountain, *in* Robert R. E. Reynolds and Reynolds J., (eds.), Punctuated Chaos in the Northeastern Mojave Desert: San Bernardino County Museum Association Quarterly 43 (1, 2), p. 73-76. <https://www.desertsymposium.org/>
- Vredenburg, L.M., 1996c, History of Mining in the Halloran Hills, Shadow Mountains, and Silurian Hills *in* Reynolds, R.E. and Reynolds J., (eds.), Punctuated Chaos in the Northeastern Mojave Desert: San Bernardino County Museum Association, Quarterly Vol. 43 (1, 2), p. 135-138. <https://www.desertsymposium.org/>
- Vredenburg, L.M., 2013, Calico—a brief overview of mining history *in* Reynolds, R. E., (ed.), Raising Questions in the Central Mojave Desert: California State University Desert Studies Center 2013 Desert Symposium, p. 92-94. <https://www.desertsymposium.org/>
- Vredenburg, L.M., 2014, Chubbuck, California *in* R. E. Reynolds (ed.), Not a drop left to drink: California State University Desert Studies Center, 2014 Desert Symposium. p. 57-59. <https://www.desertsymposium.org/>
- Vredenburg, L.M., Silver Mountain and the Oro Grande Mining Company, *in* R.E. Reynolds, (ed), Mojave Miocene: California State University Desert Studies Center, 2015 Desert Symposium p. 244 - 249.
- Vredenburg, L. M., 2017, Mineral potential within the Eastern California Shear Zone, *in* Reynolds, R. E., ed. ECSZ Does It Revisiting the Eastern California Shear Zone: 2017 Desert Symposium, p. 118-119. <https://www.desertsymposium.org/>
- Vredenburg, L.M., 2020, The Mojave Mining District: a brief history of gold mining, *in* Miller, D. M., (ed.), Changing Facies, The 2020 Desert Symposium Field Guide and Proceedings: Desert Symposium Inc., p. 121 – 125. <https://www.desertsymposium.org/>
- Vredenburg, L.M., Curtis Howe Springer and Zzyzx, this volume.
- Walker, J.D., Burchfiel, B.C., and Davis, G.A., 1995, New age controls on initiation and timing of foreland belt thrusting in the Clark Mountains, southern California: Geological Society of America, Bulletin 107 (6), scale 1:33,300.
- Watts, K.E., Haxel, G.B., Miller, D.M., 2022, Temporal and Petrogenetic Links Between Mesoproterozoic Alkaline and Carbonatite Magmas at Mountain Pass, California. *Economic Geology*, 117 (1): 1-23. doi: <https://doi.org/10.5382/econgeo.4848>.
- Weber, F.H., 1976, Geology of the Calico Silver district, San Bernardino County California, *in* Geologic guidebook to the southwestern Mojave Desert Region, California: prepared by the South Coast Geological Society for the October 9-10, 1976 field trip. p. 83-94.
- Whistler, D.P., 1984. An early Hemingfordian (early Miocene) fossil vertebrate fauna from Boron, western Mojave Desert, California: Los Angeles County Museum of Natural History Contrib. in Science, p. 355.
- Wikipedia, Baker, California. https://en.wikipedia.org/wiki/Baker%2C_California.
- Wilkinson, Gregg, 2015, Geology and mining history of the Cronese, Cave and northern Cady Mountains, San Bernardino County, California, *in* R.E. Reynolds (ed.), Mojave Miocene, California State University Desert Studies Center, Desert Symposium Proceedings.
- Wise, W. S., 1990, The mineralogy of the Mohawk Mine, San Bernardino County, California, San Bernardino County Museum Association Quarterly Vol. 37, No. 1.
- Wise, W. S., 1993, Die mineralien der Mohawk mine. im San Bernardino, County, Kalifornien/USA, Mineralien Welt, 4, p. 26-44.
- Wise, W. S., 1996. The Blue Bell Claims and the Mohawk Mine: Two prolific mineral localities in San Bernardino County, California, *in* R. E. Reynolds (ed), Punctuated chaos: A field trip to the northeastern Mojave Desert: San Bernardino County Museum Association Quarterly, 43 (1, 2), p. 91-94.
- Wright, L.A., Stewart, R.M., Gay Jr., T.E., and Hazenbush, G.C., 1953, Mines and mineral deposits of San Bernardino County, California: California Division of Mines, California Journal of Mines of Geology 49 (1,2), p. 93.

Into the mines: the road log for the pre-meeting field trip

Larry M. Vredenburg and Gregg Wilkerson

Pre-meeting field trip, April 20, 2023

This is an informal one-day trip with no provision of food or water. Be prepared with your own provisions. Make sure vehicles are packed with all your personal gear and a full tank of gas. Carry water and snacks, plan your clothing for the conditions. Wear hard toed boots. Bring hats and sunscreen. Watch for harmful plants and animals. Note that some roads are on Federal lands managed by the Bureau of Land Management and National Park Service. Respect the land and leave it as you found it: no rock or artifact collecting, digging, or harming of plants and wildlife is allowed. Part of this day's route is within the Mojave National Preserve where special use permits are required for field trips with more than a limited number of vehicles or visitors.

We will visit two active mines and tour an underground mine. Please be mindful that we are guests on the mine properties and show the respect that is deserved: honor their rules and requests.

STOP 1 — Mountain Pass mine

UTM 11S 633510 3925680; 35.465662, -115.528572

The field trip starts when we meet at the Mountain Pass mine at 7:30 a.m. Don't be late: the tour starts at 8:00 a.m. sharp! The tour of the facility is limited to 20 people. You must have signed up prior to the trip.

Take exit 281 for Bailey Rd., Mountain Pass mine. TURN SOUTH away from the facility, then straight onto a dirt road heading south. Pull out in a wide area (Figure 1).

Mining at Mountain Pass began with base and precious minerals. Between 1900 and 1920 several small lead, zinc, copper, gold, and tungsten deposits were mined and some production recorded. The Sulphide Queen gold mine, adjacent to the future Mountain Pass orebody, was not discovered until 1936. A 100-ton

cyanide plant was built, and small production achieved prior to World War II (Warhol, 1980, p. 359) to process the gold and base metal ores.

In April 1949 an area of intense radioactivity was discovered in Mountain Pass by Herbert Woodward (later a metallurgist for Molycorp) and James Watkins, who were prospecting for uranium with a friend's Geiger counter. They were invited to this location by Fred Piehl, half owner of the Sulphide Queen gold mine. After they discovered an area of radioactivity, they located the Birthday claims north of Piehl's claims, and sent a specimen of the mineral to the U.S. Bureau of Mines in Boulder City, Nevada, for identification. The sample was tentatively identified as bastnaesite, a rare-earth fluorocarbonate. USGS geologist Donnell F. Hewett confirmed the identification, examined the property in July, and arranged for detailed study. USGS geologists W. N. Sharp and Lloyd C. Pray began mapping the discovery on November 3rd. Within days enough had been learned about the nature and extent of the deposit to warrant an announcement by the Secretary of Interior on November 18. In February 1950 the Molybdenum Corporation of America purchased the Birthday claims and began



Figure 1. Mountain Pass area, showing parking area south of the Interstate 15. (ESRI imagery).

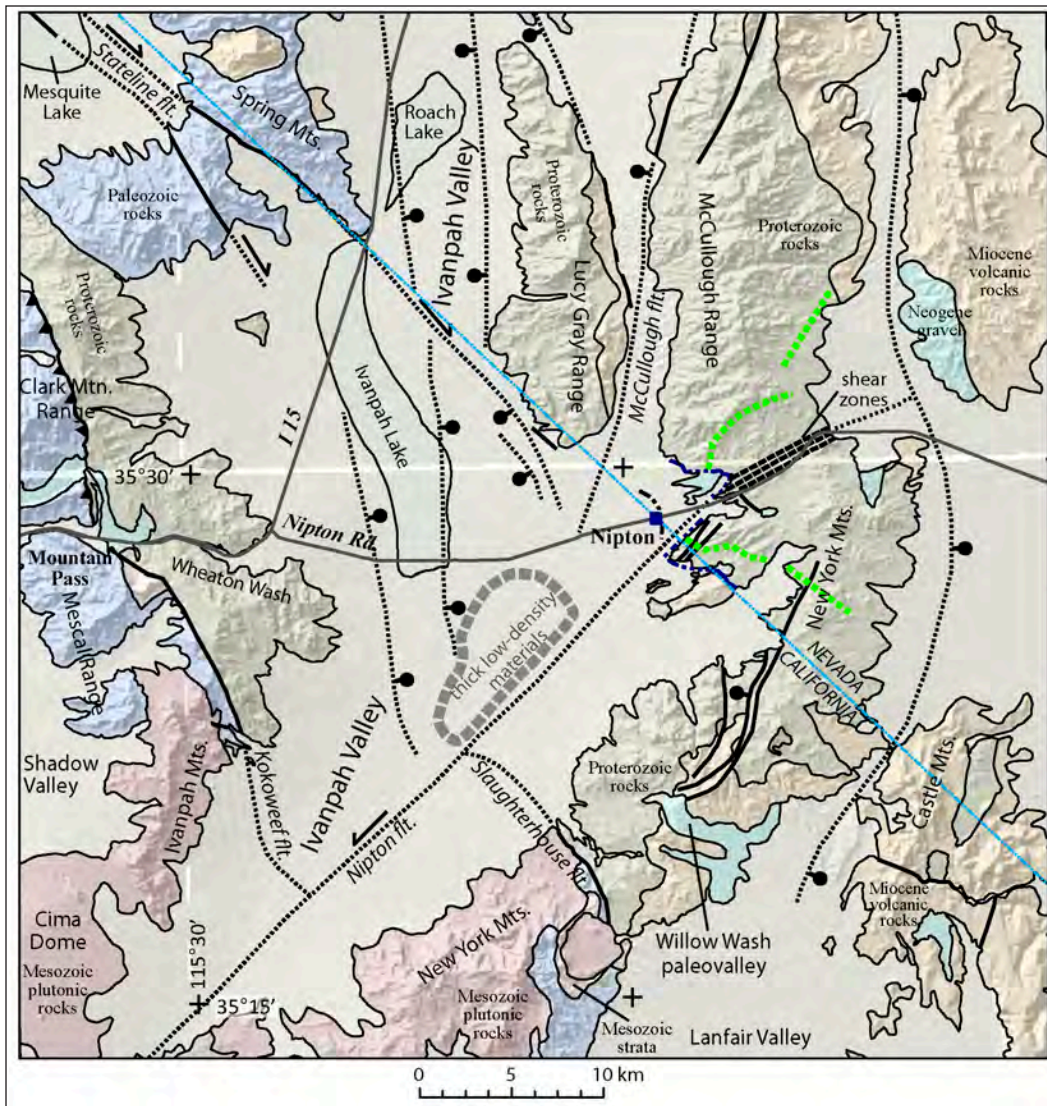


Figure 2 (left). Geology and physiography of the Ivanpah Valley area (Miller and others., 2019, p. 13). Major Cenozoic faults are shown as well as a few important Mesozoic faults. Most thrust faults of the Mescal and Clark Mountain ranges are omitted for simplicity. The 1.4 Ga ultrapotassic intrusive suite of the Mountain Pass area straddles I-15; Bar-and-Ball—on downthrown side of normal fault; Arrow shows sense of offset on strike-slip fault. Green dashed lines show transects along which apatite was sampled by Mahan and others (2012).

Figure 3.(below). Mountain Pass Rare Earth Mine and Processing Facility. <https://mpmaterials.com/what-we-do/> Accessed Feb. 24, 2023



developing the property, which is now the world's richest known concentration of rare earths (Hewett, 1954; Olson and others, 1954; USGS MRDS id=10212814).

Mountain Pass is the site of the most economically important rare earth element (REE) deposit in the United States. From the mid-1960s to the early 1990s, the United States was the world's largest producer of REEs with production coming entirely from the Mountain Pass mine. In the late 1980s, China began mining REE deposits in their country and quickly gained control of global REE production, providing 95 percent of the global market of processed REE by 2011. Between 2011 and 2017, China produced approximately 84 percent of the world's REEs, followed by Australia with about 8 percent of production. Within this period, the United States only produced REEs between 2012 and 2015, entirely from the Mountain Pass mine, which contributed only about 4 percent of the world REE supply (Van Gosen and others, 2019, p.4). The Mountain Pass mine (Figure 3) was acquired in 2017 by MP Materials. From 2020 through 2022, the company has produced 38,500 Mt, 42,413 Mt and 42,499 Mt annually of rare earth oxides in concentrate. In 2020 they produced about 15% of the rare earth content consumed in the global market. The company is currently working on adding heavy rare earth separation capability at Mountain Pass (<https://mpmaterials.com/>).

Following the discovery of the Mountain Pass deposit this area has been the subject of numerous studies. A few of the more recent ones include Verplanck and others (2014, 2016), Poletti and others (2016), and Denton and Ponce (2016). However, since 2017, a flood of studies has been published (Ponce and Denton, 2018a; Ponce and Denton, 2018b; Ponce and Denton, 2019; Denton and others, 2019; and Watts and others, 2022). Studies underway at Mountain Pass include Ramo (this volume) and Miller and Wooden (this volume). The following is condensed from Watts and others (2022):

Mountain Pass is located within the Mojave crustal province, a crystalline basement terrane

that spans most of southeastern California and parts of Nevada, Arizona, and Utah as inferred from radiogenic Nd and Pb isotope data. Though the age of this basement terrane is Paleoproterozoic (~1800–1600 Ma),

Archean components are apparent from Nd isotope data and detrital zircons with ages that extend to >2000 Ma. The Paleoproterozoic rocks that are widespread in the Ivanpah Valley area (Figure 2) record superimposed episodes of sedimentation, arc magmatism, plutonism, and metamorphism. The oldest rocks (~1800 Ma) are metasedimentary gneisses and metaigneous calc-alkaline rocks with a magmatic arc affinity. The ~1700 Ma Ivanpah orogeny was a regional, high-grade metamorphic event, forming granitic and intermediate biotite garnet gneisses, lesser amphibolite, and migmatites. Synorogenic intrusions are represented by augen orthogneisses and granitic and pegmatitic dikes. Voluminous postorogenic granitic plutons were emplaced along a north-south trend in the middle of the Mojave crustal province ~1690–1640 Ma, manifest in part as coarse alkali-feldspar porphyritic gneisses that lack the granulite-grade fabrics and migmatization associated with the Ivanpah orogeny.

At Mountain Pass a suite of Mesoproterozoic (~1400 Ma) alkaline silicate intrusions (Figure 4) range in composition from shonkinite (most voluminous) to syenite (less voluminous) to alkali granite (minor) that are spatially and temporally associated with a series of carbonatite dikes and intrusions. The most significant carbonatite intrusion is the Sulphide Queen stock. Though

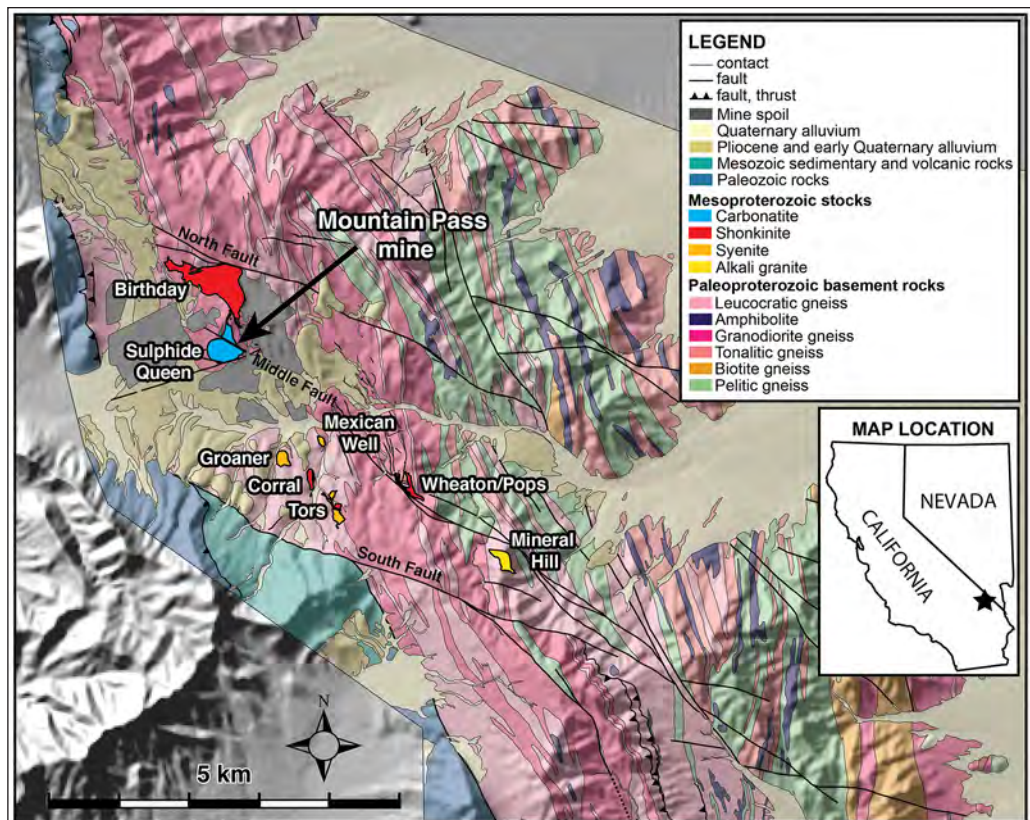


Figure 4. Mountain Pass regional geologic map (Watts and others, 2022). Note small intrusion of ultrapotassic rocks and related bodies.

moderate in its areal extent (700 m in widest dimension) and thickness (up to 150 m), the orebody is high grade. The Sulphide Queen deposit, although mined for over 50 years, has an estimated remaining resource of 20 to 47 million metric tons (Mt) at an average grade of 8.9% rare earth oxides (REOs). As is characteristic of most carbonatite ore deposits, it has an extreme enrichment in light REEs (LREEs: atomic numbers 57–63) relative to heavy REEs (HREEs: atomic numbers 64–71), with bastnasite ($[\text{LREE}]\text{CO}_3\text{F}$) constituting the predominant ore mineral.

Outcrops of ~1400 Ma alkaline and carbonatite stocks and dikes at Mountain Pass form a 3 X 10 km northwest-southeast belt. Similar dikes are found in the Ivanpah Valley region up to 30 km away, however these dikes lack the potassic alteration (finitization) present at Mountain Pass. At Mountain Pass there are eight stocks which are limited to the 3 X 10 km area mentioned above; they range in size from 0.1 to 2 km in their widest dimensions. The Birthday shonkinite stock and the Sulphide Queen carbonatite stock are the two largest intrusive bodies at Mountain Pass. Smaller syenite-shonkinite stocks include Mexican Well Groaner, Corral, Tors, and Wheaton (also known as Pops) (Figure 4). Mineral Hill is the lone alkali granite stock. Stocks are accompanied by hundreds of mapped dikes of shonkinite, syenite, alkali granite, and carbonatite, 0.3 to 10 m wide and as much as 1 km long. Many dikes strike northwest, parallel to the orientation of some stocks.

The study by Watts and others (2022) supports a model in which alkaline and carbonatite magmatism occurred over tens of millions of years, repeatedly tapping a metasomatized mantle source, which endowed magmas with elevated REEs and other diagnostic

components (e.g., F, Ba). Some of the shonkinite dikes represent the youngest phase of alkaline magmatism that overlapped in space and time with the intrusion and alteration of carbonatite magmas at 1396–1371 Ma. Miller and Wooden (this volume) conclude “that the widespread intrusion of geochemically unusual, highly LREE-enriched melts at 1.4 Ga indicates that melting of metasomatized mantle was regional in scope.”

Mines in the nearby Mescal Range to the south were worked well before the Mountain Pass REE discovery (Figures 5, 6).

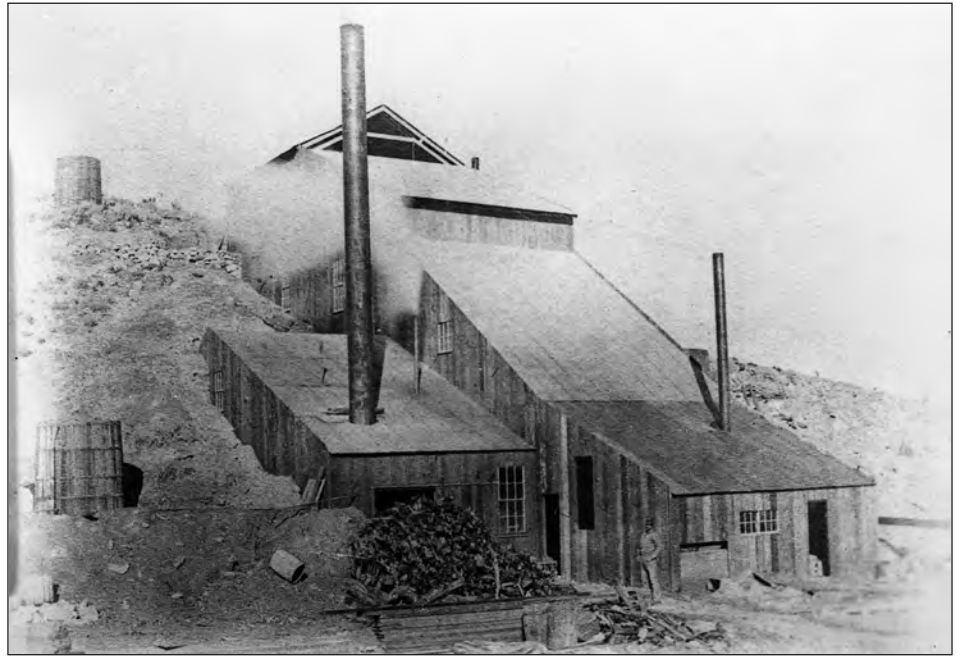


Figure 5. Mescal Mill c. 1880. E.L. MacFarland collection.



Figure 6. Mescal Miners c. 1880, (L-R): a Russian, a Mexican or Indian?, Jim McCormick, a Piute Indian. E.L. MacFarland collection

Leave Mountain Pass and proceed to the Techatticup mine (Eldorado Canyon Mine Tours) located near Nelson, Nevada, a drive of about 75 Miles.

U-Turn and retrace the route to Interstate 15.

0.0 (0.0) TURN RIGHT North (East) on I-15 toward Las Vegas. RESET YOUR ODOMETER

Caution: Maintain speed and be aware of closing traffic going down-grade here on the interstate. High-speed, truck heavy traffic makes this stretch of highway more dangerous than others. From this point to the Nipton exit, we drive through Proterozoic gneiss and granitoids.

5.0 (5.0) EXIT 286 **Nipton Road**. Turn right onto Nipton Rd. Nipton Road was built in the 1930s to support the construction of Hoover Dam.

8.4 (3.4) Pass Ivanpah Road.

15.1 (6.7) **Cross the Union Pacific Railroad and pass through Nipton**. Nipton was a mining camp at the crossroads of two wagon trails. It became a town when on February 9, 1905, the first train on the newly constructed San Pedro, Los Angeles & Salt Lake Railroad arrived. It was called "Nippeno Camp" following a nearby discovery of gold. The name was changed to Nipton when the San Pedro, Los Angeles & Salt Lake Railroad merged with the Union Pacific Railroad around 1910. In addition to being a cattle-loading station for several local ranches, the town and depot also supplied numerous mines in the area, becoming a social center for the sparse population of the region (Wikipedia.com: Nipton, California).

17.9 (2.8) **Enter Nevada** – the road name changes to Nevada State Highway 164 / Joshua Tree Highway. The location of the state line has been controversial since California was accepted into the Union in 1850. Several surveys and re-surveys were conducted, and the matter was not resolved until issuance of a Supreme Court decision in 1970.

20.5 (2.6) Pass Crescent Peak Road, site of the abandoned town of Crescent (Figure 7). To the northwest are the McCullough Mountains. To the southeast are the

New York Mountains (Miller and Wooden, 1993). The rocks in both ranges in this area are Paleoproterozoic gneisses.

The Crescent District: Mineralization in the Crescent district was first discovered by Native Americans who mined small amounts of turquoise along the south flank of Crescent Peak. These deposits were mined commercially from 1894 to 1906, producing approximately \$1 million in turquoise. Gold and silver were also discovered in the early 1900s, with intermittent periods of mining activity over the next 40 years. Principal producers were the Nippeno, Big Tiger, Lily, and Double Standard mines. Total production is unknown but likely was less than \$100,000.

During the uranium prospecting rush of the 1950s, the district was examined for its uranium and thorium potential. Thorium and lesser uranium, with associated rare earth elements, were discovered at the Thor claim, southwest of Crescent Peak. An examination by U.S. Atomic Energy Commission reported a sample from the Thor Claim with 0.15% ThO₂ and 1.54% REE. Much of the area was staked and numerous prospect pits and trenches were dug. Recent geochemistry, SEM, microprobe, and field studies concluded that primary rare earth bearing ore minerals at the Thor claim include the phosphate minerals apatite, monazite, and xenotime as well as allanite, a Ca-REE fluoride, thorite and/or thorumgumite, and thorianite (Baltzer and Housley, 2019). Host rocks for the gold mineralization and REE minerals are Paleoproterozoic gneisses (Hewett, 1956; Miller and Wooden, 1993; Miller and others 2007).



Figure 7. The Jordan boarding house at Crescent, Nevada. Right, Mrs. Jordan (hostess). Left, F. B. Home, miner and guide. August 1913. U.S. Geological Survey photo collection. Photo by D.B. Sterrett. Photo #sdb00571

29.5 (9.0) Pass the Walking Box Ranch / Viceroy Mine Rd.
 After visiting the Techatticup mine we will return here to travel to the Castle Mountain mine.

36.4 (6.9) Arrive at Searchlight. TURN LEFT (north) on U.S. Highway 95.

Searchlight, Nevada. On May 6, 1897, G. F. Colton discovered a gold-rich vein that became the Duplex mine. A mining district was organized in 1898 and the mining camp of Searchlight was established. Three mines were equipped with stamp mills: the Quartette, Duplex, and Southern Nevada. In 1902 the Quartette's newly constructed 20-stamp mill on the Colorado River was operational. It was connected to the mine by a 15-mile-long narrow-gauge railroad. After water was struck in the mine in 1906, the mill was moved to Searchlight and expanded to 40 stamps. A branch of the AT&SF railway was extended to Searchlight from Barnwell in 1907 but the rails were torn up in 1924. The Searchlight boom period lasted until 1910.

The Quartette mine, located three quarters of a mile south of Searchlight, was the district's largest producer. Its most productive period was between 1902 and 1923, but there was limited production in 1934, 1935, and 1951. Searchlight has a recorded production of nearly \$7,000,000 (Longwell and others, 1965). The primary product of the veins in the Searchlight mining district has

been gold with some copper and lead. The majority of Searchlight production came from oxidized ores (Brown, 1977; Paher, 1980, p. 280-284; Longwell and others, 1965 p. 112 -116; Callaghan, 1939).

The area is underlain by a Precambrian complex consisting of granitic gneiss that was intruded by Cretaceous and Tertiary silicic to intermediate rocks, and Tertiary volcanic rocks. Andesites and basalts predominate with rhyolitic flows and pyroclastic beds present throughout the exposed section. Wide rhyolite dikes cut the quartz monzonite and granite plutons and small lamprophyre dikes are common in the mapped area of intrusive rocks. Mineralized veins in the district varied greatly with a few up to 3,500 feet long and many productive over 1,000 feet. The width of veins ranged up to 50 feet. One vein was mined up to 900 feet down dip (Brown, 1977).

62.3 (25.9) TURN RIGHT (east) onto Nevada State Highway 165

73.5 (11.2) Pass through the tiny community of Nelson.

75.1 (1.6) ARRIVE at the Techatticup mine – Eldorado Canyon Mine Tours

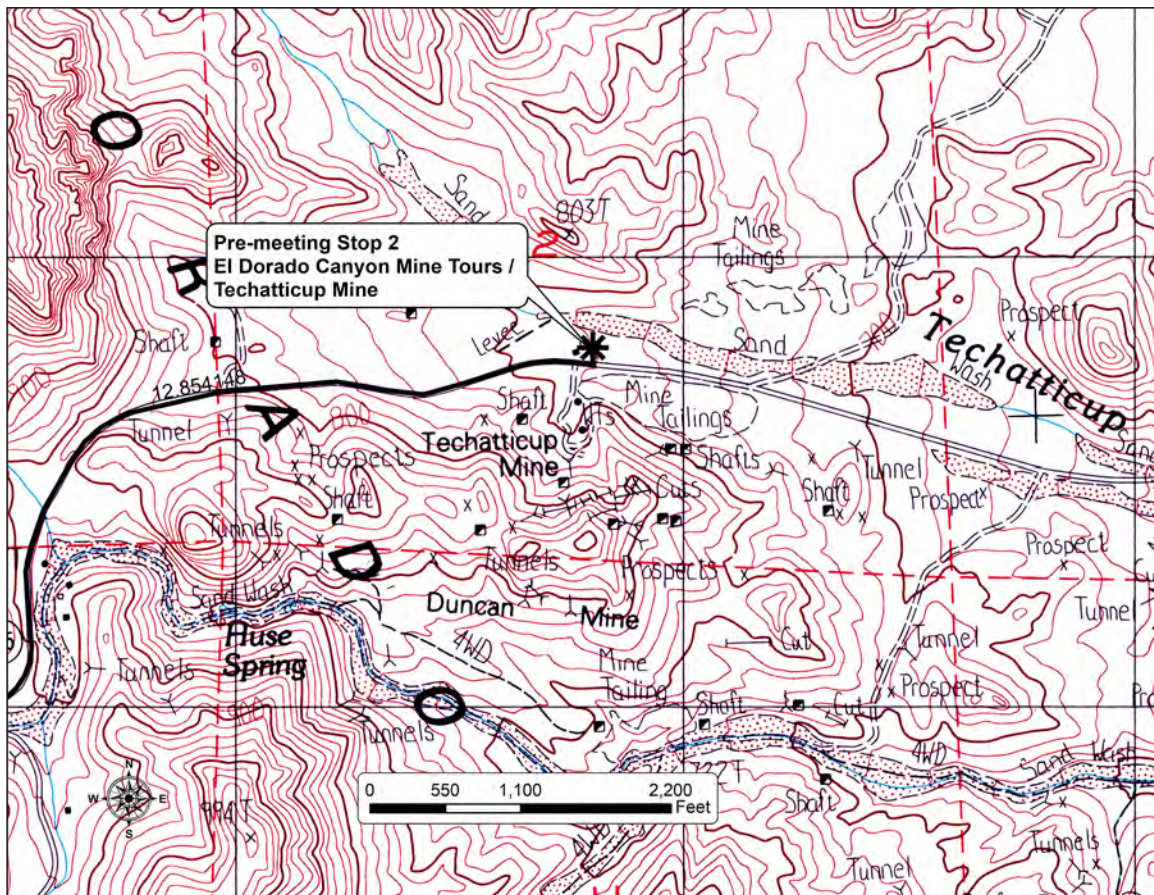


Figure 8. Topographic map of the Techatticup Mine area <https://eldoradocanyonminetours.com/index.html>.

STOP 2 — Techatticup mine

UTM 11S 698719 3953995;
35.709884, -114.803324 (Figure 8)

We have scheduled an underground tour of the mine at 12:00 noon for 20 people. Bring \$15 in cash for the cost of the tour.

Mining in Eldorado Canyon dates from 1861, although there are legends that early prospectors found arrastras and prospect pits, suggesting that the area was previously mined by the Spanish. Rich gold discoveries were made in the area resulting in a stampede of prospectors from Los Angeles. In 1862 Rudolph d'Heureuse was hired by promoters to scout out the new discovery and take photos along the way.

After he arrived, he mapped the district in exquisite detail (Lapides, 2018). Also In 1862, the Southwestern Mining Company purchased the Techatticup mine from the original locators and erected a 15-stamp mill on the Colorado River. The Techatticup mine is the largest

producer in the district. Between 1907 and 1954, 100,616 ounces of gold were produced from 580,255 tons of ore. Geology of the district primarily consists of fine-grained quartz monzonite of Tertiary age. Ore occurs in veins filling fissures, which can be traced on the surface for more than a mile (Figures 9, 10). On the north side of Eldorado Canyon the quartz monzonite intruded a series of andesitic and rhyolitic lavas, breccias, and tuffs. Two and one-half miles of Eldorado Canyon, Precambrian gneiss and schist are cut by dikes of pegmatite, aplite, fine-grained quartz monzonite and andesitic porphyries. The Techatticup mine was developed by about 3 miles of underground workings (Figure 11). Ore consisted of free gold with a small percentage of pyrite, sphalerite, galena, and chrysocolla. Sulfides increased slightly with depth, but gold and silver values remained constant. Gangue was principally quartz and calcite (Longwell and others, 1965).

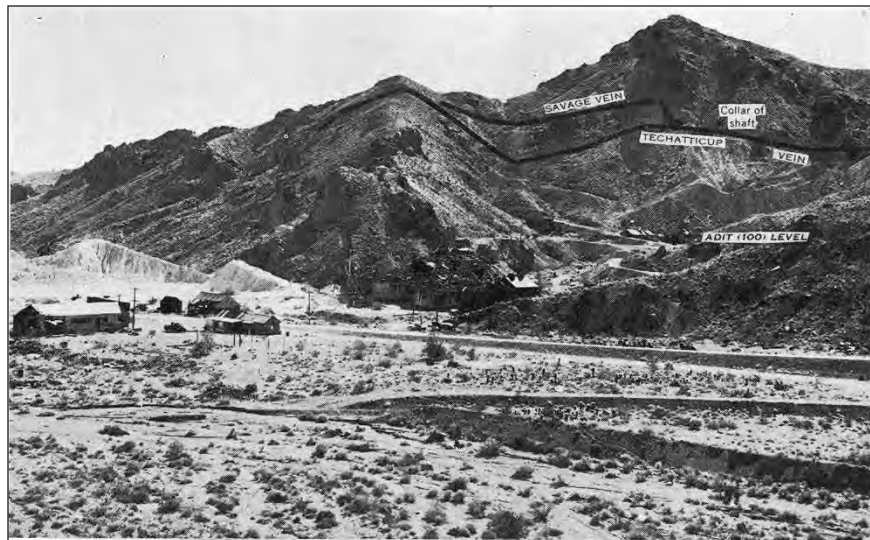


Figure 9. Techatticup vein from Longwell and others (1965).

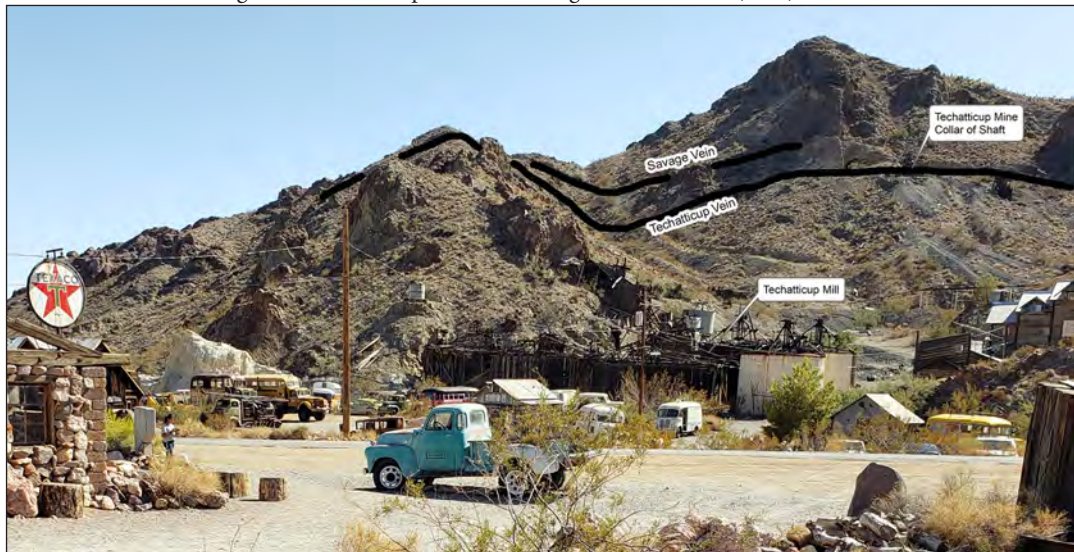


Figure 10. Techatticup mine and mill, view to south. Photo: L.M. Vredenburg, Oct. 13, 2019. Veins after Longwell and others (1965)

In 1994 the 51-acre property was purchased by Tony and Bobbie Werly. The buildings were in disrepair and strewn with trash. It took the family 5 years to restore the buildings and clean the site. Two days before escrow closed on the property Tony discovered a mine entrance that was obscured by rock and dirt (Figure 12). After cleaning out the tunnel and stringing lights, family members began giving tours of the underground mine in 2000. For more information about the restored mine go to YouTube.com and search for Nelson Ghost Town, or Tony Werly (Libby, 2001; Jones, 2019; Wadsworth, 2021).

Upper Camp was nearby and served miners in the area (Figures 13, 14).

Leave the Techatticup mine and proceed to the Castle Mountain mine – About 65 miles.

0.0 (0.0) RESET YOUR ODOMETER. Leave the Techatticup Mine. GO WEST on NV-165 W to U.S. 95.

12.8 (12.8) TURN LEFT (south) on U.S. 95.

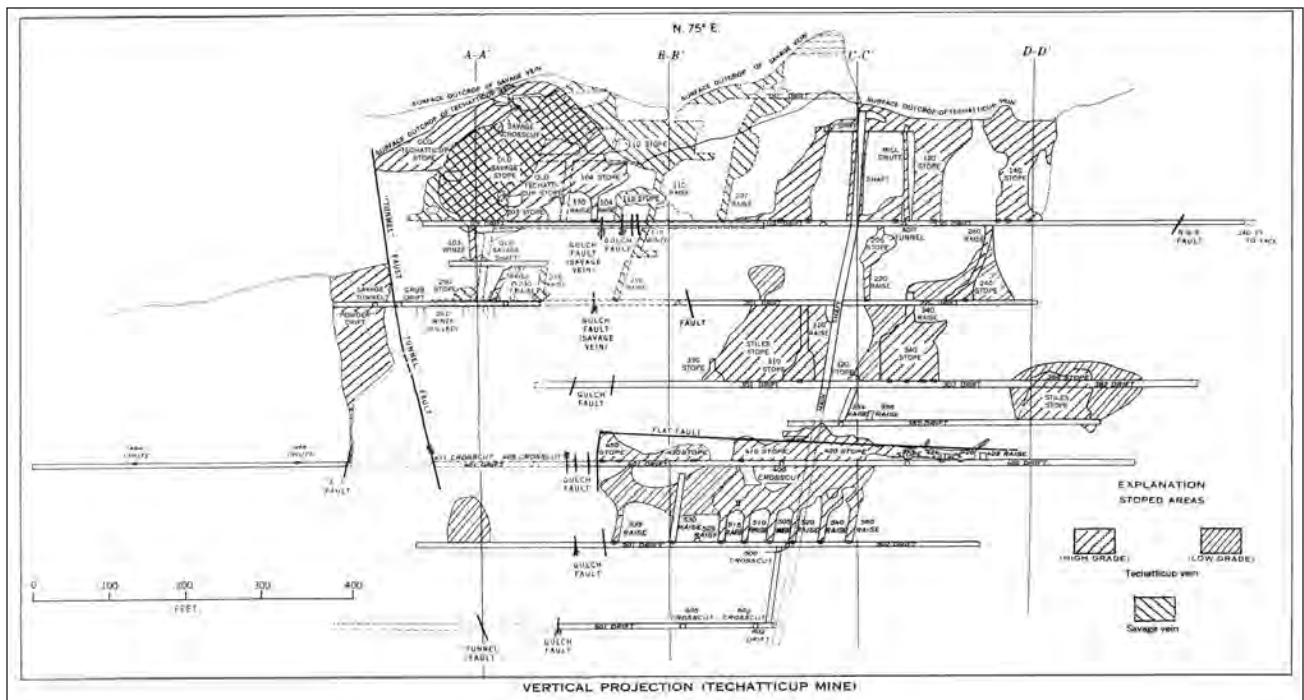


Figure 11. Vertical section of the Techatticup mine (Longwell and others, 1965, plate 11).

38.7 (25.9) Arrive at Searchlight. Turn right (west) on Nevada Route 164 (Joshua Tree Hwy.)

45.7 (7.0) mi TURN LEFT onto Walking Box Ranch Rd toward the Castle Mountain mine.

The Highland Range is to the north and the New York Mountains are to the southwest. As we drive to the Castle Mountain mine, the New York Mountains expose Precambrian metamorphic rocks (Miller and others, 2007;

Miller and Wooden, 1993). The Castle Mountains were described by Medall (1964), Nielson and Bedford (1999), Nielson and Turner (1999), Nielson, and others (1993), and Turner and Glazner (1990). Mineral resources of the Castle Peaks Wilderness Study Area were described by Miller and others (1986).

Pass Walking Box Ranch. Walking Box Ranch was founded in 1931 by the actors Rex Bell and Clara Bow as a working 400,000-acre ranch. The ranch covered 160 acres at the time it was listed on the National Register of Historic Places on January 30, 2009. It is presently managed by the Bureau of Land Management. The area around the Walker Box Ranch is a Joshua Tree woodland.

46.8 (1.1) Continue straight onto YKL Ranch Road / Viceroy Mine Road.

55.7 (8.7) **Enter California.** From this location you can see spires of Tertiary volcanic rocks underlying Castle Peaks due west about 3 miles. The New York Mountains extend both north and southwest from Castle Peaks. The Castle Mountains extend from due east to south.

7.4 (1.9) Cross the route the of the abandoned Barnwell and



Figure 12. Old El Dorado Mine. Entrance to the underground mine tour. L.M. Vredenburgh photo Oct. 13, 2019.



Figure 13. Upper Camp Eldorado Canyon [Alturas], Photographer Rudolph d'Heureuse. c. 1863. - located about 3.5 miles southwest of the Techatticup Mine (approx. 35.698n, 114.864w). UC Berkeley, Bancroft Library Collection. <https://oac.cdlib.org/ark:/13030/tf8t1nb71d/?brand=oac4>.



Figure 14. John Moss, a leader in the early Eldorado Cañon mining, and Piute Chief Tercherrum at Upper Camp. Photographer Rudolph d'Heureuse. c. 1863. UC Berkeley, Bancroft Library Collection. <https://oac.cdlib.org/ark:/13030/tf8779p406/?brand=oac4>.

Searchlight Railroad. A good view of Hart Peak is to the east. Hart Peak is about in the middle of the Castle Mountains.

65.2 (7.8) ARRIVE at the Castle Mountain mine gate. PARK outside of the gate. They are expecting us to arrive at 2:30 pm.

STOP 3 — Castle Mountain mine

UTM 11S 671934 3905179; 35.275001, -115.109593

Gold was first discovered in the Castle Mountains in 1907 by James Hart and the brothers Bert and Clark Hitt. The original discovery was in high grade veins carrying as much as 500 oz of gold per ton, but most of the ore contained 1 to 2 oz per ton. Production was not significant, despite extensive underground workings at the Oro Belle and Hart consolidated mines, and operations ceased within a few years. In 1933, operations began at the Big Chief mine (aka Valley View mine) and a mill was erected, but there was minimal production. The mine closed in 1942 (Linder, 1989a, 1989b; Capps and Moore, 1991).

Major gold deposits were discovered in 1986 by consulting geologist Harold Linder. In 1990 Viceroy Gold Corporation, operator of the newly opened Castle Mountain mine, announced combined reserves of over 38 million short tons of ore in six deposits (Hart Tunnel, Jumbo, Jumbo South, Lesley Ann, Oro Belle, and South Extension) totaling about two million ounces (62.2 metric tons) of gold.

In 1991, production began on a single open pit to mine the Jumbo South and Lesley Ann (JSLA) deposits with a combined ore grade of 0.048 oz Au/ton (Figures 15, 16). Reserves for these deposits assume a cut-off grade of 0.015 oz Au/ton. Ore grades for the other four deposits varied between 0.044 and 0.046 oz Au/ton. Gold recovery varied between 65% and 70%. By 1996 these deposits were considered exhausted, and JSLA pit was backfilled with waste rock from the Jumbo and Oro Belle pits. Mining from the Oro Belle ceased in 2001 due to low gold prices (Secret, 2021).

Heap leaching of ore ceased in 2005. The mine produced about 1,150,000 troy ounces (35.8 metric tons) of gold during its operation. Reclamation was proceeding on schedule at the Castle Mountain mine as gold prices

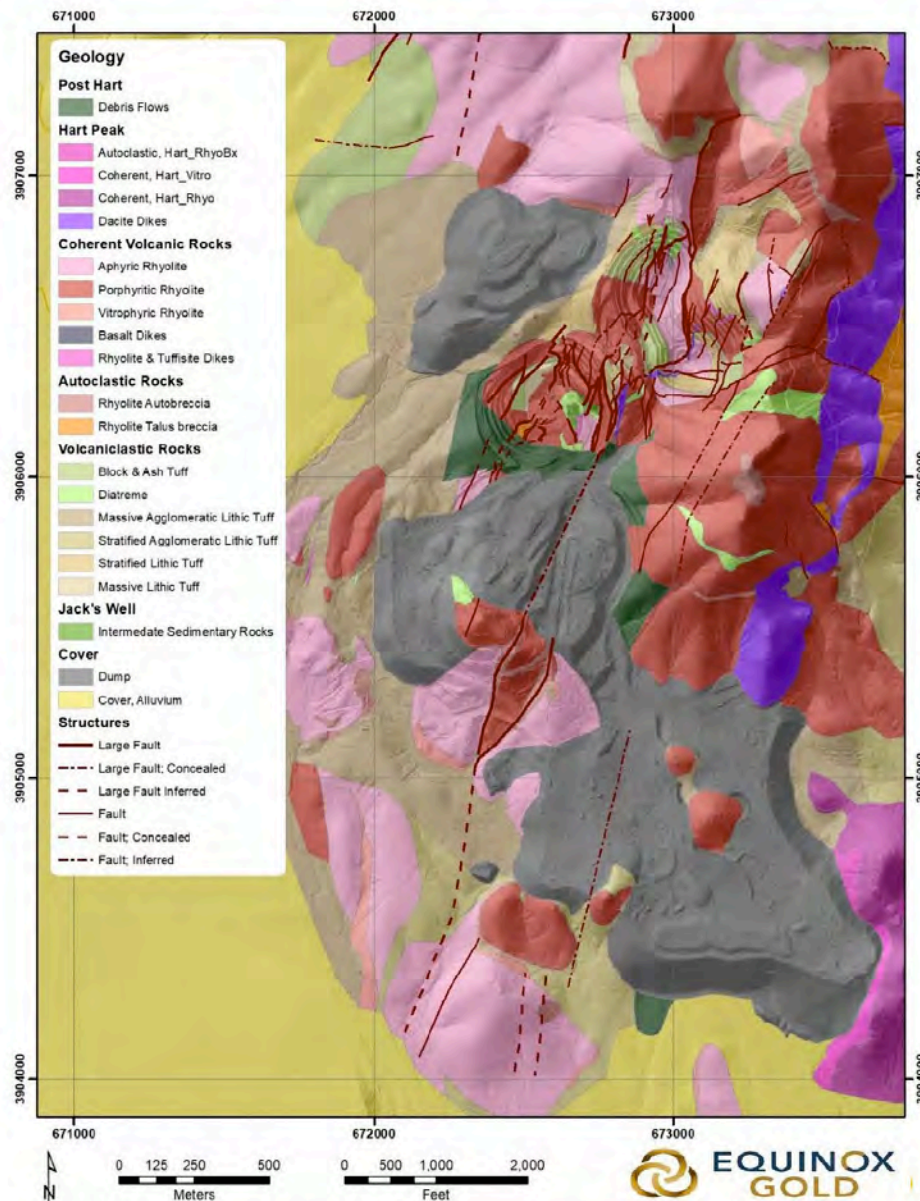


Figure 15. Castle Mountain Project Geology (Secrest and others, 2021, p. 7-8).



Figure 16. Oblique air photo of the Castle Mountain Project, 2021. (Secrest and others, 2021, p. 1)

escalated from \$490 per ounce in 1990 to \$1,800 in 2015. That escalation led to a re-analysis of mining at Castle Mountain. Waste material at Castle Mountain, carefully revegetated, was now ore-grade. Those areas of the mine are now being re-excavated and placed on heap leach piles for cyanide leaching (California Water Board, 2020).

The first phase of development was expected to run for three years beginning in 2019 and is forecast to produce an average of 45,000 oz of gold a year (Figures 17, 18). The second phase, from years four to 16, is anticipated to produce an annual average of 203,000 oz of gold. The project is estimated to produce 2.8 million oz of gold over its initial mine life of 16 years. It is expected to create up to 600 jobs during both construction and operations (Equinox (2022a, 2022b)).

Gold mineralization is widespread over an area of at least two square miles in host Tertiary volcanic rocks and has a vertical depth range of more than 1500 feet. The Castle Mountain ore bodies are classified as volcanic-hosted epithermal-type mineralization. Gold is the major metal present. Silver is present and base metal sulfides are completely absent. The overall gold-to-silver ratio is about 1:2, but in the core of the deposits the ratio is reversed with a gold-to-silver ratio of 2:1. In general, the ore bodies are associated with permeable, brecciated rock units. Significant mineralization occurs in all the hydrothermally altered Tertiary rock units, but rhyolite dome complexes and their associated hydrothermal breccias contain more ore than do lithic tuffs. Gold occurs in quartz stockwork veins, matrix silicification, and with drusy quartz in cavities. All ore

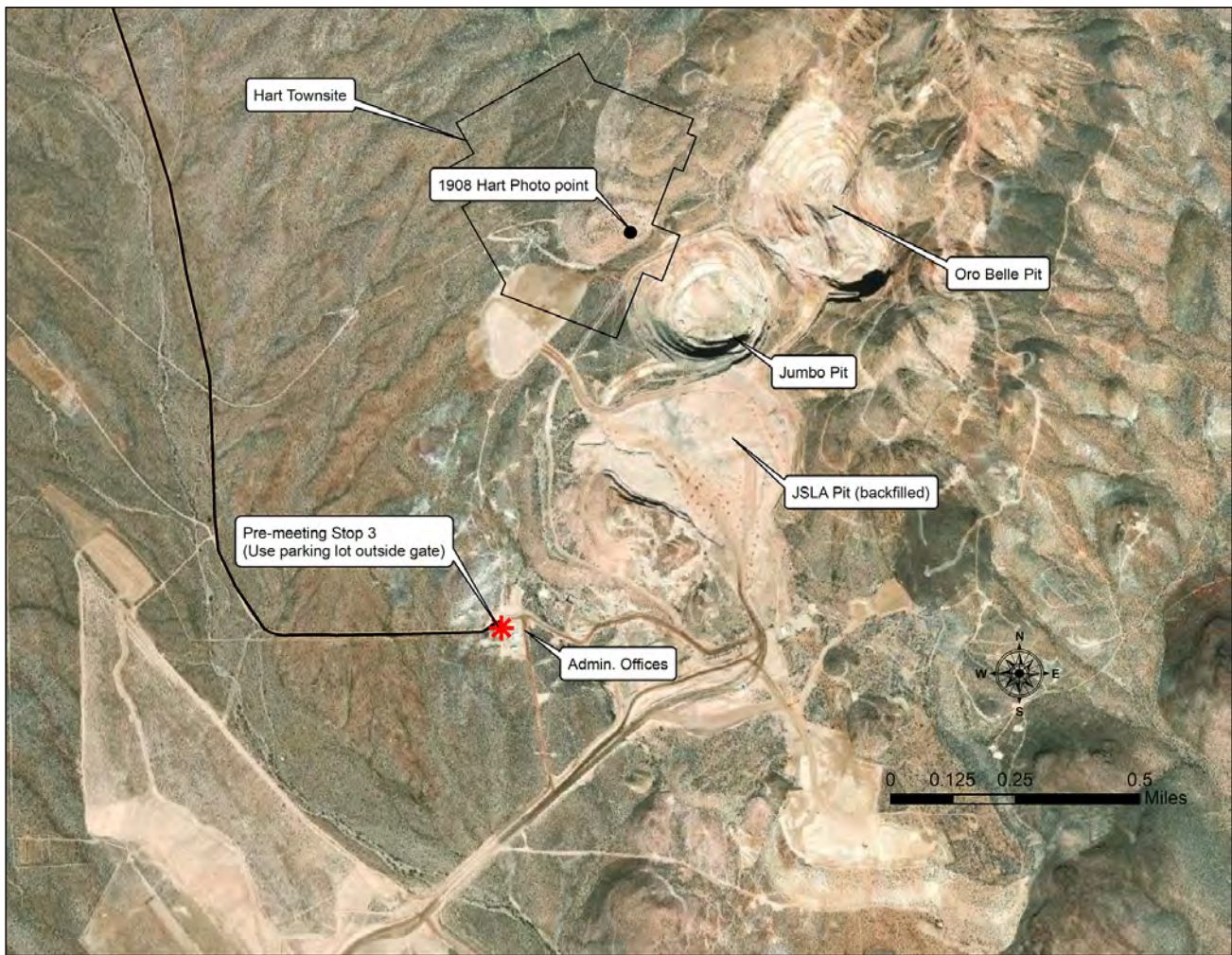


Figure 17. Castle Mountain Project with pits labeled.



Figure 18. Castle Mountain Mine, photo by G. Wilkerson Jan. 21, 2023.

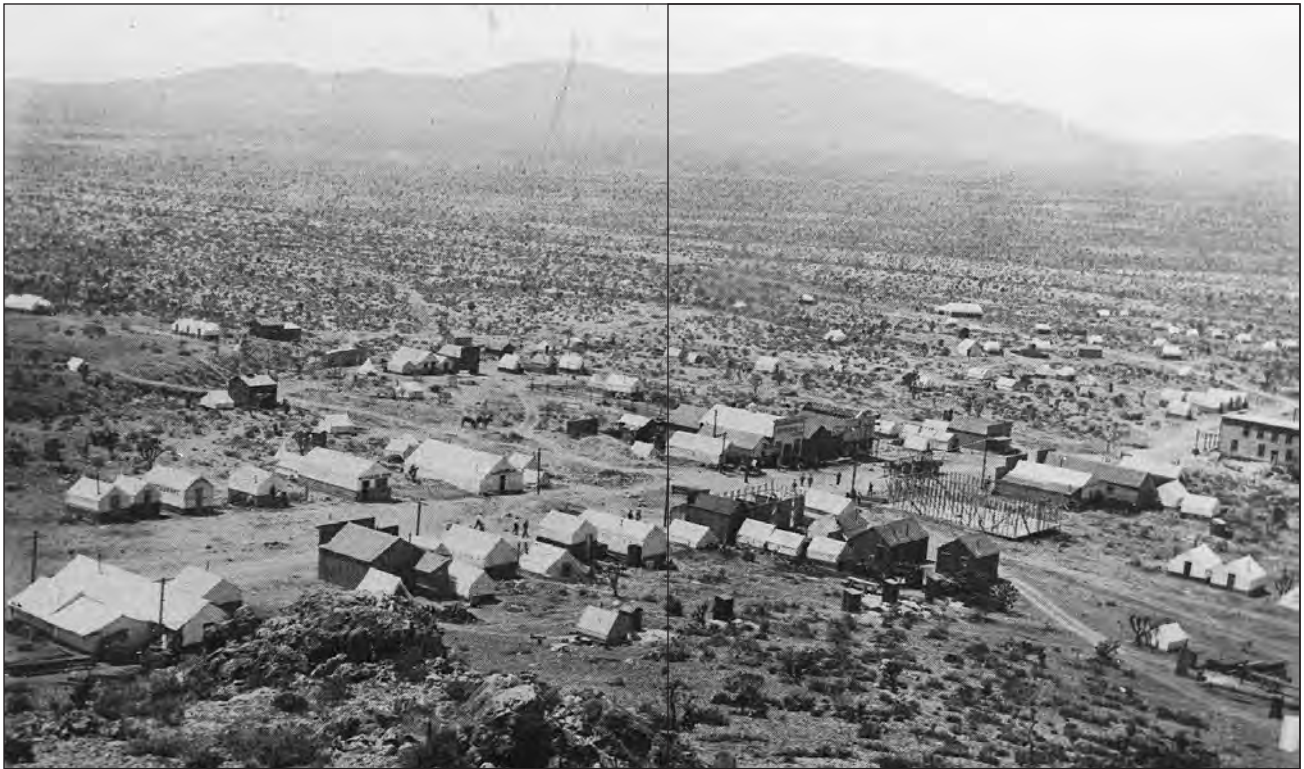


Figure 19. Hart townsite, 1908. Laereman & Phillips, c. 1908, *Souvenir of Hart, California*, 19 p.



Figure 20. Hart townsite 1984. Photo taken from 35.286119n, 115.104986w by L.M. Vredenburg, 1984.

reserves are in the oxidized zone, and only rare sulfide grains occur above the water table, which is at a depth of about 550 feet (Linder, 1989a; Capps and Moore, 1991, 1997; Kohler, 2002, 2006 and USGS MRDS id=10310700).

Historic photos of the Hart mine illustrate the size of the camp and the barely recognizable remnants of the town in 1984 (Figures 19–21).

Leave the Castle Mountain mine.

From here you can follow a field trip leader back to Interstate 15 via the way you came—Nevada State Route

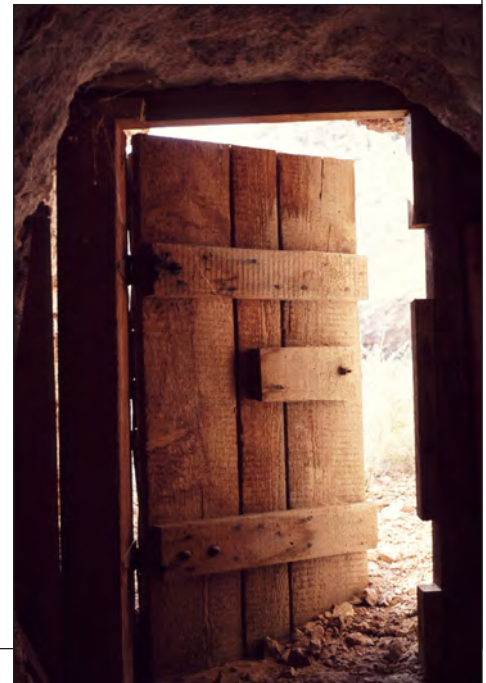


Figure 21. Door at Hart. Photo taken from the inside of an abandoned powder magazine(?). Approximate location was 35.286n, 115.097w now located within an open pit. Photo by L.M. Vredenburg, September, 1974.

164 and Nipton; it is 42 miles. If you have a high clearance vehicle and would like to save about 15 miles follow the other field trip leader via Hart Mine Road and Ivanpah Road.

References Cited

- Baltzer, S., and Housley, R., 2019, Mineralogy of the Thor rare earth deposit, New York Mountains, southern Nevada in D.M. Miller (ed.), *Exploring ends of eras in the eastern Mojave Desert: Desert Symposium Inc.*, p. 98- 103. <https://www.desertsymposium.org/>
- Brown, J.S., 1977, *The Geology of the Searchlight Mining District, Clark County, Nevada*: University of Missouri, Rolla. MS thesis. 84 p. https://scholarsmine.mst.edu/cgi/viewcontent.cgi?article=4255&context=masters_theses
- California Water Board, 2020, Waste discharge requirements for castle mountain venture, operator Equinox Gold Corporation and U.S. Bureau of Land Management, owners Castle Mountain Mine heap leach pad, tank pond, event pond, and conveyance system San Bernardino County, Order R7-2020-004, Castle Mountain Venture, Equinox Gold Corporation: U.S. Department of Interior, Bureau of Land Management.
- Callaghan, E. 1939, *Geology of the Searchlight District, Clark County, Nevada*: U.S. Geological Survey Bulletin 906D, 188 pp.
- Capps R.C., and Moore J., 1991, Geologic setting of mid-Miocene gold deposits in the Castle Mountains, San Bernardino County California and Clark County, Nevada: Geological Society of Nevada, Great Basin Symposium, v. 2, p. 1195-1219.
- Capps, R.C., and Moore, J.A., 1997, *Geologic Map of the Castle Mountains, San Bernardino County, California and Clark County, Nevada*: Nevada Bureau of Mines and Geology, Map 108.
- Denton, K.M. and Ponce, D.A., 2016, Gravity and magnetic studies of the eastern Mojave Desert, California and Nevada: U.S. Geological Survey, Open File Report 2016-1070.
- Denton, K.M., Ponce, D.A., Peacock, J.R. and Miller, D.M., 2019, Geophysical characterization of a Proterozoic REE terrane at Mountain Pass, eastern Mojave Desert, California, USA: *Geosphere*, v. 16, no. 1, p. 456–471. <https://doi.org/10.1130/GES02066.1>
- Equinox Gold, 2022a, Castle Mountain Phase 1, Equinox Gold - Castle Mountain: <https://www.equinoxgold.com/operations/operating-mines/castle-mountain-operating/>
- Equinox Gold, 2022b, Castle Mountain Expansion: <https://www.equinoxgold.com/operations/growth-projects/castle-mountain-expansion/>
- Hewett, D.F., 1954, History of the discovery at Mountain Pass, California, in Olson, J. C., Shawe, D. R. Pray, L. C. and Sharp, W. N., *Rare-Earth Mineral Deposits of the Mountain Pass District San Bernardino County California*: U.S. Geological Survey Professional Paper 261, p. iii – vi.
- Hewett, D. F., 1956, *Geology and mineral resources of the Ivanpah Quadrangle California and Nevada*: U.S. Geological Survey Professional Paper 275, 170 pp.
- Jones, Jay, April 5, 2019, Eldorado Canyon Mine Tours, where they first went to strike gold, Los Angeles *Times*: <https://www.latimes.com/travel/la-tr-vegas12-2009apr12-story.html>
- Kohler, Susan, 2002, California's non-fuel mineral production 2001: California Geological Survey web site, http://www.consrv.ca.gov/CGS/minerals/min_prod/non_fuel_2001.pdf.
- Kohler, Susan, 2006, California non-fuel minerals 2005, in *Mining Engineering*, May 2006, pp. 70-74.
- Lapides, J., 2018, *The Mojave Road in 1863, Tales of the Mojave Road Publishing Co., Mojave Desert Heritage and Cultural Association, Goffs, California*, 129 pp.
- Libby, Jeffrey, Feb. 15. 2001, All Mine: Trek to Eldorado Canyon is a trip back in time, *Las Vegas Sun*. <https://lasvegassun.com/news/2001/feb/15/all-mine-trek-to-eldorado-canyon-is-a-trip-back-in/>
- Linder, H., 1989a, Castle Mountains gold deposit, Hart mining district, San Bernardino County, California: *California Geology*, v. 42, no. 6, p. 134-144.
- Linder, H., 1989b, The Castle Mountains gold deposit, Hart district, San Bernardino County, California, in *The California Desert Mineral Symposium (Compendium)*, U.S. Department of the Interior-Bureau of Land Management, p. 177-193. <https://archive.org/details/california-gold-symposium-II-1989>
- Longwell, C.R., Pampeyan, E.H., Bowyer, B and Roberts, R.J., 1965, *Geology and mineral deposits of Clark County, Nevada*: Nevada Bureau of Mines and Geology, Bulletin 62, 218 pp.
- Medall, S.E., 1964, *Geology of the Castle Mountains, California [M.S. thesis]*: University of Southern California, 106 pp.
- Miller, D.M., Frisken, J.G., Jachens, R.C., Gese, D.D., 1986, *Mineral Resources of the Castle Peaks Wilderness Study area, San Bernardino County, California*: US Geological Survey Bulletin 1713-A, 19 pp.
- Miller, D.M., and Wooden, J.L., 1993, *Geologic map of the New York Mountains area, California and Nevada*: U.S. Geological Survey Open-File Report 93-198, 10 pp.
- Miller, D.M., and Wooden, J.L., this volume
- Miller, D.M., Miller R.J., Nielsen, J.E., Wilshire, H.G., Howard, K.A., and Stone, P., 2007, *Geologic Map of the East Mojave National Scenic Area, California*: U.S. Geological Survey Bulletin 2160, Plate 1, Scale 1:125,000
- Miller, D.M., Langenheim, V.E., Denton, K.M., and Ponce, D., 2019, Strike-slip fault interactions at Ivanpah Valley, California and Nevada, in David Miller (ed.), *Exploring Ends of Eras in the eastern Mojave Desert, Desert Symposium Field Guide and Proceedings: Desert Symposium, Inc.* p. 91-97 <https://www.desertsymposium.org/>
- Nielson, J.E., Turner, R.D., and Glazner, A.F., 1993, Tertiary stratigraphy and structure of the Castle Mountains and Castle Peaks, Calif. and Nev., in Sherrod, D.R., and Nielson, J.E., (eds.), *Tertiary stratigraphy of highly extended terranes, California, Arizona, and Nevada*: U.S. Geological Survey Bulletin 2053, p. 45–49.
- Nielson, J.E., digital database by D.R. Bedford, 1999, *Geologic map of the east of Grotto Hills quadrangle, California*:

- U.S. Geological Survey Open File Report OF-99-35, scale, 1:24,000.
- Nielson, J.E., and Turner, R.D., digital database by D.R. Bedford, 1999, Geologic map of the Hart Peak quadrangle, California and Nevada: U.S. Geological Survey Open File Report OF-99-34, scale, 1:24,000.
- Olson, J.C., Shawe, D.R. Pray, L.C. and Sharp, W.N., 1954, Rare-Earth Mineral Deposits of the Mountain Pass District San Bernardino County, California: U.S. Geological Survey Professional Paper 261. 75 pp., 13 pls.
- Paher, S, 1980, Nevada Ghost Towns and Mining Camps: (Howell-North Books, San Diego), 491 pp.
- Poletti, J.E., Cottle, J.M., Hagen-Peter, G.A., and Lackey, J.S., 2016, Petrochronological constraints on the origin of the Mountain Pass ultrapotassic and carbonatite intrusive suite, California: *Journal of Petrology*, v. 57, p. 1555–1598.
- Ponce, D.A., and Denton, K.M., 2018a, Isostatic gravity map of Mountain Pass and vicinity, California and Nevada: U.S. Geological Survey Scientific Investigations Map 3412-A, scale 1:62,500. <https://doi.org/10.3133/sim3412A>.
- Ponce, D.A., and Denton, K.M., 2018b, Aeromagnetic map of Mountain Pass and vicinity, California and Nevada: U.S. Geological Survey Scientific Investigations Map 3412-B, scale 1:62,500. <https://doi.org/10.3133/sim3412B>.
- Ponce, D.A., and Denton, K.M., 2019, High-resolution airborne radiometric survey of Mountain Pass, California: U.S. Geological Survey data release. <https://doi.org/10.5066/P9ENLS6D>.
- Ramo and others, this volume
- Secrest, G., Tahaji, L. M., Black, E., Rabb, T., Nilsson, J. and Bartlett, R. D., 2021, Castle Mountain Project, Technical Report on the Castle Mountain Project Feasibility Study San Bernardino County, California, USA: Prepared for Equinox Gold, 453 p. https://www.equinoxgold.com/_resources/projects/technical_reports/2021-CastleMountain.pdf.
- Turner, R.D., and Glazner, A.F., 1990, Miocene volcanism, folding, and faulting in the Castle Mountains, southern Nevada and eastern California, in Wernicke, B.P., (ed.), Basin and Range extensional tectonics near the latitude of Las Vegas, Nevada: Geological Society of America Memoir 176, p. 23–35.
- Van Gosen, B.S., Verplanck, P.L. and Emsbo, P., 2019, Rare Earth Element Mineral Deposits in the United States, U.S. Geological Survey Circular 1454, 16 pp.
- Verplanck, P.E., Van Gosen, B.S., Seal, R.R. II, and McCafferty, A.E., 2014, A deposit model for carbonatite and peralkaline intrusion-related rare earth element deposits: U.S. Geological Survey, Scientific Investigations Report 2010-5070-J, 71 pp.
- Verplanck, P.E., Mariano, A.N., and Mariano, A., Jr., 2016, Rare earth element ore geology of carbonatites: Reviews in Economic Geology, Society of Economic Geologists, January 1, 2016, Vol. 18, 18 p.; <https://doi.org/10.5382/REV.18>.
- Wadsworth, Reuben, October 31, 2021, Eldorado Canyon day; from lawless gold mining mecca to a hoarder's dream: St. George News. <https://www.stgeorgeutah.com/news/archive/2021/10/31/raw-eldorado-canyon-day-from-lawless-gold-mining-mecca-to-a-hoarders-dream/#.Y-FrPXbMJD8>.
- Warhol, Warren N., 1980, Molycorp's Mountain Pass Operations, in Fife, D.L. and Brown A.R., (eds.), *Geology and mineral wealth of the California Desert: South Coast* Geological Society, p. 359-366.

Carbide lamps and hard hats

Snapshots of mines in the Mojave

Jennifer Flesher Reynolds

photographs by Robert E. Reynolds

Bob Reynolds (1943–2020) started collecting minerals as a child, and by college days he often went right to the source: mines. All he needed was a friend with a car (who didn't care much about dents and dings), a few more friends to chip in for gas, hard hats, carbide lamps, Brew 102, and—fortunately for history—an Instamatic camera. After graduation from the University of California, Riverside, and a stint as a mining geologist at the Lucky Jim mine in the Old Woman Mountains, his work as a San Bernardino County Museum curator took him afield to collect suites of minerals and photograph mines in the Mojave Desert, often accompanied by his wife Jennifer and children Jed and Kate.

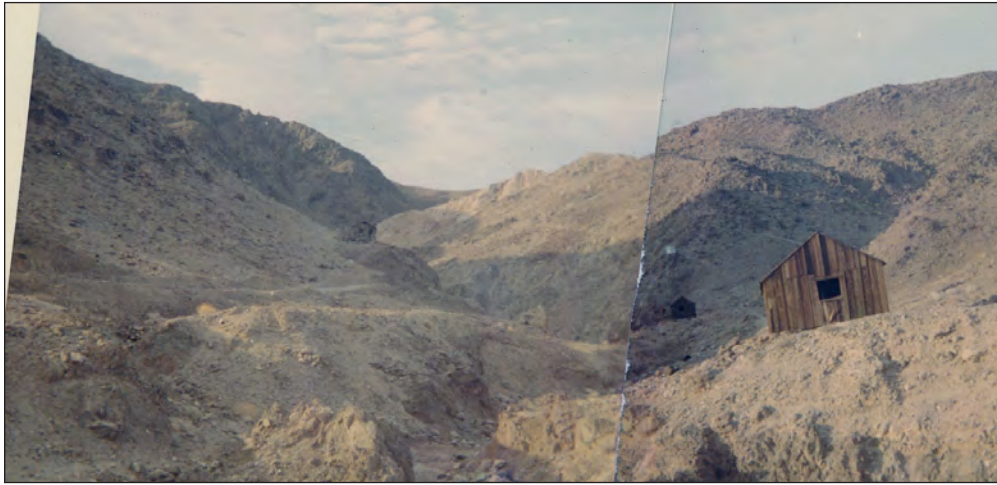


Above, UCR student geologists and other friends arrive at the Red Cloud mine, Arizona, 1967. From left, Gary Elliott, Barney Gonzalez, Dave Antrosio, Sue McCoy, Carol and Jerry Brem, Paul Allen, Marsha Gay Newton, Dave Doan, Kent Cartwright, Jenny Flesher, Ken Brem, and Steve Ivy.



Left, carbide lamps and hard hats: from left, Cheryl Black, Bob Reynolds, and Dion Dyer inside the Red Cloud mine, 270-foot level, March 1966.

The Red Cloud was the first mine I ever entered. Getting introduced to mines by climbing dubious wooden ladders down a 270-foot diagonal shaft, and by waiting in complete darkness while my carbide lamp could be refilled, was more than adequate preparation for mines to come in the Mojave Desert.



Alvord mine, Alvord Mountain. *Gold, copper, lead.* 1880s intermittent through 1952.

All views 1967. Above top, view south past the cabins. Center, view north toward the mine. Above, view south from the mine entrance with (from left) Jerry Brem, Carol Brem, Chuck Williams, Jenny Flesher, and Pickle the Dog. Right: trestle near mine.



Top four images: Black Metal mine, 1968.

Below, a WWII Dodge Power Wagon ambulance, reborn as the Power Flower, en route to the Black Metal mine, 1968.

Black Metal mine, Old Woman Mountains. *Gold, silver, copper.* Located before 1896; relocated 1902 and active through 1911.

Sometimes getting to places in the Old Woman Mountains (back when vehicle travel was allowed) was half the fun. All too often, roads turned out to be tank tracks left during Patton's WWII army maneuvers.



Scanlon Gulch mines, Old Woman Mountains. *Silver, gold.* Located for silver in 1889; shipped gold ore in 1890s through the 'teens.



Top and center, lower camp mill 1966;
bottom left, hilltop cabin, 1966.





Scanlon Gulch mines, 1966. Three cabins, a shed, and the rock room.



Entrance to the Rock Cabin mine, Scanlon Gulch, 1968.



Flooded adit, view north toward entrance. Scanlon Gulch, 1966.

Hidden Value mine, Carbonate Peak, Old Woman Mountains. *Tungsten*. 1943 and occasionally to 1953.
Right: in 1966.



Silver Wave mine, Carbonate Peak, Old Woman Mountains. *Lead, silver*. Production in 1902.
Center left and right: 1968.



Gemco mine, Carbonate Peak, Old Woman Mountains. *Gold, silver, lead, copper, zinc*.

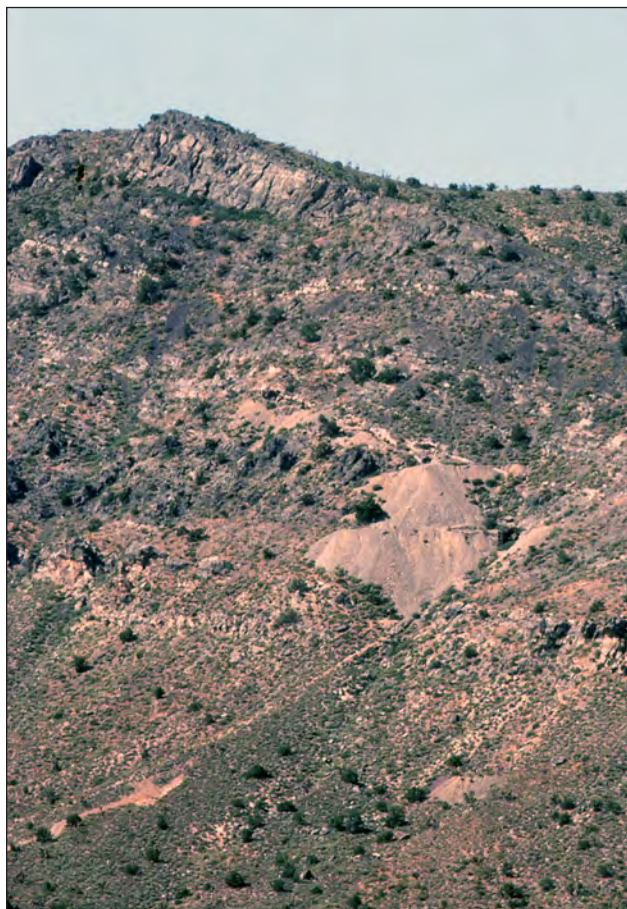
Left: 1968.

Right, Standard #2, 1968.

Below: Standard #1, 1968.



Standard mines, Ivanpah Range. *Copper, gold*. Located in 1896 when it was known as Copper Camp; leased in 1905 by Standard Mines Ltd. and produced intermittently until 1919.



Mollusc (Mescal, Cambria) mine. Mescal Range. *Gold, silver*. Discovered 1879, abandoned in 1889, and revived in 1892.

Right: 1982.



Bronze mine, New York Mountains.
Copper, lead, silver, tungsten, zinc.
Operated during 1951.

All images from 1971.



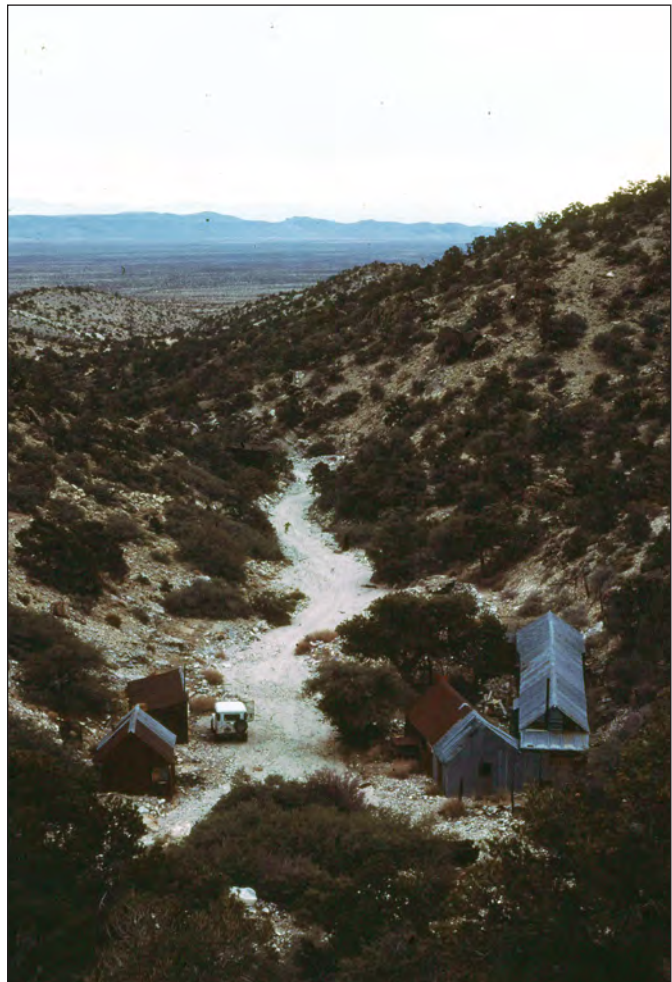


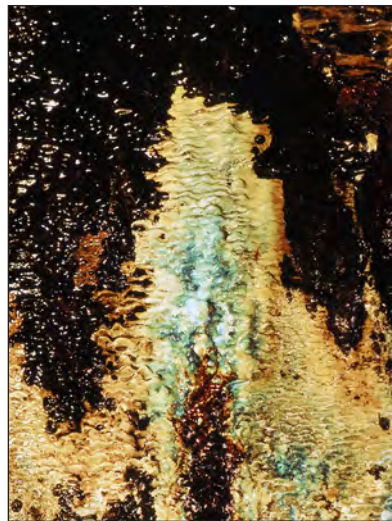
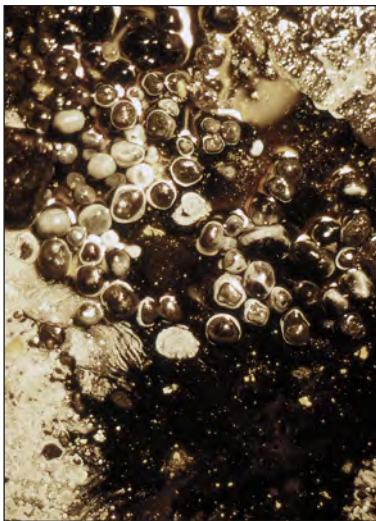
Sagamore mines,
New York Mountains.
Lead, silver, zinc,
copper, tungsten, gold.
Production in 1907-08,
1917, 1942-45, 1951.



The stone cabin complex (above, with chimney) may date to 1867; the lower camp (top and right) from the 1940s. Images from 1973.

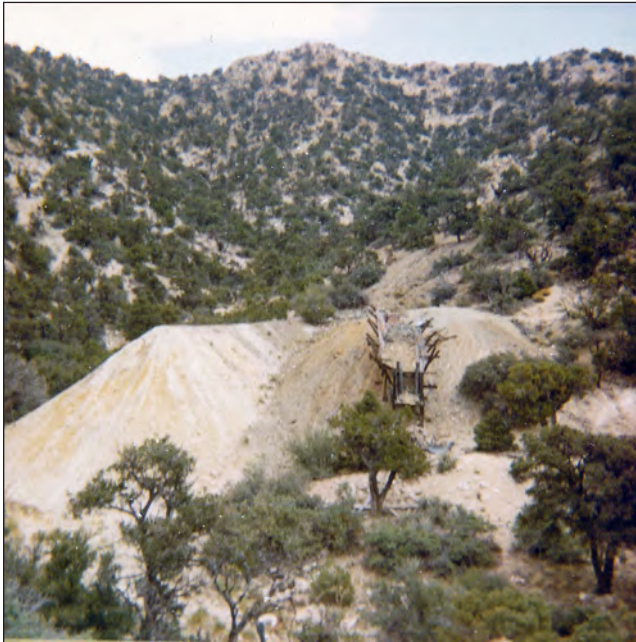
Sheltering in the tin cabin meant adjusting to a nightly visit from a spotted skunk who never altered his path from hither to yon via the top of our sleeping bag.





Sagamore mine, 1971.

One of the adits at the Sagamore mine was very wet, with colorful, actively depositing aragonite, conichalcite, and other minerals. To avoid stepping into a pool with cave pearls, I put my hand out and it sunk right into one of the waterlogged mine timbers. Our party made a careful but immediate retreat and skipped further exploration of that particular tunnel.

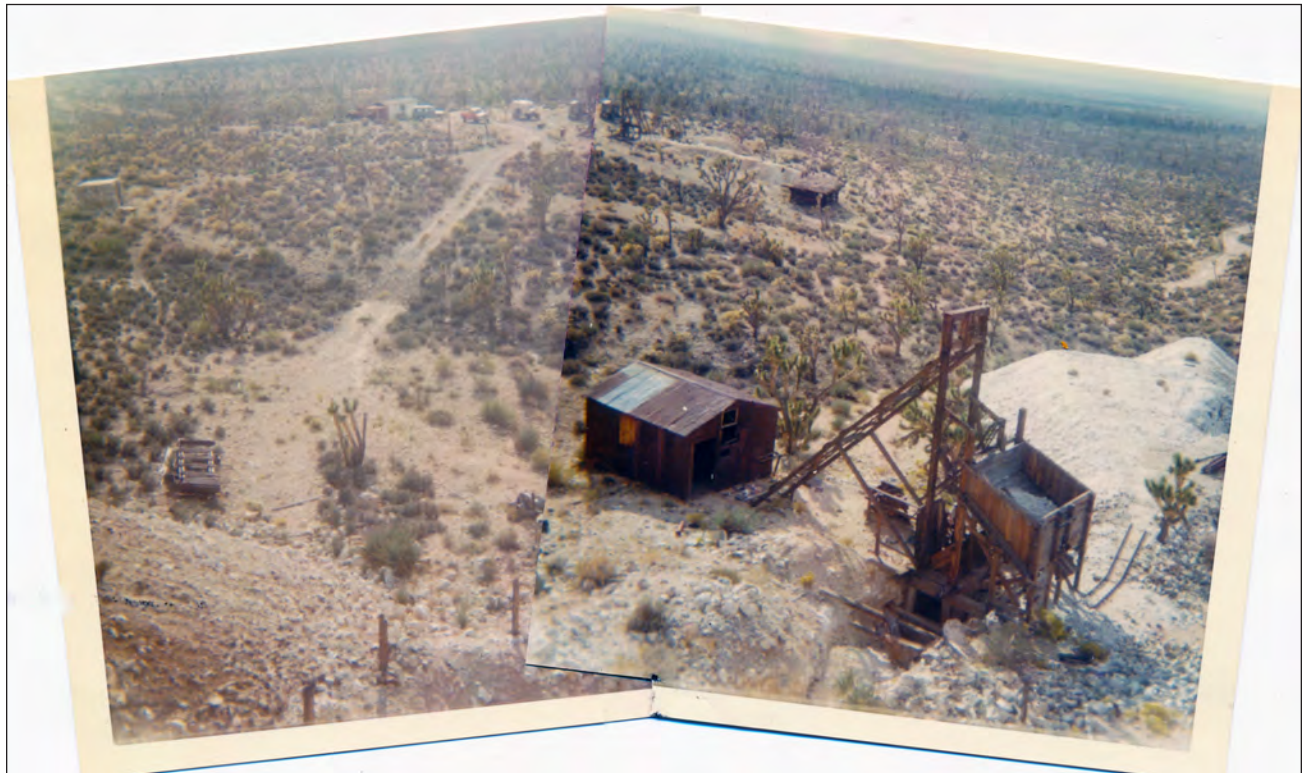


Giant Ledge (Hard Cash) mine, New York Mountains,
Copper, lead, silver, tungsten, and zinc.

Above and left, 1968.



Right, Giant Ledge mine, 1998.



Evening Star mine, Ivanpah Mountains. *Copper, gold, tin, tungsten, zinc.* 1939–1944.

Images this page: 1967.

J. Riley Bemby located the Evening Star tin deposit in 1938 and sold the claim within the year.



CIMA, CALIF.
8/3/81
P.O. Box 51. 92323

Mr. Robert Reynolds
2024 Orange Tree Lane
Redlands,
Ca. 92373

Good Morn'n Bob;

When you were here months ago, and took pictures, you promised to send me two pictures each of the three men in front of my house, and allso of the Ranch, Kessler Ranch."

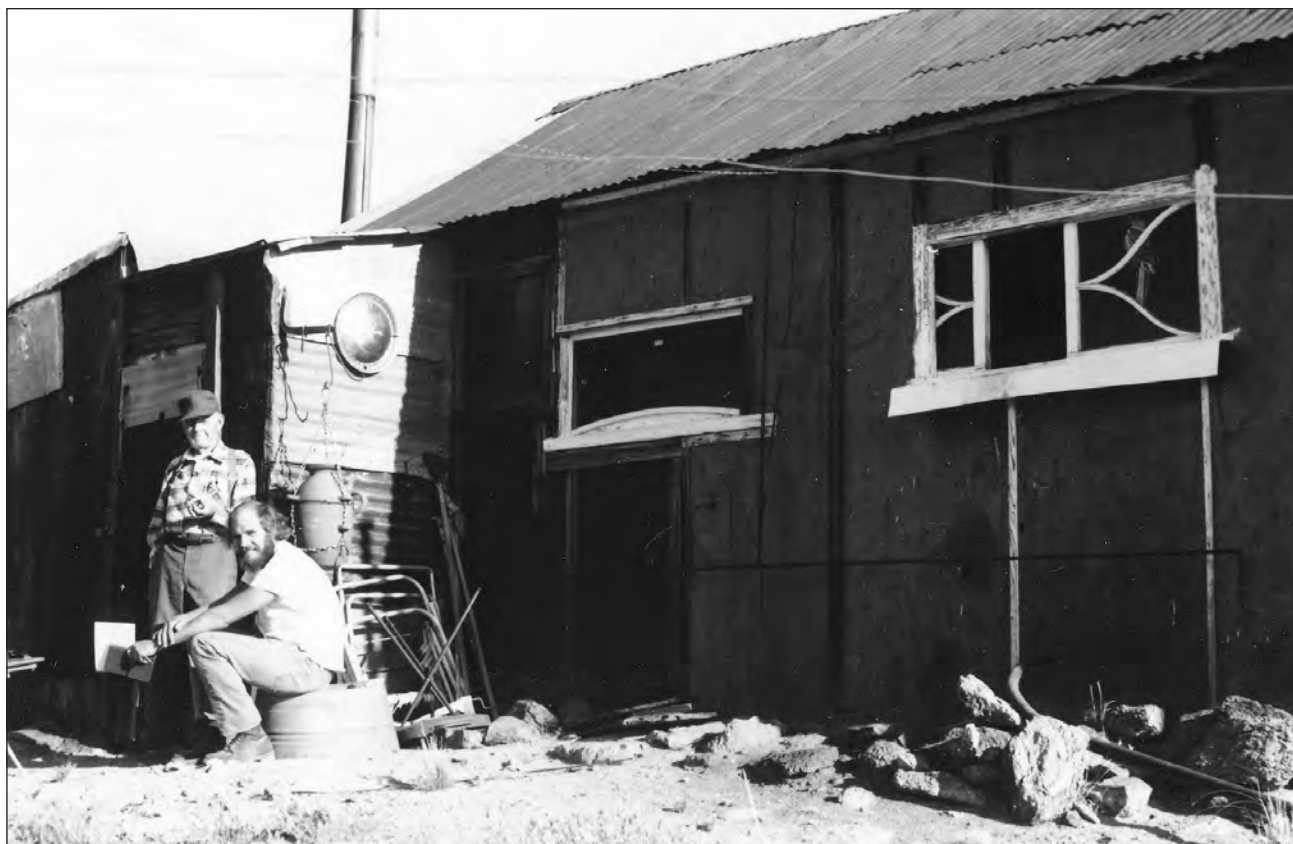
when do I get them ?..?

Maybe a gentle nudge in the developers postarior with a no IO boot will get tham on the way,

Its IO degrees hotter'n hell,

Thanks in Advance.

J. Riley Bemby



J. Riley Bemby and Quintin Lake (seated), Riley's Camp near Cima, 1981.



Evening Star mine, south headframe, 1967.



Evening Star mine, headframe, 1968



Evening Star mine, truck with Jennifer Flesher, 1967.



Evening Star mine, generator, 1967.



Bill Nye mine,
Goodsprings
district. *Lead, zinc,
copper, silver, gold.*
Production from
1914.

All images 1967.





Potosi mine, Goodsprings district. *Zinc, lead, silver, gold, copper, uranium*. Production from 1913.

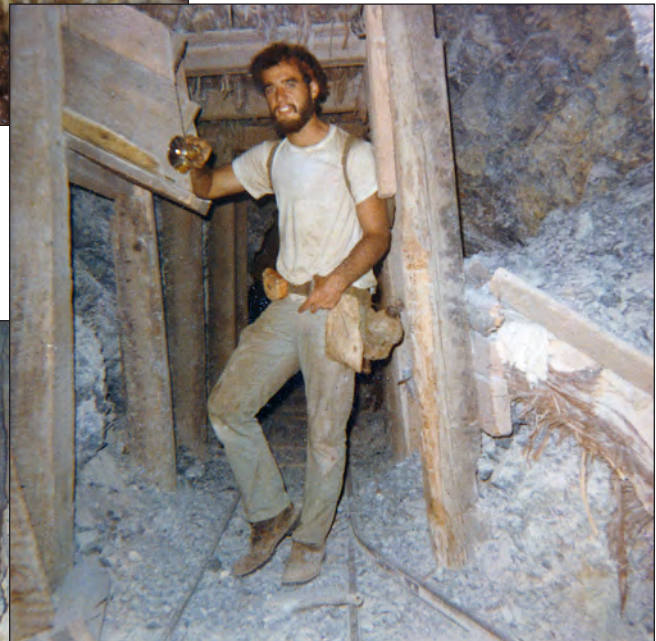
Above, tracks leading from mine to the loader, 1967.

The most memorable mine in the Goodsprings district that I ever explored was the Argentina. Its several levels were accessible, and it looked like it could start up again at any moment: ore cars on the tracks, and huge ore buckets still hanging from the tramway lines leading down from the mine. It had been set up as a civil defense shelter and some of the larger stopes were still piled with folded cots, canned water, and crates of “Nutriwafer” survival biscuits (they looked like hardtack and tasted like you forgot to remove the wrapper).



Stonewall Jackson mine, Clark Mountain district. *Copper, gold, lead, silver.*

Inside the mine in 1965: Bob Reynolds (below); Dion Dyer (lower left).





Copper World mine, Clark Mountain district. *Copper, lead, silver, and gold* 1906-08, 1916-20, 1944; *“Royal Gem Azurite”* in 1977.

All images on this page: 1968.





Left, Copper World tunnels at chrysocola cut, 1977.

Center, heavy equipment at chrysocola cut, 1978

Below left: chrysocola cut, 1988. *Sugar White photo.*



Route to the Copper World mine, 1968, likely still littered with VW parts.



Rosalie (Valley Wells), 1968. The 1918 mill site and smelter for the Copper World mine and (perhaps occasionally) the Mohawk mine.

We often camped at Valley Wells in 1967 and 1968 while collecting Pleistocene fossils for the San Bernardino County Museum. Paul Ink, who told us he lived at Rosalie as a caretaker, was a frequent visitor to our campsite, sharing improbable tales and borrowing food and beverages. Paul was convinced that he was a Publishers Clearinghouse winner and promised to pay us back for the supplies as soon as he received his million-dollar check.



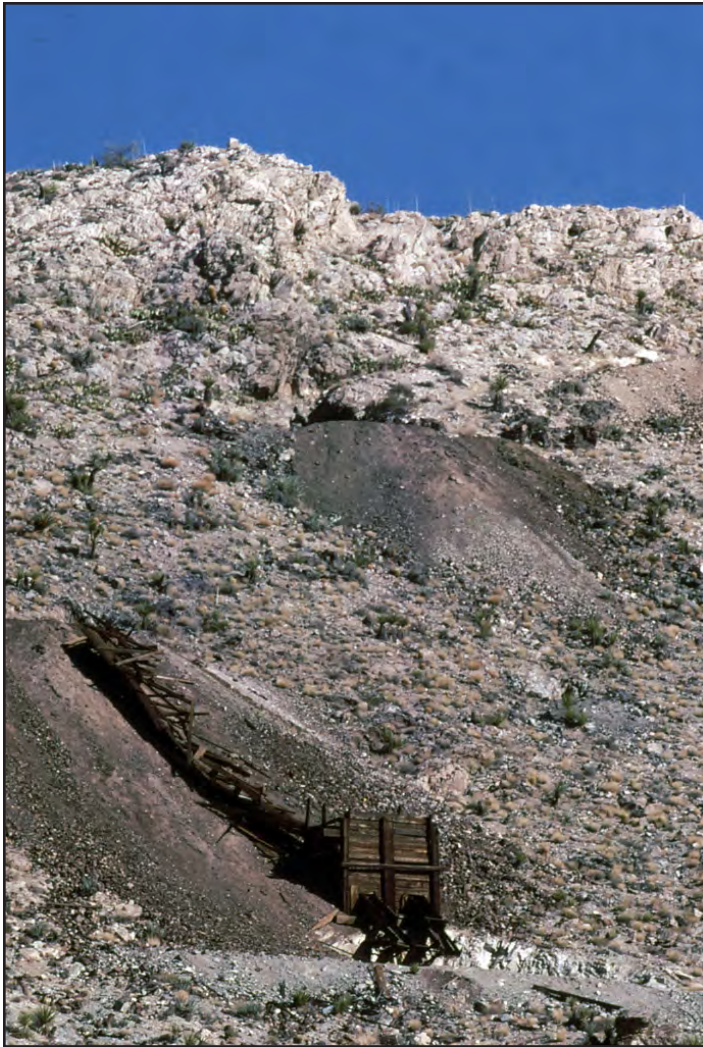
Valley Wells copper smelter, 1991.



Valley Wells copper smelter, 1968.



Dugout cabins at Valley Wells, 1968.



Mohawk mine, Clark Mountain district.
Zinc, copper, silver, lead, gold. Pre-1900 to
1921, 1944–1952.

Left, mines and structures on the
south-facing slope of Mohawk Ridge,
1971.



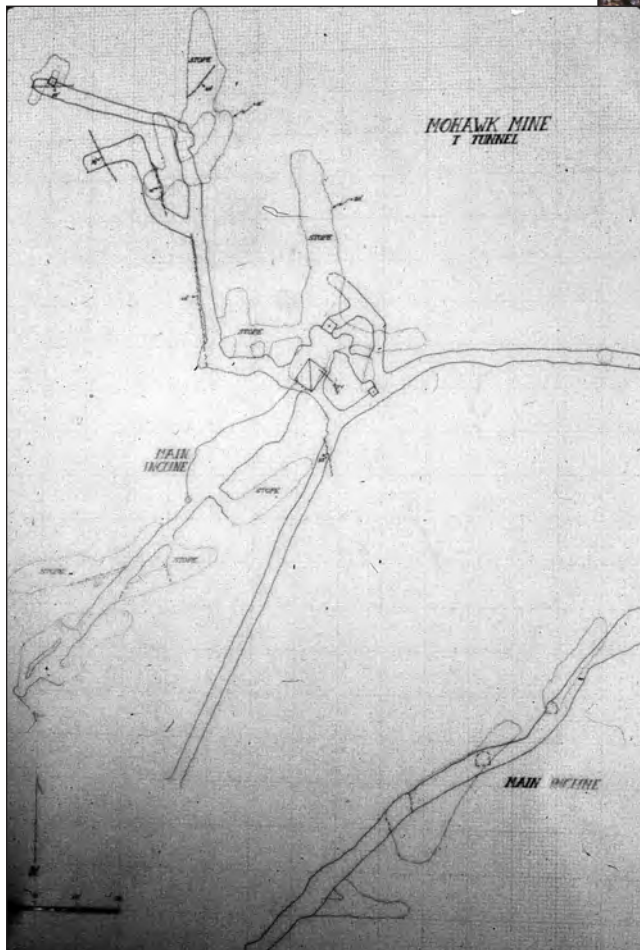
Jenny, Jed, and
Kate Reynolds
collecting empty
dynamite boxes.
Mohawk mine,
south-facing ridge,
1979.



Mohawk Ridge, 1971.



Mohawk mine, south-facing ridge, 1968.



Loading chute, Mohawk mine, 1968.



Mohawk mine, 1986. Jed Reynolds (standing).



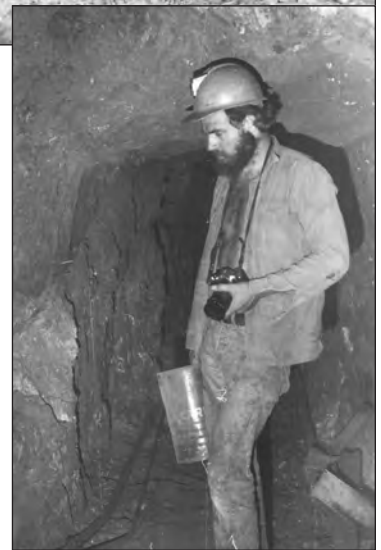
Mohawk mine, 1971.



Mohawk mine, 1967, Grant Richards after a day of collecting.



Mohawk mine, 1971, view easterly.



Mine on the north side of Mohawk Ridge, circa 1980. Top right, loading bin; right, Quintin Lake inside the mine; below right, Bob Reynolds at mine shaft entrance; left, ladders and ore car tracks leading up the mine shaft.

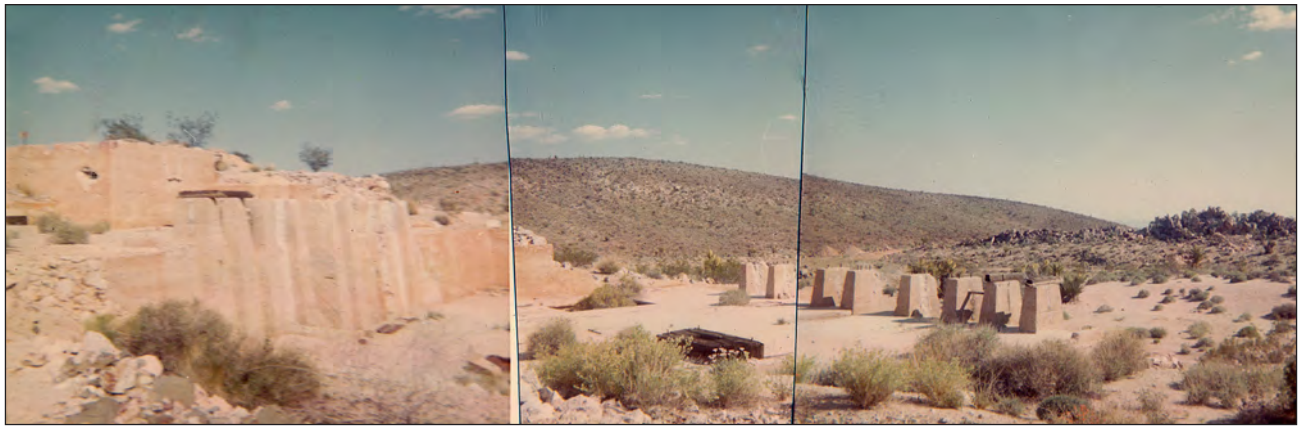




True Blue mine, Bobcat Hills near Vontrigger. *Gold, copper*. 1890s.

All images 1968.

In 1968 a very suspicious Fish and Game ranger arrived as I was preparing our morning meal. He quizzed everyone outside about their intentions, and then crept up to the cabin where I was standing inside by a window opening, scrambling eggs. I saw the crown of his hat appear at the bottom of the window frame; it slowly rose up until I saw his forehead and then his eyes—about three feet away from my skillet. “Just what are you cooking?” “Eggs.” “Eggs?” “Chicken eggs.” Once that was established, he joined us for breakfast.



Leiser Ray mine and mill, Signal Hill, Vontrigger mining district. *Copper, gold, zinc, tungsten, silver; vanadium* ore was shipped during World War I. Top image, mill site 1987. Above, mine entrance and dumps, 1970s.

We were searching for vanadinite specimens and instead found the then-owners of the Leiser Ray. They invited us to look around inside the mine entrance: no vanadinite, but some attractive, tiny, lime green descloizite crystals.



Golden Quail claims, Lanfair Valley. *Gold*.

image ca. 1979

One of the open vertical shafts here was a reliable spot to see a barn owl nest and chicks.



Noonday mine, Tecopa. *Gold, copper, lead, silver, zinc.* From 1907.

Images ca. 1985.

Illuminating the Waterloo silver deposit in three-dimensions using multi-element data

C.E. Fitzgerald,¹ C.S. Gallagher,² and W.T. Pratt³

¹Apollo Silver Corporation, Vancouver, B.C., Canada. Email: cathy@apollosilver.com;

²Rogue Geoscience Inc., Kimberley, B.C., Canada;

³Specialised Geological Mapping Ltd., Moray, United Kingdom.

ABSTRACT — The Waterloo deposit is a stratiform disseminated silver and gold deposit, one of 50 silver occurrences within the historic Calico silver mining district, part of a northwest-trending belt of precious metals locales related to Tertiary volcanic centers in the Mojave Desert of California. Unlike most occurrences at Calico, which are hosted in faults and veins in volcanic rocks, Waterloo is a stratiform, disseminated style deposit hosted within the finely laminated siliceous sediments and sandstones of the lower Barstow Formation (Miocene). The deposit is interpreted as a syngenetic, hot spring and replacement type formed in an active non-marine sedimentary basin, strongly controlled by faulting.

The Waterloo deposit was acquired by Apollo Silver Corporation in 2021 and soon after a preliminary estimate of the silver mineral resource was published. Since then, the primary objective for the company was to recalculate and improve the confidence in the estimate using new geologic mapping, drilling and a refined three-dimensional (3D) geological model. This was accomplished in early 2023, and using the new 3D model, the company declared a silver mineral resource of 110 million oz at a higher confidence level than that disclosed in 2022. For this work there was a strong emphasis on using new mapping, new tools, and multi-element chemistry to produce a more robust and geologically refined model. Multi-element chemical data was critical for improving the understanding of this exceptional deposit. The data had several uses including identifying key elements that fingerprint contacts not identifiable visually; highlighting key stratigraphic horizons such as exhalite zones, beneath which most of the silver mineralization occurs; and identifying important vectors toward silver and gold mineralization, allowing real-time targeting of mineralized horizons using a portable X-Ray fluorescence tool (pXRF). Further, Gaussian mixture modeling using historic geochemical data highlighted numerous laterally continuous horizons that form a “chemostratigraphy” that roughly parallels the modeled surface bedding planes. This work highlights the folding of silver- and gold-mineralized rocks at Waterloo and helps map strong geochemical zonation within the lower Barstow. The numerous key relationships identified using multi-element geochemical data support previous geologic hypotheses and establish new ones. A much better understanding of these relationships allows for highly efficient exploration not only at Waterloo, but also of similar style deposits.

Introduction and work history

The Waterloo deposit is a stratiform disseminated silver and gold orebody with some fault-hosted higher grade mineralization. It occurs within the lower Barstow Formation in the historic Calico silver mining district, near Barstow, California. It is located on private land owned by Apollo Silver Corporation (Apollo), approximately 1 mile northwest of Calico Ghost Town. Apollo acquired the land in 2021 from Pan American Silver Corporation, along with the adjacent Langtry property (option to earn 100% ownership), which hosts a similar silver deposit (Figure 1), combining the deposits under a common operator for the first time.

The Calico district has a long history beginning with mining between the 1880s and 1890s (a reported 15–20 million oz [Moz] of silver extracted), well documented by many authors (including Lindgren, 1887; Storms, 1893; Storms and Fairbanks, 1965; Weber, 1966; Weber 1967a

and 1967b; Harthrong, 1983). The mineralization, geology and tectonics of the broader region have also been well studied (Lindgren, 1887; Storms 1893; Erwin and Gardner, 1940; DeLeen, 1950; McCulloh, 1965; Weber, 1965; Dibblee 1970; Tarman and Thompson, 1988; Dokka, 1986; Dokka and Travis 1990; Woodburne et al., 1990; Singleton and Gans 2008; Jessey, 2014). Waterloo is amongst more than 50 silver occurrences in the district, which is part of a northwest-trending belt of precious metal districts related to Tertiary volcanic centers (Lindgren, 1887; Weber, 1966, 1980). Over the last 130 years, interest in the geology and mineralization of the district has not waned.

Most silver occurrences in the Calico district comprise northwest-striking mineralized faults and veins with silver-barite, mostly hosted by rhyolitic tuffs and andesite lavas, pyroclastics, and breccias of the Tertiary (~24–19 Ma) Pickhandle Formation (Singleton and Gans, 2008). Supergene enrichment was important for enhancing silver

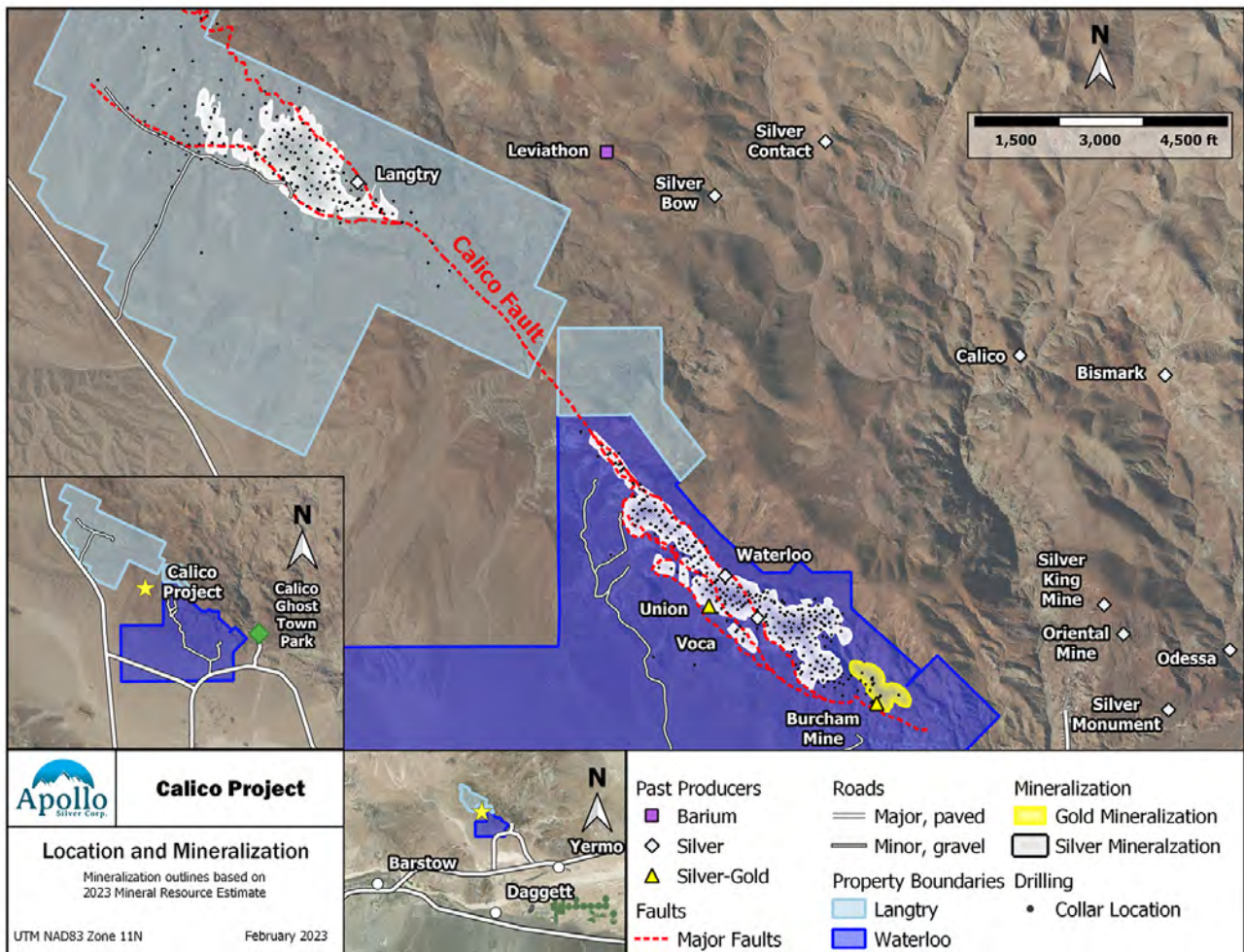


Figure 1: Calico Project, highlighting the Waterloo and Langtry properties and silver deposits.

grades. Waterloo and Langtry are unique in the area because they are stratiform, disseminated ore deposits, hosted by the Barstow Formation, which overlies the Pickhandle Fm. These sedimentary rocks include finely laminated siliceous sediments (“cherts”) of probable hot spring origin. Silver is fine grained, primarily oxidized, mostly as native silver, silver salts (Cl, Br, I), supergene acanthite and lesser argentojarosite. It is hosted by the “cherts” and also in interbedded, variably barite and adularia-altered sandstones, siltstones and minor tuffs. Disseminated gold is also present at Waterloo at the contact between the Barstow and Pickhandle formations. Northwest-striking, steep mineralized faults, similar to those in the Pickhandle, also occur within the Barstow Formation sediments; these host some high grade silver (up to 1,600 g/t) and gold (up to 211 g/t). They were reportedly mined underground in the late 1800s (silver at Waterloo, Union and Voca mines) and 1940s (gold at Union and Burcham) (Figure 1). An estimated 6.4 Moz of silver was extracted from Waterloo mine and 70,000 oz of gold from Burcham (Fletcher, 1986). Recent work by Apollo and Pratt (2022) shows that the Waterloo mine, one of the largest in the district, also targeted the

mineralized, brecciated and variably faulted contact between the Barstow and Pickhandle formations.

Despite the period of intense mining in the late 1800s, the stratiform disseminated deposits were not discovered until the 1960s. The discovery of Waterloo (1965 by ASARCO) and Langtry (1964 by Superior Oil Company) triggered new exploration in the Calico Mountains. Between their discovery and 2012, there was significant exploration at both. This included ground geophysics (magnetics, electromagnetics, gravity and induced polarization (IP) in the 1970s); surface and underground grab sampling, surface trench bulk sampling for metallurgical test work, drilling (272 reverse circulation (RC) drill holes (62,024 ft) and 11 diamond drill holes (2,487 ft); and detailed and extensive surface mapping (Kirkpatrick 1965; Watson, 1968; Smith, 1977; Fletcher, 1986; Pratt 2008, 2012). Several researchers also completed studies at Waterloo (Mayo, 1972; Jessey, 2014; Jessey and Tarman, 1994; Schuiling, 1999; Strom, 2003 among others). Work by ASARCO culminated in a mining permit for Waterloo in 1980, valid for 24 years, but the mine was never developed. After 2012, no work was undertaken on the properties until Apollo acquired them in 2021.

Apollo undertook a comprehensive desktop review, organizing and validating the historic data. The objectives were to better understand the exploration history and district geology, to create a 3D geologic model, and to produce the first public silver resource estimate. In February 2022, Apollo published an inferred mineral resource estimate for the combined Waterloo/Langtry properties (the “Calico Project”). This comprised 166 Moz of silver in 64.1 Mst at 2.59 opt (troy ounces). Of this, Waterloo comprised 116 Moz of silver in 42.8 Mst at 2.71 opt (troy ounces) (Loveday, 2022). The preliminary 3D model and this early resource estimate were then used to optimize Apollo’s work in late 2021 and during 2022. The program comprised geophysical surveys (ground 3D IP and resistivity, drone magnetic survey); detailed geological mapping and sampling (Pratt, 2022); and an RC drill program (88 holes/32,283 feet) at Waterloo. The objective was to refine the geological understanding of the deposit, with a strong emphasis on multi-element geochemistry, and produce a more robust 3D model that could be then used to produce a more confident silver resource estimate. This was accomplished in March 2023, when Apollo declared a more confident silver mineral resource estimate of 110 Moz of silver in 37.7 Mst at an average grade of 2.93 oz per ton (opt) in the measured and indicated categories.

Apollo’s work at Waterloo benefited greatly from the excellent historic work of many workers, including historic drilling (Pan American Silver Corp., and ASARCO), surface mapping and cross sections by Fletcher (1986), Pratt (2008 and 2012), and many other publications.

Geology

This central region of the Mojave Desert experienced widespread volcanism during late Oligocene–Early Miocene (24 to 19 Ma) crustal extension (Dokka, 1986; Dokka and Woodburne, 1986; Woodburne, 2015). This deposited the andesite lavas and felsic pyroclastics of the Pickhandle Formation, which now forms much of the Calico Mountains. Between approximately 19 and 13 Ma there was extensive non-marine sedimentation related to Basin and Range-type extensional faulting (Singleton and Gans, 2008; Miller et al., 2013; Woodburne, 2015). The Barstow sediments were deposited in this interval. Post-Barstow andesitic and dacitic volcanic rocks (~17.1 to 16.8 Ma) sit unconformably on the Pickhandle and Barstow formations at the southern end of the Calico Mountains (Dibblee, 1970, Singleton and Gans 2008). Because hydrothermal alteration has been dated at ~17 Ma at Waterloo (Fletcher, 1986), this suggests a link between Post-Barstow volcanism and mineralization (Tarman and Jessey 1989; Jessey, 2014; Pratt, 2022).

The 19 to 17 Ma window was clearly critical, with emplacement of late dacite domes, strong extension, rapid erosion, sedimentation, and silver-gold mineralization. This was followed by periods of further erosion and deformation, largely by regional strike-slip faulting and

transpression along major northwest-striking dextral faults, such as the Calico fault, and west-striking sinistral faults, such as the Manix fault (Dibblee, 1961; Garfunkel 1974; Dokka and Travis 1990; Glazner et al., 2002). These faults are largely responsible for the fragmented nature of an originally extensive, stratiform silver orebody between Waterloo and Langtry. The Calico fault shows a flexure (restraining bend) at Waterloo; this caused transpression and reverse offsets (Pratt, 2022). It also caused intense folding of the Barstow sediments, with beds becoming overturned close to the fault, on both foot- and hanging-walls (Singleton and Gans, 2008; Tarman and Thompson, 1988). Oskin et al. (2007) noted a threefold drop in slip rate of the Calico fault, with strain in the restraining bend distributed into folds and faults in the Calico Mountains. The Barstow Formation at Waterloo forms a NW-plunging anticline, meaning the deepest portions and the contact with the Pickhandle Formation occur at the Burcham mine (Figure 2). Erosion has removed the stratiform silver mineralization at Burcham.

At Waterloo, the Barstow-Pickhandle contact seems mostly conformable but is faulted and brecciated in some places (Pratt, 2022). Mapping and core logging by Fletcher (1986) and Pratt (2008, 2012, 2022) identified three main lithostratigraphic units above the Pickhandle. These are the lower and upper Barstow Formation (Tertiary) and the poorly consolidated Yermo Formation gravels (Quaternary) (Figure 2). The Barstow Formation, comprising fluvial and lacustrine sandstones, siltstones, and cherty mudstones (Fillmore and Walker, 1996; Ingersoll et al., 1996; Jessey, 2014; Pratt, 2022) is split into lower (mineralized) and upper (non-mineralized) units. The lower Barstow is further split into 1) a basal pebbly tuffaceous sandstone/conglomerate, with biotite, granitoid, schist and volcanic clasts (Figure 3c). This may be the Owl Conglomerate Member, mapped in the Mud Hills (MacFadden et al., 1990; Woodburne et al., 1990; Ingersoll et al., 1996; Murray and Hames, 2021); 2) well-bedded sandstones/siltstones with variable tuffaceous material; 3) an upper mixed assemblage including cherty, silver-mineralized sediments (“cherts”) and sandstones (Figure 3a and 3b) (Pratt, 2022). Some of these sandstones form major, non-bedded, barite-adularia-rich slumped and disturbed beds up to 30 m thick, forming distinct topographic ledges. Rare shelly (non-marine) fossils occur in these sandstones.

Syn-sedimentary slumping is widespread in Lower Barstow. This reflects contemporaneous strong extension and nearby active fault scarps, possibly including a precursor of the Calico fault. These scarps shed a mix of volcanic (Pickhandle?), plutonic, and metamorphic debris. There are also common sandy phreatic breccias and sand dikes, originally feeding sand volcanoes (Figure 3b). Both are classic features of geothermal districts. The sediments were probably deposited in alluvial fans and braided rivers. At times clastic input waned and evaporitic lakes formed. These produced stromatolites and tufa-coated

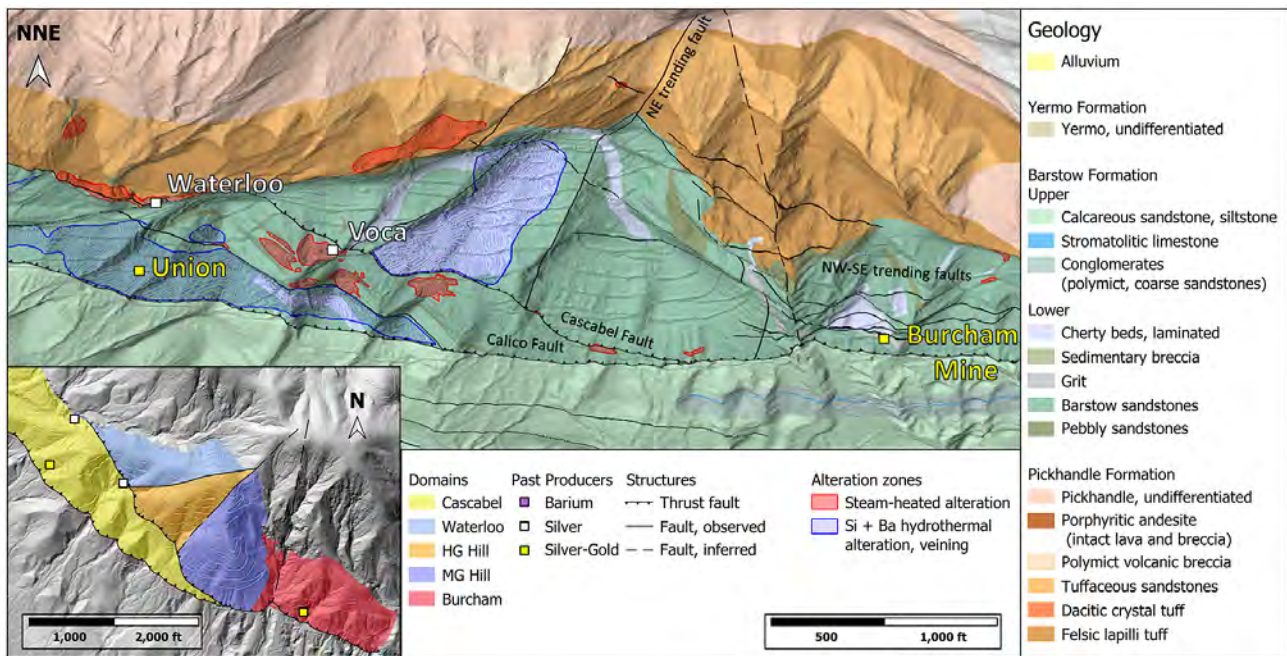


Figure 2: Geological Map of the Waterloo Property.

branches in swamps. Some of these lakes were clearly oversaturated with silica and contain algal mats and pisoliths. These cherty, laminated sediments (“cherts”) resemble sinter and suggest a hot spring origin (Figure 3a). This interpretation is reinforced by the contained silver mineralization and widespread disseminated silver sulfides + barite. Thin sections (Pratt, 2012) clearly show barite crystals growing during accumulation of these siliceous hot spring deposits.

The upper Barstow, mostly cropping out in the Calico fault footwall, but also present in the hanging wall northwest of Langtry, comprises distinctly coarser and less well consolidated conglomerates, boulder beds (with metamorphic clasts) and brown pebbly calcareous sandstones. There are also widespread green calcareous and smectitic sandstones and siltstones. There are some thin beds of very distinctive tubular stromatolitic limestone. Disseminated gypsum is widespread, suggesting evaporites are present.

The Calico fault comprises a zone of anastomosing, sub-parallel, mostly northeast-dipping faults with some exhibiting friable, white, possible steam-heated alteration (Figure 3d). These faults dissect and bound the stratiform silver deposits at both Waterloo and Langtry.

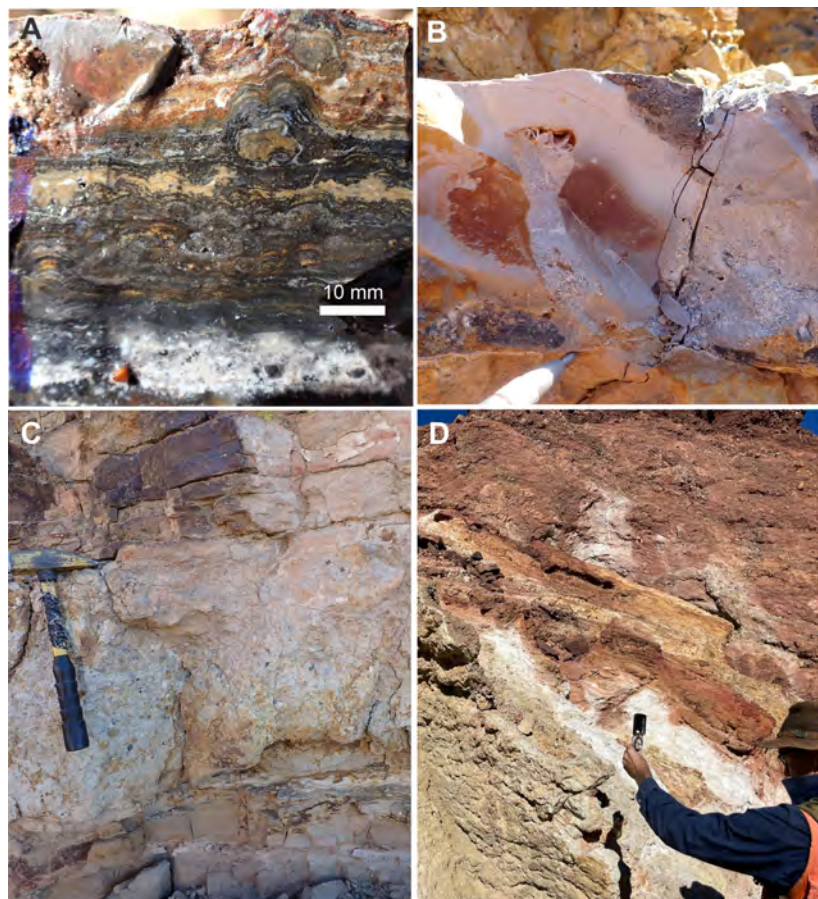


Figure 3: Key textures from Waterloo: (A) Laminated cherty algal mats with convex-upward growth. Note “pisoliths” with concentric chalcedony coats. Dark color comes from >5% disseminated marcasite or pyrite. (B) Cherty mudstone/siltstone cut by sandstone dikes with open (geopetal) spaces filled with barite. This is clear evidence of phreatic activity. (C) Lowermost Barstow Formation pebbly conglomerate bed, close to the contact with the Pickhandle. This is the gold host at Burcham. (D) Steam-heated alteration (?) along the Calico fault.

The principal strands are the Calico thrust fault, and two sub-parallel splays (Cascabel Northeast and Southwest) (Figure 2). The fault system was reactivated after silver mineralization; it effectively thrusts the mineralized lower Barstow southwest over the upper Barstow footwall. The absence of stratiform silver mineralization between Waterloo and Langtry reflects subsequent erosion of the Barstow Formation. (The geometry is not the result of strike slip offset.) There are also several post-mineralization northeast-striking faults that have apparent normal offsets. These faults appear to offset mineralization, but the offsets are much smaller. They usefully define five structural domains at Waterloo: HG Hill, MG Hill, Waterloo, Cascabel and Burcham (Figure 2).

Mineralization and alteration

We recognize three types of mineralization at Waterloo:

1. Northwest-striking, high-angle mineralized faults/veins within the Pickhandle (Jessey, 2014) and Barstow formations. These were targeted by the historic mines mentioned above.
2. Stratiform and disseminated ore within the siliceous and adularia/barite-altered lower Barstow Formation. This hosts mostly silver, with some anomalous gold. This stratiform orebody is cut at HG Hill by abundant sinuous, branching epithermal-type veins, with crustiform and colloform chalcedony, barite, and calcite. These veins clearly developed very close to the paleosurface, with low confining pressure. The stratiform mineralized body has a strike length of more than 6,500 ft, measured NW-SE, and is up to 1,640 ft wide.
3. Disseminated gold at the contact of the Barstow and Pickhandle formations. This was also targeted for mining at the Waterloo and Burcham mines; our surface mapping supports that this contact was a hydrothermal fluid upflow zone.

All three types probably formed in a single event; the paragenesis of the silver mineralization is similar (Tarman and Jessey, 1989; Jessey, 2014; Fletcher, 1986). Four stages of mineralization and alteration were identified with the bulk of silver mineralization

occurring in the silver-silicification stage (Fletcher, 1986). We interpret the stratiform deposit to be hot-spring, low sulfidation epithermal type with replacement mineralization, as do several others (Schuiling, 1999; Jessey, 2014; Pratt, 2008, 2012, 2022). The evidence for syngenetic mineralization is persuasive. Fletcher (1986) also suggested a syngenetic origin, with mixing of hydrothermal fluids and connate waters beneath a lake. The steep mineralized faults/veins in the Barstow and Pickhandle formations are interpreted as feeders to the hot springs.

Two K-Ar radiometric dates from altered wall rocks constrain the hydrothermal event to 17 Ma (Fletcher, 1986), contemporaneous with the deposition of the Barstow sediments and extrusion of the nearby dacite domes. Fluid inclusion work by Fletcher (1986) on barite crystals supports this; he identified formation temperatures of 185–195°C and determined that they formed at depths of less than 100 ft below the surface. Recent petrography and mapping confirm widespread adularia alteration of detrital grains and minor illite/sericite, typical of low-sulfidation epithermal deposits.

Chemostratigraphy

Whole rock X-ray fluorescence (XRF) geochemical analyses are expensive and time consuming to complete and there is little historic data of this type from Waterloo. Apollo investigated other ways to assess rock geochemistry, notably ICP-OES/MS (with a four-acid “near-total” digestion) and portable XRF. To do this we submitted samples for whole rock analysis from the lower Barstow using three historic diamond drill holes

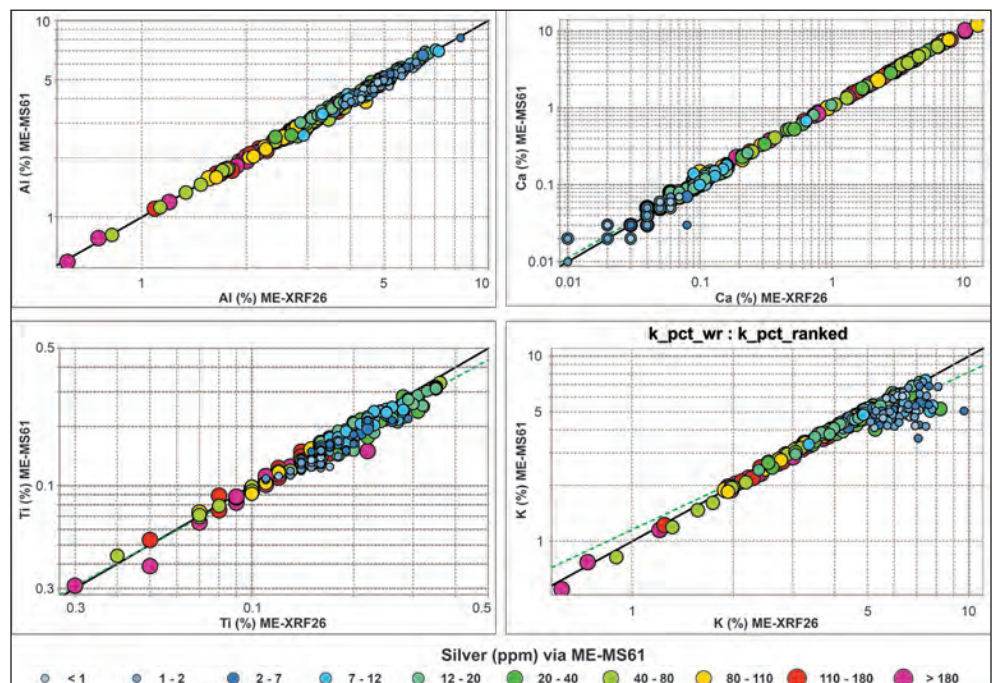


Figure 4: XY plots of whole rock major element data vs. four-acid ICP data for selected elements classified by silver (ppm) (lower Barstow samples). Ca and Al have a one-to-one relationship, whereas Ti and K show a negative bias in four-acid ICP data at low silver values.

and four of the 2022 RC holes. The new whole rock results compare very favorably with the four-acid ICP data and pXRF results (Figure 4). The 2022 drill program collected 4-acid ICP data from all samples, and pXRF from approximately one third of samples. Armed with the confidence of results from the different analytical methods we then used immobile elements from the four-acid ICP data to identify original lithologies and try to quantify subsequent hydrothermal alteration. The four-acid ICP data also allowed for the assessment of associations between, amongst other things, major elements and silver/gold. Figure 4 shows the excellent correlation between whole rock and four-acid ICP data for Al, Ca, Ti and K. Simple XY plots for each element from the two analytical methods show excellent correlation between Ca and Al. Ti and K show a slightly negative bias at lower silver values. These plots also illustrate several element populations, such as that for K, showing a separate population at low silver values. They also show the relationships between these elements and silver (e.g., high silver correlates with lower Al, Ti and K).

We used the new geochemical data to refine the 3D geological model, initially by coding downhole lithology based on RC logging and then by creating probability plots to characterize the relative values of key immobile elements for each lithology. By plotting ratios of these elements, the lithologies can be fingerprinted. For example, Barstow rocks can be distinguished from Pickhandle rocks because the latter rocks have a much higher Al/V ratio (Figure 5). Plotted in 3D, the high Al/V ratios correlate well with the inferred Pickhandle/Barstow contact in historic cross sections (Fletcher, 1986; Pratt 2012).

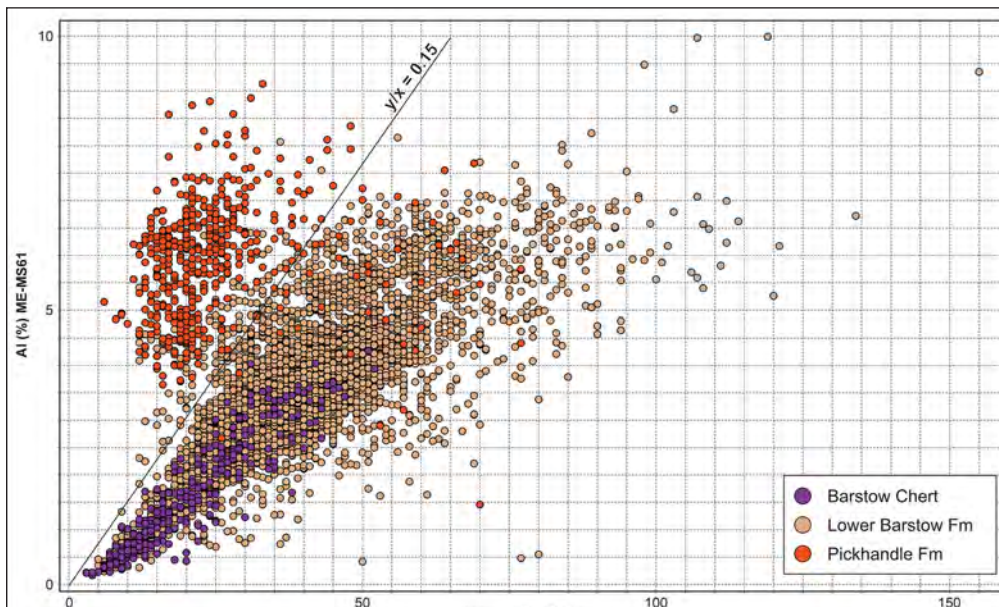


Figure 5: XY Plot of Al vs. V showing clusters defined by the Pickhandle and Barstow Formations. An Al/V ratio of 0.15 is utilized to discriminate the two rock types. Note that the “chert” population is characterized by overall low Al and V concentrations.

The absolute abundance of elements such as Th, Al, Ti, and Sr clearly identify potential exhalite/replacement zones. These are zones (probably stratigraphic units) where primary concentrations were initially very low, or subsequently leached by hydrothermal alteration. Figure 6 is an XY plot of Sr against selected elements, color-coded by silver values. This plot shows: 1) negative correlation between Sr and other immobile elements; 2) negative correlation between silver and immobile elements; and 3) an inverse correlation between silver and Sr. (*We consider Sr to be a good proxy for Ba (interpreted to be primarily hosted in barite), which tends not to dissolve in four-acid digestion.*) These populations of low immobile elements seem to be replacement zones and are dominated by Si and Ba (+Sr). They form discrete, mostly bedding-parallel horizons, up to 25 ft thick, in the upper part of the lower Barstow, up to HG Hill and MG Hill. The highest silver values are not clearly associated with these low immobile element zones, nor with the highest Sr values. Instead, they occur in the transition from high to low immobile concentrations and with low to moderate Sr values. It is important to emphasize therefore that the bulk of silver mineralization at Waterloo does not occur in the hot spring (“chert”) beds, but in sandstones beneath.

Gaussian mixture modeling

Unsupervised Gaussian mixture models (GMM) are a statistical analysis tool that can identify distinct groupings of elements in geochemical data. These clusters can then be used to better understand relationships between samples and interpret processes that may produce the clusters. GMM use a silhouette score which is a commonly used evaluation metric for clustering algorithms. It measures the similarity of an instance (data point) to its

own cluster compared to other clusters and determines the optimal number of clusters to use. The score is calculated for each instance as the difference between the average intra-cluster distance and the mean nearest-cluster distance, divided by the greatest of these two values. Scores range from -1 to 1. A high value indicates that the instance is well matched to its own cluster and poorly matched to other clusters. Low values indicate the opposite. The average score over all instances is used as a

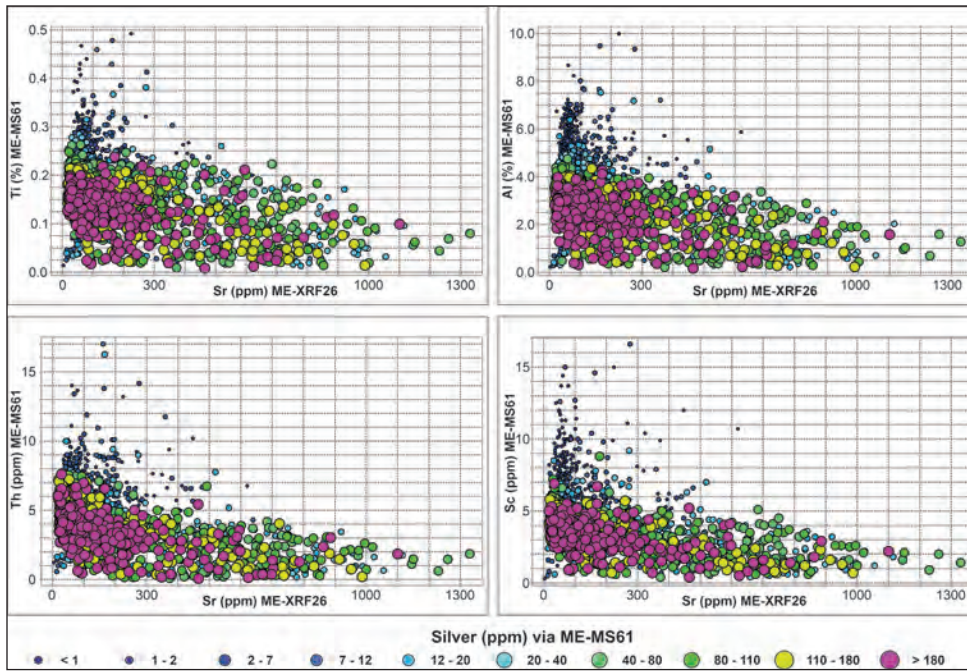


Figure 6: XY plot of selected immobile elements vs. Sr from the lower Barstow.

global performance measure for the clustering solution: a high average silhouette score indicates that the clustering solution has identified well-separated and dense clusters.

GMM analysis was completed using four-acid ICP data from historic drill samples to assess potential geochemical and spatial trends not obvious via the chemical analyses discussed above. The historic data were used because our GMM analysis was completed before 2022 drill assays were received. Furthermore, Apollo planned to use GMM as a predictive tool during ongoing drilling. The analysis was completed within the HG Hill, Waterloo, and Cascabel domains, using elements typically associated with low sulfidation hydrothermal systems (Ag, Au, Bi, Cu, Fe, Mn, S, Sb, W, As, Mo, Pb, and Zn). GMM shows four clusters were optimal for the dataset, with each sample coded with one of four numbers (a class or cluster) (Table 1).

Each GMM cluster shows a unique multielement geochemical signature and highlights geochemical zonation at Waterloo, consistent with the zonation commonly encountered within low sulphidation deposits. When clusters (classes) for each sample are plotted

Table 1: Gaussian mixture model classes for the Waterloo deposit

Class	Highly Elevated	Elevated	Low	Highly Depleted	Interpretation
0	None	Ag	Fe, Mn, Sb, As, W	None	Elevated silver, and low concentrations of volatile elements. Above background gold to 0.1 g/t and gold associated elements
1	Sb	Ag, S, As	Mo, Zn	Au, Cu, Pb	Upper volatile element-rich population with highly elevated Sb and As values with elevated silver and no gold.
2	Fe	Mn, Cu, Pb, Zn	S	None	Fe-rich, S-poor "oxide" zone highly elevated in Zn and Mn. Above background gold (+0.2 g/t).
3	Au, W, Pb	Cu, Mo, Bi	None	None	Most distinct population of all; gold-rich with igneous signature (W, Bi, Mo, etc.). Occurs at Barstow-Pickhandle contact.

downhole they define a zoned chemostratigraphy, comprising an upper volatile element-rich/silver-poor "cap", underlain by a silver-rich zone relatively depleted in volatile elements. Below this is a mixed zone of Fe-rich "oxide" and gold-rich magmatic signatures at the inferred contact between the Pickhandle and Barstow formations (Figure 7).

3D geologic model

A 3D model of Waterloo geology and mineralization was created in early 2022 using implicit modeling software (Seequent Leapfrog 3D®), a powerful

tool for subsurface visualization. The model relied on mapping data, former cross sections (Fletcher, 1986; Pratt, 2012 and 2022), and multi-element chemical data from historic RC drilling. Bedding measurements were useful for interpolating bedding in the subsurface and were used to bias the interpretation of silver distribution and to identify new structures. Modeling also leaned heavily on multi-element chemistry from historic drilling because it is difficult to interpret lithology, mineralization and structures from RC chips.

This preliminary 3D model was used to design Apollo's 2022 RC drill program. As drilling progressed and the suite of chemical elements expanded, certain trends were observed in 3D. This led to improved understanding of associations related to lithology and mineralization. Initially, during Phase 1 drilling, the model was updated iteratively as laboratory assay and multi-element data were received. During Phase 2, the model was updated in near-real time using the pXRF. This allowed for rapid model evolution, optimization of drilling, and for real-time decisions regarding grades and geologic interpretation.

RC logging data were captured, and key observations

incorporated into the model. Examples include possible faults, sulfide minerals, and significant changes in alteration. However, in many cases the RC chips appear almost identical on either side of the Pickhandle/Barstow contact; it is much easier to identify this contact

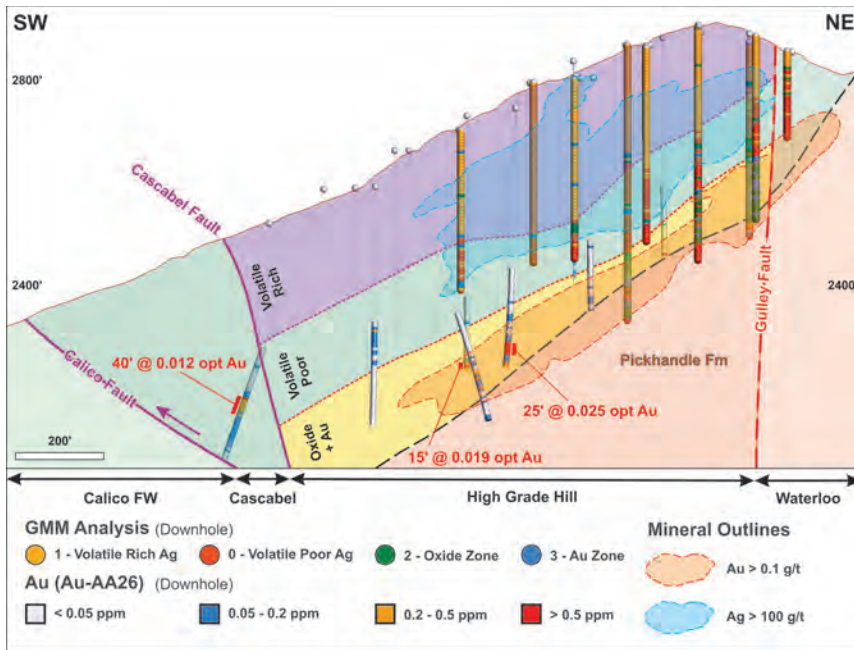


Figure 7: NE-SW cross section of HG Hill showing the three geochemical zones identified by GMM.

in multi-element data. Figure 8, a cross section through HG Hill, shows the primary and hydrothermal horizons. These include two 25 to 50 ft thick “chert” (+ barite) horizons that are above the 0.003 ounce per ton (0.1 g/t) gold grade shell. This correlates with the volatile-element rich horizon identified in the GMM model (Figure 7). Below this is a 250 ft thick sequence of mudstones, sandstones and rare fine conglomerates. This sequence hosts the bulk of the silver mineralization at Waterloo and corresponds with the Class 0 GMM cluster (Table 1). Below this is the mixed oxide/gold zone defined in the GMM cluster analysis (characterized by elevated Fe, base metals, and commonly gold, near the Barstow-Pickhandle

contact). Gold mineralization continues well into the Pickhandle Formation, remaining open at depth.

Conclusions

The Waterloo and Langtry silver deposits are interpreted as erosional outliers of a formerly continuous Miocene stratiform deposit. Hosted by the lower Barstow Formation, the deposit was of syngenetic, hot spring and replacement origin. It developed in a non-marine sedimentary basin, strongly controlled by active faults. Throughgoing mineralized faults in the Pickhandle volcanics, targeted by historic mining, are interpreted as feeders to this mineralization. We draw comparisons with the Navidad low sulfidation epithermal deposit in Argentina, which also encompasses the feeder vein/hot spring transition (Pratt and Ponce, 2011; Bouhier et al., 2023). As with

Navidad, at Calico there were periods of energetic fluvial sedimentation, which overwhelmed contemporaneous geothermal/hydrothermal activity. During quieter periods, lakes developed, and hot springs were active. There were probable geysers, sediment volcanoes and phreatic eruptions. Si-rich chemical sediments (“cherts”) were deposited, with algal mats, syngenetic barite, hydrothermal adularia and disseminated pyrite/marcasite/silver sulfides. However, most of the silver resource occurs in the adularia-barite-altered sandstones beneath the “cherts”. This may be of largely replacement origin. The fragmented geometry of the stratiform orebodies

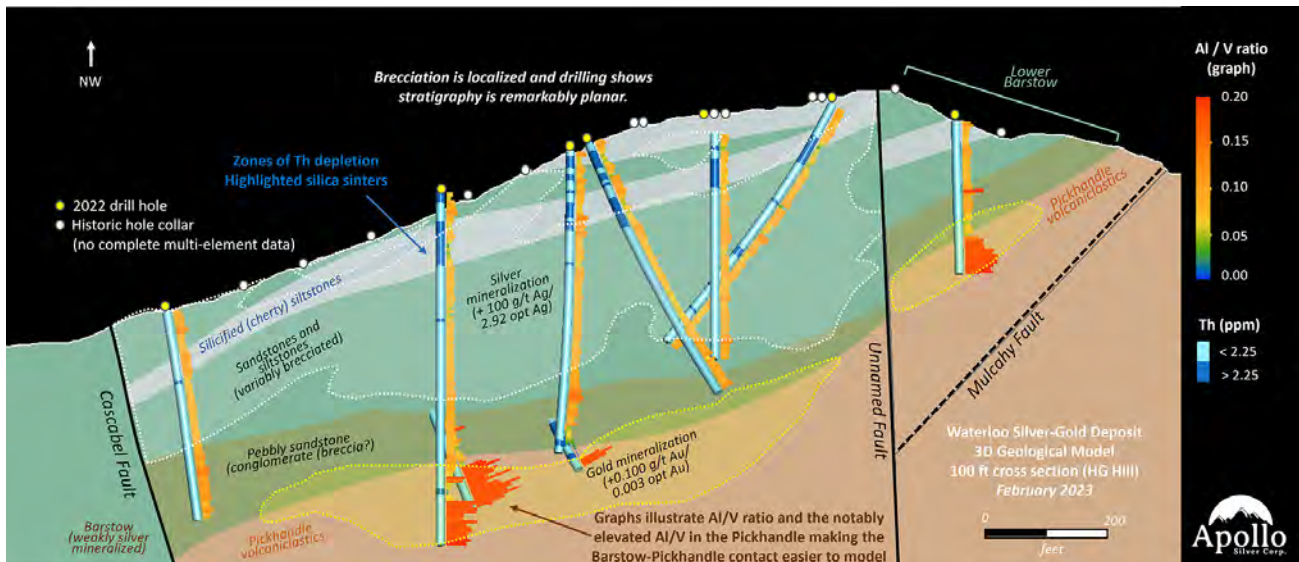


Figure 8: Cross section through updated Waterloo 3D model showing example of chemistry used to refine stratigraphy in the subsurface.

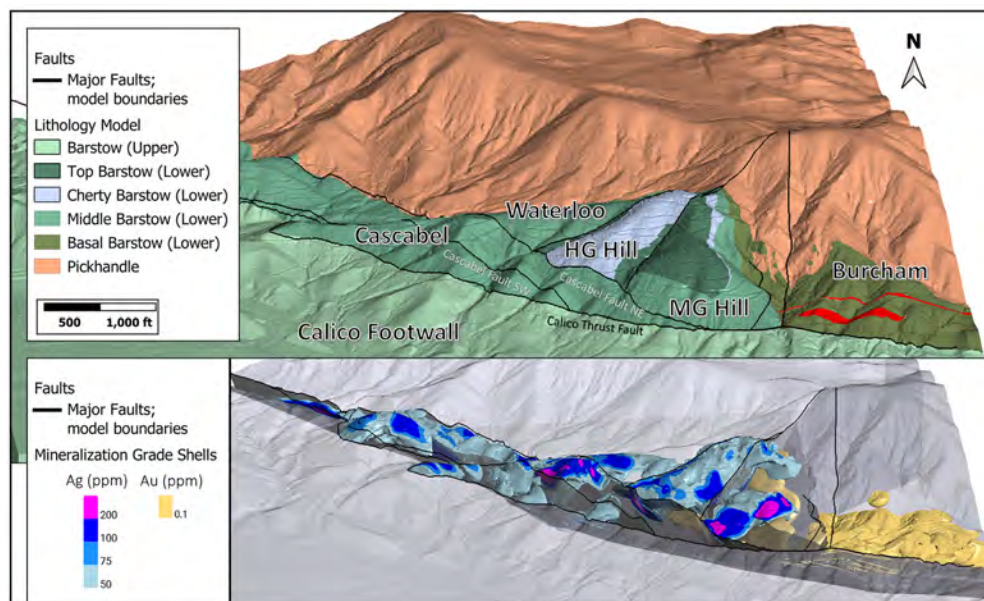


Figure 9: Updated 3D model of geology, structural domains and silver and gold mineralization for the Waterloo deposit.

reflects major post-mineral fault offsets, mostly reverse and southwest-verging, though some strike-slip cannot be ruled out, on the different strands of the Calico fault system.

Analysis of four-acid ICP data from both historic and new drilling at Waterloo helped refine the 3D geology. Four-acid ICP data compare very favorably with limited whole rock XRF data, greatly increasing the confidence in its use. Furthermore, this allowed for the confident use of pXRF while drilling was ongoing. Sample analysis in as little as 10 seconds per sample provided real-time feedback to enable near-real time decision making and geological model refinement.

Silver and gold mineralization at Waterloo is strongly zoned geochemically and has undergone significant deformation.

Multi-element chemical data were critical for understanding of this exceptional deposit with several key outcomes:

- key rock-forming and hydrothermal elements showed relatively large response ratios. These were then used to identify cryptic relationships between rock types that were not always seen in RC chips. For example, this improved confidence in the modeling the Barstow-Pickhandle contact;
- highlighted the stratiform “cherty” hot spring deposits at HG Hill and MG Hill;
- demonstrated disseminated gold mineralization along the Barstow-Pickhandle contact.
- identified important vector elements for gold (Pb, Cu) enabling the use of pXRF to highlight gold-mineralized horizons and undertake selective sampling for cost savings.
- improved confidence in inferred faults where offset is observed in “cherty” horizons.

GMM analysis was completed on historic four-acid ICP data and highlighted numerous laterally continuous horizons that form a “chemostratigraphy” that roughly parallels modeled subsurface bedding planes. They include:

- an uppermost horizon enriched in silver and volatile elements (Sb and As);
- an underlying volatile element poor horizon that hosts the highest silver grades; and
- a basal mixed zone that hosts both base metal oxides and gold-

bearing strata. This straddles the Barstow-Pickhandle contact.

Investigation with four-acid ICP geochemical data identifies numerous relationships that help establish new geologic interpretations and support hypotheses from previous workers. These interpretations, backed by an ever-growing dataset, allow for rapid and accurate geologic modeling of the system. In addition, a much better understanding allows for efficient exploration in the district for similar deposits.

Acknowledgements

The authors would like to thank Apollo Silver Corp. for permission to publish and host a site visit as part of the 2023 Desert Symposium. They would also like to thank Meagan Hogg for figure production.

Note: this scientific contribution does not represent technical disclosure by Apollo Silver Corporation and the authors take responsibility for the contents of this paper.

References

- Bouhier, V, Franchini, M, Tornos, F, Rainoldi, A. L., Partier, P, Beaufort, D, Boyce, A J, Pratt, W T & Impiccini, A. 2023. Genesis of the Loma Galena Pb-Ag Deposit, Navidad District, Patagonia, Argentina: a unique epithermal system capped by an anoxic lake. *Economic Geology*, 118, 433-457.
- DeLeen, J., 1950, Geology and mineral deposits of the Calico Mining District: Unpublished Master's Thesis, University of California-Berkeley, 86 p.
- Dibblee, T.W., Jr., 1961, Evidence of strike-slip movement on northwest trending faults in Mojave Desert, California: U.S. Geological Survey Professional Paper, v. 424-B, p. 197-198.

- Dibblee, T.W., 1970. Geologic map of the Daggett Quadrangle, San Bernardino County, California. U.S. Geological Survey, Miscellaneous Geologic Investigations Map I-592, scale 1:62,500.
- Dokka, R.K., and Woodburne, M.O., 1986, Mid-Tertiary extensional tectonics and sedimentation, central Mojave Desert, California: L.S.U. Publications in Geology and Geophysics-Tectonics and Sedimentation, no. 1, 55p.
- Dokka, R. K., 1986, Patterns and modes of early Miocene crustal extension, central Mojave Desert, California: Boulder, Colorado, Geological Society of America Special Paper 208, p. 75–95.
- Dokka, R.K., and Travis, C.J., 1990, Late Cenozoic strike-slip faulting in the Mojave Desert, California. *Tectonics* v 9(2), p. 311-340.
- Erwin, Homer D., and Dion L. Gardner, 1940, Notes on the geology of a portion of the Calico Mountains, San Bernardino County, California: California Division of Mines Report 36, pp. 203-304. (Burcham mine, pp. 302-303; Calico-Odessa mine, pp. 243-244; includes generalized geologic map).
- Fillmore, R.P., and Walker, J.D., 1996. Evolution of a supradetachment extensional basin: The lower Miocene Pickhandle Basin, central Mojave Desert, California. Special paper of the Geological Society of America, v. 303, p. 107-126.
- Fletcher, I.D., 1986. Geology and Genesis of the Waterloo and Langtry Silver-Barite Deposits, California. M.Sc. Thesis Stanford University, Ph.D., 158 p.
- Garfunkel, Z., 1974, Model for the late Cenozoic tectonic history of the Mojave Desert, California, and its relation to adjacent regions: Geological Society of America Bulletin, v. 5, p. 141–188.
- Glazner, A.F., Walker, J.D., Bartley, J.M., and Fletcher, J.M. 2002. Cenozoic evolution of the Mojave Block of southern California. In Glazner, A.F., Walker, J.D., and Bartley, J.M., eds. Geologic evolution of the Mojave Desert and Southwestern Basin and Range: Boulder, Colorado, GSA Memoir 195, p. 19-41.
- Harthrong, D.S., 1982. Renewed mining activity in the Calico Mountains, a report on the ASARCO-Waterloo project, California Division of Mines and Geology 1982 Mining Review., vol. 36 (10), October 1983, p. 216-225.
- Ingersoll, R.V., Devaney, K.A., Geslin, J.K., Cavazza, W., Diamond, D.S., Heins, W.A., Jagiello, K., J., Marsaglia, K., M., Paylor, E.D., and Short, P.F., 1996. The Mud Hills, Mojave Desert, California: Structure, stratigraphy and sedimentology of a rapidly extended terrane. In: Special papers of the Geological Society of America, v. 303, April 1993, p. 61-84.
- Jessey, D. R., and Tarman, Donald W., 1994, Implications of fluid inclusion P/T data from Miocene hydrothermal barite deposits, central Mojave Desert, San Bernardino County, California: Quarterly of San Bernardino County Museum Association, 1994, v. 41, p. 22-23.
- Jessey, D.R., 2014. Geology and ore genesis of silver-barite mineralization in the Central Mojave Desert, CA. Geological Sciences Dept Cal Poly U – Pomona. 16 pp.
- Kirkpatrick, R.K., 1975. Waterloo property geology. Internal ASARCO report and maps.
- Lindgren, W., 1887. The Silver mines of Calico, California. Transactions of the American Institute of Mining Engineers. Vol 15, p 717-734. Scranton Meeting, Feb 1887.
- Loveday, D., 2022. NI 43-101 Technical Report for the Mineral Resource Estimate of the Calico Silver Project, San Bernardino County California, USA. Completed by Stantec Consulting Services on behalf of Apollo Silver Corporation. March 28, 2022, 148 pp.
- MacFadden, B. J., Swisher, C. C., III, Opdyke, N. D., and Woodburne, M. O., 1990. Paleomagnetism, geochronology, and possible tectonic rotation of the middle Miocene Barstow Formation, Mojave Desert, southern California: Geological Society of America Bulletin, v. 102, p. 478–493.
- Mayo, A. L., 1972, Geology and ore deposits of the south-central Calico Mountains: Unpublished Master's Thesis, Calif. State University-San Diego, 74 p.
- McCulloch, T. H., 1965, Geologic map of the Nebo and Yermo Quadrangles, San Bernardino County, California: U. S. Geological Survey Open-File Map OFR-65-107.
- Miller, D.M., Leslie, S.R., Hillhouse, J.W., Wooden, J.L., Vazquez, J.A., and Reynolds, R.E., 2010. Reconnaissance geochronology of tuffs in the Miocene Barstow Formation: implications for basin evolution and tectonics in the Central Mojave Desert. 2010 Desert Symposium, p 70-85.
- Miller, D.M., Rosario, J.E., Leslie, S.R., and Vazquez, J.A., 2013. Paleogeographic insights based on new U-Pb dates for altered tuffs in the Miocene Barstow Formation, California. 2013 Desert Symposium, p. 31-38.
- Murray, B.P., and Hames, W.E., 2021. Evidence of early Miocene synextensional volcanism and deposition in the northern Calico Mountains, central Mojave metamorphic core complex, southern California USA. *Geosphere*, v 17, p1-30.
- Oskin, M., Perg, L., Blumentritt, D., Mukhopadhyay, S., and Iriondo, A. 2007. Slip rate of the Calico Fault: implications for geologic versus geodetic rate discrepancy in the Eastern California Shear Zone. *JGR*, V 112, B03402, 16 pgs.
- Pratt, W.T., 2008. Waterloo Project, Barstow California. Internal report and map for Pan American Silver Corp., September 2008. 32 pp plus map.
- Pratt, W.T. and Ponce, M. 2011. Controls on mineralization in the Navidad Trend. Unpublished report for Pan American Silver Corp., December 2011. 25 pp.
- Pratt, W.T., 2012. Controls on silver mineralization at Waterloo, California. Internal report and map for Pan American Silver Corp., December, 2012. 46 pp plus map.
- Pratt, W.T., 2022. Geological mapping at the Langtry and Waterloo silver targets, California. Internal report and map for Apollo Silver Corp., December 2021, 34 pp plus map.
- Schuiling, T. 1999. A Miocene hot spring exhalate in the southern Calico Mountains. In: Tracks along the Mojave. Eds. Reynolds, R.E., and Reynolds, J. San Bernardino County Museum Quarterly vol 46(3) p 89-93.
- Singleton, J.S., and Gans, P.B., 2008. Structural and stratigraphic evolution of the Calico Mtn: Implications for early Miocene

- extension and Neogene transpression in the Central Mojave Desert, California. *Geosphere*, June v 4(3), pp 459-479.
- Smith, D.M., 1977. Geological map of the Waterloo area, Calico District, San Bernardino County, California. Internal ASARCO report and map
- Storms, W.H., 1893. San Bernardino County: California Mining Bureau, Report 11, pp. 337-349.
- Storms, W.H., and Fairbanks, H.W., 1965. The Calico Mining District in: Old Mines of Southern California: Desert-Mountain-Coastal areas including the Calico-Salton Sea Colorado River Districts and Southern Counties. Reprinted From 1893 Report of the California State Mineralogist. Frontier Book Company, p. 50-58.
- Tarman, D.W., and Jessey, D.R. 1989. Relationship between extensional tectonism and silver-barite mineralization of the Calico Mining District, SB County, California. Dept of Geol Sciences Cal Poly. P 201-218.
- Tarman, D. W., and Thompson, D.M., 1988, Folding of the Barstow Formation in the southern Calico Mountains, in *Geologic Excursions in the Eastern Mojave Desert*, Lori Gaskin editor: National Association of Geology Teachers Far Western Section, Spring Conference, p 31-42.
- Watson, B.N. 1968. Further geologic study of ASARCO's Waterloo Deposit. Internal ASARCO Memo. 11 pp.
- Weber, F. H., 1965, Reconnaissance of silver-barite deposits of the Calico Mountains and vicinity: California Division of Mines and Geology Open File Map, Los Angeles.
- Weber, F. H., 1966, Silver deposits of the Calico District: Calif. Division of Mines and Geology Mineral Info. Service, v. 19, pp. 71-80.
- Weber, F.H., 1967a. Economic Geology of The Calico District, California. SME of AIME, presented at the SME Fall Meeting – Rocky Mtn Minerals Conference, Las Vegas, NV, Sept 6-8 1967.10 pp.
- Weber, F.H., 1967b. Silver deposits of the Calico District. Part 3. February. California Division of Mines and Geology Mineral Info. Service, Vol 20(2). February 1967, p.11-15.
- Weber, F.H., 1980. Calico Silver District, San Bernardino County, California – update. In *Geology and mineral wealth of the California Desert*; South Coast Geological Society, p. 339-345.
- Woodburne, M.O., Tedford, R.H., and Swisher, C.C., 1990, Lithostratigraphy, biostratigraphy, and geochronology of the Barstow Formation of the Mojave Desert, southern California: *Geological Society of America Bulletin*, v. 102, p. 459–477.
- Woodburne, M.O., 2015. Mojave Desert Neogene tectonics and onset of the Eastern California Shear Zone. USGS 2015 Desert Symposium, pages 153-174.

Memories of Old Borate

Wm. H. Smitheram^{1,2}

Preface

The Cornish, as an emigrating and mining people, have left their mark around the world, especially in America. Their genius in mining was a skill inherited from generations of forebears. It is said that, "Wherever there is a hole in the ground, you will find a Cornishman at the bottom of it." And so it was true at the Borate borax mines at the turn of the century. Rich borax deposits in the Calico Mountains, twelve miles from Daggett, California, were developed and worked from 1890 through 1907 (Fig. 1).

My grandparents, William and Florence Smitheram (Figure 2), arrived at Borate in 1899 with their children, four-year-old Myrtle and Frank (my father), age two. William assumed the job as Mines Superintendent and Florence was a wife and mother living under primitive conditions. She also maintained a notebook and at random intervals recorded events and described personalities. Most of the entries were written in the first decade of the century and others appear as recollections in later years. I have transcribed her Borate memories into this paper.

Her flair for detailed events presents a highly interesting and amusing story as well as a true insight into

the life of a miner's wife in old Borate (Figure 3). Perhaps it can be said, "She held the day's wonder and joy in her heart, to recall in the delight of memories."

Life at the Borate mines

Will and I, with our children, Frank and Myrtle, arrived in Borate in 1899. We thought we had come to the end of the world upon seeing the borax mining camp, so barren and isolated in a mountain canyon, and faced with primitive living conditions (Figure 4).

Fred Corkhill, from the Isle of Man, was superintendent at the time and Will was to be his replacement. Corkhill was being sent with a group to search for new borax deposits in Chile, South America. We lived for several weeks in a tent cabin opposite Corkhill's house located at the top of Borate Canyon. My cook stove was out doors and supplies were shipped in from Daggett some twelve miles away. With Corkhill's help and direction, Will soon assumed his responsibilities. When the Corkhills moved away, we moved into the superintendent's redwood house (Figure 5). For a mining camp it was roomy and adequate, the roof was solid, and my cook stove was inside.

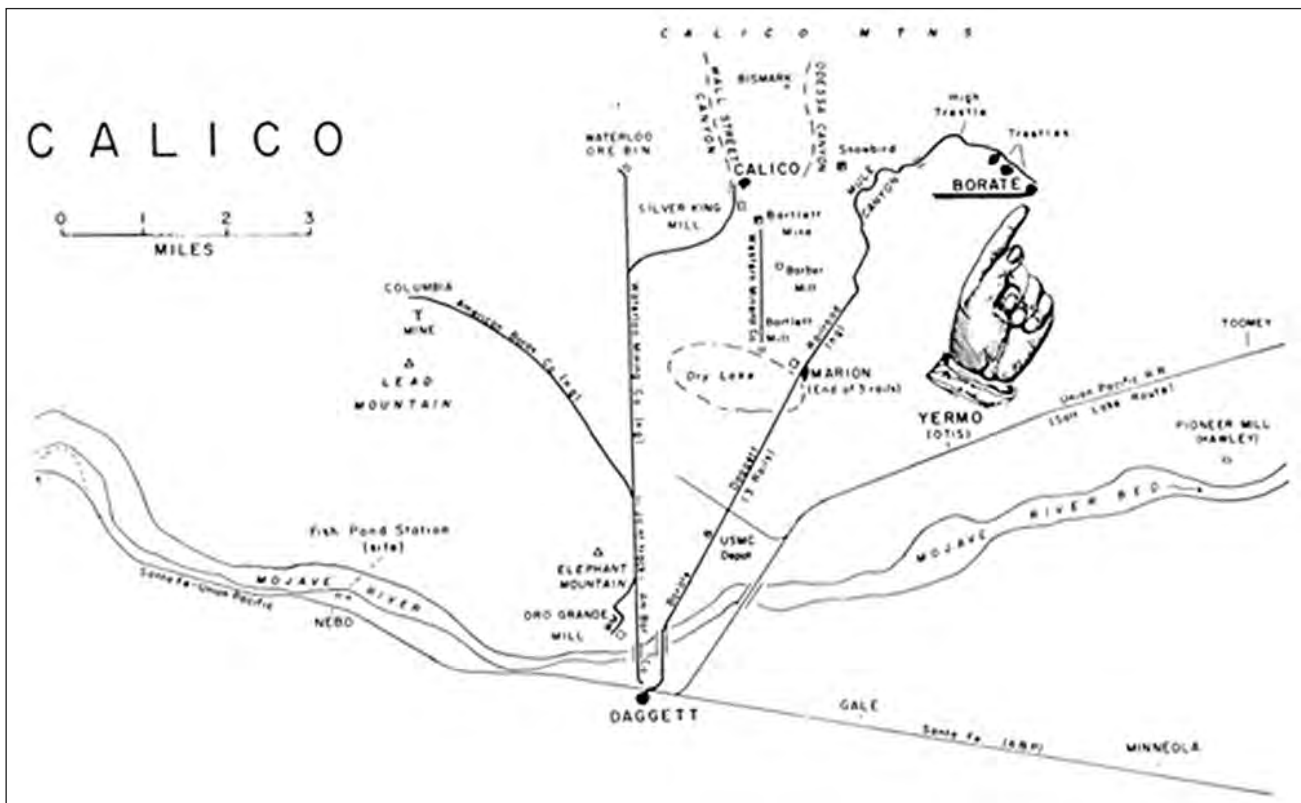


Figure 1. Map of Calico Mining District showing Borate in relation to nearby sites and railroads.



Figure 2. Wedding portraits of William and Florence Smitheram. William b. July 11, 1865, Cornwall, England; d. Sept. 1, 1916, Riverside, CA. Florence b. Nov. 27, 1875, Toronto, Ontario, Canada; d. July 31, 1971, Riverside CA. Wm. H. Smitheram collection.

Corkhill had been faced with labor troubles when several miners demanded a schedule of no Sunday work. In order to maintain adequate ore production, the mines were on two twelve hour shifts, seven days a week (Figure 6). Corkhill had continued this schedule and Will soon determined this was necessary as well, in order to keep the roaster mill at Marion in production (Figure 7). Those miners who could not abide by this decision soon left.

We lived in Borate almost seven years. The only times I was away for a few weeks was in 1900 when our daughter, Gertrude, was born and in 1905 when our son, George, was born (Figure 8). Both times I went by train to Redlands where I had an aunt and uncle and also a trusted

doctor. Everyone in camp was very helpful to me. Some of the families were: Julianne and James Nevill, Pearl and Ed Mott, and Osborne, Haggerty, Jennings, Willoughby, Mulcahy, McShane, and Falconer. John and Ella Allen had a daughter, Mary, and she and our children were friends, even into adulthood.

About seventy-five people, including single miners, lived and worked at Borate. The number varied each year. We visited often and our house, the largest in the camp, seemed to be a general meeting place. I well remember one of the shift bosses, John Harrigan, a jolly Irishman with a multitude of stories about his travels. He often brought small gifts to our house: licorice for the children and oranges and berries from a ranch at Fishponds on the Mojave River. Sometimes I gave him tea and rice pudding and I suspected he looked forward to this.

Our house became like a bake oven during the hot summer months and we slept out doors at night. We decided to live during the hottest period at a place called Round Rock (Figure 9). This was down the canyon and a few hundred yards along the main railroad track. Alongside a massive volcanic rock was a small cottage, and at its rear was an adit running about thirty feet into the hillside. An air shaft had been sunk from the hilltop directly into this tunnel and that is where our family had its sleeping quarters. It was the coolest place in the entire camp.

Will was at the mines twelve hours a day and sometimes I felt lonely and deserted. The engineer on the ore train, Ed Roach, always stopped daily in front of the cottage on the morning haul into Marion, and threw off a supply of scrap lumber. It was my chore to cut up the scrap lumber into kindling for my cook stove. He also delivered a barrel of water when needed. His brother, John Roach,

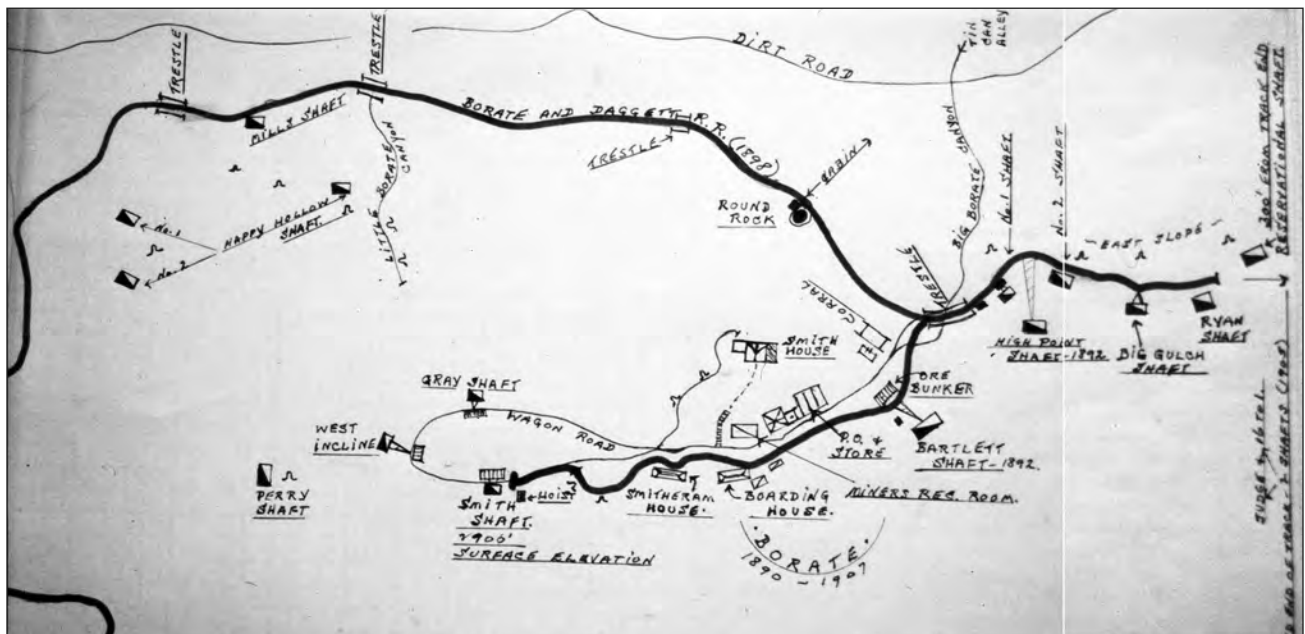


Figure 3. Sketch map by William H. Smitheram of the Borate and Daggett Railroad and workings at Borate. Additional structures existed at Borate, and some of the features on the map are located incorrectly. For example, the Bartlett shaft was actually near the No. 1 shaft, north of the trestle in Big Borate Canyon.



Figure 4. Tent cabins at Happy Hollow, west Borate, 1897-1898. These borax workings were also used as a work camp during the construction of the Borate and Daggett Railroad. Wm. H. Smitheram collection.



Figure 5. Superintendent's house at the top of Borate Canyon 1903. Wm. H. Smitheram collection.



Figure 6. Mine workers and the shift boss at the town of Borate in front of the recreation room, after 1898. The Ella Pitchess house is top left; the Smith house peeks over the horizon. Wm. H. Smitheram collection

was the foreman of the roaster mill at Marion, situated on the desert flats near Daggett. Other engineers on the ore train were Jerome Connelly and Enyon Timmons.

Several of the Cornish miners retained their speech mannerisms which were always amusing to me. They called tea leaves "Brownshans" and coffee dregs were "Grishans." There was no hard liquor available in Borate but sometimes the miners brought in their own ale. If one became tipsy he was said to be "Tadly Odly." If a man was helped into camp, unable to walk straight, he was "Prilled." The miners often made a New Years drink called a milk punch. It was boiled condensed milk, brandy, and orange or lemon rind. Another favorite was called a mahogany, made with three parts gin and one of treacle.

We depended on many home remedies for common ailments. I had no experience in relieving childhood colic and fever until an old Cornish miner advised that rhubarb brandy would cure the problem. He brought in some rhubarb from Daggett and proceed to boil it into a mush consistency, added a cup of gin and another of wine, and then strained it all through a cloth. When cool, the liquid was given in small amounts and within a few hours fever and coughing was contained.

The nearest doctor was located in Barstow. If one had an infected tooth needing extraction, he usually held whisky in his mouth as he rode the first train out of Daggett into Barstow or even to San Bernardino where care could be found. Sometimes a worker would become injured accidentally—a crushed finger, a fractured wrist, or a broken arm. I recall only one time that an accidental death happened, that of a young miner, Dave Jenkins. The powder team, three workers, was setting dynamite fuses in holes in a stope preparing it for blasting. Jenkins was inspecting the work when the powder suddenly exploded, and he was crushed by falling rock. A man was dispatched to Daggett to telegraph the coroner, John Keating, in San Bernardino. However, the coroner did not arrive in

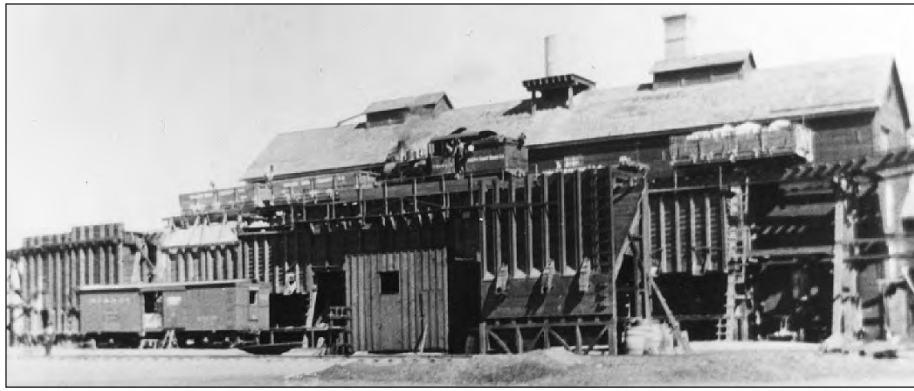


Figure 7. The borax roasting plant at Marion, five miles from Daggett, circa 1900. The Borate and Daggett ore train offloads from an elevated track into bins awaiting “benefaction,” or enrichment. The Wm. H. Smitheram collection, from U.S. Borax & Chemical Co.



Figure 8. Three Smitheram children at Borate, 1903. Gertrude, far left in bonnet; Mary Ellen seated in wagon; Frank about age 6, far right. Wm. H. Smitheram collection.

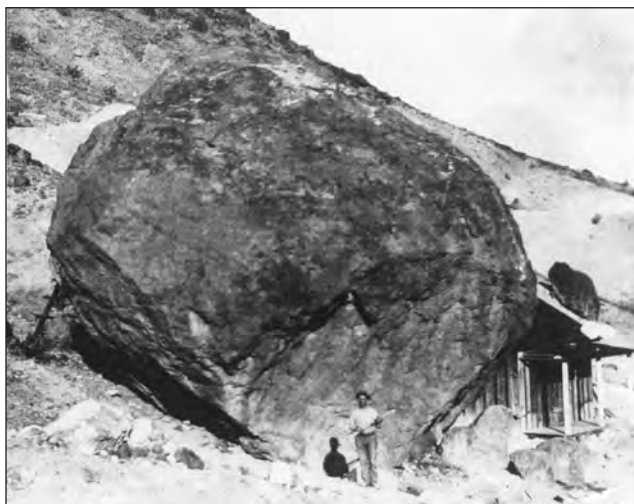


Figure 9. Smitheram summer cottage at Round Rock, Borate, 1903. Wm. H. Smitheram collection.

Borate until the third day. The poor victim had been laid out on a sheet of corrugated tin in an abandoned tunnel. The inquest was held in the boarding house and that same day the body was taken to Calico for burial.

Shortly after we arrived in Borate an amusing incident occurred. I was a witness to the beginning of the tale and the ending was related to me by Jerome Connelly, an engineer on the Borate and Daggett Railroad. It concerns two young miners who left their jobs in

a rush after the explosion of a water barrel. It was the custom of the miners to maintain a barrel of water just inside the tunnel where work was being done. The water was used to wash their hands after handling explosives. After several months the water barrel became thick with mud.

On this particular day, Charlie Williams and Jack Delameter had washed their hands when another miner put his candle out by dipping the tip into the water barrel. As soon as the fire touched the water there was a heavy, loud explosion. The two men were not injured, but were covered with thick, dripping mud. Enough nitroglycerin to cause the explosion had washed off the hands of many men and collected on top of the water. We were all laughing at the sight of the frustrated young miners as they walked to the bunk house to clean up. The two decided to quit and go where they could work without getting a mud bath. They collected their pay and packed up their belongings. Jack owned what was called a telescope valise which was composed of two parts, a top and bottom. The top lid fit tightly down over the bottom half and the valise was held together with leather straps.

They had barely assembled their few belongings when the shrill blast of the engine whistle announced the departure of the ore train. They ran for the tool car attached to the rear of the borax train where they had been given permission to ride. A few miles from camp Jack discovered he had forgotten to strap the two pieces of his valise together, and had only the empty top half. He had left all his earthly belongings behind in the bunk house. There was nothing he could do about this and his anger increased the more he talked about his calamity. He then drew out his pocket knife and vigorously started cutting the valise into small pieces. He was heard to say, “I may lose my best shirt and pants but I’ll save my sweethearts addresses,” which he had carefully written on the valise top.

Desert characters

Many itinerant miners drifted into Borate seeking work, and if they were qualified, Will found them a place,



Figure 10. Death Valley Scotty (Walter E. Scott) standing at left center next to his mules on Daggett's main street in 1903. San Bernardino County Museum Association collection.

sometimes for a week or two. One I well remember was "Little Jack," a five foot Cornish miner whose real name was John Kitto. He was a barber and cobbler by trade and a miner when necessary to keep body and soul together. He usually appeared in camp twice a year and headed for our house on arrival. I saved our children's worn out shoes for him as his feet were very small and he never spent money for new shoes. Somehow he repaired the worn out shoes and was as happy as one with a fortune. After I gave him a meal, Will found a few days work for him around the mines—menial jobs, but honest work. He often worked with the ore car gang. Although Will was not prejudicial, he was wary of people. I suppose being around rough miners from all walks of life had attuned his senses. He was very good in determining a man's character when hiring mine workers.

Another miner we came to know well was Marcus Pluth. He often walked into camp asking for temporary work. With several earned dollars he soon went on his way. He was very polite, self-educated, and a man with much foresight. He was one of a few individuals who made money from his mining claims around the Mojave desert. One time he and John Merritt teamed together and located valuable iron claims at Eagle Mountain. They held the claims for a long time and eventually sold them to the Harriman-Kaiser Company. About 1907 Pluth located a rich lime deposit at Alvord Mountain and later sold it for \$9,000.00. He died in 1939 and sleeps now in the Daggett cemetery.

One day in the spring of 1906, a fellow came riding up Borate Canyon and was soon recognized as Death Valley Scotty, at that time about 30 years old (Figure 10). He was astride a big black mule and led another black one loaded with camping equipment. Following along was a young burro. Scotty wanted to give the burro to our children for a pet. Will was very reluctant to accept the burro, saying he could not take it on as he had no means to obtain hay or grain for its feed. The children cried when they learned they would not be able to keep the burro. It was very gentle, and since Will

had noticed a brand mark on its ear, he was concerned that Scotty may have picked it up as a stray on his way out to the desert.

Will never fully trusted Scotty although he treated him well and had given him water and canned goods on past occasions. Some weeks later, as it turned out, Will had gone over to the nearby Brunswick mine in the Calico Mountains to investigate a small borax deposit. There were three families living on the site, the men being engaged in working the tailings of the old silver mine dump. The little burro had been left in their care and Will was told Alex Hastings, a Mojave River rancher, had claimed ownership. No one will ever know how Scotty really obtained that burro.

Borax Smith remembered

At least once a year, Francis Marion Smith (Borax Smith) came to Borate on an inspection tour. He stayed in a cottage on the hill top just above the main section of the mining camp, the dwelling being somewhat spacious and insulated (Figures 11, 12). I recall that the corner roof



Figure 11. The Borate post office, store, and bunkhouse, with the Borax Smith house on the horizon and the Ella Pitchess house upper left in the distance, probably 1903. Wm. H. Smitheram collection.



Figure 12. The Borax Smith house was the only painted house in Borate. The spur leads to the West Borate workings, including the Smith shaft.

points were tied into concrete pillars by strong wire cables. This was necessary as frequent gale force winds blew in from the desert. Will and Borax Smith got along very well together, and many times sat up until morning hours at our house discussing mining problems.

Smith appeared to me to have a strong facial resemblance to Theodore Roosevelt with his glasses, mustache, and hair style. He had consolidated all his holdings in 1890 into the Pacific Coast Borax Company and soon assumed the Twenty Mule Team as a trademark (Figures 13, 14). In 1898 he built the Borate and Daggett Railroad from Borate into Daggett, on the main line of the Santa Fe Railroad (Figures 15, 16). The following year Smith and his English friends desired to acquire new sources of borax and outlets for their products. They formed an organization called Borax Consolidated, Ltd. and Smith became managing director in America.

Whenever Smith was at our house, I gave him tea and corn bread, his favorite, and he never failed to say, "Tis the best in the West." He usually had his meals at the boarding house and I was told that he was very particular in that he insisted his eggs be cooked to perfection and his pancakes be dollar bite size. There was usually a Chinese cook at the boarding house but on one occasion the cook was a man named Hardcastle. After Smith had left, the cook was heard to have exclaimed, "Good God Almighty, he's gone at last."

Smith was an excellent story teller and I have since forgotten many of his tales. However, a laughable one has stuck in my mind. It concerns a burro that was owned by a desert prospector, Shorty Harris. He noticed one night that his burro seemed kind of sickly, so he gave him a bucket of water, cold out of a spring. The burro took a sip and let out a moan like a squaw with a belly ache. At supper time Harris gave him a hot flap jack and the burro held it in his mouth for several minutes before he swallowed it. Later on, the burro was found drinking some warm water Harris had set aside to wash up with. All of a sudden Harris realized the burro had a tooth ache. The next morning the burro had disappeared. About two days later it showed up as full of ginger as a burro can get, and no more tooth ache. The burro walked right up to Harris, opened his mouth, and let out a terrific bray, and there in the tooth was a gold filling. Harris spent a month looking for the ledge that contained the gold but never found it. "Yes, a far-fetched amusing story, perhaps one that has not faded away in the desert heat."

In 1904, Borax Smith approved a plan to send the Twenty Mule Team around the country to visit cities on an advertising and publicity tour. The first appearance was at the St. Louis World's Fair that year. Ed Stiles, one of the original team drivers, trained the mules and drove the team. Bob Wilson, another original teamster, also drove the team on the tour. On and off for many years the Twenty Mule Team was called out for festive and important occasions such as President Wilson's inauguration in 1917, and often in the Pasadena Rose Parade.

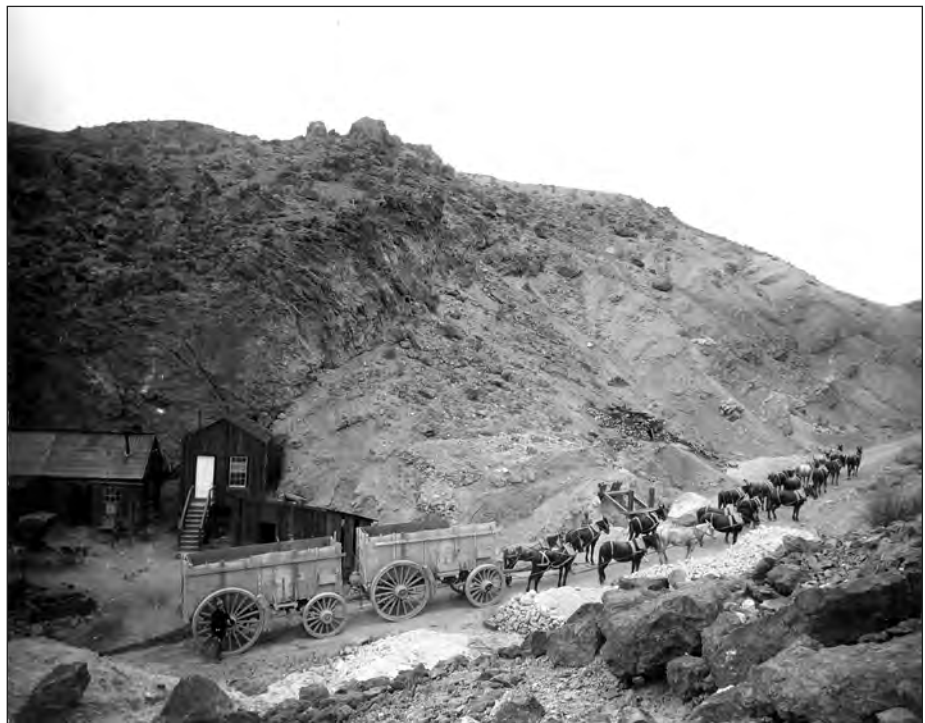


Figure 13. A 20-mule team hauls borax wagons in front of the first superintendent's cabin, with a white door. The second, larger superintendent's cabin where the Smitheram family lived was built about 1895 to the right of the small cabin.



Figure 14. Twenty mule team hitched to ore wagons, Borate, circa 1897. Wm. H. Smitheram collection.

At the time of the San Francisco Exposition in 1915, Smith invited his old-time friends and employees to a grand party at his Oakland estate. Will was somewhat reluctant to go, but I persuaded him to do so. Will enjoyed every minute being among so many friends. He often related what an impressive sight it was when the mule team and wagons circled into the estate entrance as a “salute” to Borax Smith. I recall seeing the team in 1924 when it paraded along Broadway in Los Angeles. The team also paraded at the opening of the San Francisco Bay Bridge in 1937. A major tour of the country in 1940 hailed the release of MGM’s “Twenty Mule Team” starring Wallace Beery.

In 1913, when we were living at the Lila-C borax mine, we sadly learned that Smith had declared insolvency. His holdings went into a trustee committee in Oakland as he had overextended his capital and defaulted on his notes. He had invested in the transportation system in Oakland and in the ferry service on San Francisco Bay. We knew him as an energetic man who had an abundance of optimism for everything he did. I shall always think of Borax Smith as a very warm-hearted and kind man. On the day of my Wills’ funeral in 1916 we talked at length of former times, and when he left he handed me his personal check which he insisted I accept. He died in Oakland in August, 1931.

Farewell to Borate

As time progressed, the colemanite ore veins became low grade and difficult to

work. The borax deposits at the Lila-C mine near the eastern edge of Death Valley had been developed, and in October 1907 the Borate mines were shut down. Wash Cahill closed the company store and our little post office closed forever. The Cahill family had been working at Borate since the early 1890s and Wash liked to tell how they received the mail before the railroad was completed in 1898. The Mulcahy family lived at nearby Calico so the Borate miners each paid one dollar per month to their young daughter, Fannie, to ride horseback from Calico to deliver the mail once a week. Since a majority of the Borate miners were unmarried, they all enjoyed the sight of her and the opportunity for conversation.

Will left Borate in October for the Lila-C mines and the children and I packed up our few belongings and within a few days our departure arrived. Our move did not prove completely successful for on the very day we climbed up on a flat car for the ride down to Daggett, a strong desert wind blew into a gale. As the ore train slowly negotiated the steep grades down through Mule Canyon, hot sparks flew backward from the locomotive stack onto its train. When the train emerged from the canyon the bone-dry cabins on several flat cars were burning furiously. By the time the fires were extinguished at Marion, all we were able to save were a few boxes of clothing and cooking utensils and my sewing machine. Our table and chairs and beds were a pile of bits and pieces.

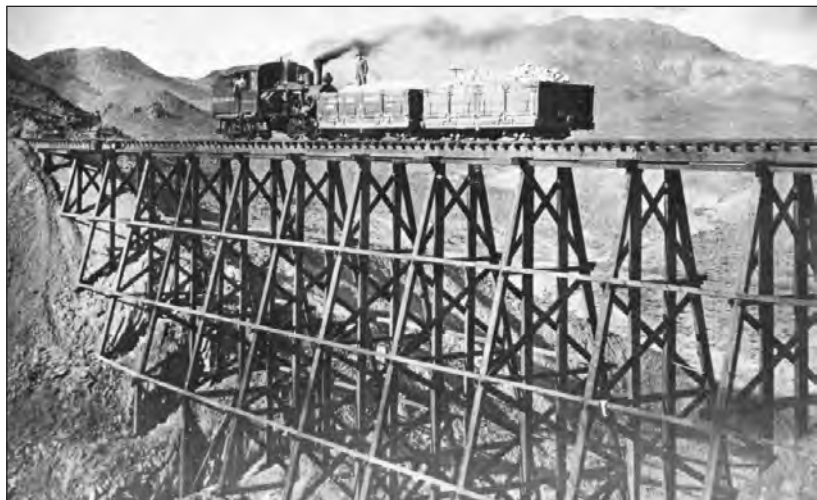


Figure 15. Heisler locomotive and ore cars on the Borate and Daggett railroad in 1903. The trestle spans Little Borate Canyon at the entrance to Happy Hollow. Wm. H. Smitheram collection

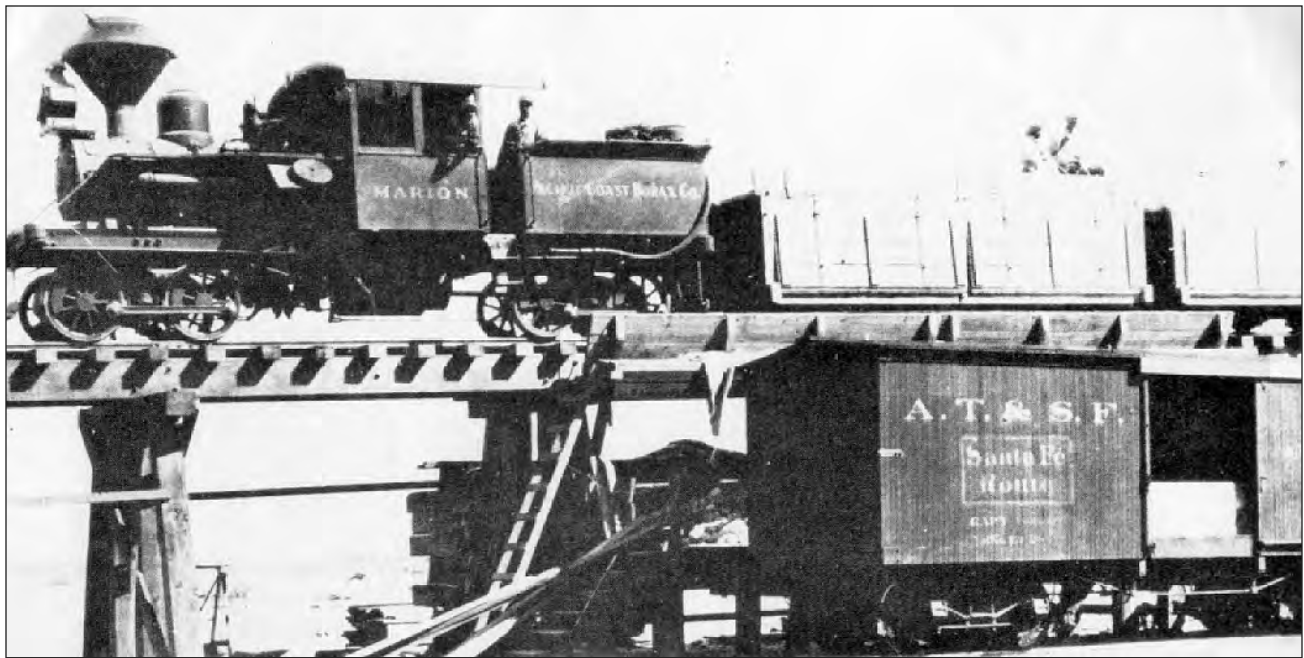


Figure 16. Narrow-gauge ore train from Borate on a high trestle at Daggett unloading borax ore into Santa Fe cars for shipment to Alameda, after 1898. Wm. H. Smitheram collection.

All the supplies, machinery, cabins, and heavy lumber were moved by rail from Borate to the new location at the Lila-C mine. Alex McLaren was given the contract to salvage everything and supervise the removal. Everything was loaded on narrow gauge flat cars at Borate and hauled on the Borate and Daggett Railroad down the mountain to the intersection with the standard gauge trackage at Marion. Everything was then skidded over to the standard gauge flat cars of the Santa Fe Railroad for movement from Daggett to Ludlow. From there the Tonapah and Tidewater Railroad transported the shipments to the Lila-C mine.

Although our life at Borate seemed uneventful and monotonous, I now reflect on the people who were friendly and charitable. Debts were paid and no violence occurred. Their word was as good as a bond and women were held in high respect. If someone became injured, or died, everyone contributed to a collection for those who remained.

The miners received two days off each year. The Fourth of July was usually celebrated with a baseball game and a pot luck dinner. On Christmas Day everyone banded together for a chicken dinner. Sometimes we sang carols with music supplied by an accordion or violin. We learned that a person is richest whose pleasures are the simplest. St. Patrick's Day was special as the Irish miners and many others celebrated by singing songs after their work shift. Everyone wore a bit of green ribbon on their shirts. One time a young scamp tied a green ribbon on a dog's tail who promptly ran down the canyon waving it. This gesture aroused much indignation among the Irish miners.

Many nationalities were represented over the years, all good workers for the most part: American, Cornish,

English, Irish, Welsh, Greek, Dutch, German, French, Italian, Bohemian and Scandinavian. All contributed to the wealth and history of old Borate.

References

- ¹ *Text from Smitheram, W. H., 1997. "Memories of Old Borate," in Memories, minerals, fossils, and dust, J. Reynolds (ed.). San Bernardino County Museum Association Quarterly 44(1), 1-7.*
- ² *Caption information in part from Reynolds, R. E., 1999. A walk through Borate: rediscovering a borax mining town in the Calico Mountains. San Bernardino County Museum Association Quarterly 46(1), 31 p.*

ἱστορία: Hunting for Old Calico's silver output

Douglas Steeples

Historian, dwsteeples@gmail.com

ABSTRACT — Production records for the Calico Mining District are diverse, discordant, and do not correspond to physical evidence for district development. Government records, newspapers, journals, mine surveys, stockholder reports, business periodicals, and scientific papers are sources of information about mine production. After statehood in 1850, the California State Legislature recognized that geologists could provide valuable information about mine activities. In 1851 the Legislature named John B. Trask, a medical practitioner and active member of the California Academy of Sciences, as Honorary State Geologist. In 1853 the Legislature passed a joint resolution asking him for geological information about the state. In 1880 the California State Mining Bureau, predecessor to the California Division of Mines and Geology and later the California Geological Survey, was established. These organizations produced annual or biannual Reports of the State Mineralogist which summarized mine production, but in ways that were general, inconsistent, and unverifiable. The U.S. Bureau of Mines (USBM) was established in the Department of the Interior on May 16, 1910, pursuant to the Organic Act (Public Law 179) to deal with a wave of catastrophic mine disasters. One of the USBM's ancillary responsibilities was to record mine and mineral processing production. Much of this government interest was in monitoring income for taxes, and in California there was a depletion tax associated with commodity production. Tax, depletion, and production records were almost always reported in dollars. Deducing silver production requires a calculation based on assumptions about the price of silver at the time its production was reported. The value of silver when compared to real estate and wages shows that it is influenced by world and national events, policies, and population changes. The raw data of production estimates, then, are a veil over the truth and the historian must reconstruct a series of assumptions to evaluate and interpret them. This paper examines these variables in relation to the history of the Calico District and concludes that previous reports of Calico mine production are likely under reported by a factor of 50%. Total production could have been as high as 40 million ounces of silver.

Introduction

A business historian may seem to be a sheep among goats, or a thief among strangers, when he shares a paper with such an audience as this. But that is not actually the case. Both he and his readers pursue a common task. Both “inquire,” for which the classical Greek word is “ἱστορία” but about different things and with evidence that is messy, partial, broken, and deformed, can be elusive, and may be difficult to shape into a coherent account. Research toward writing this paper began in 1954 and led to several presentations; it now informs the epilogue of a forthcoming book. In the 1950s, several familiar figures in Calico's history were still alive and available for interviews. We begin here with an anecdote about two well-known Calicoans, merchant and mine owner John Lane and once manager of the Garfield-Runover group of mines Jim Patterson. Then we become metaphorically a fox hunting a hedgehog, to borrow a phrase from Isaiah Berlin. We are in pursuit of Calicos' dodgiest, most important prey: the actual yield of local silver mines during their best years. We seem now to be gaining ground, but the hedgehog might even yet escape. Happily, there is still more evidence to be found and assayed, and expertise competent to continue the chase.

In March 1898, John Lane was staying in Los Angeles' Hollenbeck Hotel while on a business trip. At one point the proprietor asked him if he knew a former superintendent of Calico's Runover-Garfield Mines named Jim Patterson. Lane replied, “Yes.” Pointing to a drooping figure at the bar's end, the owner said it was Jim. Fearing that Jim would fill his boots with whiskey and die without aid, the bartender asked John for help. John wired his wife, Lucy, that he was bringing Jim to Calico.

After sobering up there, Jim remained a few days. He said that he had seen some rough days after his mines closed, including time wasted trying to farm in his old Missouri home. He was now waiting for the sea ice to clear so that he could head to a job with the Hudson's Bay Company in the new gold fields in northwest Canada's Klondike. While present he reminisced and played cards with the Lanes and a few old friends. In words evocative of Thomas Wolfe's 1934 novel, *You Can't Go Home Again*, he sighed “I never found another Calico” (Lane, 1964). Soon afterward he left, never to be heard from again. Many others shared his nostalgia. Some at times reunited into the 1940s, but they knew that they could not recapture a life like theirs in the old camp. Some clung to memories fairly accurately and were more matter of fact than

sentimental. Lucy Lane's *Calico Memories* (Lane, 1954), while her recollections were at times in error, falls into that class. One can say more or less the same of Herman Mellen and others who told of their experiences in Calico, and Borate as well. Later, historian Remi Nadeau rightly wrote that "Calico is more apt to be famous as a ghost town than it was in real life" (Lane, 1964; Nadeau, 1965).

Nadeau's statement is true, and its accuracy is unfortunate. Certainly, Calico harbored no one as famous as a Big Nose Kate to marry a Doc Holliday. Wyatt Earp, his father, and a brother farmed around San Bernardino and Redlands after leaving Tombstone. There is no evidence that any member of the Earp family ever traveled to Calico. Lucy Lane harrumphed, "Never heard of her," when asked if she knew of a Diamond Lil, the madam of a local house of prostitution. "Ma" and "Pa" Preston's notoriety and famed escape from Calico to Daggett might have been distorted into the unfounded tale of Lil. W.L.G. Soule was no match in real life or in any other way with Wild Bill Hickok or Bat Masterson as a lawman. Harry Dodson's unfortunate turn to robbery lacked the drama or importance of any of the raids of Jesse James, the Daltons, the Wild Bunch, and others like them. Mayhem at the 1885 May Day Strawberry and Ice Cream Festival cannot compare with the shootout at the OK Corral or that in which Billy the Kid died. "Jack" ("Dorsey") the mail dog's

work for the postal service does not rival that of Snowshoe Johnson.

Population and production

Exact totals and values of Calico's fluctuating population and silver output are, with some exceptions, unavailable. In a general way, population was related to silver production. Business directories for 1888 and 1889 and the 1890 census give only snapshots of particular moments. Silver and borax output, like population, varied seasonally and yearly. Records were poor, flawed, incomplete, sometimes ruined in a flooded archive, and much production went unreported because operators were often reluctant to discuss their mines' yields. Memories faded. If the 1890 silver purchase act brought 700 miners to Calico, a continued decline in silver prices cut a mining revival short, "leaving only the 30-stamp Silver King Mill and a 15-stamp mill in Daggett operating in 1892" (Wright and others, 1953). Discussion here must, then, be limited. It will turn first to discover what can be learned by examining the origins and sizes of the fortunes of a few persons who were important in Calico's history. Then it will consider various estimates of local silver production. Last, it will use the most conservative estimate, referencing contemporary southern California events, to see what that silver might have done.



The town of Calico viewed from the Silver King mine. *R.E. Reynolds collection.*

Henry Markham

Henry Markham was by far the most notable California figure active in Calico affairs. Born in Wilmington, New York, in 1840, he studied in Wheeler Academy, then taught school for three years. He fought for the Union, 1863–65, sustaining a severe wound in February 1865. After an honorable discharge, he learned that Milwaukee was emerging as a major port for shipping grain and lumber, and a rising center of manufacturing and railroad construction. He moved there, studied law, and shrewdly entered a practice that specialized in maritime and fire insurance law. Bright and energetic, he quickly developed good relationships with that city's leading businessmen, including Daniel T. Wells. In 1879, for reasons of health, Markham responded to an advertisement and bought a 23-acre site with 750 orange trees in Pasadena, California. He was soon one of Pasadena's leading boosters. He encouraged many wealthy persons to move there and build palatial homes on Orange Grove Boulevard and Grand Avenue as far south from Colorado Boulevard to present Markham Place and east to Hill Boulevard. He quickly developed a strong law practice and interest in gold and silver mining. Meanwhile, his promotional efforts began to bear fruit. Over time August Busch (beer), the David Berry Gambles (Proctor and Gamble), William "Bill" Wrigley (chewing gum), the George Holmes Maxwells (coffee), Albert Goodwill Spalding (sporting goods) and others built mansions on what became known as "millionaires' row." By 1887 he had the means to build a three-story, \$33,500 (\$1.65 million in 2023 dollars) house. In 1886 demand pushed land prices from \$400 such that a thousand lots sold for \$5 million. Twelve hundred carpenters erected 400–500 new buildings in Pasadena, 1886–1887, when a boom ballooned land and housing prices and sales. In 1886, house prices began at about \$600, averaged about \$4,200, and with land sales in 1886 topped about \$20 million.

At that time factory and farm workers earned an average of about \$420 a year (Bureau of Labor Statistics for California, 1883–1884). How much Markham's mansion, demolished in 1939, would sell for in today's inflated southern California market is anybody's guess. To his credit, Markham served on the city school board and campaigned successfully for creation of a public library. His connection with mining informed his support for the conversion of Throop University into the California Institute of Technology. However civic-minded he might have been, business held his keenest attention. He was also a director of the First National Bank of Los Angeles, the San Gabriel Valley National Bank (in Pasadena) and the Southern California Oil Supply Company. None of these things, except his family, was as important to him as mining gold and silver. That is why he was so prominent in Calico affairs. His role in creating and securing financing for the Oro Grande Mining Company predated his entry into mining in the Calico Mountains. Inability to mine and mill Silver Mountain's stubborn ores

coincided with rich new silver finds in the painted hills abutting modern Yermo. The hills immediately attracted his attention. When Sheriff John King could not raise the capital needed to develop the Silver King, Markham could scarcely resist paying \$60,000 for a lease on it with an option to buy. The contract required him to sink a 150' shaft. In doing so he struck paydirt. He found "ore so rich that ... [he] took up the option and bought the claim for only \$60,000, paying for it "out of production from the mine" and extracting \$150,00 more than that sum in silver early in 1882. On June 1, the Mining and Scientific Press (1882) reported that he had sold the Silver King to the Oro Grande Mining Company some weeks earlier.

Calico Union Mining Company

On June 7, 1882, he and six other Angelenos incorporated the Calico Union Mining Company. They capitalized it at \$1,000,000, in 10,000 shares at \$100 each. Markham was to take \$150,000 (15 percent) of its stock. The company's stated purposes were to buy, sell, and work mines. It appears that the Calico Union shortly afterward bought the Silver King back from the Oro Grande company. In August the Los Angeles Herald (1884) reported that "Negotiations" have been "going on for some time for

Articles of Incorporation

Calico Union Mining Company

Know all Men by these Presents: That we, the undersigned, have this day voluntarily, associated ourselves together for the purpose of forming a corporation under the laws of the State of California, and we hereby certify:

FIRST—That the name of said corporation is *The Calico Union Mining Company*

SECOND—That the purposes for which it is formed are: *To acquire and dispose of Mineral lands in the County of San Bernardino, State of California, and the making of the same to do and perform all other and necessary acts for the prosecution of the aforesaid purposes.*

THIRD—That the place where its principal business is to be conducted shall be *the City of Los Angeles, County of Los Angeles, State of California.*

FOURTH—That the term for which it is to exist is *fifty* years from the date of its incorporation.

FIFTH—That the number of its Directors or Trustees shall be *seven*, and that the names and residences of those who are appointed for the first year are:

<i>Henry K. Markham</i>	<i>Los Angeles</i>	<i>Los Angeles, California</i>
<i>William Calaney</i>	<i>Los Angeles</i>	<i>Los Angeles, California</i>
<i>George P. Johnson</i>	<i>Los Angeles</i>	<i>Los Angeles, California</i>
<i>J. Johnson</i>	<i>Los Angeles</i>	<i>Los Angeles, California</i>
<i>A. H. Johnson</i>	<i>Los Angeles</i>	<i>Los Angeles, California</i>
<i>G. P. Rusby</i>	<i>Pasadena</i>	<i>Los Angeles, California</i>
<i>W. K. Wallis</i>	<i>Pasadena</i>	<i>Los Angeles, California</i>

the sale of the King mine at Calico to San Francisco capitalists." The asking price was \$300,000. As such talk spread one assayer warned that "while it is a good mine, it was not worth the money asked." One could scarcely have been more wrong. Official records have Calico emerging as an important silver producer a year later, in 1883. The trail of evidence for the following years is thin. We've no evidence how much money the Calico Union's incorporators actually paid in. In October, 1882, the Calico Union leased the Silver King back to the Oro Grande Mining Company. It appears that the lease continued in effect until the Waterloo Mining Company merged with the Oro Grande, although a search for the lease's terms has been fruitless. In 1884, the Oro Grande bought the Silver King-Oriental mill on the side of the Mojave River opposite Daggett.

Markham and Jonas Osborne (introduced below) early in that year began to talk about building a railroad to serve Calico's mines and in March 1885, they formed the Daggett & Calico Railroad Company. It was to build via the "most practicable route from a point to intersect with the Atlantic and Pacific Railroad at the Town of Daggett, thence via the Oro Grande Company's mill to the Town of Calico, with a Branch Road or spur to the Snowbird Mine via Barber's Mill." Surveyors projected the line on a straight course to Calico, then work stopped. That it was to be a common carrier hints that Markham may no longer have owned an interest in the Oro Grande Mining Company and that the Calico Union was defunct. Nothing came of this plan, and the railroad's articles of incorporation remain elusive. When the Waterloo Mining Company built a rail line two years later, it was a private carrier. Markham's bid to build a line independent of any mine may have been his last attempt to profit from Calico's mines, unless he was an unnamed fifth incorporator of the Waterloo Mining Company (Los Angeles Herald, 1884; Hees, 2023; Gooley, No Date; Myrick, 1992).

Waterloo

When mining began in the Waterloo mine is not quite clear. Hints survive showing that mining started before 1885. That may be true, although there are no official records of the discovery of the Waterloo claims 1, 2, and 3 until April 19, 1888. The next day, April 20, two Milwaukeeans, Daniel T. Wells, Jr. and Charles T. Bradley, along with Angeleno Judge William Clancy, capitalized the Waterloo Mining Company for \$150,000, by means of 1,500 \$100 shares. Milwaukee lumber magnate Casper Melchior Sanger became known as the fourth director when he joined these three to patent the Waterloo Quartz Mine on November 13, 1888. The Milwaukeeans had bailed out the Oro Grande company, in response to Markham's request, years earlier. To make things even murkier, the April 16, 1888 incorporation of the Waterloo Mining Company involved transferring to it the assets of the Oro Grande Mining Company. Among other things, following this action the firm patented claims under both

corporate names and owned the Silver King, Oriental, and some nearby mines. That same year it put down rails between the Waterloo mine and its mill, adding a spur to the Silver King's Calico ore-loading bunkers in 1889. Also in 1889, the Silver King Mining Company, Ltd., of London, England, arrived—to mine the Occidental and Odessa silver mines (Huntington Library, 1879-1896; Gooley, No Date; Myrick, 1992; Vredenburg and Hensher, 1988). The original Silver King reopened on January 10, 1891, and closed definitively a year later. The Silver King Mining Company, Ltd., went bankrupt in 1896. It is unsurprising that California's Bureau of Mines, given this partial record, could do no better than essay a \$13 to \$20 million range for Calico's silver output.

The Milwaukeeans involved in these transactions give some indication of Markham's standing. Bradley, with William H. Metcalf, both millionaires before their deaths respectively in 1893 and 1892, partnered in ownership of the Badger State's largest shoe-manufacturing firm. Wells, a native of Maine, had taught school and been a merchant before he relocated in Milwaukee in 1836 at the age of 24. He began to amass a huge fortune by speculating in grain, land, and lumber. In 1847, he established a lumber mill in Escanaba, Michigan, later acquiring interests in several more mills. After holding local political offices, he served in the Territorial Legislature's upper chamber, and then a term in Congress. Coming to own vast timberlands, he was for a time president of the Lacrosse & Milwaukee R.R., and of the Chicago, Milwaukee & St. Paul R.R. He was also a director of the Wisconsin Marine and Fire and of the North-western National Insurance companies, and held banking interests throughout the state. When he died in 1903 at the age of 95, people thought him to be the richest man in the state. Markham, who lived until 1923, had chosen his associates well (Anonymous, 1818-1893; Anonymous, 1871; Beutner, 1871; Sanger, 2015).

Markham was only one of several southern Californians who profited from silver from the painted hills. The other shareholders of the Calico Union Mining Company picked dividends of at least \$257,000 and Markham at least \$42,850. To this sum must be added at least \$350,000 (and perhaps another \$150,000) from sales of the Silver King to the Oro Grande Mining Company, the Calico Union, and back to the Oro Grande, and unknown income from leasing that mine. The balance of his fortune derived from further, unpublicized sources.

Another New York native who appeared in Calico was Jonas Osborne, born in Attica in 1831. He was active in Lincoln County, Nevada, in the late 1870s, and then California's eastern Mojave Desert. There he bought some claims and a related townsite that he named after a local Indian headman, Tecopa. Lacking capital to develop his properties there, he found news of possible silver strikes in the colored hills to be irresistible. He hastened to the Calico Mountains area in 1881. That year carpenters built for him Daggett's first house, and he picked up the Sue Mine for \$1,600. After removing an unknown quantity of

ore he sold the mine in 1882 for \$60,000. He was quickly prominent among early settlers. Liberal spending had taken him to the brink of poverty when the Tonopah & Tidewater R.R. opened. The new line reduced shipping costs so much that his mines near Death Valley could be worked profitably. Again short of the means to develop his mines, he sold them for \$350,000. Carefree spending and his inability to resist grubstaking prospectors let him live long enough to sink into penury before he died on April 28, 1913. His remains have rested ever since in the Daggett Pioneer Cemetery.

John Daggett

John Daggett was a migrant from Elmira, New York, who found riches in Calico. He and his brother, David, had arrived in California during its days of gold, in 1852. After serving as postmaster in Sawyer's Bar, he moved to Nevada during the Civil War. He returned to the Golden State in 1865, and soon after he became owner of the Black Bear Gold Mine in Siskiyou County. Reports of silver finds in the painted hills drew him to southern California in 1882, while he was Lieutenant Governor. He dwelled in Los Angeles until he returned to San Francisco in 1888 and later reactivated the Black Bear Mine. In April 1882, he and W.W. Stow partnered and incorporated the Odessa Mining Company. They capitalized it at \$7,500, the amount paid for the Silver Odessa mine. That same year he paid \$9,000 in cash to add the Bismarck to his lengthening list of holdings. He also purchased surface rights to build a road up to his Odessa mines from the Alabama mine, which his firm later bought. The State Geologist knew that the "average grade of the ore" in the Odessa and the Silver Odessas "was probably the highest of any silver mine in the Calico district." They were so rich that Daggett added a mill in 1883. Although they "removed [ore] rapidly and unsystematically," the Odessa and Silver Odessa produced many \$100,000s in silver, and perhaps more, before they closed in 1886 (Hencher, 2005; Daggett, Van Dyke, 2023; Find a Grave, 2023; Lane, 1964; Hyde, 1949; Wright and others, 1953, p. 128).

Orson Johnsons

Orson Johnsons was of a piece with these men. His family moved from Ohio to Galesburg, Illinois, in 1844, when he was five years old. At the age of 16 he began clerking in a local store. A gifted manager, he bought the building that housed it a year later. In 1864, now 25 years old, he added a store in Galesburg, where he had worked previously. It soon grew to become a three-story emporium. It contained an arcade, an elevator, a vacuum tube to transfer cash from counters to the office, a restaurant, and 225 employees including a youth named Ronald Reagan. People described his establishment as "equal to all the best in Chicago." Also a civic-minded banker, he was mayor for two terms, a trustee and benefactor of Knox College for 25 years and creator of a free public library.

Johnsons moved to Los Angeles in 1876, two years after a visit. In 1879 he bought land in present Riverside. This was the same Johnsons who in 1881 bought the Sam Houston filings 1, 2, and 3 from (borax discoverer) Hugh Stevens and his brother, Robert. The sale was the result of a foolish mistake on the part of the brother, neither of whom wished to mine their claims' tough earth. Johnsons struck rich silver ore close to the surface and, concealing his find, obtained the ground for \$1,100. He formed a corporation and restyled the claims the Blackfoot Consolidated Mines Nos. 1, 2, and 3, in Odessa Canyon opposite the Silver Odessa mine. After earning "a nice sum" he "sold out to two Frenchmen for \$40,000". Their close personal and investing association led Johnsons to make Markham president of the Los Angeles Furniture Company. Markham maintained an office in it even while he was governor of California, 1891–1895. Occupying an entire city block, it both manufactured and sold furniture. Johnsons also built a block of retail outlets, and, on a third block, a hotel. This elegant hostelry, the Westminster Hotel, was the city's finest. It was the scene of many high-profile events, including a reception at which Theodore Roosevelt was one of the guests. In time this strategic block passed to the City of Los Angeles, which later built the present city hall on it. Johnsons, always charitably minded, in 1914 gave Occidental College a building that bears his name. Also an Occidental trustee, he paid for construction of the Los Angeles Young Men's Christian Association (YMCA) building and a clinic for poor children. His generosity extended, to funding the Anna Craven Johnsons Home, a 75-suite home for widows and children. Upon his death, Anna inherited an estate of "several million dollars" and continued charitable work until she died in 1930 (Lane, 1954, 1964; Hogan and Johnston, 2023).

Langtry Project

In 2008 and 2021 experts wrote reports about the Langtry Project (Matson, 2008; Samari and Breckenridge, 2021). The purpose of these reports was to determine how much silver might be hiding on a group of claims northwest of Calico. They did not attempt to use existing records of actual silver mining there while offering an important beginning toward a second approach toward detecting the importance of Calico's silver. Under the heading for the mining history of the district they wrote three noteworthy sentences. They began "1881-1896," accurately: "Silver ore was discovered in the Calico Mountains in 1881 with exploration centered around high-grade oxidized deposits of vein-related silver ore (Dibblee 1970)." They followed with two inaccurate, contradictory remarks. First they wrote, "Silver production from ...Calico ... from 1881 to 1896 was never recorded". Then they observed that "historical estimates vary from 15 to 25 million troy ounces". Their distinction between "records" and "estimates" is accurate and telling. It indicates that an attempt to get at the district's importance through a

search through such records as exist is unlikely to be conclusive (Hamid and Breckenridge, 2021; Matson, 2008).

The estimates to which they referred may in a way hint at local silver production. They must be used with caution. A geologist in the 1960s wrote that engineering reports from local mines “apparently no longer exist.” Another wrote of “reticence” of mine owners to share information about their properties. Official county, state, and federal records are scarcely better than those from the mines. They sometimes disagreed and were always incomplete. For example, in one set of state and U.S. Treasury archives, there is no report at all for 1886, and in the other there is no report for both 1885 and 1886. In years for which both sets of reports survive, they differ by as 50%. Two confidential letters, one from the San Francisco U.S. Mint and one from the U.S. Bureau of Mines, stated that official records under-reported Calico’s silver output ... but neither writer knew by how much (U.S. Bureau of Mines, 1958).

Between 1919 and the present, official statements about Calico’s silver output bounced up and down before stabilizing. H.T. Cloudman and others, (1919 pp. 823–826) is illustrative. The report set Calico’s silver output, 1881–1913, at \$13.8 million, nearly all of it before 1900. It also noted that the county records from which the figure was derived were incomplete before the year 1896, effectively rendering the total recorded doubtful. In 1940, California’s state geologist forwarded a brief challenge, offering a \$20 million estimate. Three years later the official total fell back, after recalculation, to \$13.997 million. In 1953 and 1954 state geologists threw up their hands, granting only that Calico’s mines “yielded silver ore worth a total value estimated variously at 13 to 20 million dollars.” The official state figure, with some minor tinkering, has not changed since then. Muriel Sibell Wolle, architect of Colorado University’s Fine Arts Program, took this broad range as a given in her *The Bonanza Trail* (Wolle, 1953). David Myrick’s *Railroads* (Myrick, 1992, pp. 822–823) accepted that range. It apparently hardened into Gospel truth when State Geologist F. Harold Weber confirmed it verbatim in one of three articles (Weber, 1966, 1967). In 2011, amateur historian and desert naturalist Walter Feller reiterated it. Historian Remi Nadeau chose to omit a production reference in two books that treated Calico. His choice was prudent given the absence of a substantial report based on a thorough inspection of local mines, mills, and tailings. As a rule, investigators have been content to settle for these figures for silver production down to the present. They turned instead to generate a mass of important studies unraveling the Calico Mining District’s geology. Many writers settled on the \$20 million production sum (U.S. House of Representatives, 1899; U.S. House of Representatives, 1893–1896; Bureau of Mines, 1883–1884; Cloudman, 1919; Wolle, 1953; Myrick, 1992; Vredenburg and Hensher, 1986).

This aggregation of estimates persisted until the present, although a handful of little-known challenges emerged in the shadows. The first to come to light arrived in a May 8, 1958, personal letter with confidential enclosures. The writer was Joshua T. Weakely, an Angeleno. Owner of the Silver King and Waterloo Mines during the 1920s, he held such corporate records of these properties as existed. Those for the Silver King showed a production of \$12 million, roughly the \$11.7 million low estimate for the entire Calico Mining District discussed later. The Waterloo Mine’s recorded bullion was another \$9 million. Weakely also provided two private contractual special manuscript reports, both from mining engineer F.B. Weeks. One of them, “Bismarck Mine, Calico Mining District, San Bernardino County, California,” (Weeks, 1958) showed that the Bismarck held considerable promise. The other, “Possibilities of the Calico Mining District,” slated for publication in the *Engineering and Mining Journal*, Vol. 119, p. 757 (E&MJ, May 1925), reported that existing records for the district were inadequate, but its content was changed prior to printing. Weakely did not claim that his records fully captured local silver output, but they cast serious doubt on official reports (Vredenburg, 2020; Vredenburg and others, 1981; Feller, 2023; Coke and Coke, 1941).

Larry and Lucille Coke

Larry Coke and two partners reached Calico in 1935, after learning to mine and refine gold ore and tailings in Randsburg. They set out to mine and refine silver ore and tailings there. The partners left after early work paid little. Larry and Lucille met in Yermo early in 1937, soon married, and partnered in mining and refining, both of them exploring and working Calico’s old mines as well. They lived rent free in an old Calico building as Larry’s compensation for watching over the townsite, which the Zenda Gold Mining Co. owned.

Their work led Larry to estimate that Calico production totalled \$65 million in silver (Cokes, 1941). Geologist David R. Jessey in 2011 found that the “Calico Mining District produced over \$20,000,000 of silver,” 1880–1940. Pressure was building for a major revision of Calico’s importance (Jessey and Tannan, 1988; Jessey, 2011).

Erik Melchiorre and mine volumes

In 2009, geologist Erik Melchiorre of California State University at San Bernardino began work that challenges every previous measure of Calico’s silver output. That work led to a preliminary presentation to the Mining History Association in June 2016. Melchiorre’s work began with mapping accessible parts of the Silver King Mine employing a Brunton compass and tapes. Now he has re-mapped the stopes and many underground workings using more sophisticated LIDAR techniques. The A.W.M. Keck Foundation grant funded use of portable X-ray fluorescence (XRF) and Light Detecting and Ranging

(LIDAR) to gauge pockets of “black breccia ore, and stopes and pillars” and measure ore content and density in the mine. Collection of hundreds of ore samples from mine and mill tailings accompanied work underground. Conversion of stope volumes to tonnages of ore extracted, and analysis of samples for ore content by conventional fire assay followed. The result was an estimate that the Silver King produced 20–24 million troy ounces of silver. Work since 2016 has extended to the entire set of accessible mines on the Silver King vein system in Wall Street Canyon, a system that includes the Orientals, Silver King, Burning Moscow, Red Jacket, Red Cloud, and Sue. It has also included collection and fire assaying of more hundreds of samples from tailings and dumps. Given Melchiorre’s expertise and thoroughness, and hints from earlier sources, it is not surprising that as of early 2023 he revised his previous estimate upward. He now concludes that the Wall Street Canyon mine system produced 26 million troy ounces of silver. He does not plan to investigate the Waterloo, as it is still an active corporate prospect. However, if Weakely’s record for the Silver King was more than 50% short of reality, it may have erred just as much in the case of the Waterloo. Adding \$4.5 million to the Waterloo would credit it with 13.5 million troy ounces of silver. If the yet unexplored, very rich Garfield, Runover, and Occidental mines in upper Odessa Canyon prove to have produced 25 million troy ounces of silver, the district total would be about 65 million troy ounces. That total would not include the still active Snowbird, intermittently active Thunderer and unmentioned chloriding. Moreover, and in any event, Calico’s total substantiated silver product will prove to be far higher than any previous investigation has found (Melchiorre, 2022).

World events and silver production

While these estimates may prove to be close to the truth, they do not answer one critical question. How much silver did Calico’s mines yield before 1903, and especially during its glory years, 1882–1888? Here a reminder of the character of California will be useful. Silver production at Calico was influenced by world events and economics. The gold rush of 1849 had jump-started populating northern California with a regional version of the eastern United States: Western-European-Anglo-American culture. The camp’s and mining district’s populations and recorded shipments of silver were tiny compared to those of the era’s great bonanza camps. In that respect they were like all of southern California of the late nineteenth century. The entire region lagged in development behind areas north of the Transverse Ranges and west of the Sierra Nevada and Coast Ranges. The 14 counties on the outside of those montane borders were in general physically

Table 1. Silver Output in San Bernardino County (Cloudman, 1917)

Year	Silver	Year	Silver	Year	Silver	Year	Silver
1881	\$0,100,000	1886	\$ 1,204,000	1891	\$711,131	1896	\$130,714
1882	\$0,150,000	1887	\$ 0,733,000	1892	\$ 0 67,072	1897	\$054,407
1883	\$3,706,000	1888	\$ 1,200,000	1893	\$447,000	1898	\$032,000
1884	\$2,283,000	1889	\$ 0,824,000	1894	\$148,243	1899	\$015,603
1885	\$2,363,000	1890	\$ 0,795,000	1895	\$219,410	1900	\$172,759

and culturally rural, hilly, chaparral-clothed, or desert. Outside of the districts that the gold rush had peopled and Americanized, they harbored only a handful of towns and lay under a lingering patina of Spanish and Mexican culture. Of their half dozen settlements of consequence, Los Angeles, with 11,183 residents in 1880, was by far the largest. Santa Barbara’s population was but 3,460; San Diego’s, 2,600 or so; San Bernardino’s, about 1,700; and Ventura’s, even fewer. Pasadena was only a tiny hamlet. By and large a pattern of smallish, 1,000- to 15,000-acre landholdings (some called ranchos) had replaced the huge ranchos granted during the period of Mexican rule. From the air above Los Angeles, one would have looked down on a patchwork of fruit and nut groves, vineyards, pastures dotted with sheep or black cattle, barley and other grainfields, and undeveloped lands. The occupied spots were usually on alluvial fans where streams had deposited their loads upon leaving the mountains, and bordering the few rivers that fed the Pacific Ocean. Pairs of ruts marked such roads as there were. What might not have been evident from an aerial perspective was the presence of a number of men who were waiting for some great event that would draw masses of immigrants to whom they could sell off parcels of their lands profitably. The surnames of many of them still appear on maps: Wilson, Downey, Chapman, Van Nuys, Markham, Lankershim, Chaffey, Griffith, Slauson, Baldwin, with other persons among them.

Transportation

The other factor that effected silver production was improvements in transportation. We have heretofore examined the growth of local railroad systems to support the Calico mines. The great event for which these people were waiting was an outgrowth of the incorporation of the California Southern Railroad. Entrepreneurs in National City and San Diego, with support from the Santa Fe, had chartered the line, which began to lay track from National City to San Bernardino on January 1, 1882. The line reached Colton on August 16 and San Bernardino on September 13. Flooding in January and February 1884 destroyed 30 miles of track, idling the road for nine months because it could not afford to repair the damage. To avert an S.P. takeover of the stricken line, the Santa Fe through an exchange of stock and bonds took control. It immediately placed the California Southern’s construction chief, Fred Perris, in charge of building an

81-mile extension from San Bernardino over the Cajon Pass to Waterman Junction (Barstow's site). The first train reached Waterman on November 16 after climbing a grade of up to 3.4%. Passenger fares from St. Louis immediately dropped from \$100 to \$95 as the S.P. for the first time faced competition for southern California business. The S.P. leased trackage to Los Angeles to the A.T.&S.F. to forestall construction of a rival line.

The lease arrangement failed to block the Santa Fe from becoming a serious competitor. It began to lay a web of lines around L.A., then in January 1886, withdrew from the Transcontinental Traffic Association. Freed now from membership in a pool that maintained rates and apportioned traffic, the upstart line turned to fierce rate-cutting to garner business. The loss of income as it cut rates led the Santa Fe's management in January 1887 to propose a new traffic sharing arrangement. At the time rates from New York, Chicago and Kansas City were still \$70. After the S.P. rejected the proposal, William Barstow Strong, the Santa Fe's president, determined to "destroy once and for all the [S.P.'s] monopoly in ... [California]" (Myrick, 1992).

The ensuing merciless competition climaxed on March 4–6, 1887. On the 4th Strong's line cut fares to San Francisco from Boston, New York, and Chicago to \$47, \$45, and \$32, and then again to \$42, \$40, and \$25 (respectively). The fares bottomed on March 6, when the S.P. met the Santa Fe's opening \$12 fare from Kansas City, then followed suit again at \$10. That afternoon the S.P. underbid itself three times to a \$1 fare from Kansas City. Later the Santa Fe reported that it had sold no tickets for less than \$8. Within two days fares were rising again, but they remained below former levels for a year.

The rate war, with extravagant promotion of the state's appeal, probably lured as many as 300,000 people to California. By 1888 the Santa Fe had brought more than 65,000, the S.P., Denver & Rio Grande, and the Burlington and Iowa railroads 78,437, and other lines, more. Arriving passenger trains per railroad had more than doubled in number when the frenzy was at its height. During early 1887, three to five trains, "each with multiple sections," entered California on both the Santa Fe and S.P. at the rate of three to five per day per railroad. The rate war's greatest import was the real estate and population boom that it brought to southern California. It Anglo-Americanized southern California much as the gold rush had in points north (Dumke, 1944) Its chief value here is that it offers one further approach toward gauging the significance of Calico's silver.

Population and real estate

The arrival of the S.P. in Los Angeles had prompted a 100% growth of its population in the 1870s. Writers have credited the Santa Fe with adding 500% more in 1886–1888. In Los Angeles, 2,300 individuals hawked lots in 2,700 tracts described in a 178-page tract book. Hucksters hosted visitors from especially-built grand

hotels that offered free meals, excursions, and brass band entertainment to promote newly-platted tracts of land. Besides tourists, potential settlers thronged the region. Land that had sold for \$150 to \$500 per acre in large plots came to fetch \$500, even \$1,000 per acre. Single-home city lots of 34 by 130 feet could command \$350. Scores of tracts failed, but such places as Redlands, Pasadena, San Marino, Azusa, Monrovia, Long Beach, Alhambra, Burbank, Whittier, and Santa Ana incorporated and took off.

Growth in population and assessed property values displayed the boom's transformative effects. Los Angeles grew from 11,183 people in 1880 to perhaps 80,000 in 1888 and fell back to 50,395 in 1890. San Bernardino numbered 1,673 residents, then 8,000, and finally 4,012; Santa Barbara 3,460, 8,000, then 5,864; San Diego 2,637, 15,000, and at last 16,159. City assessed property values rose in L.A. from \$4,775,373 to \$45,056,436; San Bernardino from \$470,000 to \$3,720,702; Santa Barbara from \$469,826 to \$2,894,833. Concurrently county assessed property values increased for Los Angeles from \$13,731,872 to \$60,012,280; San Bernardino from \$2,156,253 to \$17,188,555; Santa Barbara from \$4,395,076 to \$13,074,112; and San Diego from \$2,382,795 to \$24,451,740. In contrast the 1883 fire that burned out one-third of Calico's businesses required only \$25,000 in repairs and that of 1887 just \$100,000 to replace 135 incinerated buildings. Placed in this context, is Calico's lowest estimated \$11.7 million silver yield for 1882–1888, worth considering?

No, and yes. No, if those dollars were simply hoarded or left idle. No amount of money has value in and of itself. Unused, even the greatest fortune is merely riches. It becomes wealth, gains value, only when it is used to provide a service or good, or to create, sustain or strengthen an entity that does so. Silver was a commodity of value that could be quickly converted to goods and services and that's why the mines were successful at this time.

Thus did silver become wealth, capital. In the year 1886, as a land boom took off, expenditures increased the value of property in Los Angeles by \$10 million and in 1887 by \$11 million. Those numbers recorded increases in the value of physical assets. In 1880 a single store, a post office, and two daily coach runs served 391 people who dwelled where Pasadena grew. In 1886, 53 real estate agencies in Pasadena facilitated \$5,000,000 in sales of land valued at \$1,000 an acre. That land in turn put 1,200 carpenters to work erecting between 400 and 500 buildings. In 1886, five trains a day served Pasadena. In 1887, 22 trains did so. Again, in 1886 "about one hundred new houses per month were erected, representing an estimated investment of \$5,000,000" (Dumke, 1944) on Washington Street (now West Washington Boulevard) near Los Angeles's tony West Adams neighborhood. These examples show that even a few million dollars can produce large results.

The true measure of Calico's importance was what a sum of money equal even to the lowest estimate of

its silver product could do. This shows that we need to shift from counting ounces and dollars to finding their impact. Suppose that Calico's mines gave up 40 million ounces of silver, a total well within reach as we add figures for the Waterloo Mine to what Melchiorre has already documented. That total would be roughly the amount that assessed property values in Los Angeles increased between 1880 and 1890. If that much silver came out of local mines through 1888, the result would be to make it a major driver of economic growth, even if the money had been dispersed widely across the country.

It presently appears that continuing research is likely to end with an output total of between \$50 million and \$65 million and possibly inclining to the higher end of the range. There are now new hedgehogs to hunt. The most important is to attempt to develop a chronology of silver production, so as firmly to place Calico in an historical context.

References cited

- Anonymous, 1818-1893, Daniel T. Wells, Jr., Historical Essay, Dictionary of Wisconsin History, Wisconsin Historical Society Library, Madison Wisconsin.
- Anonymous, 1871, Charles Truworth Bradley, Historical Essay, Dictionary of Wisconsin History, Wisconsin Historical Society Library, Madison Wisconsin.
- Anonymous, 1871, Charles Truworth Bradley, Walking Tour of Milwaukee, Bradley and Metcalf Shoe Company, brass plate in sidewalk, historical marker No. 34, 3rd Ward, Milwaukee, Wisconsin: National Register of Historic Places.
- Beutner, Jeff, 1871, Downtown Milwaukee, 1871, photograph of shoe factory, newspaper clipping, unknown publisher.
- Bureau of Labor Statistics of California, 1883-1884, Annual Report, Wages, Tables I and II, pp. 211-214.
- Cloudman, H. T., and others, 1919, Calico - San Bernardino County-Silver, Report XV of the State Mineralogist: California Bureau of Mines, pp. 823-826.
- Coke, Lawrence and Lucille Coke, 1969, Mining on the Trails of Destiny, Vantage Press, New York, 1969. Also more interviews with the Cokes, Alfs, Dix Van Dyke and L. Burr Belden, San Bernardino journalist-historian.
- Coke, Lawrence and Lucille Coke, 1941, Calico, Barstow Peer Review, Yermo, 1941. Also several interviews, 1959-1961.
- Daggett, Van Dyke, 2023, No. 104; headnote, Jonas B. Osborn Papers, On-line Archives of California, Collection Number BANC: MSS 2011/226, <https://oac.cdlib.org/search?style=oac4:idT=UCb177154445>
- Dibblee, T.W., 1970, Geologic map of the Daggett quadrangle, San Bernardino County, California, U.S. Geological Survey, Miscellaneous Geologic Investigations Map I-592, scale 1:62,500.
- Dumke, Glenn, 1944, The Boom of the Eighties in Southern California, Huntington Library, San Marino, California, 1944, pp. 21-27, numbers of trains, pp. 26-27. Quotations, illustrations, population and assessed valuations, pp. 45, 55, 89, 277, 278.
- Engineering and Mining Journal, 1925, Volume 119, p. 757.
- Feller, Walter, 2023, "Calico Ghost Town" <http://mojavedesert.net.mining-history-calico/> Accessed March 1, 2023.
- Find a Grave, 2023, Julias Osborn, Daggett Pioneer Cemetery and Osborne, FindaGrave.com. [Find a Grave - Millions of Cemetery Records](http://www.findagrave.com/Find-a-Grave-Millions-of-Cemetery-Records). Accessed March 1, 2023.
- Gooley, Lawrence P., No Date, Wilmington's New York Henry Markham, California Governor, Adirondack Almanac. www.facebook.com, on-line publication, irregular posting.
- Hamid, S., and Breckenridge, L., 2021, Technical report on the Langtry project (Denver, 12/2/2021) https://apollosilver.com/wp-content/uploads/2021/12/12.2.2021_Apollo-Silver-NR-Langtry-43-101-CorpSec_Final-Clean-1.pdf.
- Hees, Randy, 2023, The Calico Railroad, <https://www.pacificng.com/> Accessed Aug 1, 2023.
- Hensher, Alan, 2005, The Historical Mining Towns of the Eastern Mojave Desert, in Robert E. Reynolds and Ted Weasma, editors, Old Ores: mines and mineral marketing in the east Mojave Desert—a field trip guide: Desert Symposium, California State University, Desert Studies Consortium and LSA Associates Inc., pp. 29-40.
- Hensher, Alan and Vredenburg, Larry, 1987, Waterman, Calico, Bismarck, in Ghost Towns of the Upper Mojave Desert, Third Ed., Los Angeles: 31-55.
- Hogan, Terry and O.T Johnson, 2023, Galesburg's Dream Machine, Biographical summary; <http://tjezephyr.com/backtrack/otjohnsons.html>.
- Huntington Library, 1879-1896, Henry Markham Paper Collection, Huntington Library.
- Hyde, Leslie, 1949, John Daggett, Grand Army of the Republic, Records of California Pioneers, unpublished manuscript, Sacramento, 1949, pp. 60-62.
- Jessey, David R., 2011; Calico Mining District, Field Guide, California State University, Pomona. unpublished field guide, 3 p.
- Jessey, David R., n.d., Geology and ore genesis of silver-barite mineralization in the central Mojave Desert, California, pdf and Chicago, Yumpu.
- Jessey, David R. and D.R. Tarman, 1988, "Geology of the Calico Mountains," in Don Gaskin, ed., Geologic Excursions in the Eastern Mojave Desert.
- Lane, Lucy, 1954 to 1964, oral interviews with Douglas Steeples.
- Lane, L. B., 1993, Calico Memories. Barstow: Mojave River Valley Museum, 173 p.
- Los Angeles Herald, 1884, June 7, 1884.
- Matson, H., 2008, Minerals Evaluation Report on the Langtry-Leviathan Project, on-line prospectus (link broken), Marana, Arizona, 2008
- Melchiorre, Eric, 2022, Letter to Steeples, January 6, 2022, and several telephone conversations, January-February 2023.
- Mining and Scientific Press, 1982, July 1, Sale of Silver King Mine.
- Myrick, David F., 1992, Railroads of Nevada and Eastern California, Volume II, pp. 817-822; Howell North Publishers, San Francisco.

- Nadeau, Remi, 1965, *Ghost Towns and Mining Camps of California*, Ward Ritchie Press, Los Angeles, pp. 245-252.
- Nadeau, Remi, 2003, *Silver Seekers: They Tamed California's Last Frontier*, Crest Publishing, pp. 243- 260.
- Samari, Hamid and Larry Breckenridge, 2021, *Waterloo Project, Stronghold Silver*, Resource Engineering, Ltd., Denver, Colorado, unpublished company report, May 12, 2021.
- Sanger, Pete Ehrmann, 2015, <http://onmilwaukee.com/buzz/articles.caspersangennurder.html>, April 21, 2015. This link is broken.
- U.S. House of Representatives, 1883-1896, *Precious Metals 1883-1896*, 48th to 52th Congress, Annual Report, Government Printing Office, Washington, 1883-1896.
- U.S. House of Representatives, 1899, *Report of the Director of the Mint: Precious Metals of the United States 1899*, 56th Congress, 2nd Session, Document No. 239, Government Printing Office, Washington, D. C., 1899.
- U.S. Bureau of Mines, 1958, *Mint Records, Calico Mining District*, San Francisco, unpublished report and confidential letters.
- U.S. Treasury Department, 1958, *Report of the Director of the Mint: Precious Metals*, Government Printing Office, Washington D.C.
- U.S. Treasury Department, 1958, unpublished confidential correspondence.
- Vredenburg, Larry, and Allen Hensher, 1988, *Waterman, Calico, Bismarck, Ghost Towns of the Upper Mojave Desert*, 3rd edition, Living West Press.
- Vredenburg, Larry, M. 2013, *Calico: A Brief Overview of Mining History*, in Robert E. Reynolds, editor, *Raising Questions in the Mojave Desert*, California State University Desert Studies Center, 2013 Desert Symposium, pp. 90-95.
- Vredenburg, Larry, Gary L. Shumway, and Russell D, Hartill, 1981, *Desert Fever: An Overview of Mining History of the California Desert*, The Living West Press, 323 p.
- Weber, F. Harold, 1966, *Silver Deposits of the Calico Mining District*, Volumes II and III, Calif. Division of Mines and Geology Mineral Info. Service, Volume 19, May, 1966, pp. 71-80.
- Weber, F. Harold, 1967, *Silver deposits of the Calico District. Part 3*. February. California Division of Mines and Geology, Mineral Information Service, Volume 20, February, 1967, pp. 11-15.
- Weeks, F. B., 1958, *Bismarck Mine, Calico Mining District, San Bernardino County, California*. Personal letter by Joshua T. Weakely to the Douglas Steeples, May 8, 1958.
- Wolfe, Thomas, 1934, *You Can't Go Home Again*, Simon and Schuster, New York.
- Wolle, Muriel Sibell, 1953, *Bonanza trail*, Indiana University Press, Bloomington, Tennessee.
- Wright, L.A., and others, 1953, *Mines and mineral resources of San Bernardino County, California: California Journal of Mines and Geology: Vol. 49, No. 1-2*, pp. 71-73 and 128.

A review of geology and mining in the Marble Mountains, southeastern California

David C. Buesch¹ and Bruce W. Bridenbecker²

¹ U.S. Geological Survey, Moffett Field, California, USA, E-mail: dbuesch@usgs.gov

² E-mail: bwbridenbecker@gmail.com

ABSTRACT—Mining in the Marble Mountains of southeastern California was active in the earliest 1900s and gradually declined to very few active mines by 1959, after which small claims were worked until the early 2010s. Most mining consisted of hard-rock prospects and mines, with a few soft-rock prospects and one mine. The Marble Mountains are a 10 km by 30 km, gently NE-dipping structural block composed of Proterozoic plutonic and metamorphic rocks, Paleozoic sedimentary rocks, and Jurassic granitoids exposed along the western anti-dip slopes, and Miocene volcanic and sedimentary rocks exposed along the range crest and eastern dip slopes. Mineralization occurred in metamorphic aureoles of intrusions, as contact metasomatic replacement bodies in carbonate rocks, and adjacent to thrust faults. Mineralization locally formed gold, copper, malachite, azurite, bornite, chalcopyrite, magnetite, specularite, limonite, quartz, epidote, actinolite, and garnet. Hard-rock prospects and mines are clustered in five locations. Most mines are small open pits, along with a few shafts and adits. There are a few small open-pit marble mines, and one open pit fossil mine. Eight prospects were developed in the Miocene tuffaceous deposits: three in the northwest and five in the south along with a single adit. Much of the Marble Mountains is within the Trilobite Wilderness or adjacent Areas of Critical Environmental Concern, and the area of the Golden Cycle district (Castle mine area) and prospect areas in the southern part of the range are in the Mojave Trails National Monument. The Iron Hat mine and nearby areas, and a paleontology mine in the southern range are privately owned. Most rock or mineral mines are closed, but as of 2020, one lode and four placer claims were active. South of the paleontology mine is the Marble Mountain Fossil Area of Critical Environmental Concern, where the public can collect trilobites for personal use.

Introduction

The Marble Mountains are located in the Mojave Desert, bounded by Interstate 40 along the north end of the range, Kelbaker Road on the west, and the National Trails Highway (Route 66) in the south. The range is an ~10 km by ~30 km, 135° elongate, 2–12° N60°E dipping structural block as defined by Miocene rocks that includes Proterozoic, Paleozoic, and Jurassic rocks exposed along the western anti-dip slopes, and Miocene volcanic and sedimentary rocks exposed on crests of the range and eastern dip slopes (Hall, 1985; Figure 1). There is a long history of geological work in the range on the local and regional stratigraphic correlations, paleontology, and mining (references throughout this report). Mineralization occurred in several locations and by varying processes. Mining in the range consisted of predominantly hard-rock prospects and mines, with a few soft-rock prospects. Indigenous peoples first worked the Castle mine area prior to 1900 and this area was rediscovered by the Great Gold Belt Mining Company in 1907 (Wright and others, 1953; Figure 1). Mining in this and other areas of the southern part of the range was intermittently active until 1953 (Bonham et al., 1959; Cooksley and Schafer, 1959; Neumann and Leszykowski, 1993). However, mining claims remained active through

the 1990s to 2010s when they were closed, and only two very small claims remain active (The Diggings[†], 2023).

The history of mining in the Marble Mountains is documented in by the U.S. Bureau of Land Management that maintains databases on (1) land use and management of federal lands, and (2) the surface and subsurface mines and claims using the Mineral and Land Records System (MLRS) and its predecessor Legacy Rehost System (LR2000) (U.S. Bureau of Land Management, 2023a,b). The Diggings[†] (2023) has an online database of the locations and status of mining claims on public land that is based on the MLRS. These databases contain historical data in the Marble Mountains beginning in the early 1900s to the 2020s. The U.S. Geological Survey (2023) maintains the Mineral Resource Data System (MRDS), which indicates that 17 mines existed in the Marble Mountains, most of which were active in the 1910s to 1950s.

The Southern Pacific Railroad was granted as many as eight sections within each township and range and commissioned mineral assessments in the late 1950s, as internal (unpublished) reports and maps. These geologic and mineral assessment maps cover the entire mountain range and describe economic and non-economic resources (both developed and potential). The maps for the Marble

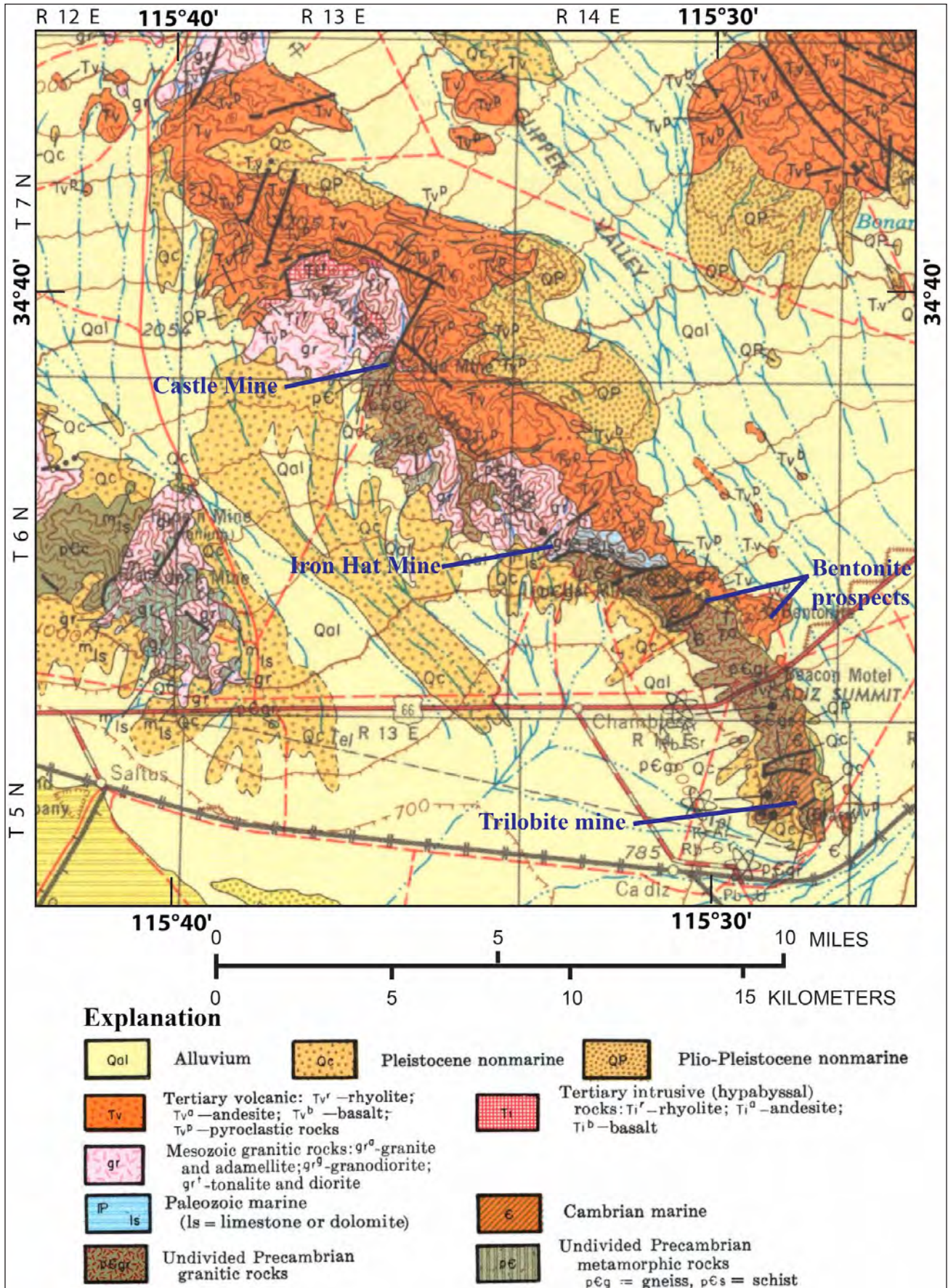


Figure 1. Geologic map of the Marble Mountains with locations of prospected or mined areas (modified from Bishop, 1963).

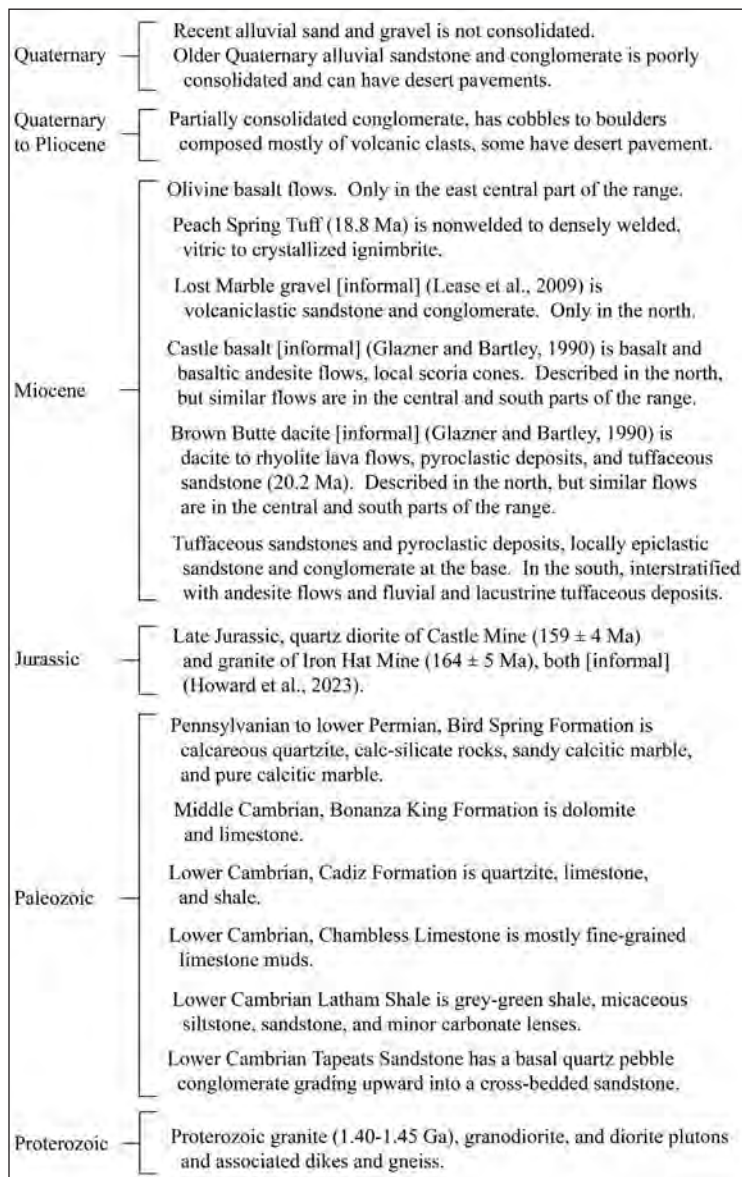


Figure 2. Simplified stratigraphic section of the Marble Mountains, southeastern California.

Mountains are Bonham et al. (1959), Cooksley and Schafer (1959), and Danehy (1959).

Land use in the Marble Mountains has evolved since the early 1980s with development of the first Areas of Critical Environmental Concern (ACECs) (U.S. Bureau of Land Management, 2015a) and in general was led by the passage of the California Desert Protection Act (1994) (U.S. Congress, 1994). Most land is administered by the Bureau of Land Management, and currently is a mixture of wilderness areas, national monuments, and conservation areas. Other holdings are by the State of California and private land. Most of the Marble Mountains are in the Trilobite Wilderness (U.S. Congress, 1994). Parts of the range and surrounding areas include the Bristol ACEC (established 2016), Chemehuevi ACEC (established 2002), and the Marble Mountain Fossil Bed ACEC (established 1980) (U.S. Bureau of Land

Management, 2015b,c). The areas of the Golden Cycle mining district (west side of the range) and altered tuff prospect areas in the southern part of the range are in the Mojave Trails National Monument (U.S. Presidential Proclamation, 2016). There are a few privately or corporately owned land holdings such as the Iron Hat mine.

The stratigraphic names used in this paper include formal and informal names as determined by the U.S. Geological Survey. The names for the Paleozoic formations and the Miocene Peach Spring Tuff are formal names. All other names are identified at first usage with the designation “[informal]” and the author(s) and date of the publication in which each was introduced.

Geology of the Marble Mountains

The Marble Mountains range is a structural block consisting of Proterozoic plutonic and metamorphic rocks, a thick section of Paleozoic sedimentary rocks, intrusions of two Late Jurassic granitoids, and a middle Miocene volcanic sequence, all surrounded by Quaternary alluvial fan deposits (Figure 1, 2).

Stratigraphy

Proterozoic igneous and metamorphic rocks crop out along the foot of the range in the south and central portion of the Marble Mountains. Granite, granodiorite, and diorite are the predominant rocks, and each have associated dikes. Dated samples of granite have ages of 1400 to 1450 Ma using K-Ar, Rb-Sr, U-Pb methods on biotite, potassium feldspar, and zircon grains (Lanphere, 1964; Silver, 1964).

Paleozoic marine sedimentary rocks in the Marble Mountains consist mostly of a conformable sequence of Cambrian shallow marine, clastic, and carbonate strata that

are capped by the Bonanza King Formation; the Pennsylvanian to Permian Bird Spring Formation occurs in a separate fault block (Figure 2; Kilian, 1964; Stone et al., 1983). These formations can be correlated across the Mojave Desert and to the Grand Canyon area (Mount, 1980; Palmer and Hazzard, 1956; Stewart, 1970; Stone et al., 1983). The general Paleozoic stratigraphy, from highest (6) to lowest (1) in the section, consists of:

- (6) The cliff-forming, Pennsylvanian to lower Permian, Bird Spring Formation composed of dolomitic limestone with fossils of crinoid stems and brachiopods, faulted against the older Paleozoic and Proterozoic rocks (Bonham et al., 1959; Stone et al., 1983).
- (5) The cliff-forming, Middle Cambrian, Bonanza King Formation composed of dolomite and limestone that

forms the capping sequence in much of the southern to central Marble Mountains (Kilian, 1964).

- (4) The cliff-forming, Lower Cambrian, Cadiz Formation composed of quartzite, limestone, and shale (Hazzard and Mason, 1936).
- (3) The cliff-forming, Lower Cambrian, Chambless Limestone composed mostly of fine-grained limestone muds. The most conspicuous feature in the rock unit is algal oncolites of genus *Girvanella* (Hazzard, 1937, 1954; Stewart, 1970).
- (2) The Lower Cambrian Latham Shale composed of grey-green shale, micaceous siltstone, sandstone, and minor carbonate lenses (Hazzard, 1954; Stewart, 1970), with an assemblage of fossils, most notable are Early Cambrian olenellid trilobites (Mount, 1980).
- (1) The Tapeats Sandstone that includes Zabriskie Quartzite overlying the Wood Canyon Formation. These units form the lowermost Cambrian to uppermost Proterozoic age rock unit area (Stewart, 1970). It is composed of a basal quartz pebble conglomerate grading upward into a cross-bedded sandstone in the southern part of the Marble Mountains. Other authors described these rocks as the Zabriskie Quartzite (Hazzard, 1937), Wood Canyon Formation (Nolan, 1929) or Prospect Mountain Quartzite (Hazzard, 1937).

Jurassic granitoid rocks either intrude or are in fault contact with Proterozoic granitoids and Paleozoic marble in the vicinity of the Castle and Iron Hat mine areas (Figure 1). These rocks are a mixture of equigranular granite, alkali feldspar granite, and older porphyritic granite to granodiorite with a minimum age of 165 Ma (Hall et al., 1988). A series of felsic dikes that appear to have an origin related to the Jurassic granites and a series of mafic dikes injected along preexisting structural weaknesses have a K-Ar age of 160 Ma (Hall et al., 1988). Howard et al. (2023) used single-crystal zircon analysis for U-Th-Pb age and Lu-Hf isotopes to date and characterize the 164 ± 5 Ma granite of Iron Hat Mine [informal] and the 159 ± 4 Ma quartz diorite of Castle Mine [informal] (which was renamed from the Castle granite of Cooksley and Schafer, 1959). The granite of Iron Hat Mine has undergone hydrothermal or deuteric alteration along fractures, joints, and shear zones, and this alteration bleached feldspars and either removed the biotite or chloritized the biotite (Bonham et al. 1959).

The Marble Mountains are capped along the length of the range and eastern dip slopes by ~700 m of Miocene lava flows, pyroclastic and volcanoclastic deposits (Kilian, 1964). The general (Neogene) Miocene stratigraphy, from highest (6) to lowest (1) in the section, consists of:

- (6) In the east central part of the range, thin olivine basalt flows deposited on the Peach Spring Tuff (Bonham et al., 1959).
- (5) The 18.8 Ma Peach Spring Tuff composed of nonwelded to densely welded, vitric to crystallized, ignimbrite. Typically, it was deposited on basalt or basaltic andesite lava flows or dacite lava flows, but locally on the Lost Marble gravel (Glazner and Bartley, 1990; Buesch, 1991; Lease et al., 2009). It was mapped as a rhyolite welded tuff (rhyolitic lithic crystal tuff, in large part welded) by Bonham et al. (1959) and Cooksley and Schafer (1959).
- (4) The Lost Marble gravel [informal] (Lease et al., 2009) composed of sandstone and well-sorted, clast-supported, pebble to cobble conglomerate beds, deposited on the Castle basalt and overlain by the Peach Spring Tuff. The Lost Marble gravel was described by Lease et al. (2009) only in the northern part of the Marble Mountains.
- (3) The Castle basalt [informal] (Glazner and Bartley, 1990) composed of basalt and basaltic andesite flows and local scoria cones, and basaltic dikes intruded the underlying dacitic tuffaceous rocks (Glazner and Bartley, 1990). This sequence was described by Glazner and Bartley (1990) only in the northern part of the Marble Mountains, although similar mafic lava flows occur beneath the Peach Spring Tuff to the south.
- (2) The Brown Butte dacite [informal] (Glazner and Bartley, 1990) composed of dacite to rhyolite lava flows and domes with associated pyroclastic flow and tephra deposits and tuffaceous sandstone. A dacite lava flow was dated with K-Ar at 20.2 Ma (Glazner and Bartley, 1990). This sequence was described by Glazner and Bartley (1990) only in the northern part of the Marble Mountains, although similar lava flows and tuffaceous rocks occur to the south. Cooksley and Schafer (1959) and Glazner and Bartley (1990) mapped dikes and stocks that were intruded into Precambrian and Paleozoic rocks, the Castle granite (renamed to quartz diorite of Castle Mine), and the Miocene lower tuffaceous and pyroclastic rocks.
- (1) Tuffaceous sandstone and pyroclastic ash and lapilli fallout tephra deposits that locally have interstratified epiclastic sandstone and conglomerate at the base. In the south, tuffaceous deposits have interstratified andesite flows and fluvial and lacustrine tuffaceous deposits.

Alluvial deposits typically have been mapped with three general age designations. From youngest (3) to oldest (1), they consist of:

- (3) Recent alluvial sediments that are unconsolidated and associated with active alluvial fans and drainages (and can include aeolian deposits). Bonham et al. (1959) and Cooksley and Schafer (1959) mapped these deposits as Recent fan and pediment deposits. Bedford et al. (2010) mapped these as intermediate alluvial fan deposits (late to middle Pleistocene) and young alluvial fan deposits (Holocene and latest Pleistocene).

- (2) Older Quaternary, alluvial fan, sandstone, and conglomerate that are poorly consolidated, typically dissected by erosion, form terraces, and have variously developed desert pavement with moderate to strong desert varnish. Bonham et al. (1959) and Cooksley and Schafer (1959) mapped these deposits as Pleistocene older fan alluvium. Bedford et al. (2010) mapped these as older alluvial fan deposits (middle to early Pleistocene), and intermediate alluvial fan deposits (late to middle Pleistocene).
- (1) Partially consolidated conglomerates, many with volcanic clasts from cobbles to boulders in size, that unconformably overlie Miocene rocks. These deposits (some have dips up to 20°) typically dip more steeply than younger (Quaternary) deposits, and they have no relations to modern drainages. Bonham et al. (1959) and Cooksley and Schafer (1959) mapped these rocks as Pleistocene and Pliocene-Pleistocene conglomerate, respectively. Bedford et al. (2010) mapped them as partially consolidated pre-Quaternary deposits, but based on the stratigraphic position, location, dips, and lack of relations to modern drainages, these can be mapped as extremely old alluvial fan deposits (early Pleistocene to Pliocene).

Metamorphism

There have been several types and periods of metamorphism. In the Proterozoic rocks, metamorphic rocks (gneisses) that have only been mapped as undifferentiated are interspersed between the plutonic rocks. In both plutonic and metamorphic rocks, there is a metamorphic overprint characterized by chlorite replacing ferromagnesian minerals; however, the timing of this event is not known. The Paleozoic section has been very weakly, regionally metamorphosed (Stone et al., 1983), converting the quartz sandstone and limestone to quartzite and marble, respectively. This metamorphism probably occurred during the Mesozoic prior to the localized contact metamorphism. Contact metamorphism and associated mineralization probably occurred during the emplacement of the Late Jurassic 164 ± 5 Ma granite of Iron Hat Mine and the 159 ± 4 Ma quartz diorite of Castle Mine plutons. In the area near the Castle mine, the country rock for mineralization included Paleozoic sedimentary and metamorphic rocks, the quartz diorite of Castle Mine, and Miocene volcanic rocks; the country rock has been strongly chloritized (Cooksley and Schafer, 1959; Neumann and Leszczykowski, 1993). Because Miocene volcanic rocks were chloritized, some of this alteration was probably related to shallow intrusions of dikes and stocks associated with the trapdoor intrusion of an equivalent of the Brown Butte dacite (Cooksley and Schafer, 1959; Glazner and Bartley, 1990).

Faulting

In the Proterozoic and Paleozoic rocks, most faults strike east to northeast with a few to the northwest, and several form splaying to anastomosing fault zones. These faults typically are normal and thrust faults and some strike-slip (Bonham et al., 1959; Cooksley and Schafer, 1959; Danehy, 1959; Kilian, 1964). Most faults in the Proterozoic and Paleozoic rocks do not cross the unconformity at the base of the Miocene section, although a few might have been reactivated with minor separation in the Miocene rocks (Figure 3). Throughout the range, the Miocene rocks are cut by a few north-striking, a few northwest-striking, and a few northeast-striking steeply dipping faults that have high-angle normal separation. In the northern part of the range, Glazner and Bartley (1990) described two sets of faults that cut the Miocene rocks. There are a few northwest-striking faults that cut the Brown Butte dacite section but do not cut the overlying Castle basalt. Of the 24 faults measured in the Brown Butte dacite, 22 vary from north- to south-southwest-strikes and dip moderately to steeply east to north-northwest, one has east-northeast-strike and dips steeply north-northwest, and one has north-northeast-strike and dips steeply west-northwest. The Castle Mine fault and intrusive dacite along the margins and within the block bounded by the Castle Mine fault were associated with a trapdoor intrusion of the dacite. Fault segments along the Castle Mine faults are vertical to steeply northeast-dipping and strike north to west. Along the western boundary of the Marble Mountains structural block, but mostly buried by Quaternary deposits, is the Bristol-Granite Mountains fault zone that forms the eastern fault of the eastern California shear zone (Dokka and Travis, 1990; Howard and Miller, 1992). Bedford et al. (2010) documented a strand of the Bristol-Granite Mountains fault that cuts middle to early Pleistocene deposits.

Mining in the range

Mining in the range began with indigenous peoples, and all historic mining claims except for four have been closed (Neumann and Leszczykowski, 1993; The Diggings[†], 2023). Mining, including exploration and development potential, are based on and influenced by 7 conditions: 1) the presence of mines and prospects with identified resources or significant production; 2) favorable geologic terrain; 3) areas where recent mineral exploration or development activities have been conducted; 4) areas of alteration, 5) logistics and costs of extraction, 6) costs of transportation to market, and 7) demand for the commodities (Neumann and Leszczykowski, 1993).

Hard-rock prospects and mines

Bonham et al. (1959), Cooksley and Schafer (1959), and Danehy (1959) all identified small prospects in the Proterozoic rocks. Some prospects far from the Late Jurassic granite and quartz diorite are labeled as possibly containing [queried] uranium (Bonham et al., 1959;

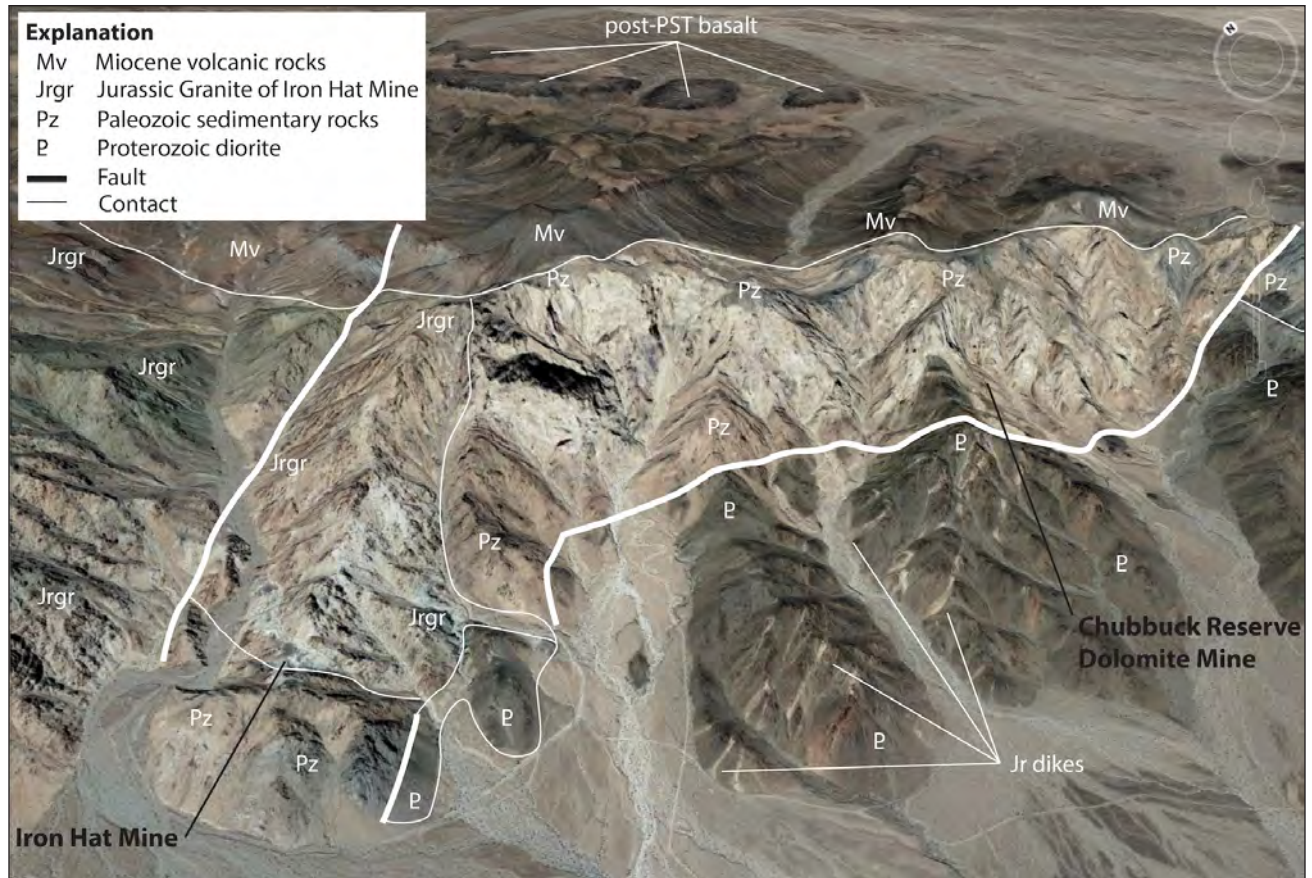


Figure 3. Oblique aerial image of the western slopes of the Marble Mountains showing the location of the Iron Hat mine and Chubbuck Reserve dolomite mine. Contacts, faults, and generalized rock units are based on Bonham et al. (1959). The fault on the left is one of the few pre-Miocene faults that were reactivated to cut the pre-Miocene unconformity. Mesas formed by the post-Peach Spring Tuff (PST) basalt are labeled to show the top of the Miocene section. View direction is along an azimuth of 040°. Google Earth image†.

Danehy, 1959). Some prospects in the Proterozoic rocks that are near the granite of Iron Hat mine have azurite and malachite. Some prospects in the Proterozoic rocks near the quartz diorite of Castle Mine were identified only as having quartz. For the prospects near the mines, it is likely that the mineralization was related to the Late Jurassic intrusions. However, in the Castle Mine area, chloritic alteration of the volcanic rocks indicates at least some alteration occurred during the Miocene intrusion of the dikes and stocks equivalent to the Brown Butte dacite (Cooksley and Schafer, 1959; Glazner and Bartley, 1990).

According to Hall et al. (1988), hydrothermal alteration formed skarn deposits in the Marble Mountains in three distinct episodes. Evidence for all of the episodes of skarns is in calcareous wall rocks adjacent to granitic intrusions. Iron poor contact skarns were the first to form. Second to form were iron-rich skarn envelopes, which encircle felsic dikes. Hall (1985) believed the dikes are the result of late-stage differentiates of the pluton. The third skarn formed at fault contacts between dolomitic marble and granite. Ore formation likely occurred as deep, iron-bearing solutions circulated along normal faults, reacted with shallow fluids and/or adjacent marble, and deposited magnetite, specularite, and limonite as both vein filling

material and replacement ore bodies, according to Hall et al. (1988).

Iron Hat mine

The Iron Hat mine is in the central part of the Marble Mountains (Figures 1, 3). The mine consists of several open pits and two tunnels that are 12.2 and 30.5 m long (Bridenbecker, 2008). Magnetite and both specular and massive hematite were reported by Lamey (1948) to be the chief ore minerals found at the seven claims reported to be the Iron Hat group, formerly called the Ironclad group (Tucker and Sampson, 1930). Hall (1985) stated that traces of copper, gold, and silver were also at the site. Bonham et al. (1959) described garnet, epidote, serpentine, calcite, wollastonite, actinolite, quartz, and small traces of chalcopyrite. From the Iron Hat mine to the southern part of the range, there were 47 mineral claims (Neumann and Leszczykowski, 1993).

Castle mine and Okanogan mine

The Golden Cycle district was developed in and along the margins of the Castle granite of Cooksley and Schafer (1959), later called [not formally named] the quartz diorite of Castle Mine by Howard et al. (2023). The Castle mine area was worked intermittently through 1941 and

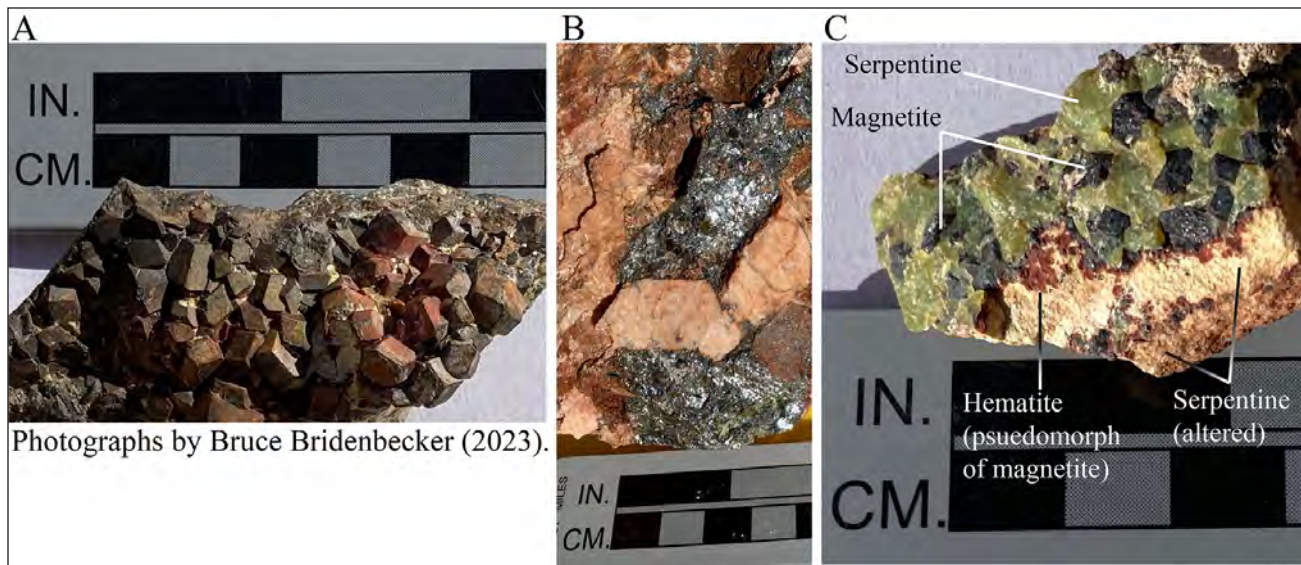


Figure 4. Rock and mineral samples from the Iron Hat mine, Marble Mountains, California. A, Magnetite crystals from edge of main adit in the ore body. B, Specularite with potassium feldspar crystals in granite from main adit. C, Magnetite and serpentine from edge of main adit.

produced a small amount of gold (Wright et al., 1953). The country rock for mineralization included Paleozoic sedimentary and metamorphic rocks, the quartz diorite of Castle Mine, and Miocene volcanic rocks; the country rock has been strongly chloritized (Cooksley and Schafer, 1959; Neumann and Leszczykowski, 1993). Polymetallic mineralization (gold, silver, and copper) is in quartz veins filling north-trending, steeply dipping shear zones (Neumann and Leszczykowski, 1993). The Castle mine consists of an excavation and two shafts that are connected at two levels. Near the Castle mine, several prospects in quartz veins occur within the Proterozoic diorite (Cooksley and Schafer, 1959). The Okanogan mine is ~1 km west of the Castle mine and consists of an excavation and three shafts. The mine and shafts targeted mineralized dikes and veins in the plutonic rock that produced gold, copper, malachite, chalcopyrite, bornite, and pyrite (Cooksley and Schafer, 1959). Chloritic alteration of the rocks (including the volcanic rocks) indicates at least some alteration occurred during the Miocene intrusion of the dikes and stocks equivalent to the Brown Butte dacite; however, mineralized fractures in the volcanic rocks have not been described (Cooksley and Schafer, 1959; Glazner and Bartley, 1990). In contrast, in the western Clipper Mountains, a vein in andesitic country rock (which was bleached adjacent to the vein) contains chalcopyrite, malachite, azurite, pyrite and presumably minor amounts of gold and silver in quartz or silicified gangue material (Cooksley and Schafer, 1959). The mineralization in the andesite country rock indicates localized mineralization during the Miocene.

Marble mines

Extensive deposits of limestone, marble, and dolomite crop out in the Marble Mountains, including occurrences of almost pure marble and marbleized limestone. The

Chubbuck Reserve dolomite mine is located ~2 km ESE of the Iron Hat mine (Figure 3), and ~2,000 tons of dolomite were mined and shipped for testing for steel flux by Kaiser Steel Corp. (Wright et al., 1953; Bonham et al., 1959). The Vaughan marble quarry, in the southernmost part of the range, produced highly colored and variegated marble that was cut, polished, and used as facing stone in buildings in the Los Angeles and San Francisco areas (Danehy, 1959; Neumann and Leszczykowski, 1993). However, in most locations, despite the high quality of occurring marble, conventional quarry mining is not feasible because of the thickness and steepness of bedding, and steep topographic slopes formed by the marble or limestone.

Fossil mine

In the southernmost Marble Mountains, paleontology specimens have been mined (Danehy, 1959). The mine is on private land, but the Marble Mountain Fossil Bed ACEC is on adjacent land, and the public can hunt there for trilobites for personal use (U.S. Bureau of Land Management, 2017).

Soft-rock prospects and mines

In the southeastern part of the Marble Mountains, Bonham et al. (1959) mapped three prospects, one mine, and one adit. In the same area, the Cadiz Summit 7.5-minute quadrangle topographic map (USGS, 1985) shows the adit of Bonham et al. (1959) with three adjacent prospects, and one prospect mapped by Bonham et al (1959) as a mine (shown by the prospect or mine leader in Figure 5). These prospects and the adit are all developed in the same part of the lower tuffaceous, pre-dacitic lava flow rocks, about two-thirds to three-fourths of the way up in the section. In this part of the section, the rocks are fine- to medium-grained tuffaceous sandstone and tuff and locally gypsiferous siltstone (Figure 6). A 1–3 m thick

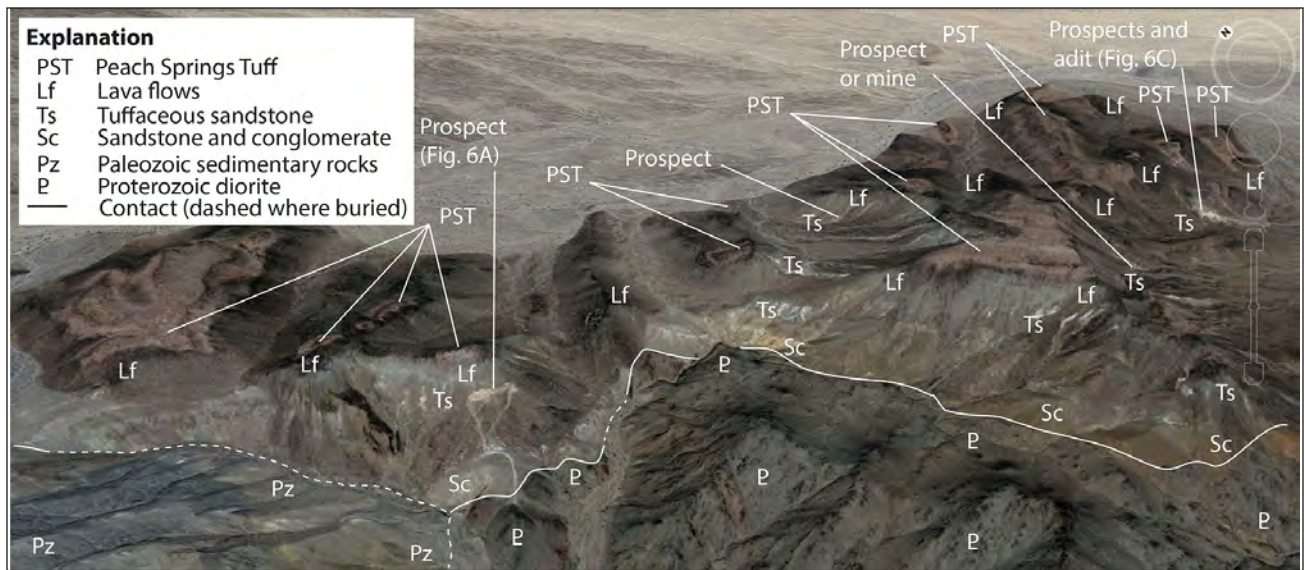


Figure 5. Oblique aerial image of the Miocene volcanic and sedimentary rocks on the east-dipping slopes of the southern Marble Mountains showing locations of the prospects and an adit. View direction is along an azimuth of 040°. Google Earth image†.

tuff has minor amounts of biotite, quartz, and feldspar crystal clasts, and the vitric components were altered to a pink-red to red, highly expandable clay (identified as bentonite by Bonham et al., 1959). The finer grain sizes, thinner bedding, locally gypsiferous beds, and low-relief of cut-and-fill structures are consistent with distal fluvial or lacustrine depositional environments (Bonham et al. 1959; Figure 6). In addition to the argillic alteration of the tuff bed, the deposits just beneath it are altered and oxidized to reddish-yellow to brownish-yellow clay; however, beds deeper in the section are not altered. Bonham et al. (1959) speculated the alteration occurred within a lake environment, but this model has not been rigorously evaluated. The stratigraphic relations indicate that these deposits occupied a relatively broad, low-relief

basin. The mine, adit, and prospects are collectively referred to as the La Feure clay deposits, and the bentonite was used for the cosmetic industry and veterinary poultice packs (Bonham et al., 1959; Neumann and Leszykowski, 1993).

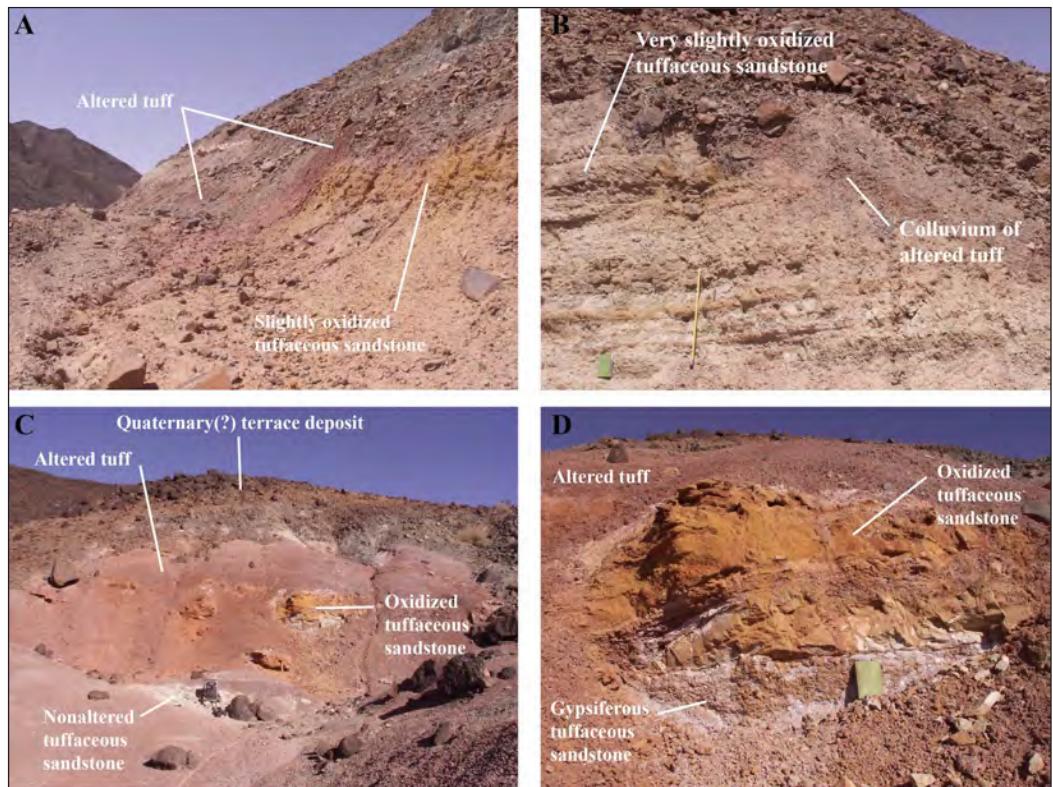


Figure 6. Photographs of Miocene tuffaceous beds in which prospects were developed in the southern Marble Mountains. A, Prospect on the western slope in the southwest part of the range with argillic altered tuff and slightly oxidized tuffaceous sandstone. B, Detail of slightly oxidized tuffaceous sandstone. Tape is 1 m. C, Prospect near the adit on the southern slope in the southeast part of the range with argillic altered tuff and oxidized tuffaceous sandstone. Daypack is 50 cm tall. D, Detail of oxidized tuffaceous sandstone with white gypsiferous beds. Book is 25 cm tall. Locations for A and C are labeled in Figure 5.

In the northwest part of the range, in the Brown Butte area, Cooksley and Schafer (1959) mapped one prospect in the lower part of the pre-lava flow, lower tuffaceous rocks. The Brown Buttes 7.5-minute quadrangle topographic map (USGS, 1985) shows two additional prospects that are higher in the section, and one is near the top of the tuffaceous section. The prospects in the tuffaceous rocks in the northern Marble Mountains were not as stratigraphically focused as those in the southern part of the range.

Stream sediment and geochemical sampling

No stream sediment sampling has been done in the Marble Mountains (Neumann and Leszczykowski, 1993). Limited geochemical sampling done in the area, through the NURE (National Uranium Resource Evaluation) program, delineated anomalous concentrations of cerium, lanthanum, uranium, and thorium in the Marble Mountains (Gray and others, 1989).

History of mining claims

The Marble Mountains have long been recognized as having metallic and nonmetallic deposits with the first mining claims registered (recordation notice) in 1907 and the most recent claims registered in the 2010 decade (Wright et al., 1953; Neumann and Leszczykowski, 1993; The Diggings[†], 2023). Although a few deposits in the range have high mineral concentrations, most are typically small and the mining is logistically challenging or expensive, the range is typically farther from markets than other resources in the Mojave, and the demands for the commodities are low (Neumann and Leszczykowski, 1993). Neumann and Leszczykowski (1993) stated that there was no mining in the Marble Mountains after 1953, and that all mines are currently idle. This is true for the larger mines such as the Castle mine and Iron Hat mine, but there were >375 mining claims registered after 1960, and there were ~4 times more claims northwest of Castle mine than those southeast of Iron Hat (The Diggings[†], 2023). Most claims were abandoned or forfeited in the 1990s to 2000s (The Diggings[†], 2023), many of which were abandoned during the establishment of the Trilobite Wilderness and Mojave Trails National Monument. Two small locations have active lode mining claims: in the Castle Mine area, registered in 1969, and three closely spaced deposits in the southeast, registered in 1987 (The Diggings[†], 2023).

Conclusions

In the Marble Mountains, several locations and periods of mineralization and metamorphism are known. During the Proterozoic metamorphism formed gneiss, and possibly minor mineralization during igneous intrusions. Regional low-grade metamorphism of the Proterozoic rocks is of uncertain age. Paleozoic rocks were weakly metamorphosed (forming quartzite and marble from respective protoliths). This metamorphism probably

occurred during the Mesozoic prior to localized contact metamorphism, and it may have been the event recorded in Proterozoic rocks. Late Jurassic intrusions of the 164 ± 5 Ma granite of Iron Hat mine are associated with dike and skarn deposits and hydrothermal or deuteric alteration. Late Jurassic intrusions of the 159 ± 4 Ma quartz diorite of Castle mine are associated with skarn adjacent to dikes. During the Miocene, a low-grade chloritization and alteration event in the Castle mine area affected some of the volcanic rocks and was associated with trapdoor faulting and intrusion of dacitic stocks. Alteration of Miocene tephra deposits to bentonite possibly occurred in a lacustrine environment.

Most of the Marble Mountains are now in the Trilobite Wilderness or adjacent Areas of Critical Environmental Concern, and the areas of the Golden Cycle district and altered tuff prospect areas in the southern part of the range are in the Mojave Trails National Monument. The Iron Hat mine area and the paleontology mine are privately owned. Most mines and prospects were closed before or during the transfer of land to the wilderness, Areas of Critical Environmental Concern, and monument areas. One small lode claim near the Castle mine and three placer claims in the south are active. The public can collect fossils in the Marble Mountain Fossil Bed Area of Critical Environmental Concern at the south end of the range.

References

- Bedford, D.R., Miller, D.M. and Phelps, G.A., 2010, Surficial geologic map of the Amboy 30' x 60' quadrangle, San Bernardino County, California: U.S. Geological Survey Scientific Investigations Map 3109, scale 1:100,000.
- Bishop, C.C., 1963, Geologic Map of California, Needles Sheet: California Division of Mines and Geology, scale 1:250,000.
- Bonham, H.F. Jr., Schafer, Max, and Cooksley, J.W., 1959, Geology and mineral resources of Township 6 North Ranges 13 and 14 East San Bernardino Base and Meridian, San Bernardino County, California: Southern Pacific Company, Land Department, Regional geologic mapping program and mineral survey, 42 p., map scale 1:24,000.
- Bridenbecker, B.W., 2008, The Iron Hat (Ironclad) ore deposits, Marble Mountains, San Bernardino County, California: Reynolds, R.E., ed., "Trough to trough: The Colorado River and the Salton Sea", California State University, Desert Studies Consortium, p. 44-47.
- Buesch, D.C., 1991, Changes in depositional environments resulting from emplacement of a large-volume ignimbrite: in Fisher, R.V., and Smith G.A., eds., Sedimentation in Volcanic Settings, Society of Economic Paleontologists and Mineralogists (Society for Sedimentary Geology) Special Publication No. 45, p. 139-153.
- Bureau of Land Management, 2023a, Bureau of Land Management California data library: Bureau of Land Management California Geospatial Data website, accessed 20Mar23, at <https://gbp-blm-egis.hub.arcgis.com/pages/california>.

- Bureau of Land Management, 2023b, Bureau of Land Management Reporting Applications -LMS and MLRS: Bureau of Land Management Reports website, accessed 20Mar23, at <https://reports.blm.gov>.
- Cooksley, J.W., and Schafer, Max, 1959, Geology and mineral resources of Township 7 North Ranges 13 and 14 East San Bernardino Base and Meridian, San Bernardino County, California: Southern Pacific Company, Land Department, Regional geologic mapping program and mineral survey, 19 p., map scale 1:24,000.
- Danehy, E.A., 1959, Geology and mineral resources of Township 5 North Ranges 13 and 14 East San Bernardino Base and Meridian, San Bernardino County, California: Southern Pacific Company, Land Department, Regional geologic mapping program and mineral survey, 22 p., map scale 1:24,000.
- Dokka, R.K., and Travis, C.J., 1990, Late Cenozoic strike-slip faulting in the Mojave Desert, California: *Tectonics*, v. 9, no. 2, p. 311–340.
- Glazner, A. F., and Bartley, J. M. 1990. Early Miocene dome emplacement, diking, and limited tectonism in the northern Marble Mountains, eastern Mojave Desert, California. in Foster, J. H., and Lewis, L. L., eds. Lower Colorado River extensional terrane and Whipple Mountains. Santa Ana, CA, South Coast Geological Society, p. 89–97.
- Gray, F., Griscom, A., Nowlan, G.A., Raines, G.L., Hodges, C.A., and Huber, D.F., 1989, Planning document for the mineral resource assessment of the Needles 1° x 2° quadrangle, California and Arizona: unpublished U.S. Geological Survey Administrative Report, 273 p.
- Hall, D.L., 1985. Contact Metamorphism, Hydrothermal Alteration, and Iron-Ore Deposition in the South-Central Marble Mountains, San Bernardino County, California: Unpublished M.A. thesis, University of California, Riverside. 240 p.
- Hall, D.L., Cohen, L.H., and Schiffman, 1988., Hydrothermal alteration associated with the Iron Hat Iron Skarn deposit, Eastern Mojave Desert, San Bernardino County, California: *Economic Geology*, v. 83, p. 568-587.
- Hazzard, J.C., 1937., The Paleozoic section of the Nopah and Resting Springs Mountains: Doctor's Dissertation, Univ. So. California. 150 p.
- Hazzard, J.C., 1954., Rocks and structure of the Northern Providence Mountains, San Bernardino County, California: California Division of Mines Bull. 170, Chapter IV, Contr.4, p. 27-35.
- Hazzard, J.C., and Mason, J.F., 1936., Middle Cambrian formations of the Providence and Marble Mountains: *Geol. Soc. Am. Bull.*, v. 47, p. 229-240.
- Howard, K.A., and Miller, D.M., 1992, Late Cenozoic faulting at the boundary between the Mojave and Sonoran blocks, Bristol Lake area, California, in Richard, S.M., ed., Deformation associated with the Neogene Eastern California Shear Zone, southwestern Arizona and southeastern California: San Bernardino County Museum Association Special Publication 92–1, p. 37–47.
- Howard, K.A., Shaw, S.E., and Allen, C.M., 2023, Magmatic record of changing Cordilleran plate-boundary conditions—Insights from Lu-Hf isotopes in the Mojave Desert: *Geosphere*, v. 19, p. 1–18, <https://doi.org/10.1130/GES02438.1>.
- Kilian, H. M., 1964., Geology of the Marble Mountains, San Bernardino County, California: Unpublished M.A. Thesis, Univ. of So. Cal., 109 p.
- Lamey, C. A., 1948, Iron Hat (Ironclad) iron-ore deposits, San Bernardino County, California: *Calif. Div. Mines Bull.*, v. 129, p. 99-109.
- Lanphere, M. A., 1964., Geochronologic studies in the Eastern Mojave Desert, California: *Jour. Geol.*, v. 72, p. 381-399.
- Lease, R.O., McQuarrie, N., Oskin, M., and Leier, A., 2009, Quantifying dextral shear on the Bristol-Granite Mountains fault zone: Successful geologic prediction from kinematic compatibility of the Eastern California Shear Zone: *Journal of Geology*, v. 117, p. 37-53. doi: 10.1086/593320.
- Mount, J. D., 1980., Characteristics of early Cambrian faunas from Eastern San Bernardino County, California: *So. California Paleo. Soc. Sp. Pub.*, no 2, p. 19-29.
- Neumann, T.R., and Leszczykowski, A., 1993, Identified mineral resources of the Needles 1° X 2° Map Quadrangle, California: U. S. Bureau of Mines, Mineral Land Assessment Open File Report 14-93, 349 p., 2 plates.
- Nolan, T. B., 1929., Notes on the stratigraphy and structure of the northwest portion of Spring Mountain, Nevada. *American Jour. Sci.* v. 17, p. 461-472.
- Palmer, A.L., and Hazzard, J.C., 1956, Age and correlation of Cornfield Springs and Bonanza King Formations in southeastern California and southern Nevada: *American Association of Petroleum Geologists Bulletin*, v. 40, p. 2494-2513.
- Silver, L. T., 1964., U/Pb radiometric date quoted on Geologic Maps of California, Needles Sheet.
- Stewart, J. H., 1970, Upper Precambrian and Lower Cambrian strata in the southern Great Basin, California and Nevada: U.S. Geological Survey Professional Paper 620, 206 p.
- Stone, Paul, Howard, K.A., and Hamilton, W., 1983, Correlation of metamorphosed Paleozoic strata of the southeastern Mojave Desert region, California and Arizona: *Geological Society of America Bulletin*, v. 94, p. 1135-1147.
- The Diggings¹, 2023, Online database of the locations and status of mining claims on public land: The Diggings website, accessed March 18, 2023, at <https://thediggings.com/usa/california/san-bernardino-ca071/map>.
- Tucker, W. B. and Sampson, R.W., 1930, San Bernardino County, in Report XXVI of the State Geologist, State of Cal., Div. of Mines, p. 261-262.
- Wright, L.A., Stewart, R.M., Gay, T.E., and Hazenbush, G.C., 1953, Mines and mineral resources of San Bernardino County, California: *California Journal of Mines and Geology*, vol. 49, nos. 1 and 2, p. 49-192.
- U.S. Bureau of Land Management, 2015a, Desert Renewable Energy Conservation Plan – Proposed Land use Plan Amendment and Final Environmental Impact Statement: U.S. Bureau of Land Management website, accessed March 23, 2023, at <https://eplanning.blm.gov/eplanning-ui/project/66459/510>.

- U.S. Bureau of Land Management, 2015b, Desert Renewable Energy Conservation Plan – Proposed Land use Plan Amendment and Final Environmental Impact Statement – Appendix L, Chemehuevi ACEC: U.S. Bureau of Land Management, p. 973-984, Bureau of Land Management website, accessed March 24, 2023, at https://eplanning.blm.gov/public_projects/lup/66459/20012656/250017253/ACEC_Piute_Valley_and_Sacramento_Mountains_Subregion.pdf.
- U.S. Bureau of Land Management, 2015c, Desert Renewable Energy Conservation Plan – Proposed Land use Plan Amendment and Final Environmental Impact Statement – Appendix L, Bristol Mountains and Marble Mountain Fossil Bed ACECs: U.S. Bureau of Land Management, p. 1036-1046, and p.1074-1083, Bureau of Land Management website, accessed March 24, 2023, at https://eplanning.blm.gov/public_projects/lup/66459/20012656/250017254/ACEC_South_Mojave-Amboy_Subregion.pdf.
- U.S. Bureau of Land Management, 2017, Mojave Trails National Monument - Marble Mountain Trilobite Fossil Collection: Bureau of Land Management, Mojave Trails National Monument website, accessed March 24, 2023, at https://www.blm.gov/sites/blm.gov/files/uploads/NLCS_CA_Mojave-TrailsNM_Marble-Mountains-trilobite-fossil-colection.pdf.
- U.S. Bureau of Land Management, 2017, Mojave Trails National Monument - Marble Mountain Trilobite Fossil Collection: Bureau of Land Management, Mojave Trails National Monument website, accessed March 24, 2023, at https://www.blm.gov/sites/blm.gov/files/uploads/NLCS_CA_Mojave-TrailsNM_Marble-Mountains-trilobite-fossil-colection.pdf.
- U.S. Congress, 1994, California Desert Protection Act 1994: U.S. Government Public Law 103-433, 55 p.
- U.S. Presidential Proclamation, 2016, Presidential Proclamation -- Establishment of the Mojave Trails National Monument: The White House, Office of the Press Secretary (February 12, 2016), <https://obamawhitehouse.archives.gov/the-press-office/2016/02/12/presidential-proclamation-establishment-mojave-trails-national-monument>.
- U.S. Geological Survey, 1985, Brown Buttes 7.5-minute quadrangle topographic map, scale 1:24,000.
- U.S. Geological Survey, 1985, Cadiz Summit 7.5-minute quadrangle topographic map, scale 1:24,000.
- U.S. Geological Survey, 2023, USGS Mineral Resource Data System (MRDS): U.S. Geological Survey website, accessed March 20, 2023, at <https://www.usgs.gov/programs/mineral-resources-program>.

† Any use of trade, firm, or product names is for descriptive purposes only and does not imply endorsement by the U.S. Government.

Early Miocene volcanism, sedimentation, and extensional faulting in the Van Winkle hills, Mojave National Preserve, southeastern California

Phillip B. Gans,¹ Elizabeth OBlack Gans,² and Andrew Kylander-Clark¹

¹University of California, Santa Barbara

²Santa Barbara City College

ABSTRACT — Our knowledge of the ages, distribution, and tectonic framework of Miocene volcanic and sedimentary successions in the eastern Mojave Desert region is incomplete. This contribution describes in detail the Miocene volcanic, sedimentation, and structural history of the Van Winkle hills (VWH) southeast of the Granite Mountains, near the southern boundary of the Mojave National Preserve. Detailed mapping, structural and stratigraphic analysis, and geochronologic investigations focused on the northern VWH, where a superbly exposed ~ 350 m-thick section of Miocene sedimentary and volcanic rocks rests on Cretaceous granite. The Miocene succession consists, in ascending order, of: (a) Basal arkose conglomerate and sandstone (*Tc*); (b) A lower tuffaceous sediment interval comprised of pumiceous debris flow deposits, plane-laminated volcanoclastic sandstone and minor intercalated lapilli- and ash-fall deposits, conglomerate beds, and debris avalanche deposits (*Tts1*); (c) A crystal-poor hbl-plag rhyodacite lava that pinches out abruptly to the east (*Trd*); (d) A middle tuffaceous sediment interval with abundant primary thin pyroclastic flows surge, and fallout deposits, grading upward into fluvial and alluvial deposits with abundant granitic detritus (*Tts2*); (e) A “capping” sequence dominated by mafic to intermediate lavas that includes, in ascending order, olivine basalt, tuffaceous sediment, pyroxene andesite, and hornblende andesite (*Toa*, *Tts3*, *Tpa*, and *Tha*). New LA-ICPMS U-Pb zircon ages were obtained on 3 primary fallout deposits, yielding ages of 23.56 ± 0.07 and 23.03 ± 0.11 for tephra horizons near the base and top of *Tts1*, and 21.35 ± 0.23 for a tephra near the middle of *Tts2*. The capping lava sequence is likely 21 to 19 Ma, given its projected position beneath 18.8 Ma Peach Spring tuff in the hills to the south. Thus, the entire section at VWH is earliest Miocene.

Sedimentary units are comprised largely of intermediate to silicic volcanic debris that accumulated in lowlands adjacent to active intermediate to silicic volcanic centers. Paleocurrent data and the eastward pinch out of *Trd* suggest these volcanic highlands lay to the west, perhaps in the Old Dad and northern Marble Mountains. The capping basalt to andesite lavas appear to have been fed by local fissure eruptions as evidenced by numerous E-W striking feeder dikes of identical composition. The older part of the Miocene sections at VWH are tilted ~25° southward and repeated on N-dipping normal faults, displaying a classic domino-style block rotation geometry. Dips shallow abruptly in the upper parts of *Tts2* and in overlying lavas to ~10–15°, across a conspicuous angular unconformity. Normal faults dip 50–55° to the north with nearly pure dip-slip slickenlines and the larger displacement faults terminate upward against (or only slightly offset) the overlying capping sequence of lavas. The combined structural and stratigraphic relations indicate that the VWH area was extended 20–25% in a ~N-S direction between 21.5 and ~19 Ma. Early Miocene extension at VWH appears to be part of a larger domain of N-S extension that includes at least the Granite and northern Marble Mountains. In this domain, S-dipping early Miocene sections rest on diverse crystalline basement rocks that must also be tilted. We speculate that the Granite Mountains plutonic complex is a large tilt block, bound on its northern flank by the 40° N-dipping Bull Canyon Fault (Howard, 1987) and overlain by 20–25° S-dipping early Miocene strata in the VWH and northern Marble Mountains, thereby providing a cross sectional view of the upper ~ 6 km of early Miocene crust, from Jurassic and Cretaceous intrusions with tectonite fabrics at deeper levels, to late Cretaceous intrusions at higher structural levels. Structural and stratigraphic relationships at VWH bring into focus questions about the distribution, magnitudes, timing, and directions of extension throughout the eastern Mojave Desert region and highlight the need for careful examination of other Miocene strata in this region.

Introduction

Our knowledge of Miocene volcanism and sedimentation in the eastern Mojave Desert region is woefully incomplete. Extensive alluvial cover and erosion have left only isolated exposures of Miocene rocks, and the few well-exposed sections that are present have received scant attention. Though Miocene volcanic and sedimentary rocks occur throughout southeastern California (Hewett, 1955; Dibblee, 1980; Dokka, 1986; Glazner et al, 2002; Theodore, 2007), there remain fundamental questions about them, including: (a) What are the age(s), location, and character of the major Miocene eruptive centers? (b) What is the geometry, age(s), and structural context of Miocene sedimentary basins? (c) What is the magnitude, distribution, direction, and timing of Miocene extensional tectonism?

The answers to these questions are critical if we are to make any headway on broader questions as to the ultimate origin of this early to mid-Miocene tectonomagmatic activity and how it fits into a broader regional and plate tectonic framework.

This contribution is a small step toward filling this knowledge gap with a detailed description of the Miocene volcanic, sedimentation, and structural history the Van Winkle hills (VWH) – an inconspicuous set of hills and ridges surrounding Van Winkle Mountain near the southern boundary of the Mojave National Preserve. Geologic mapping was carried out at 1:4000 in the northern portion of the VWH (Fig. 1) and complemented by reconnaissance work elsewhere in the hills and collection of samples for petrographic and geochronologic analysis. The VWH are just north of interstate 40 and SE of the Granite Mountains and Kelbaker road in the southernmost part of the Mojave National Preserve (Fig. 1) The detailed map area encompasses 3 km² centered on the northern ridge of these hills, where diverse plutonic, volcanic, and sedimentary rocks are well exposed. Mapping was conducted on high resolution Google Earth imagery, using the FieldMove Clino App (Vaughan et al, 2014) as the primary data collection and location device.

Lithologic/stratigraphic units were subdivided and carefully mapped out, with a critical appraisal of which contacts are depositional versus faulted (Fig. 2). Individual units were carefully described in the field, and representative samples from each rock type were examined petrographically. A wealth of orientation data was collected on bedding, laminar flow fabrics, and faults, to assess the average and spatial variations in structural

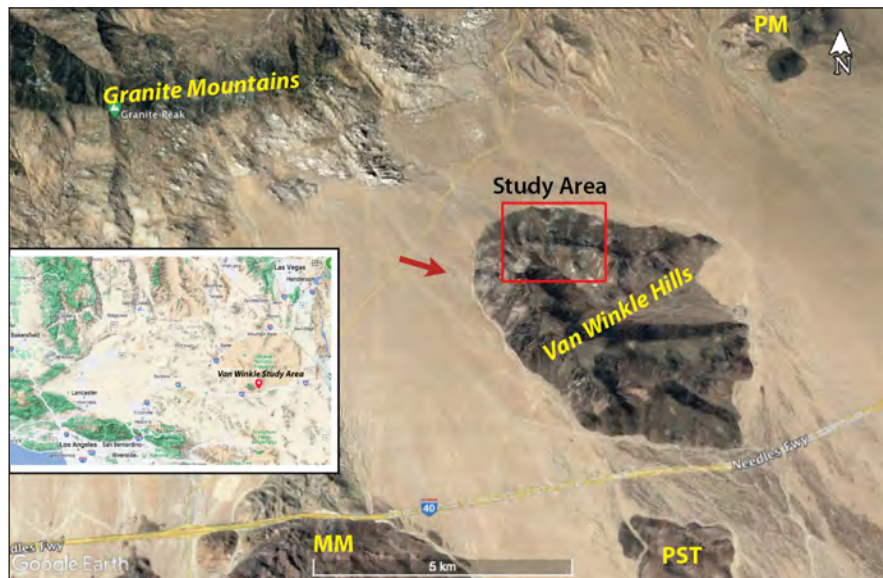


Figure 1: Google Earth image of the Van Winkle hills and surroundings, highlighting major geographic features and roads. Red box shows outline of the area mapped in this study (Fig. 2), and red arrow shows approximate orientation of the oblique view of the VWH described in Figure 11. Inset shows location of study area in context of the broader Mojave Desert region of southeastern California. **PM**–Providence Mts.; **MM**–Marble Mts.; **PST**– Peach Spring Tuff exposures south of the VWH.

orientations of each unit. The combined stratigraphic and structural data was then used to reconstruct the sequence of volcanic, depositional, and deformational events in the area and to interpret this geologic history in the context of Miocene extension and magmatism in the region. It should be emphasized that this is a preliminary report and that work in progress will complete mapping of the entire VWH and provide much additional stratigraphic, structural, and geochronologic information for this area.

Stratigraphic framework

Overview

The Van Winkle hills (formal name is Van Winkle Mountain) expose a thick succession of Miocene sedimentary and volcanic rocks that rest depositionally on a crystalline basement of Cretaceous(?) biotite granite (**Kg**) (Miller et al, 1985). The Miocene section, which was the focus of this study, locally exceeds 350 m in thickness and was divided for mapping purposes into seven different lithostratigraphic units. In ascending order these are: **Tc** - basal arkose/fanglomerate, **Tts1**- lower tuffaceous sediments, **Trd** – rhyodacite lava dome, **Tts2** – middle tuffaceous sediment, **Tob** - olivine basalt lavas, **Tts3** – upper tuffaceous sediment, and **Tpa**, **Tha** – two pyroxene andesite and hornblende andesite lavas (Fig. 2). The younger units (Tob, Tts3, Tpa, and Tha) form a capping succession that sits in a modest angular unconformity on the faulted and tilted older units. The Miocene section is particularly well exposed on the northern flank of the northernmost E-W trending ridge in the VWH (Fig. 3). Each of these units is described separately below and their

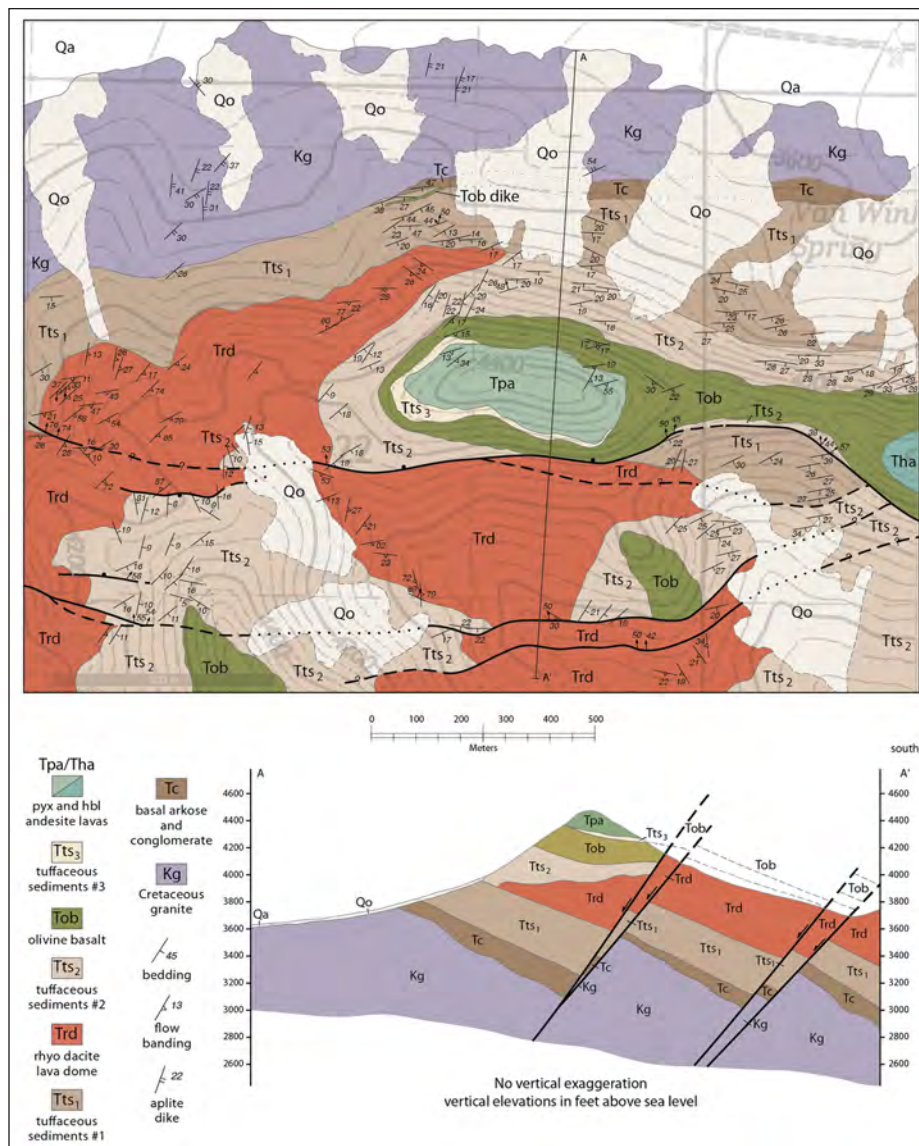


Figure 2: Geologic map and cross section of the northern Van Winkle hills. Geologic mapping was completed at 1:4000 on high resolution Google Earth imagery by P. Gans during several multi-day sessions in 2020-22. North-south geologic cross section of the northern ridge of the Van Winkle hills (viewed eastward. No vertical exaggeration, but vertical axes are in feet (elevation above sea level) while horizontal scale is in meters.

general stratigraphic relationships and variations in thickness are illustrated schematically in Figure 4.

Although the relative ages and stratigraphic position of these units within the map area are clear, volcanic units (lavas) and their proximal volcanoclastic sedimentary deposits such as these are inherently discontinuous and show marked lateral variations in thickness and character. The table below summarizes thickness variations of

Figure 3 (right): View south of the exposed Miocene section on the north-facing slope of the main ridge in the study area. Units are dipping gently (~25°) away from the viewer, such that the full Miocene succession is well exposed from this vantage point. Unit labels as on geologic map and cross section (Fig. 2).



these units as measured in a series of N-S cross sections of the northern fault block and illustrates the rapid changes that occur even within this fairly limited map area. Even a few kilometers distant a very different local stratigraphic succession might be found.

Rock unit descriptions:

Cretaceous Granite (Kg)

The oldest exposed rock is a granite that forms the crystalline basement for the Miocene succession. This poorly exposed unit forms low rounded outcrops and extensive slopes underlain by light-colored grus along the northernmost flanks of the Van Winkle hills (Fig. 2). It is almost certainly a continuation of the large late Cretaceous porphyritic monzogranite body, described by Howard et al (1987) and dated at 74.19 ± 0.44 by U-Pb zircon (Hess, 2017), that underlies the southern Granite Mts and the broad pediment to the south of the Granite Mts and NW of the Van Winkle Hills. It is a coarse-grained biotite granite with ~25–30% large blocky pink K-feldspar, 30% grey quartz, 30–35% chalky white plagioclase, ~5–8% biotite, and accessory sphene. It has a hypidiomorphic

Table 1: Thicknesses (in meters) of litho-stratigraphic units as measured off cross sections from west to east across the study area. Note the dramatic changes in the thicknesses of Tts1, Trd, and Tts2 across distances of less than 2 km.

Section	Tc	Tts1	Trd	Tts2	Tob	Tts3	Tpa/Tha
1-1'(west)	20	na	170	130	5	na	na
2-2'	10	92	110	40	10	0	na
3-3'	0	90	130	55	15	12	>30
4-4'	0	85	72	67	30	16	>30
5-5'	35	110	0	115	60	50	>45
6-6'(east)	30	140	0	162	40	0	>30

granular texture with a somewhat seriate grain size distribution. The granite is cut by occasional 10 to 50 cm thick late-stage aplite/pegmatite veins and dikes that consistently dip gently to the east and southeast.

these exposures, faint bedding is defined by moderately dipping layers of pebbles within the dominantly coarse sandy material (Fig. 3). The basal arkose is very weakly consolidated and appears to consist entirely of pebbles,

Basal Arkose and Conglomerate (Tc)

A thin, discontinuous band of very poorly exposed arkosic sandstone and conglomerate locally intervenes between the underlying Cretaceous granite and the overlying volcanoclastic section (Figs 2, 4). This unit weathers to a pale red to tan and is evident by the distinct soil color and a few deeply weathered exposures on the walls of steep ravines. In

these exposures, faint bedding is defined by moderately dipping layers of pebbles within the dominantly coarse sandy material (Fig. 3). The basal arkose is very weakly consolidated and appears to consist entirely of pebbles, grus, and sand derived from the underlying granite. Its age is unknown other than being bracketed between the ~ 75 Ma underlying granite and the immediately overlying early Miocene (~24 Ma) volcanoclastic rocks.

Tuffaceous Sediments

Intervals (Tts1, Tts2, Tts3)

Thick accumulations of well-bedded tuffaceous sedimentary rocks make up most of the Miocene section in the northern Van Winkle hills (Fig. 3,4). These include intervals of thinly bedded volcanoclastic sandstone, massive pumiceous debris flows, discontinuous conglomerate lenses, clast-supported boulder breccia, and subordinate pyroclastic fallout and flow deposits (fig. 5AA, B). These rocks weather white, light grey, or cream colored due to the abundance of silicic ash and pumice detritus and tend to form recessive or ledgy slopes. The tuffaceous sediments are dominated by volcanic detritus—glass (ash or pumice), volcanic crystals, and volcanic lithic grains of assorted sizes and compositions—but some horizons also include basement derived arkosic sand and granite clasts. It is

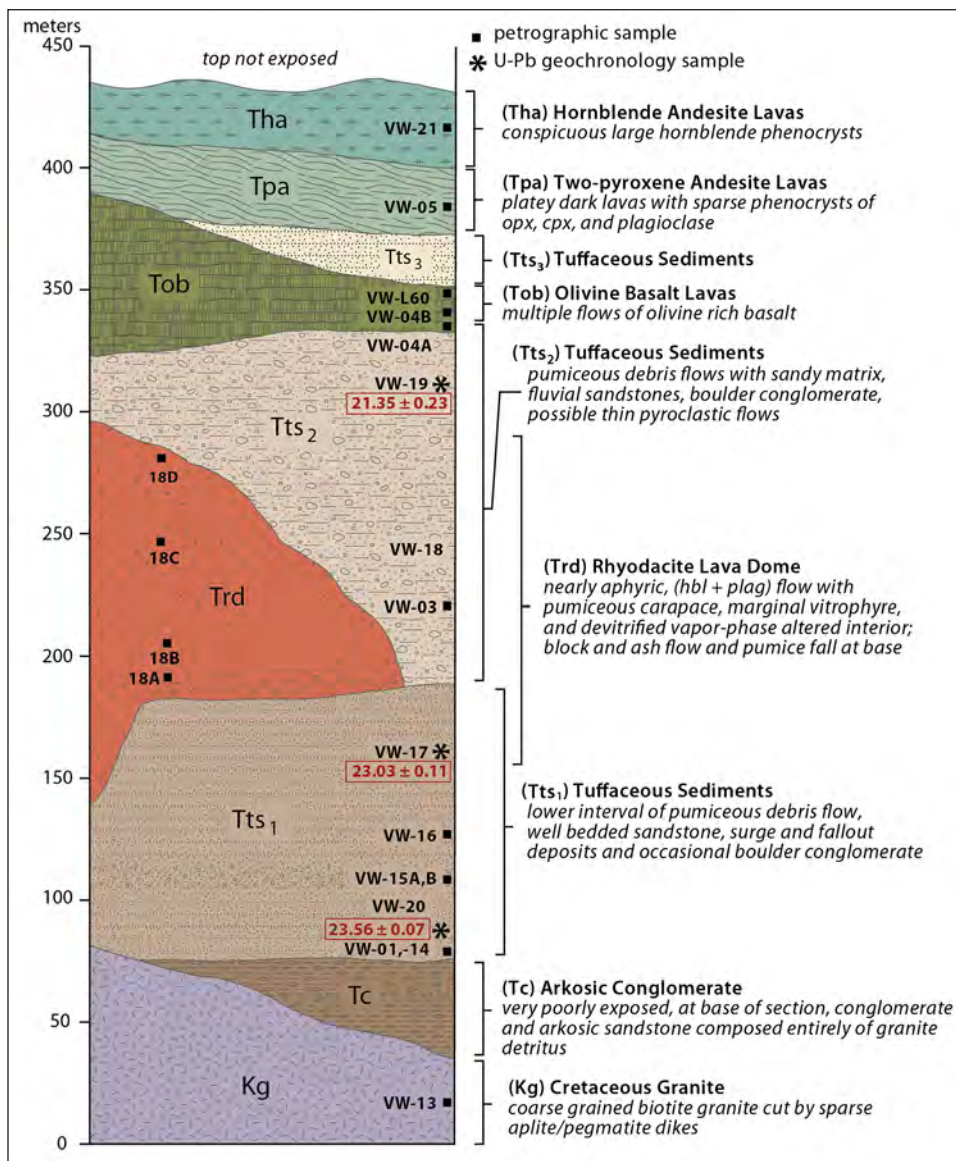


Figure 4: Generalized columnar section of the Miocene volcanic and sedimentary succession exposed in the northern Van Winkle hills, illustrating approximate thicknesses and variations in lithostratigraphic map units. See text for discussion. Approximate positions of representative petrographic and geochronologic samples (VW-___) discussed in the text are indicated by filled circles and stars, respectively.

not straightforward, on a bed-by-bed basis, to distinguish water-laid sediments (fluvial sandstones, debris flows) from primary volcanic pyroclastic deposits (fallout, surge, unwelded pyroclastic flows), particularly if the sediments represent juvenile pyroclastic material that has been only slightly reworked by fluvial and alluvial processes. The criteria we find most helpful is that water-laid sediments generally have a much higher proportion and more diverse assemblage of crystals and dense lithics in their sand sized fraction, and the grains typically display some rounding (Fig. 6A, B) compared to the equivalent grain sizes in primary pyroclastic fall, surge, and flow deposits. The latter generally have angular crystals belonging to a single magmatic phenocryst suite and an abundance of ash and lapilli-sized glass fragments, including delicate bubble wall shards (Fig. 6C) and frothy pumice clasts. Degree of sorting, grading, grain size distributions and the presence (or lack thereof) of laminations and cross beds, and cut and fill structures can further aid in determining a depositional environment (e.g., Fig. 5B, E), but ambiguities remain, especially where significant weathering and clay alteration obscure original textures. With these caveats in mind, the Tts strata in VWH are interpreted to mainly reflect aqueous transport and deposition, but the immature nature of all the detritus and the presence of occasional primary pyroclastic horizons and intercalated lavas indicates that this sedimentation occurred concurrently with and proximal to active volcanism. Several distinct lithofacies, listed below in decreasing order of abundance, make up these sections:

(a) *Pumiceous sandy debris flow deposits*: These are typically 0.5 to 2.0 m-thick, light-greyish green to tan massive beds with relatively planar tops and bottoms that are poorly sorted and lack internal stratification (Fig. 5A). The poorly sorted matrix is dominated by variably rounded fine-grained sand to grit-sized heterolithic volcanic grains, including qtz, plag, bio, hbl, and pyx crystals and assorted dacite and andesite lithics (Fig. 6B). In addition, these beds invariably contain a few percent 1-3 cm rounded white pumice and occasional large pebbles or even boulders of andesite or dacite lava and rarely granite that appear to be floating in the sandy matrix.

These beds are interpreted as debris flows (lahars) that originated in active volcanic highlands and came to rest in their current position as broad tabular sheets in the adjacent lowlands.

(b) *Plane-laminated (locally cross bedded) coarse-grained sandstone and pebbly sandstone*: Intervals up to 10 meters thick of well-bedded, reasonably well-sorted, slightly rounded coarse sandstone and pebbly sandstone occur throughout the Tts section (Fig. 5A). Volcanic crystals and dense lithic grains predominate, with relatively sparse pumice (Fig. 6A). Bedding and laminations are defined by alternations in grain size, and thicker beds may display m-scale cross stratification, cut and fill structures, and pebble lenses. All are grain- or clast-supported. This lithofacies is interpreted as primarily fluvial (bedload) deposits from braided streams or possibly meandering streams,



Figure 5: Field photographs of selected Miocene rock units from the Van Winkle hills: (A) Typical lithofacies observed in the lower sedimentary section (Tts1), including a m-scale pumiceous debris flow, thin reworked ash fall, and laminated, well-sorted volcanoclastic sandstone; (B) Juvenile rhyolite fallout deposit near base of Tts1 (sample VW-20), displaying characteristic sorting and stacking of pumice lapilli, faint laminations, and a few % small angular lithic fragments; (C) Cogenetic block-and-ash-flow deposit directly underlying the Trd lava is composed entirely of large angular blocks of pumiceous (light tan) and vitrophyric (dark grey) facies of the same rhyodacite with minor interstitial ash; (D) Large-scale flow-folding within the upper vitrophyre of the Trd lava; (E) Likely surge deposits within lower portion of Tts2 displaying characteristic large-scale cross stratification—inset shows close-up of characteristic sorting and laminations within the surge deposits; (F) Stratified dark red basaltic scoria (cinder) deposits, at the base of olivine-basalt lava sequence (Tob). 40 cm long hammer for scale in some photos.

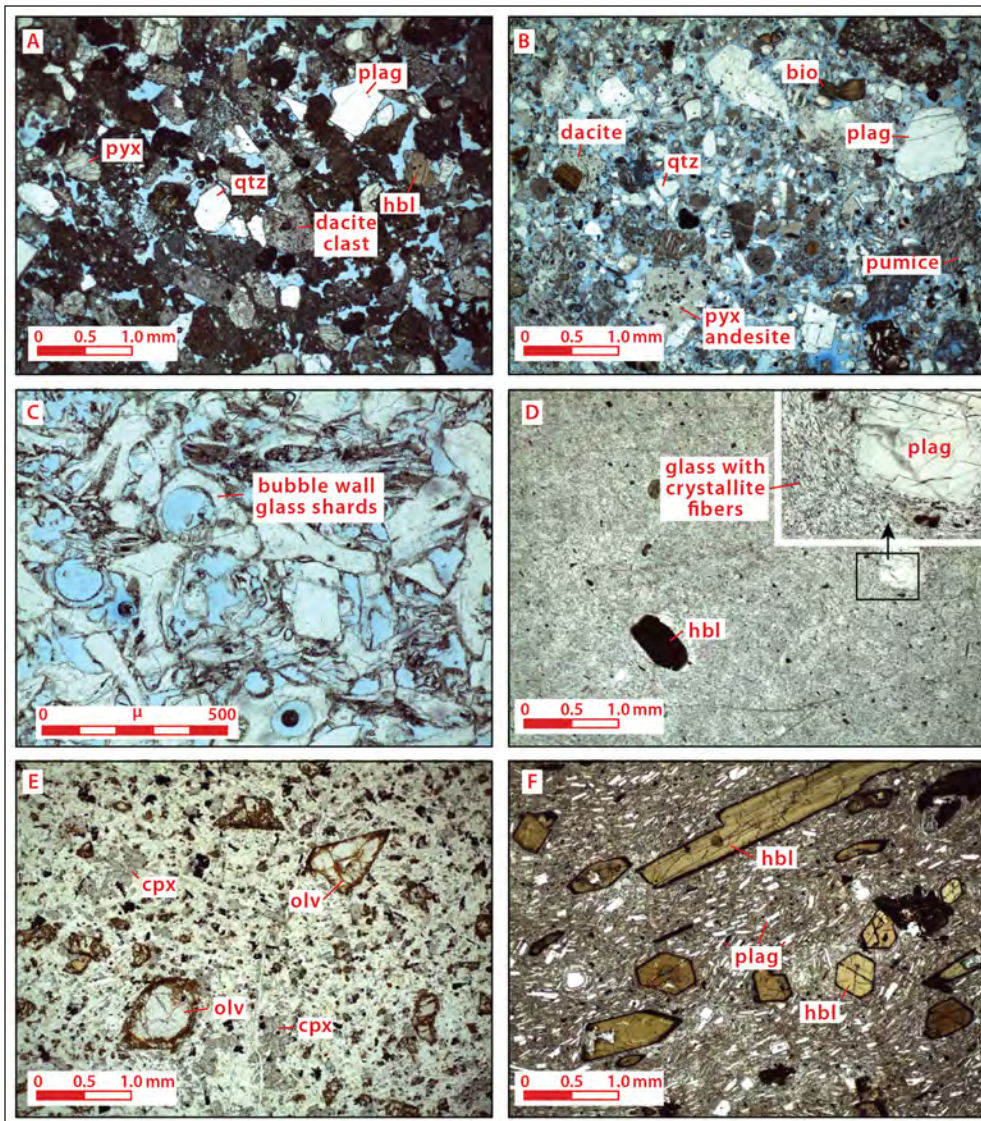


Figure 6: Photomicrographs of selected volcanic and volcanoclastic Miocene rocks from the Van Winkle hills: (A) Sample VW-01A: Well-sorted, sub-rounded, medium-grained sandstone composed entirely of volcanic crystals and lithics (pumice, dacite, andesite) but of mixed provenance; (B) Sample VW-16: Sand to silt matrix of typical pumiceous debris flow, illustrating the poor sorting and heterolithic character of these deposits; (C) Sample VW-17: The 23.0 Ma primary ash fall deposit near the top of Tts1 composed largely of delicate glass (bubble wall) shards with rare bio and plag crystals; (D) Sample VW-18A: Vitrophyre from the rhyodacite lava dome (Trd), contains very sparse (< 2%) phenocrysts of hbl and plag in a glassy groundmass riddled with flow-aligned crystallite fibers; (E) Sample VW-04A: Interior of one of the Tob olivine basalt lavas near the top of the section. Note olivine phenocrysts in a holocrystalline groundmass of iddingsitized olv, cpx, and plag; (F) Sample VW-21: Capping hornblende andesite lava in SE corner of the study area, with conspicuous large prismatic hbl phenocrysts and felted plag laths in the groundmass.

though the lack of siltstone/claystone overbank deposits is notable. Thin intervals (5–30 cm thick) of plane-laminated sandstone also commonly separate the massive debris flow beds described above, and likely represent hyperconcentrated flow deposits associated with the waning stages of the debris flow events. Differentiating some of the fluvial sandstone deposits from primary surge deposits (described below) or possibly even eolian deposits can be quite

difficult given their broad similarity.

(c) *Primary pyroclastic fallout, surge, and flow deposits:* Unambiguous “primary” pyroclastic fall and flow deposits occur sporadically within the Tts sections, though they are volumetrically minor. Ash- and lapilli-fallout deposits (tephras) form conspicuous thin but persistent white layers, 0.1 to 1.0 m thick, composed of reasonably well sorted ash (bubble-wall shards) or frothy pumice lapilli with subordinate crystal and small angular lithics (Fig. 5B, 6C). Some fallout beds grade upward into what appear to be well-stratified surge deposits, other pyroclastic intervals appear to be entirely surge deposits based on their characteristic sorting, thin discontinuous lenses of small lithic fragments, and the presence of m-scale low-amplitude cross stratification (antidunes) indicative of a high flow regime (Fig. 6E). It is possible that some of the m-scale massive, poorly sorted pumiceous debris flow beds described above may instead represent thin unwelded “hot” pyroclastic flows (ash-flow tuffs). All intervals interpreted as primary pyroclastic

deposits— i.e., resulting directly from a coeval volcanic eruption—are characterized by a much higher proportion of glass fragments relative to crystals and lithics. U-Pb dating of zircons on three tephra horizons from different stratigraphic positions within Tts yielded well-defined concordant populations of zircons representing the youngest (and dominant) age group from each sample—weighted mean ages that are in

correct stratigraphic order (see below), corroborating their interpretation as primary fallout deposits.

(d) *Clast-supported breccia and conglomerate*: A relatively minor component of the Tts intervals is lenticular bodies of clast supported cobble to boulder breccias and conglomerate. Some are clearly sedimentary in origin, occurring as discontinuous m-thick beds or lenses within the fluvial sandstone sequences and containing subrounded heterolithic volcanic and granitic clasts. These likely represent a channel fill facies. Other breccias form more continuous sheets up to several meters thick and are interpreted as either dome collapse block-and-ash-flows or small debris avalanche deposits, based on their poor sorting and the monolithologic angular m-scale clasts (Fig. 5C). Two noteworthy examples are a several m thick breccia interval in the lower part of Tts1 composed of vesicular to dense, two pyroxene andesite vitrophyre clasts, and a striking 10–15 m-thick clast-supported breccia layer that directly underlies the rhyodacite lava (Trd) that is composed exclusively of pumiceous and vitrophyric clasts of Trd (Fig. 5C).

Were it not for the intervening intervals of lava, it would be difficult to separate the Tts into the three units indicated on the map. Indeed, where Trd pinches out eastward, the distinction between Tts1 and Tts2 is fairly arbitrary and the contact is essentially a projection along form lines of bedding (Fig. 2), with the basal lapilli fallout of Trd serving as a guide. Nevertheless, there are some average differences between the three Tts mapped intervals that are worth noting. The lowest (Tts1) interval ranges from 80 to 150 m thick, thickening toward the east. Its base is marked by a sharp transition from the underlying arkose to very light colored thinly bedded pumiceous and ashy layers of well sorted and well-rounded coarse-grained volcanoclastic sandstone. The majority of Tts1 weathers a drab light greenish grey and consists mainly the pumiceous sandy debris flow lithofacies, but also includes several coarse breccia and conglomerate layers, and generally includes a higher proportion of andesitic detritus. Toward the top, Tts1 includes several discrete boulder conglomerate and breccia beds composed mainly of granitic clasts. In contrast, Tts2 (50 to 150 m thick) has a greater abundance of well-sorted coarse-grained sandstone, much of which is plane laminated or cross laminated, with thin lenses of pebble conglomerate suggesting a fluvial or alluvial environment, although some horizons display grading and cross stratification that appear to be more characteristic of surge deposits. The detritus in Tts2 is predominantly dacitic or rhyolitic, compositionally similar to the underlying rhyodacite lava.

Imbricated pebbles in a conglomerate bed near the top of Tts2 indicate WNW directed paleocurrents, but there is insufficient data to know how consistent this is. Tts2 beds become somewhat muddier with a greater proportion of debris flows and an increase in arkosic detritus in the stratigraphically highest southern part of the map area (Fig. 2). Tts3 is quite thin (≤ 50 m) and discontinuous—a local accumulation of tuffaceous sediments present between Tob and Tpa containing an appreciable component of basaltic detritus.

Rhyodacite Lava Dome (Trd)

A conspicuous cliff-forming rhyodacite lava separates Tts1 from Tts2 in the western part of the map area. It thins eastward from >150 m in its western exposures and abruptly pinches out in the central part of the map area (Table 1) The lava likely represents the remnants of a lava dome—a broad coulee or torta type edifice—that erupted to the west of the map area and flowed south or southeastward, covering a minimum of 5 km². The Trd lava displays all the classic internal color and textural variations we expect in a silicic lava dome—marked changes in appearance that arise due to variations in the cooling rate, flow field, and volatile interactions. A vertical transect through the lava reveals a thin pumiceous breccia at the base grading upward into a 5–10 m thick dark grey vitrophyre layer, followed by a pink to red devitrified interior with increasing vapor phase alteration upward (as evidenced by abundant lithophysal cavities), followed by an upper grey vitrophyre horizon and finally a 10–15 m-thick light tan glassy pumiceous carapace (Fig. 7). Laminar flow foliations defined by cm and mm scale color banding and platy partings are evident though much of the interior of the lava and are generally subparallel to its depositional contact near the base but become much more irregular in the interior due to extensive flow folding (Fig. 5D). The lava directly overlies a 1 m-thick cogenetic lapilli fallout and a ~10 m-thick monolithologic block-and-ash-flow deposit (Fig. 5C) that were emplaced during the early stages of the same rhyodacite eruption—these are included as part of the same map unit. The Trd

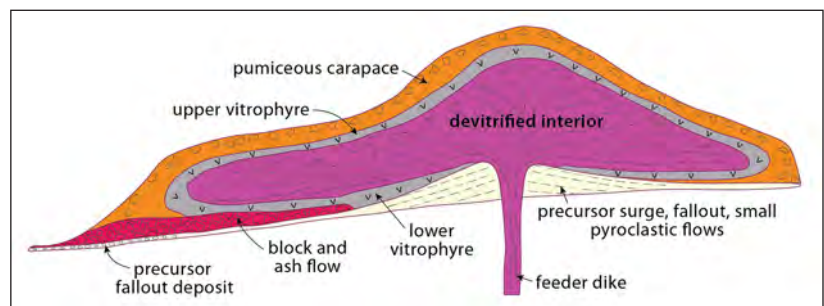


Figure 7: Architecture of a silicic lava-dome as exemplified by the Van Winkle rhyodacite (Trd). The northern face of the main east-west ridge in the study area provides a superb cross-sectional view of the facies and features that are illustrated in this conceptual model. A lobe of this lava pinches out toward the east but thickens towards the west where abundant vertical flow banding may indicate proximity to the vent.

lava is nearly aphyric, with less than 5% phenocrysts of prismatic oxyhornblende and plagioclase and trace biotite. Interestingly, many of the lithophysal cavities have large euhedral books of vapor-phase biotite in addition to chalcedony and quartz.

Olivine Basalt Lavas (Tob)

A sequence of several olivine basalt flows (Tob) overlies Tts2 at the top of the central ridge in the map area, and the same unit is inferred to form the extensive high-standing mesas of basalt in the Van Winkle hills to the south. The basal contact with Tts2 varies from concordant to clearly discordant, with Tob apparently filling in broad channels cut into Tts2 and forming a modest (10–15 °) angular unconformity with most of the Tts strata below. The exposed thickness of olivine basalt lavas ranges from ~10 m to >60 m. Where multiple flows are present, the basal one has (~10%) tiny olivine microphenocrysts—now completely replaced by red iddingsite—in a microcrystalline groundmass. Stratigraphically higher flows contain more abundant (6–8%) large (1–3mm) iddingsitized olivine and sparse dark green augite phenocrysts (Fig. 6E). Flow tops are easily recognized by their oxidized vesicular character. All these Tob flows appear to be locally derived, given the presence of bedded scoria lapilli beneath the basal flow (Fig. 5F), and the presence of compositionally identical dikes that cut stratigraphically lower units along the northern flank of the map area (Fig. 2) of Tob.

Two Pyroxene Andesite (Tpa) and Hornblende Andesite (Tha) Lavas

In the high western part of the central ridge, the Miocene section is capped by a two-pyroxene andesite lava that weather a dark brown and has a conspicuous platy parting. This unit contains 3–5% prismatic pyroxene phenocrysts (~ equal amounts of cpx and opx) in a microcrystalline groundmass of plag + pyx + minor iddingsitized olivine. At the eastern end of the same ridge, Tob is directly overlain by a different lava—a hornblende andesite with ~6–8% conspicuous large prismatic hornblende (Fig. 6F)), sparse plag phenocrysts, and occasional glomerocrysts of cpx+plag+hbl. The stratigraphic relationship between Tha and Tpa has not yet been established. A poorly exposed dike of Tha that is identical to the lava cuts the Cretaceous granite just west of the NW corner of the map area, suggesting it also was locally derived.

Age of the Van Winkle section: U-Pb geochronology of tephra horizons

New U-Pb single crystal zircon ages were obtained on three primary fallout deposits using the LA-ICPMS facility at UCSB following the procedures of Kylander-Clark et al., 2013. Zircons were separated following standard mineral separations procedures, including crushing and sieving, panning to obtain heavy mineral

concentrates, and magnetic and density separations to yield zircon concentrates that were then hand picked, mounted on epoxy pucks, polished and analyzed.

Care was taken to select the smaller ($\leq 100\mu$) euhedral prismatic (needle like) zircons in each sample for analysis, and laser spots were focused on the tips and out edges of these zircons whenever possible. Approximately 50 zircons from each sample were analyzed, and all samples yielded a coherent “young” population of concordant ages that are interpreted to represent the eruptive/depositional age of each tephra (Fig. 8). Weighted mean ages and 2 sigma (95% confidence) analytical uncertainties are reported for each sample, following the procedures of Kylander-Clark et al (2013). Even though sparse older xenocrystic zircons were present, the fact that the youngest zircons were typically the largest population in each sample and that the estimated weighted mean ages for these youngest zircon populations fall in correct stratigraphic order strengthens their interpretation as depositional ages.

Sample VW-20 (Fig 5B) was collected from a 50 cm-thick crystal rich biotite-rhyolite lapilli fallout horizon about 5 m above the basal contact of Tts1 (Fig. 2). It yielded a straightforward weighted mean age of 23.56 ± 0.07 Ma from a coherent population of 28 zircons (Fig. 8C). Sample VW-17 is a stratigraphically higher, 30 cm-thick pristine ash-fall horizon (Fig. 6C) near the top of Tts1 (~20–25 m below the contact with Trd). It yielded a weighted mean age of 23.03 ± 0.11 Ma on a coherent population of 39 zircons. Finally, sample VW-19 was collected from a 1 m-thick, slightly reworked lapilli fall horizon towards the top of Tts2, approximately 10–15 m below the depositional contact with the overlying Tob (Fig. 2). The pumice lapilli in this unit are nearly aphyric and the sample yielded relatively sparse zircons, of which only a minority proportion ($n=9$) fall in the youngest population, yielding a weight mean age 21.35 ± 0.23 Ma (Fig. 8A). Xenocrystic zircons in this sample span a broad age range and include an older Miocene (~24 Ma) population, as well as late Cretaceous and Jurassic populations. Thus, the entire Miocene section below the capping lavas at VWH appears to span slightly more than 2 Ma, from ≥ 23.5 to ≤ 21.3 Ma, and reflects an average accumulation rate of ~150 m/million years (~0.15 mm/yr). The older (23–24 Ma) part of the section, with its abundance of proximal andesitic debris, documents some of the older reliably dated local volcanic activity in the southeastern California, similar to the older ages reported by Miller et al (1994). The rhyolite lava (Trd) is bracketed between 23.0 and 21.5 Ma. The capping sequence of lavas is not yet dated ($^{40}\text{Ar}/^{39}\text{Ar}$ dating is in progress), but is likely 21 to 19 Ma, given its projected position beneath 18.8 Ma Peach Spring Tuff in the Middle Hills just south of VWH (Fig. 1). Thus, the entire section at VWH is earliest Miocene, and places important constraints on both the inception of volcanism and on the timing of extensional faulting in this part of the eastern Mojave Desert, as explored further in the sections below.

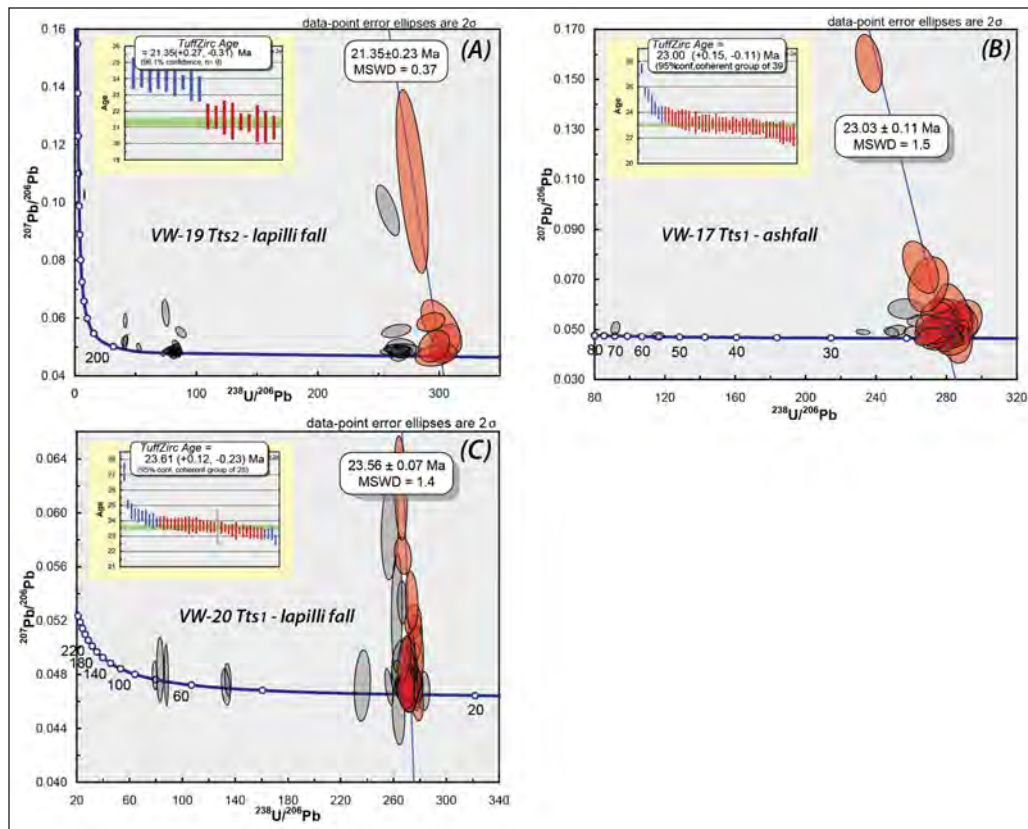


Figure 8: U-Pb LA-ICPMS zircon geochronology of three tephra layers within the Miocene succession in the Van Winkle hills. (A) VW-19—a reworked lapilli fall deposit near the top of Tts2; (B) VW-17—an ash fall deposit near the top of Tts1; (C) VW-20—a crystal rich lapilli fall deposit near the base of Tts1. Terra-Wasserburg plots for each sample shows individual zircon spot analyses with 2σ uncertainty ellipses and the weighted mean age calculated from regression through subset of younger concordant ages. Inset plot shows ^{207}Pb -corrected ages with 2 sigma error bars, arranged in increasing order, with mean weighted age of the youngest concordant zircons and uncertainty indicated by green shaded bar. See text for discussion.

Structural Framework

Overview

The overall structure of the Van Winkle hills consists of gently S-dipping volcanic and sedimentary sections, cut by steeply N-dipping normal faults of modest displacement (Fig. 2). Stratigraphically higher units (upper part of Tts2, Tob, Tpa) appear to be somewhat less tilted than lower ones, and some of the sedimentary intervals (especially Tts2) may thicken southward within each fault block, suggesting that some of these sections might have been accumulating syntectonically with movement on the bounding normal faults—e.g., growth faulting in extensional half grabens. Faults have displacements ranging from a few meters to 100s of meters and fault planes are locally well exposed, with well-developed striations (Fig. 9). As discussed below, normal faults that repeat the lower stratigraphic units (Tts1, Trd, Tts2) along the western flank of the Van Winkle hills to the south of the map area do not appear to cut (or show only minor offset of) the capping basalt sequence. These relationships require additional investigation, but all are compatible with an episode of normal faulting that occurred largely

prior to deposition of Tob.

Geometric relationships

Assessing the amount of tectonic tilting of the different stratigraphic units has large uncertainties. The most reliable data come from the Tts units, but they are poorly exposed and commonly covered by extensive veneers of Qoal (Fig. 2). More importantly, these deposits likely represent volcanoclastic and pyroclastic aprons flanking active volcanic highlands and edifices, and thus may have had moderate initial dips. Similarly, laminar flow fabrics within the intercalated lavas are notoriously unreliable as paleohorizontal indicators, given the

complex flow fields that may occur within a single lava. Nevertheless, it is clear that both Tts1 and Tts2 and most flow laminations within Trd all dip an average of $20\text{--}25^\circ$ to the SSE (Fig. 10), with an average orientation for all lower units of $\sim 075/22^\circ$. Given the amount of lateral variation and scatter in the data, it is not clear whether the tilt of Tts2 is statistically any less than Tts1, though the latter does show a marked change from SSE-dipping to SE-dipping from east to west (Fig. 10D, E). In contrast, both the basal contact and internal flow banding within Tob and Tpa appear to more gently dipping ($\leq 15^\circ$; Fig 10F).

Within the study area, there are many small-scale normal faults (<1 to 3 m offsets) that are too small to show on the map and a few larger ones with 10s to perhaps as much as 150–200 m of offset. (Fig. 2, 9). Most of the faults strike \sim E-W to WSW, and dip $50\text{--}55^\circ$ to the NNW (Fig. 10H), striking parallel to and forming a $\sim 75^\circ$ bedding-to-fault cutoff angle with the displaced strata. Slickenlines are well exposed on many of the faults and are generally very close to pure dip slip (Fig. 10H). The precise amount of displacement on the 3 or 4 bigger faults that transect the southern portion of the map area is difficult to constrain,

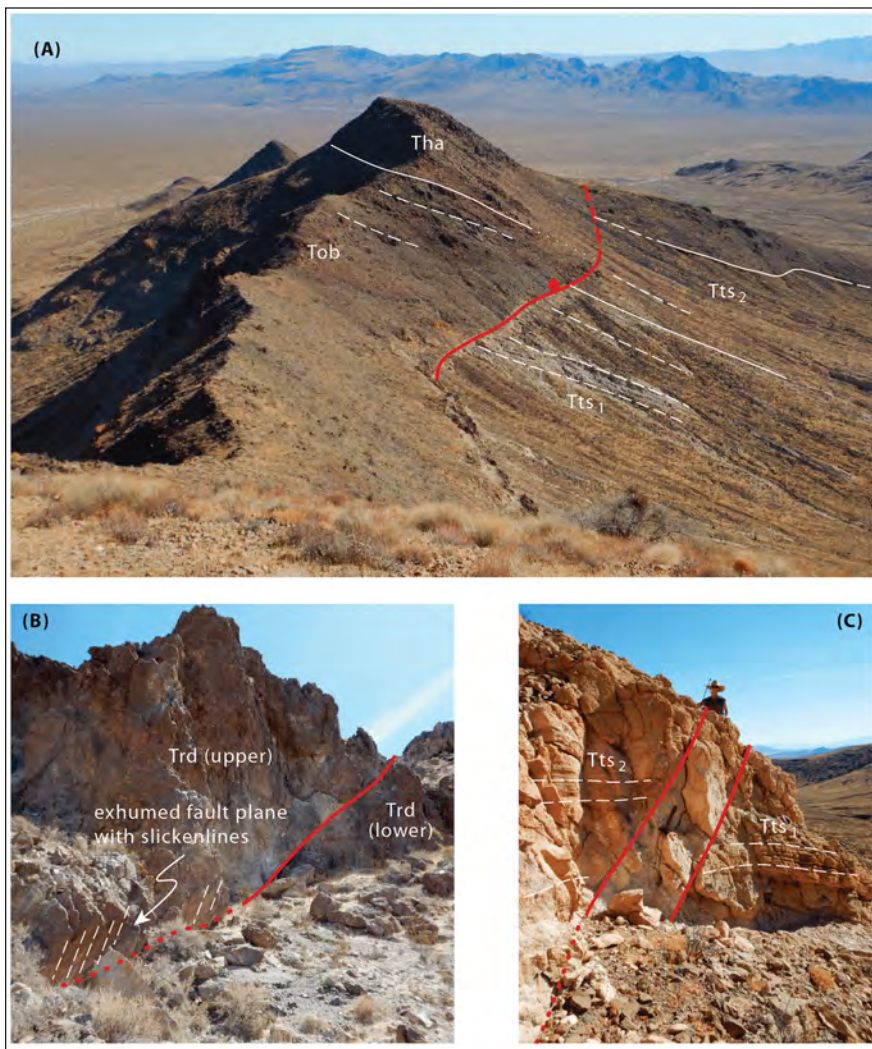


Figure 9: Field photographs of fault relations in the northern Van Winkle hills. (A) View eastward along the northern ridge, illustrating the general southward dip of bedding and the trace of one of the larger N-dipping normal faults that repeats part of the section. Note the truncation of layering in both hanging wall and footwall; (B) View east of exposed N-dipping fault that offsets Trd. Note well-exposed fault plane with slickenlines; (C) View east of N-dipping fault zone bound by two parallel slip surfaces that places lower Tts2 against upper Tts1.

mainly because of the variability and uncertainty in the thicknesses of the stratigraphic units that they cut. The best constraints are provided by the projected offset of the Tob/Tts2 contact on the northern faults and the projected Trd/Tts2 contact on the southern faults, but these have large uncertainties, yielding estimates ranging from a few 10s of meters to 50–100 m.

Magnitude and timing of extensional faulting

The faulting and tilting geometry at Van Winkle Mountain paints a coherent kinematic picture of N-dipping normal faults bounding S-tilted fault blocks reflecting modest amounts of “domino-style” N-S extension and vertical shortening (Fig. 10I). In the cross-sectional interpretation illustrated in Figure 2B, it is speculated that stratigraphic displacement may increase (slightly) downward on some of these faults due to a slight

fanning of dips and an interpreted wedge shaped geometry for some of the lower units, but most fault displacement appears to have occurred after Tts2 and pre-the capping sequence. Further mapping and structural analysis to the south and southwest will help test this hypothesis. It is clear that this style of normal faulting continues southward in the Van Winkle Mountain and is dramatically illustrated in an oblique view of the western flank of the range (Fig. 11). Detailed mapping of this area is currently in progress, but nevertheless, it is evident that repeated sections of the same Tts1, Trd, and Tts2 units described above are tilted ~20–25° southward and cut by a series of major and minor faults similar to the ones observed to the north. Simple calculations using bedding to fault cutoff angles and average stratal tilt indicate an average extension factor of ~25 to 30%, or ~ 1.5 km of N-S extension across the breadth of the Van Winkle hills – a number that will be refined with future mapping and palinspastic reconstruction. The stratigraphic relations and new age constraints from the northern ridge suggest that the majority of the extensional faulting and tilting in the VWH occurred after deposition of the ~22 Ma Trd lava, but largely predates deposition of the capping basalts (estimated to be ~19–20 Ma). This conclusion is strongly reinforced by relationships

observed in Figure 11, where several large normal faults, including one with ~ 400 m of offset, cut and offset the lower stratigraphic units but either terminate upwards or only slightly offset an angular unconformity at the base of the capping basalts. This early Miocene age for extension is in accord with relations across much of the eastern Mojave that consistently show the 18.8 Ma Peach Spring Tuff and underlying basalts is generally unfaulted and untilted (e.g. Wells and Hillhouse, 1989).

Discussion and conclusions

The VWH may not be a very impressive range, but it records a rich history of Miocene sedimentation, volcanic eruptions, and extensional faulting that provide important new insights into the early Miocene tectonic evolution of this part of the Mojave. Local volcanic activity

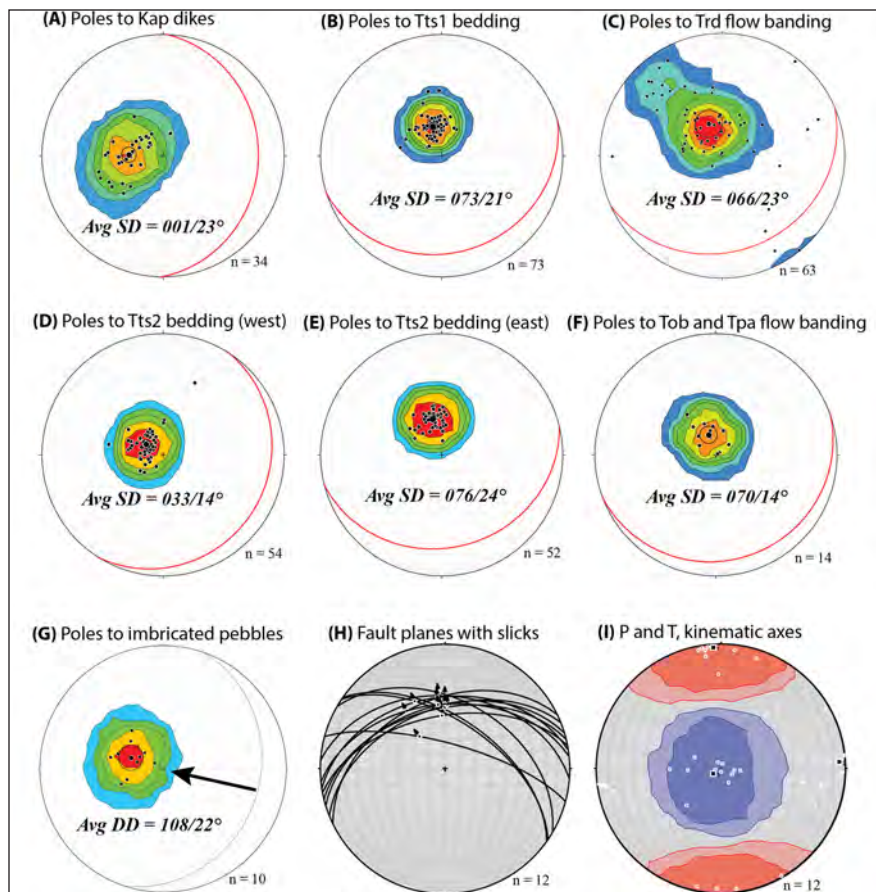


Figure 10: Lower hemisphere stereographic projections (stereonet) of structural data from the northern Van Winkle hills. (A) Poles to planar aplite dike margins within the Cretaceous granite; (B) to (F) Poles to bedding in sedimentary units and to laminar flow foliations within intercalated lavas. Great circles (red) correspond to average orientation of planar element; (G) Poles to imbricated tabular cobbles in a conglomerate bed near the top of Tts1 (after rotating bedding back to horizontal) consistently dip towards the ESE, indicating an average paleo current transport direction towards the WNW; (H) and (I) Fault planes and slickensides from measured faults, and calculated P and T axes. P and T axes and best fit kinematic axes indicate N-S extension and vertical shortening. n = number of measurements. Structural data plotted using *Stereonet* and *FaultKin* software (<https://www.rickallmendinger.net/>).

commenced ~24 Ma and resulted in the accumulation of several hundred meters of volcanoclastic sediments punctuated by deposits from nearby effusive and explosive eruptions. The Miocene section rests nonconformably on deeply weathered late Cretaceous batholithic rocks across a relatively low-relief erosion surface. The character of the sediments suggest that the area now occupied by the VWH was a lowlands but close to an active volcanic field that was erupting prodigious quantities of intermediate to silicic magmas. Following 2–3 m.y. of volcanoclastic sedimentation, the area was broken up by a system of E-W striking N-dipping normal faults and extended 25–30% in a N-S direction via domino-style block rotations—extension that is largely bracketed between 21 and 19 Ma. This extension was accompanied and followed by local fissure eruptions of basalt and minor andesite, blanketing the area with extensive thin sheets of lava. Shortly thereafter, the arrival of distal outflow sheets of

18.8 Ma Peach Spring Tuff into lowlands to the south brought an end to all the early Miocene excitement in the VWH area. Several important questions arise from the relationships and narrative described above.

What was the pre-Miocene (Early Cenozoic) tectonic history of this area?

The nonconformity between the late Cretaceous (~75 Ma) porphyritic monzogranite and the base of the Miocene section represents a major time gap (~50 Ma) and significant exhumation by processes for which we have no direct evidence. Kula (2002) estimated emplacement depths for Cretaceous plutons of the Granite Mountains of ~15 km based on Al in hornblende barometry. Even allowing for the (considerable) uncertainties in these estimates and whether they would apply to the granite directly below the Miocene unconformity in the VWH, there seems little doubt that many kilometers of section have been removed. Argon thermochronology by Hess (2017) from the SE flank of the Granite Mountain indicates very rapid cooling of these late Cretaceous intrusions from magmatic temperatures to <200° between 75 and 66 Ma, a cooling that he attributed to widespread late Cretaceous exhumation along major extensional shear zones (e.g. Wells et al. 2005). However, it is not clear why this late Cretaceous cooling would be so widespread instead of restricted to the immediate footwalls of the identified shear zones. This late Cretaceous cooling event might instead record rapid regional cooling of shallowly emplaced plutons to ambient temperatures following shutoff of the magmatic arc, rather than a specific tectonic event, and the missing section may have been removed gradually by erosion throughout the early Cenozoic. In any case, a lot of material was removed prior to the Miocene and we have little insight as to when, how, or where all the material went.

Where were the major early Miocene volcanic centers and what did they look like?

The VWH, indirectly and directly, records prolific early Miocene intermediate to silicic volcanism. The fact that the section is dominated by sedimentary (volcanoclastic)

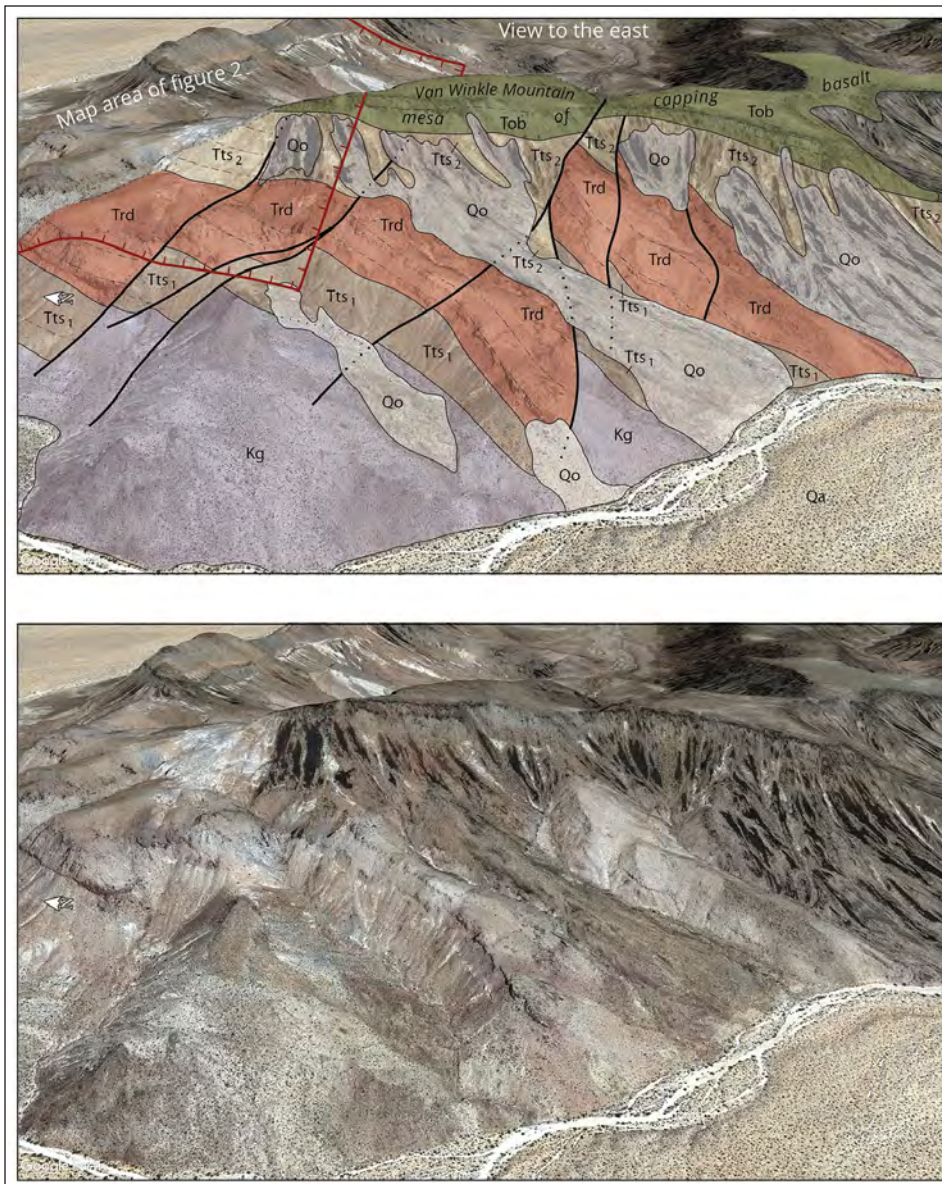


Figure 11: Oblique view of the western flank of the Van Winkle hills (Van Winkle Mountain in foreground is highest point in the VWH) illustrating key structural stratigraphic relations. Moderately S-dipping sections of the Lower Miocene (24-21 Ma) tuffaceous sediments and the rhyodacite lava (Trd) are repeated by several N-dipping normal faults that either terminate upward against, or only slightly offset, an angular unconformity at the base of the very gently-dipping sequence of “capping” lavas. (A) Geologic interpretation of the western flank of the Van Winkle Hills—based on field reconnaissance by the author. (B) Oblique view eastward of same area in Google Earth. Geologic units the same as in Fig.2. See text for discussion.

rocks and is preserved for us to examine today likely indicates that the VWH represented a lowlands at the time and that the major volcanic centers formed nearby highlands. Where were the volcanic centers located and what were their geometric and geomorphic attributes? Were they large stratovolcanoes and composite volcanoes or broad dome fields? Constructional volcanic edifices are notoriously transient in the geologic record as they are easily eroded, leaving behind only the sedimentary detritus and long runout lava and pyroclastic flows as evidence for their existence. Thick accumulations of

primary volcanic rocks occur in the Bristol and northern Marble Mountains to the W and SW and in the Clipper Mountains to the east (Miller et al, 1985; Howard et. al., 1987; Glazner and Bartley, 1990). Are these individual separate volcanic centers or relics of one larger volcanic field, now fragmented by extensional and strike-slip faulting? More investigations of the Miocene successions in these areas are sorely needed.

How widespread is the early Miocene extension that is documented in the VWH and what is the explanation for the anomalous N-S extension direction?

Much of the eastern Mojave Desert region is interpreted to be either un-extended or very weakly extended, in sharp contrast to the Colorado River extensional corridor to the east (Howard and John, 1987) with most deformation of Miocene rocks attributed to dextral shearing associated with the eastern California dextral shear zone (Dokka and Travis, 1990; Howard and Miller, 1992). This perception may stem from widespread occurrences of flat-lying to very gently tilted Miocene basalts and units such as the Peach Spring Tuff or the Woods Mountains ignimbrite sequence (Wells and Hillhouse, 1989; McCurry, 1988). However, the extension we have

documented at VWH is older than these units, raising the possibility that extension may be more widespread than previously recognized but would only be evident in the earliest Miocene strata. The early Miocene extension at VWH appears to be part of a larger domain of N-S extension that includes the Granite and northernmost Marble Mountains, perhaps truncated on the west by the younger Bristol-Granite Mountains fault (Howard et al, 1987). Further west in the Bristol Mountains and Lava Hills, thick Miocene sections are complexly faulted and

tilted, reflecting both NE-SW extension and subsequent NW-directed right-lateral shearing (e.g. Howard et al., 1987; Miller, 1994, Noorzad et al., this volume), but the connection between this extensional domain and the one described here is uncertain.

In the VWH extensional domain, consistently S-dipping earliest Miocene sections rest on diverse Mesozoic and Precambrian crystalline rocks that must also be tilted. We suggest that the entire Granite Mountains plutonic complex is part of a large tilt block within this extensional domain, bound on its northern flank by the 40° N-dipping Bull Canyon Fault (Howard et al., 1987; Hess, 2017) and overlain by 20–25° S-dipping early Miocene strata along its southern reaches in the VWH and northern Marble Mountains. This tilt block thereby provides a cross sectional view of the upper ~ 6 km of the early Miocene upper crust, from Jurassic and Cretaceous intrusions with tectonite fabrics at deeper levels, to epizonal late Cretaceous intrusions at higher structural levels. The total amount of exposed section might be less than the estimated 6 km if the block is internally broken by additional N-dipping faults—faults that might be difficult to constrain amidst the sea of granite. Future work will test this hypothesis.

Regionally, Miocene extension directions in this part of southeastern California are typically E-W or NE-SW (e.g., Dokka, 1986, 1989), including in the nearby southern Bristol Mountains (Miller, 1994). Why was the extension direction in the Van Winkle Hills apparently, N-S? Is there evidence for later rotation? If extension was initially NE-SW, it would require a major (50–60°) CCW rotation of the blocks in this area, for which there is a lack of evidence (Wells and Hillhouse, 1989). A more likely explanation is that there existed a complex strain field in the eastern Mojave during the early Miocene, with divergent extension directions in different areas. This would not be particularly surprising given the growing evidence for a similar complexity in the Colorado River extensional corridor to the east (e.g. Gans et al., 2018). In any case, the structural and stratigraphic relationships in the VWH bring into focus our lack of knowledge about the distribution, magnitudes, timing, and directions of extension throughout the eastern Mojave Desert region and highlight the need for careful examination of other Miocene strata in this region.

Acknowledgements

Thanks to Dr. Matt Rioux for first suggesting that I go take a look at the volcanic section in the Van Winkles and to the UCSB 2022 Field Methods Class students for their enthusiasm and good cheer as I dragged them out there to learn introductory mapping techniques in non-traditional geologic units. Many thanks to Evan Monroe and Ryan Eden—first as stellar TAs for that class, and later for help with the zircon dating. I have had many fruitful discussions with Dave Miller on all aspects of Mojave geology, including his prior work in the Van Winkle area,

and special thanks to him for his careful and constructive review of an earlier version of this manuscript. Partial financial support for my field work in this area was provided by a Faculty Research Grant awarded by the UCSB Academic Senate.

References Cited

- Dibblee, T. W., 1980, Cenozoic rock units of the Mojave Desert, in Fife, D.L., and Brown, A.R., eds., *Geology and mineral wealth of the California desert: Santa Ana, Calif., South Coast Geological Society*, p. 41-68.
- Dokka, R.K., 1986, Patterns and modes of early Miocene crustal extension of the central Mojave Desert, California, in Mayer, Larry, ed., *Extensional tectonics of the southwestern United States: a perspective on processes and kinematics: Geological Society of America Special Paper 208*, p. 75-95.
- Dokka, R.K., 1989, The Mojave extensional belt of southern California: *Tectonics*, v. 8, no. 2, p. 363-390.
- Dokka, R.K., and Travis, C.J., 1990, Late Cenozoic strike-slip faulting in the Mojave Desert, California: *Tectonics*, v. 9, no. 2, p. 311-340.
- Gans, P. B., Newmann, J., Monroe, E., and Kylander-Clark, A., 2018 Orthogonal (N-S) extension at the leading edge of a propagating continental rift: a reassessment of Homer Mountain and environs, lower Colorado River extensional corridor (CREC). *Geological Society of America Abstracts with Programs*, 50(5), 2018. doi: 10.1130/abs/2018RM-313804.
- Glazner, A.F., Walker, J. D., Bartley, J., 2002, Cenozoic evolution of the Mojave block of southern California. *Memoir of the Geological Society of America*. 195. 10.1130/0-8137-1195-9.19.
- Glazner, A.F., and Bartley, J.M., 1990, Early Miocene dome emplacement, diking, and limited tectonism in the northern Marble Mountains, eastern Mojave Desert, California, in Foster, J.H., and Lewis, L.L., eds., *Lower Colorado River extensional terrane and Whipple Mountains: Santa Ana, Calif., South Coast Geological Society, (Annual Field Trip Guide No. 18)*, p. 89-97.
- Glazner, A.F., Bartley, J.M., and Walker, J.D., 1989, Magnitude and significance of Miocene crustal extension in the central Mojave Desert, California: *Geology*, v. 17, no. 1, p. 50-53.
- Glazner, A.F., Nielson, J.E., Howard, K.A., and Miller, D.M., 1986, Correlation of the Peach Springs Tuff, a large-volume Miocene ignimbrite sheet in California and Arizona: *Geology* v. 14, no. 10, p.840-843.
- Hess, L.T., 2017. *Late Cretaceous Extensional Collapse of the Southern Cordillera: Evidence from the Bristol and Granite Mountains, SE California* (MS, University of Nevada, Las Vegas).
- Hewett, D.F., 1955. Structural features of the Mojave Desert region In *Crust of the Earth: A Symposium* (Vol. 62, p. 377). Geological Society of America
- Howard, K.A. and John, B.E., 1987. Crustal extension along a rooted system of imbricate low-angle faults: Colorado River extensional corridor, California and Arizona. *Geological Society, London, Special Publications*, 28(1), pp.299-311.
- Howard, K.A. and Miller, D.M., 1992, Late Cenozoic Faulting at the Boundary between the Mojave and Sonoran Blocks:

- Bristol Lake Area, California, in Richard, S.M., ed., Deformation associated with the Neogene Eastern California Shear Zone, southeastern 129 California and southwestern Arizona, *San Bernardino County Museums Special Publication*, p. 37-47.
- Howard, K.A., Kilburn, J.E., Simpson, R.W., Fitzgibbon, Todd T., Detra, D.E., Raines, G.L., and Sabine, C., 1987, Mineral resources of the Bristol/Granite Mountains Wilderness Study Area, San Bernardino County, California: *U. S. Geological Survey Bulletin*, Report: B 1712-C, p.C1-C18.
- Kylander-Clark, A.R., Hacker, B.R. and Cottle, J.M., 2013. Laser-ablation split-stream ICP petrochronology. *Chemical Geology*, 345, pp.99-112.
- Kula, J.L., 2002, *Thermochronology and Geobarometry of the Granite Mountains, southeast California; Exhumation of a Plutonic Complex During Collapse of the Sevier Orogen*: MS Thesis, University of Nevada, Las Vegas.
- Lease, R.O., McQuarrie, N., Oskin, M. and Leier, A., 2009. Quantifying dextral shear on the Bristol-Granite Mountains fault zone: Successful geologic prediction from kinematic compatibility of the eastern California shear zone. *The Journal of Geology*, 117(1), pp.37-53.
- McCurry, M., 1988. Geology and petrology of the Woods Mountains volcanic center, southeastern California: Implications for the genesis of peralkaline rhyolite ash flow tuffs. *Journal of Geophysical Research: Solid Earth*, 93(B12), pp.14835-14855.
- Miller, D. M, Miller, R., Nielson, J., Howard, K. and Stone, P., 2007, Geologic map of the Eastern Mojave National Scenic Area, in Theodore, T.G. ed., 2007. *Geology and mineral resources of the East Mojave national scenic area, San Bernardino County, California*. US Department of the Interior, US Geological Survey Bull 2160.
- Miller, D.M., 1994. Cenozoic deposits in the Lava Hills and southern Bristol Mountains, southeastern California. in *Tertiary stratigraphy of highly extended terranes, California, Arizona, and Nevada: US Geological Survey Bulletin*, 2053, pp.99-107.
- Miller, D.M., Wells, M.L., Dewitt, E., Walker, J.D., and Nakata, J.K., 1996, Late Cretaceous extensional fault system across the northeastern Mojave Desert: *San Bernardino County Museum Association Quarterly*: v. 43 (1), p. 77–83.
- Miller, D.M., Glick, L.L., Goldfarb, Richard, Simpson, R.W., Hoover, D.B., Detra, D.E., Dohrenwend, J.C., and Munts, S.R., 1985, Mineral resources and resource potential map of the South Providence Mountains Wilderness Study Area, San Bernardino County, California: *U.S. Geological Survey Miscellaneous Field Studies Map MF-1780-A*, scale 1:62,500.
- Theodore, T, ed. (2007), “Geology and Mineral Resources of the East Mojave National Scenic Area, San Bernardino County, California” *U.S. Geological Survey Bulletin 2160*.
- Vaughan, A., Collins, N., Krus, M. and Rourke, P., 2014, May. Recent development of an earth science app-FieldMove Clino. In *EGU general assembly conference abstracts* (p. 14751).
- Wells, M.L., Beyene, M.A., Spell, T.L., Kula, J.L., Miller, D.M., Zanetti, K.A., 2005, The Pinto zone; a Laramide synconvergent extensional shear zone in the Mojave Desert region of the southwest United States: *Journal of Structural Geology*, v.27, p. 1697-1720.
- Wells, M.L., and Hoisch, T. D., 2008, The role of mantle delamination in widespread Late Cretaceous extension and magmatism in the Cordilleran Orogen, western United States: *Geological Society of America Bulletin*, v. 120, p. 515-530.
- Wells, R.E., and Hillhouse, J.W., 1989, Paleomagnetism and tectonic rotation of the lower Miocene Peach Springs Tuff: Colorado Plateau, Arizona to Barstow, California: *Geological Society of America Bulletin*, v. 101, no. 6, p. 846-863.

Plant rings in the Colorado River Delta: clones, ghosts, and zombies

David K. Lynch,¹ Steven M. Nelson,² and Tomás E. Rivas Salcedo³

¹ Thule Scientific, corresponding author. david@alumni.caltech.edu

² Independent Scientist

³ Sonoran Institute

ABSTRACT — Satellite, aerial and ground surveys of the Colorado River delta and flood plain revealed circular plant growth (“plant rings”) in saltgrass (*Distichlis palmeri*), cattail (*Typha domingensis*) and mesquite (*Prosopis glandulosa*). Tides, tectonics, and climate have profound and ongoing changes to the delta. They determine when, where, and how plant rings grow, eliminating some and allowing others to take root and flourish.

1. Introduction

Circular plant growth is a rare form of development where the plant grows radially outward in ever-expanding rings as the central region dies off (necrotic zone)¹⁻⁴. It occurs when seeds, rhizomes or stolons thrive on the outer periphery of the plant but not on the inside where germination is prevented due to lack of water, nutrients or the presence of growth-inhibiting substances (allelopathy). Ring growth can be sexual or asexual (clonal)⁴ and is seen in both woody and herbaceous species^{4,5} and fungi⁵. Rings are often found in stressful or transitional environments¹⁻⁴, usually in groups of same-species rings called *ring fields*⁴. Besides rings, other patterns can occur⁶ — bands and labyrinths — and are examples of self organization⁷. Ring growth was first reported in 1947 by Watt⁸, although it has undoubtedly been known since antiquity. Such rings are found all over the world and many were recently discovered or recognized in the Colorado River flood plain and delta.

The Colorado River is one of the most controlled rivers in the world⁹. Yet despite heavy damming in the US, the delta in Mexico remains dynamic, as it has been since before the first European explorers documented it¹⁰. Today, the river is an ever-changing maze of channels and canals that are subject to the whims of nature¹¹⁻¹⁵ and human activities¹⁶⁻¹⁹. The key processes affecting the river are (1) diversion of riparian flow and groundwater pumping for domestic use and agriculture, and (2) deflation of parts of the delta from the loss of fluvial sediment²⁰⁻²². Three interacting forces give the delta its ever-changing character: *tectonics, tides and climate*.

In this paper we report plants rings and ring fields in Mexico’s Colorado River flood plain and estuary (Figure 1). In a related paper²³, we discuss how the delta’s tides, sedimentation, river water discharge and earthquakes influence tidal bores.



Figure 1. Colorado River flood plain and delta (Google Earth) overlaid with locations of ring fields from the satellite survey. Orange circles (lower right): M group *Distichlis palmeri*. Red triangles (center right): T group *Typha domingensis*. Yellow squares (center): CR group dead *Typha*. Green stars (upper left): LS group *Prosopis glandulosa*. Image from Google Earth.

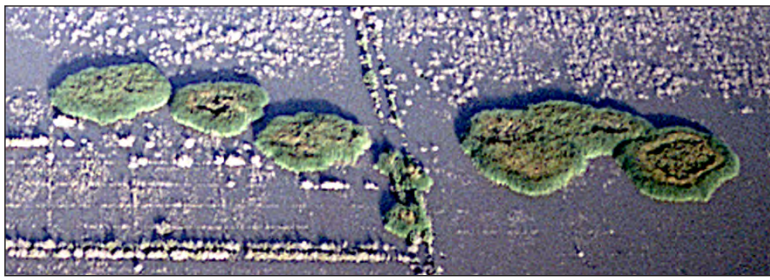


Figure 2. Living *Typha domingensis* rings near the Ayala Drain channel. Note the characteristic brown suppressed zone in the middle of the rings. On the right, several rings have merged. Rings are about 30m across. Photo by Steven Nelson, August 11 1985.



Figure 3. *Distichlis* rings. Note the characteristic starburst stolon growth patterns. The smallest ring is roughly 8 meters across. Photo by Steven Nelson, October 13 1985

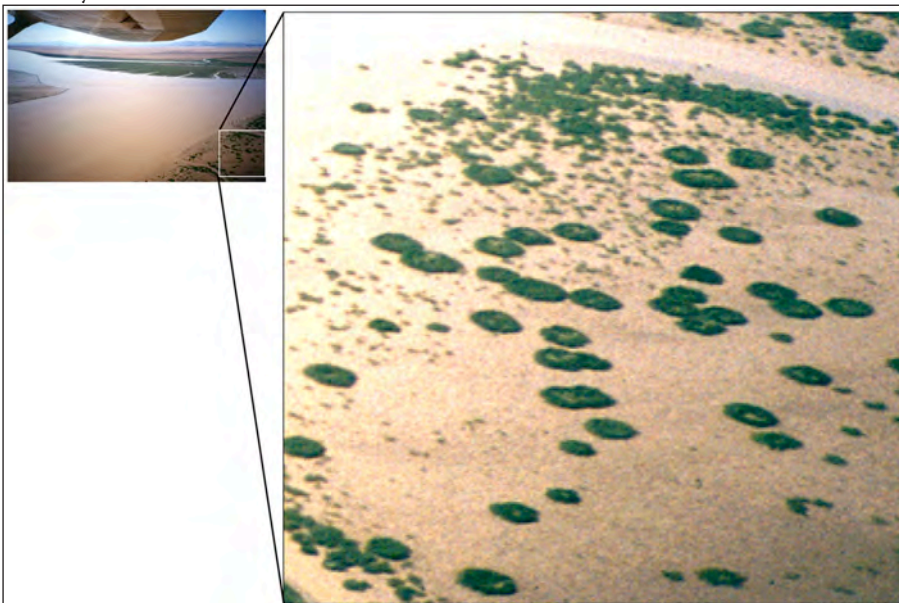


Figure 4. *Distichlis* rings. Note the obvious “doughnut” shape with central suppression zone. Photo by Steven Nelson, Aug 11 1985.

2. Aerial and Field Observations

Starting in 1984, Nelson²⁴ made several reconnaissance flights over the lower delta in light aircraft. Many of his photos showed plant rings (Figures 2–4). Over a period of several years, he and his colleagues made ground observations by gaining access with motorboats and kayaks (Figure 5).

3. Satellite Survey

Prompted by features seen in Figures 2–5, we performed a limited Google Earth search for plant rings in the area using the method described by Lynch⁴ (Figure 1). Only places near the delta and Laguna Salada were explored: agricultural fields and mountainous terrain were not. Ring fields were assigned names and their locations documented. We found many other rings not marked in Figure 1 that have not been identified and we undoubtedly missed other rings in the area.

Figure 1 shows that ring fields fall into four distinct groups of single species plants. (1) M group *Distichlis palmeri*, (2) T group *Typha domingensis*, (3) CR group dead *Typha*, and (4) LS group *Prosopis glandulosa*.

4. Rings in the delta

4.1 Saltgrass Rings (*Distichlis palmeri*)

Saltgrass^{25,26} rings were the most common in the lower estuary near Montague Island (M group) where they experience frequent tidal inundations (Figures 6, 7). This species is a halophyte endemic to tidal marshes of the northern part of the Gulf of California. Saltgrass rings are most often found in groups within half a kilometer of tidal channels, though isolated plants occurred farther inland. Rings tend to occur in lineaments, usually found along elevated flats adjacent to tidal drainage channels. In some parts of the estuary, saltgrass began growing in areas that experienced subsidence and consequent tidal flooding following the 2010 El Mayor-Cucapah earthquake. After they are established from seeds, rings grow asexually and develop starburst patterns (Figure 8) of stolons (runners), initially with suppressed zones and later with necrotic zones. Saltgrass rarely covers large areas, although rings may merge into sizable irregularly shaped masses (Figure 9). Rings show a variety of ring sizes, the smaller ones presumably being younger. Based



Figure 5. *Distichlis* ring on Montague Island with central suppression zone. Photo by Steven Nelson, May 17 1986.

4.2 Cattail (*Typha domingensis*)

Cattails²⁷ are widespread throughout the world and are found in freshwater parts of the delta, especially in lagoons and ditches of the Cienega de Santa Clara²⁸ and Hardy-Colorado Wetland^{16,29}. They are perennial, herbaceous emergents that can reproduce sexually or asexually. Cattails can grow together into large, formless masses (Figure 10). Their rings do not produce empty *necrotic zones* in the same sense that other ring plants do. Instead a central brown *suppressed zone* develops (Figure 2), perhaps because the inner thatch is inhibiting growth. But the brown plant parts are not dead and can revitalize after a fire.

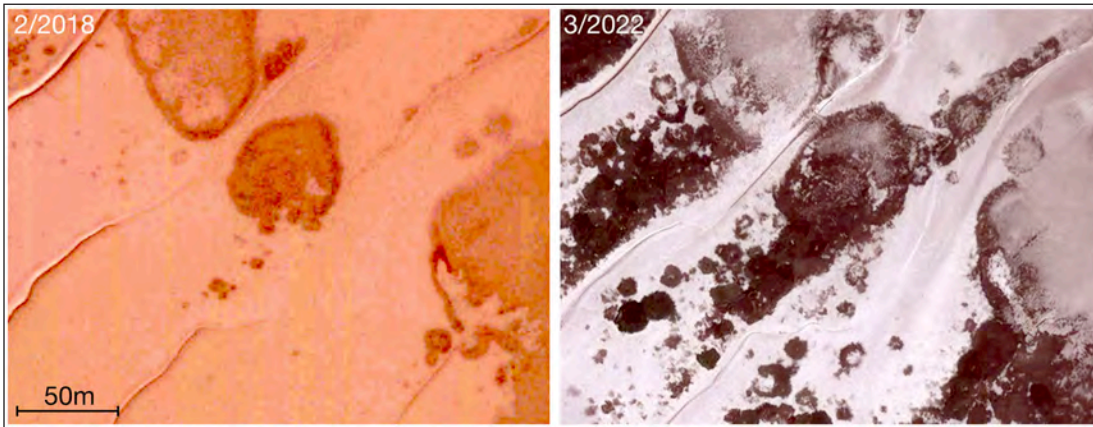


Figure 6. Development of M3 ring field of *Distichlis* on Montague Island from 2018 to 2022. Note the large preexisting rings and significant new growth of rings along drainage channels. Image from Google Earth.

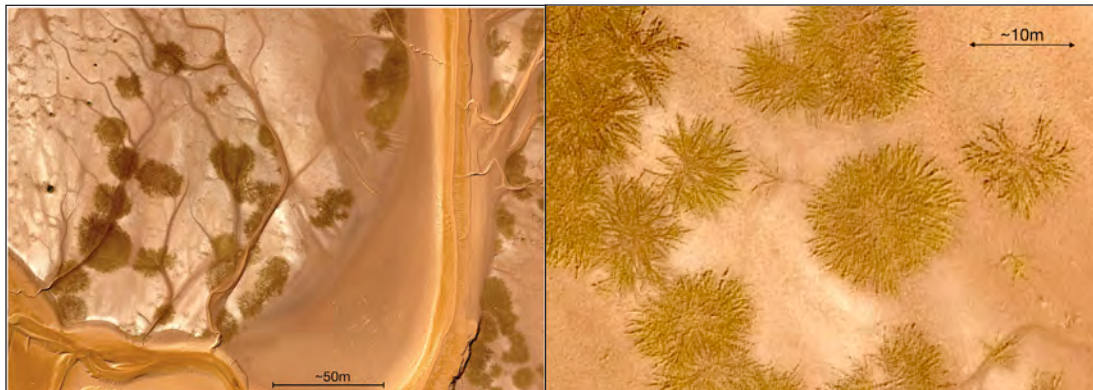


Figure 7. Former young *Distichlis* rings straddling tidal drainage channels in the upper intertidal zone on earthquake-subsided ground. Photo courtesy of the Sonoran Institute, Oct 2017.

Figure 8 - Aerial photo of young *Distichlis* showing radial stolon growth. The circular ring in the middle shows early signs of a central suppressed zone. Photo courtesy of the Sonoran Institute, October 2017.

on satellite imagery, the smaller ones (10m – 20m) enlarge at about 3m/yr, while some of the larger ones (> 20m) appear to be long-lived and ~quiescent, remaining after smaller ones have disappeared.

the centers are slightly moist soil. All the CR ghost rings are within a few km of each other. Ghost rings mark the greatest extent of the Hardy-Colorado Wetland during the floods of the 1980s.

Dead cattail rings can be seen today as “ghosts” of former living plants (Figure 11, ring field CR2 from the CR group). CR ring fields consist of many thin rings (Figure 12) with a few living iodine bush (*Allenrolfea occidentalis*) on the dead ring itself. Just inside the ring is an annulus of nearly plant-free soil while the majority of the plants in the center region are dead cattail root stalks. The darker brownish regions of Figure 11 in

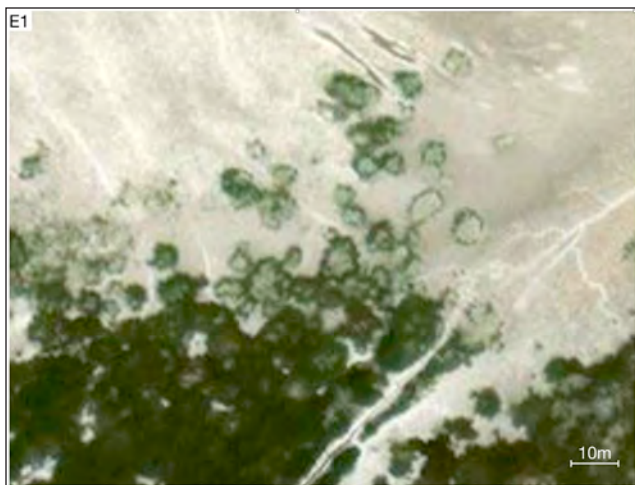


Figure 9. E1 ring field in the M group. Rings may grow and merge into consolidated ring fields that appear as irregular masses although individual clones are still faintly distinguishable. Upper middle; individual rings. Lower left; consolidated rings. Image from Bing Maps.

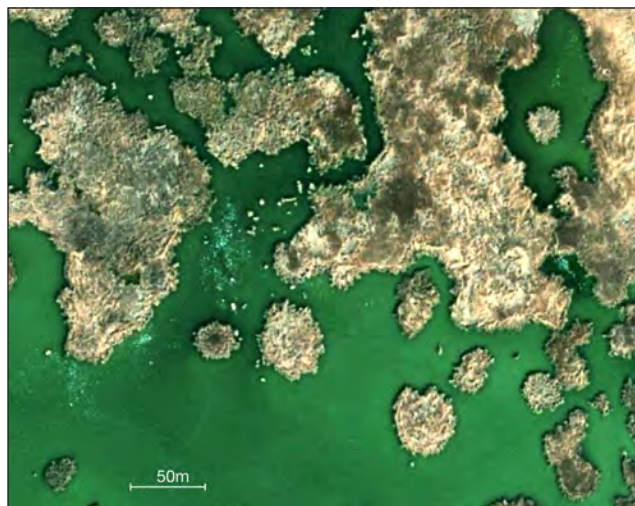


Figure 10. Image of living *Typha* ring group T3 in the Cienega de Santa Clara. In the upper part, *Typha* rings have merged into one another to form large irregular masses in which individual clones are not distinguishable. Image from Bing Maps.



Figure 11. Dead *Typha* Rings in the CR2 ring field near Yurimuri. Both rings are about 60m in diameter and almost perfectly circular. Photo by David Lynch, December 8 2022. Lower right inset: 2021 Google Earth satellite image.

4.3 Mesquite (*Prosopis glandulosa*)

Many mesquite ring fields³⁰ surround Laguna Salada. Mesquite is native to southwestern US and northern Baja. Ring LS2 (Figure 13) was remarkable for its large size, ~130m across. It did not appear to change in satellite imagery between 1977 and 2017 (Figure 14), leading to early speculation that it was either dead or was creosote (*Larrea tridentata*), a plant that grows very slowly. A subsequent site visit revealed it to be mesquite, a plant that does not reproduce clonally. The ring is on a micaceous coppice dune 3-4 meters high with significant internal topography. There were several species of attending plants, including creosote in close proximity to the mesquite. Yet despite the profusion of vigorous flowering plants (mainly desert sand verbena (*Abronia villosa*) and damianita (*Chrysactinia mexicana*), the mesquite was somewhat

brownish and appeared to be in poor health (Figure 15). No seed pods were found.

5. Discussion

Despite being in the same climate range (Köppen Climate BWh: hot desert), saltgrass, cattail, and mesquite grow in mutually exclusive aqueous environments, a situation reminiscent of the separate growing regions of mesquite and creosote ring fields in southern California deserts⁴. Saltgrass grows in tidal estuaries. Cattail thrives in fresh water. Mesquite

prefers open land, obtaining freshwater from rain and deep roots. Unlike saltgrass and cattail, both of which can reproduce asexually through rhizomes and stolons, mesquite can only propagate sexually.

5.1 Saltgrass

Distichlis only grows where tides reach, though it does not grow *everywhere* that tides reach. This suggests that tides are the main seed dispersal mechanism. Most *Distichlis* seeds are probably picked up and redistributed by spring tide inundations. Ring formation may be a two-step process. (1) First, a seed sprouts and grows to become an isolated entity in itself (sexual). (2) Then the resulting plant develops rings as stolons propagate radially outward (asexual) and take root.

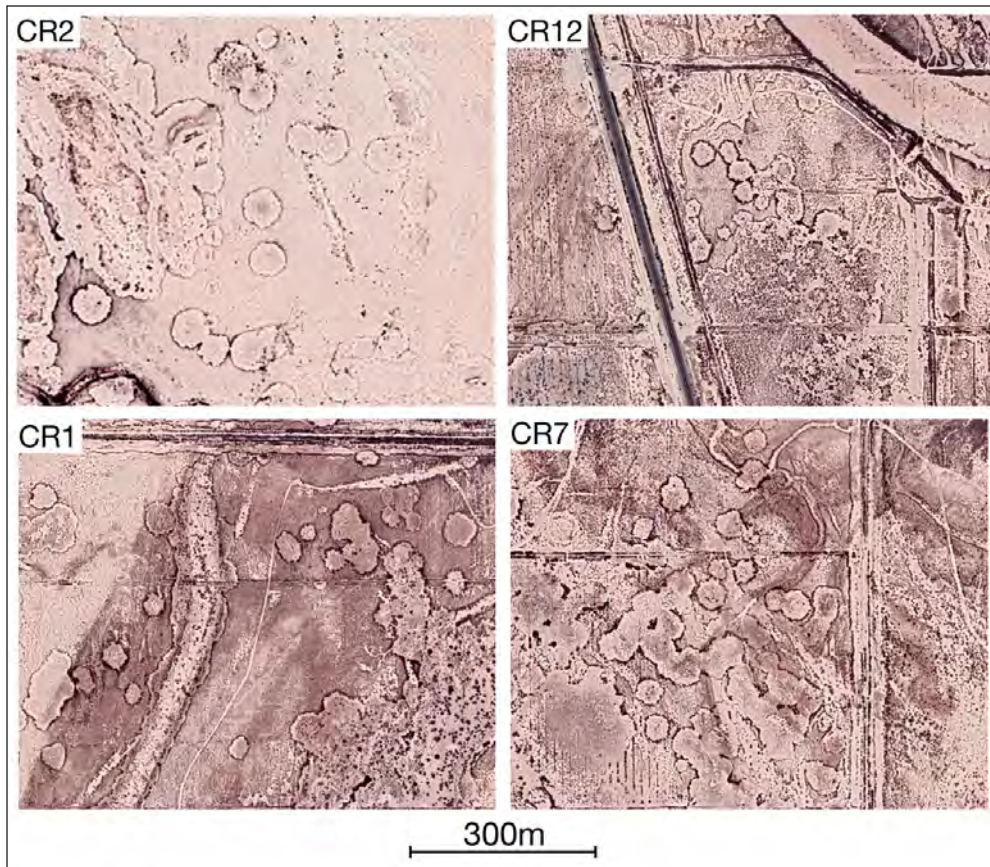


Figure 12. Google Earth Images of ghost *Typha* ring fields. Images from Google Earth.



Figure 13: Aerial picture of LS2. Photo by David Lynch, December 8 2022. LS2 is about 130m across.

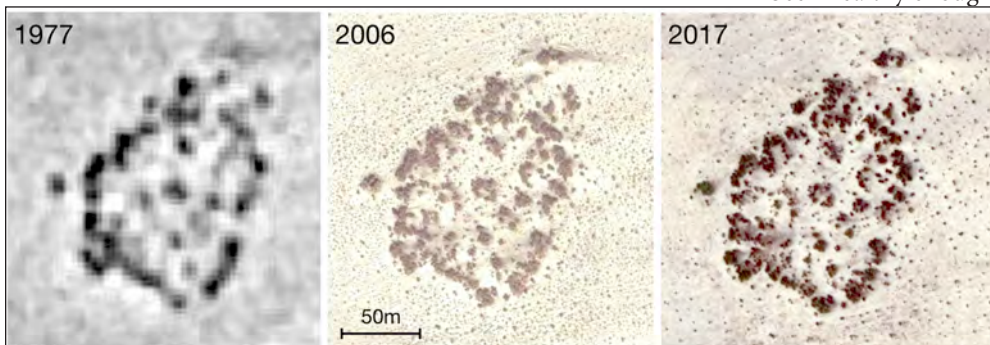


Figure 14. LS2 ring. There is little or no discernible differences between the images. Left: KH-9 image. Center and right: Google Earth historic images.

5.2 Cattails

The cattail rings making up the ghost rings of today first began when a Hardy-Colorado Wetland²⁹ started to develop at the junction of the Hardy and Colorado rivers in the 1960's and 70's. This wetland greatly expanded in 1983 following freshwater river floods in March-May¹⁸⁻²². These inundations were the results of water releases from the Hoover and Glen Canyon dams that were necessitated by extreme snowmelt in the upper river basin²⁰. After 1987 when releases ended and waters receded, the cattails died but their remains endured. The brief flood episodes in 1993 and 1997-98 were of too short duration for *Typha* to become reestablished and the

rings did not rejuvenate, nor did new *Typha* appear in the area except in the river. The extent of the flooding in the Hardy-Colorado Wetland is shown in Figure 16. Figure 17 shows the entire flood plain during and after the 1983 freshwater floods.

5.3 Mesquite

In 2022, the mesquite in LS2 was like a zombie. It looked unhealthy, spindly and brown, almost dead looking on its upper parts (Figure 15). There were no seed pods, either on the plant or the ground. Despite its apparent lack of growth or reproduction, the mesquite must have once been healthy enough to produce viable seeds

because ring growth depends on it. Prior to 1977 (Figure 13), a mesquite ring formed, grew and accreted a coppice dune. Then something happened to change the growing conditions. The plant was weakened enough to prevent growth and reproduction, but not enough to kill it.

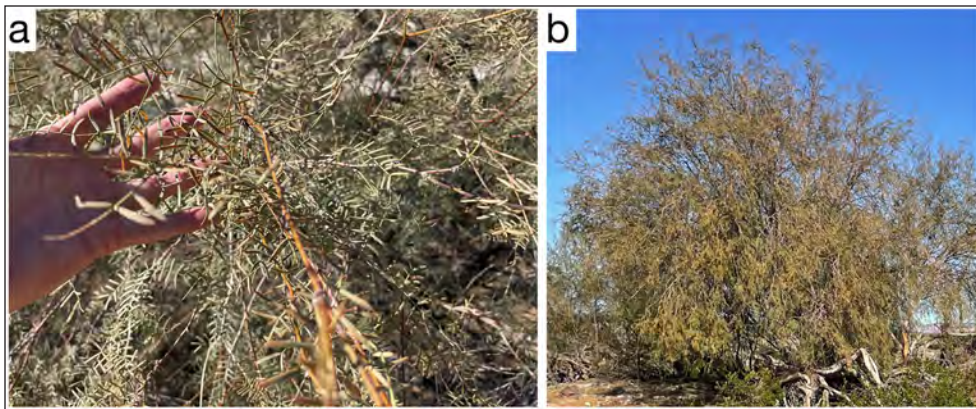


Figure 15. LS2 mesquite. (a) Mesquite branch showing thin foliage, pale green and often brown leaves. (b) One of many mesquite ring trees, greenish brown with thin foliage and no seed pods. A healthy mesquite is rich green with thick foliage and usually has seed pods lying around its base. Photos by David Lynch, December 8 2022.

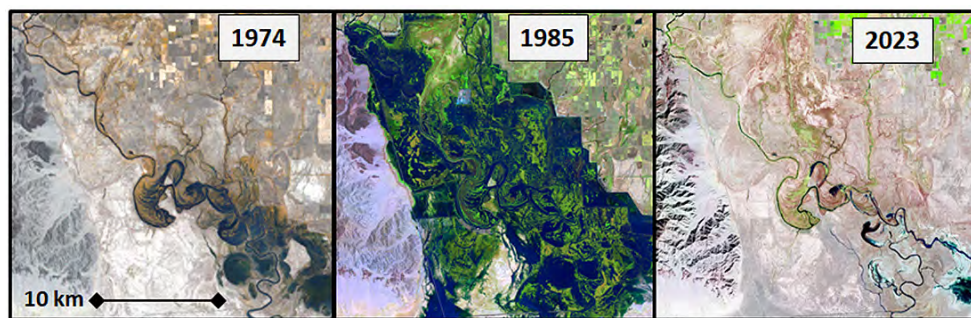


Figure 16. Influence of the dam releases in 1983-1987 on the Hardy-Colorado Wetland surface hydrology. LANDSAT 1 (1974), 6 (1985) and 9 (2023) in similar near infrared bands.



Figure 17. Google Earth images showing the extent of river flooding in 1985 and today's more usual, drier conditions.

Quite a number of conditions can force mesquite into a balance between living and dead³¹: bacterial and fungal infections, insect infestation, drought, soil chemistry changes and even being attacked by certain phytoplasmas³².

6. Summary and conclusions

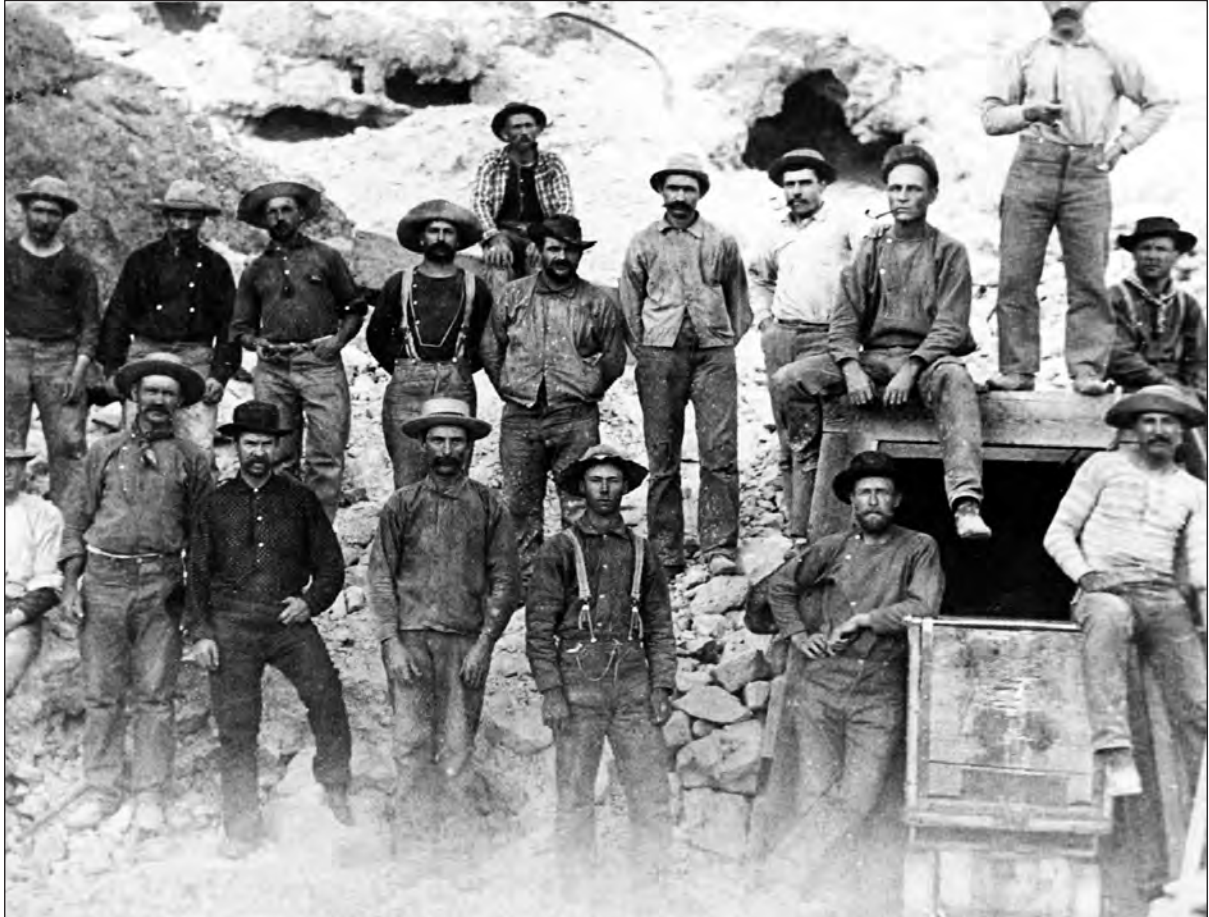
Based on *in situ*, aerial, and satellite surveys, we have cataloged a large number of plant rings and ring fields in Mexico's Colorado River floodplain. The most common are *Distichlis palmeri* (saltgrass). Saltgrass seed dispersal in the estuary is largely by tides. *Typha domingensis* (cattail) rings were found both living and dead ("ghost"). *Prosopis glandulosa* (mesquite) rings were found that did not appear to thrive

or reproduce ("zombies"). Ring growth in cattails and saltgrass takes shape clonally while mesquite are entirely sexual in origin. Historic Google Earth imagery revealed that rings come and go as the result of manmade and natural changes in the area.

References

1. Sheffer, E., H. Yizhaq, E. Gilad, M. Shachak, E. Meron. 2007. Why do plants in resource-deprived environments form rings? *Ecological Complexity* 4(4): 192-200.
2. Bonanomi, G., G. Incerti, A. Stinca, F. Carteni, F. Giannino, S. Mazzoleni. 2014. Ring formation in clonal plants. *Community Ecology* 15(1): 77-86.
3. Meron E., E. Gilad, J. von Hardenberg, M. Shachak, Yair Zarmi 2004 Vegetation patterns along a rainfall gradient. *Chaos, Solitons and Fractals* 19(2): 367-376.
4. Lynch, David K. 2002, Circular Plant Growth in Southern California Deserts, *Desert Plants*, 38(1) Aug, 22-31
5. Gregory, P. 1982 Fairy rings; Free and tethered, *Bulletin of the British Mycological Society* 16(2): 161-63.
6. Deblauwe, P. Couteron, O. Lejeune, J. Bogeaert and M. Barbier. 2011. Environmental modulation of self-organized periodic vegetation patterns in Sudan. *Ecography* 34(6): 990-1001.
7. Camazine, S., J-L. Deneubourg, N. Franks, J. Sneyd, G. Theraula, E. Bonabeau. 2001 Self-organization in biological

- systems, Princeton Studies in Complexity. Princeton University Press, Princeton, pp 562.
8. Watt, A., 1947 Pattern and process in the plant community. *Journal of Ecology* 35(1/2): 1–22.
 9. Ward, Evan R., 2003 Border Oasis: Water and the Political Ecology of the Colorado River Delta, 1940–1975, University of Arizona Press, 2003, pp208
 10. Sykes, G., 1937 The Colorado Delta. Special Publication No. 19. New York: American Geographical Society.
 11. Lynch, David K. and Brian McNeece, 2020 On the Origin and Evolution of the Salton Sea, Proceedings of the 2020 Desert Symposium, April 17-20, 2020, Zzyzx, D. M. Miller (ed.) 179-184
 12. Fletcher, John M., Orlando J. Teran, Thomas J. Rockwell, Mike Oskin, Ken W. Hudnut, Karl J. Mueller, Ronald M. Spelz, Sinan O. Akciz, Eulalia Masana, Geoff Faneros, Alex Morellan, Joann Stock, Austin Elliott, Peter Gold, Jing Liu-Zeng, Alejandro Gonzalez, David K. Lynch, Alejandro Hinojosa, Javier Gonzalez, 2014 Assembly Of A Large Earthquake From A Complex Fault System: Surface Rupture Kinematics Of The April 4,2010 El Mayor-Cucapah M_w 7.2 Earthquake, *Geosphere*, 10(4), 1-31
 13. Hauksson, Egill, Joann Stock, Kate Hutton, Wenzheng Yang, J. Antonio Vidal-Villegas & Hiroo Kanamori, 2011 The 2010 M w 7.2 El Mayor-Cucapah Earthquake Sequence, Baja California, Mexico and Southernmost California, USA: Active Seismotectonics along the Mexican Pacific Margin. *Pure Appl. Geophys.* **168**, 1255–1277
 14. Gonzalez-Ortega, Alejandro, Yuri Fialko, David Sandwell, F. Alejandro Nava-Pichardo, John Fletcher, Javier Gonzalez-Garcia, Brad Lipovsky, Michael Floyd, Gareth Funning, 2014 “El Mayor-Cucapah (M_w 7.2) earthquake: early near-field postseismic deformation from InSAR and GPS observations” *Journal of Geophysical Research*. **119** (2): 1482.
 15. Nelson, Steven M., Eric J. Fielding, Francisco Zamora-Arroyo, Karl Fless, 2013 Delta dynamics: Effects of a major earthquake, tides, and river flows on Ciénega de Santa Clara and the Colorado River Delta, Mexico, *Ecological Engineering* 59 (2013) 144–156
 16. Nelson, Steven m., Eloise Kendy, Karl W. Flessa, J. Eliana Rodriguez-Burgueño, Jorge Ramírez-Hernández, Tomás Rivas-Salcedo, 2020 Channel Incision By Headcut Migration: Reconnection Of The Colorado River To Its Estuary And The Gulf Of California During The Floods Of 1979-1988, *Hydrological Processes*. **34** 4156-4174
 17. Mueller, Erich R., John C. Schmidt, David J. Topping, Patrick B. Shafroth, Jesús Eliana. Rodríguez-Burgueno, Jorge Ramírez-Hernández, Paul E. Grams, 2017 Geomorphic change and sediment transport during a small artificial flood in a transformed post-dam delta: The Colorado River delta, United States and Mexico, *Ecological Engineering* 106 (2017) 757–775
 18. Kendy, Eloise, Karl W. Flessa, Karen J. Schlatter, Carlos A. de la Parra, Osvel M. Hinojosa Huerta, Yamilett K. Carrillo-Guerrero, Enrique Guillen, 2017 Leveraging environmental flows to reform water management policy: Lessons learned from the 2014 Colorado River Delta pulse flow, *Ecological Engineering*, 106, Part B, 2017, 683-694,
 19. Nelson, Steven M. Jorge Ramírez-Hernández, J. Eliana Rodriguez-Burgueño, 2017 A history of the 2014 Minute 319 environmental pulse flow as documented by field measurements and satellite imagery, *Ecological Engineering* Volume 106, Part B, September 2017, 733-748
 20. Nelson, Steven, Francisco Zamora-Arroyo, Jorge Ramírez-Hernández, and Edith Santiago-Serrano, 2013 Geomorphology of a Recurring Tidal Sandbar in the estuary of the Colorado River, Mexico: Implications for restoration. *Ecological Engineering*. 59. 121-133.
 21. Zamora, Hector, Steven Nelson, Karl Flessa, and Ritsuo Nomura, 2013 Post-dam sediment dynamics and processes in the Colorado River estuary: Implications for habitat restoration. *Ecological Engineering*. 59. 134-143.
 22. Carriquiry, Jose & Alberto Sanchez, 1999 Sedimentation in the Colorado River Delta and Upper Gulf of California After Nearly a Century of Discharge Loss. *Marine Geology*. 158. 125-145.
 23. Nelson, Steven M., David K. Lynch and Tomás E. Rivas Salcedo, 2023 The Colorado River (Mexico) Tidal Bore: Persistent Phenomenon in a Changing Estuary, (this volume)
 24. Nelson, Steven 2007, In search of El Burro, the tidal bore of the Rio Colorado Delta, in Dry Borders: Great Natural Reserves of the Sonoran Desert (Richard Stephen Felger, Bill Broyles, eds.) University of Utah Press, pp799, Salt Lake City
 25. Bresdin, Cyphine; Glenn, Edward P. (2016), Khan, M. Ajmal; Boër, Benno; zturk, Münir; Clüsener-Godt, Miguel (eds.), “Distichlis palmeri: An Endemic Grass in the Coastal Sabkhas of the Northern Gulf of California and a Potential New Grain Crop for Saltwater Agriculture”, *Sabkha Ecosystems: Volume V: The Americas*, Springer International Publishing, vol. 48, pp. 389–396,
 26. Pearlstein, S. L., R. S. Felger, E. P. Glenn, J. Harrington, K. A. Al-Ghanem, S. G. Nelson, 2012 Nipa (*Distichlis palmeri*): A perennial grain crop for saltwater irrigation, *Journal of Arid Environments*, 82, July 2012 60-70
 27. <https://nas.er.usgs.gov/queries/FactSheet.aspx?SpeciesID=3020>
 28. Carrillo-Guerrero, Yamilett K., Karl Flessa, Osvel Hinojosa-Huerta and Laura López-Hoffman, 2013 From accident to management: The Cienega de Santa Clara ecosystem, *Ecological Engineering*, 59, October 2013, Pages 84-92
 29. Payne, J.M., Reid, F.A., Gonzalez, E.C., 1992. Feasibility study for the possible enhancement of the Colorado Delta Wetlands, Baja California Norte, Mexico. *Ducks Unlimited/ Ducks Unlimited Mexico*, Rancho Cordova, CA.
 30. Of the ~16 LS ring fields we identified in the satellite survey, only one was reached on foot, LS2. We presume the others are also mesquite because of their locations, ecological conditions and visual similarity.
 31. <https://plantdiseasehandbook.tamu.edu/landscaping/trees/mesquite/>
 32. Huang, Weijie , Allyson M. MacLean, Akiko Sugio, Abbas Maqbool, Marco Busscher, Shu-Ting Cho, Sophien Kamoun, Chih-Horng Kuo, Richard G.H. Immink, and Saskia A. Hogenhout. 2021 Parasitic modulation of host development by ubiquitin-independent protein degradation, *Cell*, 184(20), P5201-5214.E12



Miners at the Occidental mine tunnel, Calico. San Bernardino County Museum collection.

The Colorado River (Mexico) tidal bore: persistent phenomenon in a changing estuary

Steven M. Nelson,^{1*} David K. Lynch,² and Tomás E. Rivas Salcedo³

¹Independent Scientist, 6101 NE 102nd Avenue, Apt. 5, Vancouver, WA 98662-6321, snelson467@gmail.com

²Thule Scientific, P. O. Box 953, Topanga CA 90290

³Sonoran Institute, Blvd. López Mateos SN, Zona Industrial, Mexicali, Baja California, C.P. 21010, Mexico

ABSTRACT — The macro-tidal estuary of the Colorado River, Mexico has been disconnected from the river's fluvial supply by the operation of upstream dams and diversions. Since the last major period of fluvial delivery in the 1980s and 90s an emergent and growing tidal sandbar has obstructed the river channel 40 km upstream from the Gulf of California. The estuary has assumed the characteristics of a blind tidal channel system where tidal sediment is transported landward, leading to decreased channel depth and width. Loss of fluvial flow diminished but did not eliminate tidal bores which continue to ascend the estuary channel at the head of flooding spring tides. Spring tide flood currents saw increased power after a large area of the intertidal mudflats subsided up to 1m following the 2010 M7.2 El Mayor-Cucapah earthquake, resulting in extensive channel bank erosion and headcut incision of new tidal channels. We conducted field visits and used satellite imagery to detect tidal bores over the 12-year post-earthquake period in order to estimate the frequency of tidal bores and gain a better understanding of their contribution to both erosion and aggradation of estuary channels and the surface of the intertidal flats.

1. Introduction

The estuary

The Colorado River estuary is situated at the northern end of the Gulf of California (Figure 1). The mean spring tide range in the upper Gulf is 6.4 m (Lavin and Marinone, 2003), reportedly increasing to 8 to 10 m within the estuary (Thompson, 1968) although no tide monitoring stations are maintained therein. In the mixed semidiurnal tidal regime of the upper Gulf, each day's lower low tide

immediately precedes the higher high, contributing a maximum range to one of the day's tides. The convergent estuary is hypersynchronous, compressing the flood tidal wave into a smaller cross-sectional area as it ascends the narrowing/shallowing estuary channel, enhancing tidal effects until friction ultimately dissipates the wave at the tidal limit. Compression of the flood wave also steepens it and delays its arrival, resulting in highly asymmetrical flood-dominant tide cycles: the authors' observations at various locations within the estuary have recorded spring-tide flood periods ranging from 2.5 to 4 hours, with the ebb lasting 8 to 9.5 hours. These factors combine to create conditions favoring the formation of a tidal bore wave at the head of one and sometimes both daily flood tides during spring tide (full and new moon) periods.

The tidal bore

Lynch (1982) and Graber (2012) provide introductory information and scientific theory of tidal bores. A bore is a tidally generated water wave advancing upstream and represents the instantaneous turning of the tide from ebb to flood. It occurs during spring tides when the tidal range is at its monthly maximum. Tidal bores have been documented in the Colorado River estuary since the earliest Spanish explorers visited the area in the 16th century (Freeman, 1923).

Perhaps the best introduction to the Colorado River bore is found in the description provided by James H. Gordon of the U.S. Weather Bureau who witnessed a bore at the tiny seaport of La Bomba on the south bank of

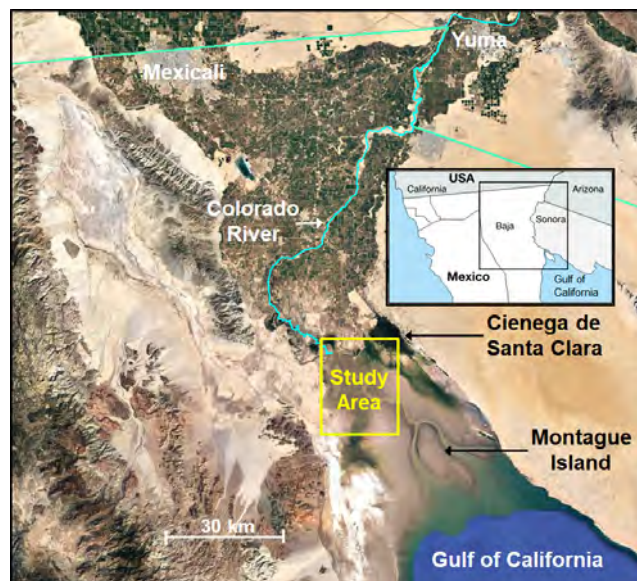


Figure 1. Regional map showing the study area in the Colorado River Estuary.

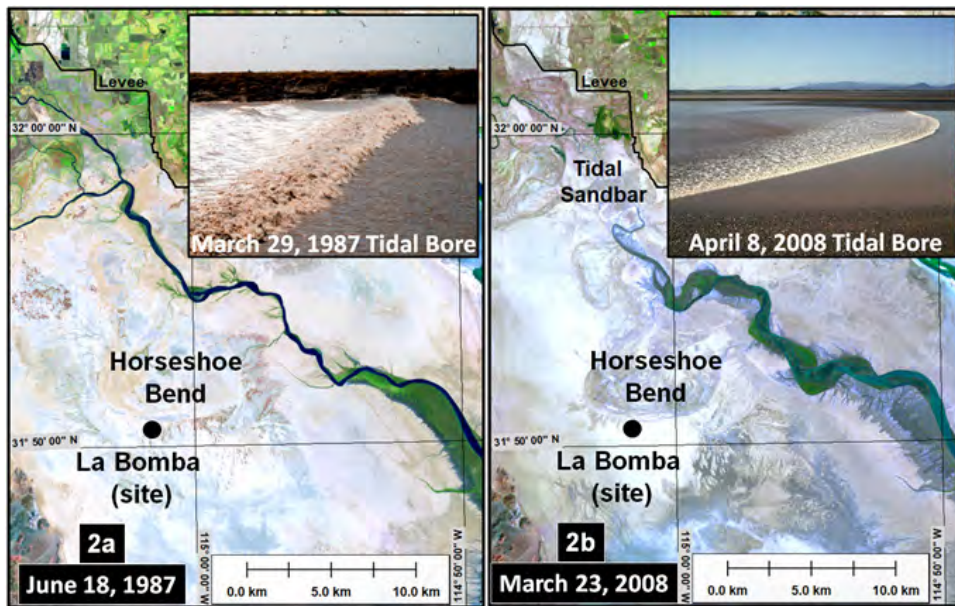


Figure 2. Estuary changes in the two decades prior to the 2010 El Mayor-Cucapah Earthquake (Landsat 5 images). Both pictured bores are advancing left to right. Fig. 2a: In 1987-88, Nelson observed tidal bores along the reach between the La Bocana fish camp and a tide gage 4 km to the south. Fluvial flow to the Gulf was occurring, producing classic river-channel tidal bores. Note the opposite channel bank just 100 m away. Fig. 2b: Fluvial flow to the Gulf was curtailed after 2000 as drought conditions developed throughout the Colorado River Basin. By 2006 a tidal sandbar (upper left) blocked the river channel and the estuary once again became a strictly tidal system. Bores in the tidal channel became smaller and appeared only intermittently in deeper and more constricted sections where the flood met opposing ebb current. 1987 photo by Lynn C. Anderson, 2008 photo by Steven Nelson.

Horseshoe Bend, a now-abandoned meander of the river (Figure 2) on December 9, 1923:

The coming of the bore was first called to our attention by the disturbance among a big flock of white pelicans fully 6 miles away. Fish always follow the bore in, we were told. The brown line of the bore itself was visible with the glass at perhaps 3 miles. Its speed appeared to be nearly 8 miles an hour. As a spectacle it was disappointing. This was doubtless due in some measure to the strong north wind that had been fighting the tide all the way up the Gulf. Up to the moment that the bore, or first wave, arrived the current was running strongly seaward. In an instant it was reversed and racing up the river. The bore was not over 3 feet high, a racing wave fully a mile long, foam crested and perhaps a foot higher over the shallows and sand bars.... The lack of turmoil between the two opposite currents was surprising. The level of the river rose 3 feet in the first minute and 5 feet in 15 minutes. The bank was 15 feet high at low tide. The high tide of two nights previous had filled the channel and overflowed the surrounding country 6 inches deep. Probably a full half mile behind the first wave something similar to a tide rip appeared, waves 3 to 4 feet high

probably not over 20 feet from crest to crest racing up the river. They would have made very rough going for a small boat (Gordon, 1924).

Gordon may have been underwhelmed by the observed bore because of a newspaper report (Henderson, 1922a) of a bore “15 to 20 ft” high that had capsized a small ship as it lay at anchor off La Bomba. A later statement by the ship’s engineer (Henderson, 1922b) said a bore “about 8 ft” high had pushed the ship onto a bar and caused it to list so severely that many people jumped or fell into the river and were drowned. The actual size of the bore would have been very hard to judge because it approached in darkness just two nights past the new moon (night of November 19–20, 1922), despite a later

account claiming the victims watched the “nearly 15 ft” bore approach in bright moonlight (Waters, 1946).

The Colorado River estuary is so remote that few people have actually witnessed a tidal bore there, which complicates accurate reporting. A survey of eyewitness accounts indicates that historical bores were generally considerably smaller than 15 ft or even 8 ft: Gordon (1924) and Sykes (1937) reported 3 ft¹ bores, Derby (1852) and Waters (1946) 4 ft bores, Leigh (1941) a 4.5 ft bore, and Ives (1861) a bore “several” feet high. The best historical photo of a bore taken by Sykes² shows one about 2–3 ft high in Horseshoe Bend, circa 1904.

While the Colorado River tidal bores are not among the world’s largest (Bartsch-Winkler and Lynch, 1988), they share with all tidal bores an important function in mixing and dispersion of sediments as the wave propagates upstream (Chanson, 2004). Understanding the occurrence and frequency of tidal bores within the estuary as modified by the 2010 El Mayor-Cucapah earthquake is an important first step in understanding erosion and sedimentation processes.

1 Sykes added that bores could “swell up to 6 or 7 feet” at constrictions in the channel or irregularities in the shoreline.
2 Sykes Family Collection PC240, Box 8, Folder 147 “Tidal Bore on Colorado River”, Arizona Historical Society Library and Archives, Tucson, Arizona

Tidal bores in the three decades prior to the 2010 El Mayor-Cucapah earthquake

Nelson (2007) observed several tidal bores in 1987 and 1988 during a period of fluvial discharge to the estuary and Gulf (Fig. 2a). River flow in the 100 m-wide channel was sufficient to keep all channel bars submerged even at low tide, and in mid-channel the bore wave was typically undular (non-breaking). Although river discharge can have a dampening effect on bore formation if the water in the channel becomes too deep (Bonneton et al., 2015), fluvial discharge in early 1987 resulted in bores similar in size to the eyewitness reports from the 19th and early 20th centuries.

Flood-dominant estuaries typically experience net landward bedload transport as fine-grained sediments mobilized by the flood tides are deposited on inundated surfaces during the long slack tide preceding the extended ebb (Dalrymple, 2010; Wells, 1995). When fluvial flow reaches the estuary, these tide-mobilized sediments are deposited near the river's mouth, but in the absence of such flow the sediments are carried inland. After fluvial flow to the estuary was curtailed in the 1960s and 70s following installation of upstream dams and diversions, landward transport of tidal sediments caused a tidal sandbar to form in the Colorado River channel 40 km above the river's mouth (ACOE, 1982). The channel reopened when fluvial flow was temporarily restored in the 1980s (Nelson et al., 2020), only to close again after 2000 as drought conditions once again curtailed fluvial flow. By 2006 a new tidal sandbar (Fig. 2b) had developed in the same location as the previous one (Nelson et al., 2013b; Zamora et al., 2013). The estuary downstream from the sandbar became a "blind" (tapering to a dry upstream terminus) tidal channel.

The blind estuary channel was significantly wider and more sinuous than the riparian channel had been in the 1980s. Bank erosion and retreat, which had begun in the 1990s, continued after the fluvial supply was

cut off, indicating that it was driven by tidal currents. Much of the sediment eroded from the banks was retained in channel bars (Nelson et al., 2013b). In contrast to the 1980s channel morphology, which had been dominated by fluvial flow, channel bedforms were now defined by bi-directional flow. A system of parallel "mutually evasive" flood and ebb dominated channels developed, meandering independently of each other with frequent intersections and interconnections as is common in tidal channels (Hughes, 2012; Wells, 1995). Tidal bores (inset, Fig. 2b) diminished in size from those seen in the 1980s, forming intermittently in places where the flood and ebb channels coincided.

Subsidence Impact of the 2010 El Mayor-Cucapah earthquake

The mainshock of the Mw 7.2 El Mayor-Cucapah earthquake occurred on Easter Sunday, April 4, 2010, producing a nearly continuous fault trace extending 120 km from the U.S.-Mexico international boundary to the Gulf of California (Fletcher et al., 2014). The current study area is at the far southern end of the rupture zone where movement occurred along previously unidentified faults, causing coseismic and post-seismic subsidence of up to 1 m (Huang et al., 2017; Nelson et al., 2013a).

Figure 3 illustrates spring tidal inundation patterns in the study area 8 months prior to and 6 months after the earthquake. Prior to the earthquake (Fig. 3a) a spring tide predicted to reach ~5.5m (at Puerto Peñasco, Sonora) inundated an area mainly aligned along the estuary

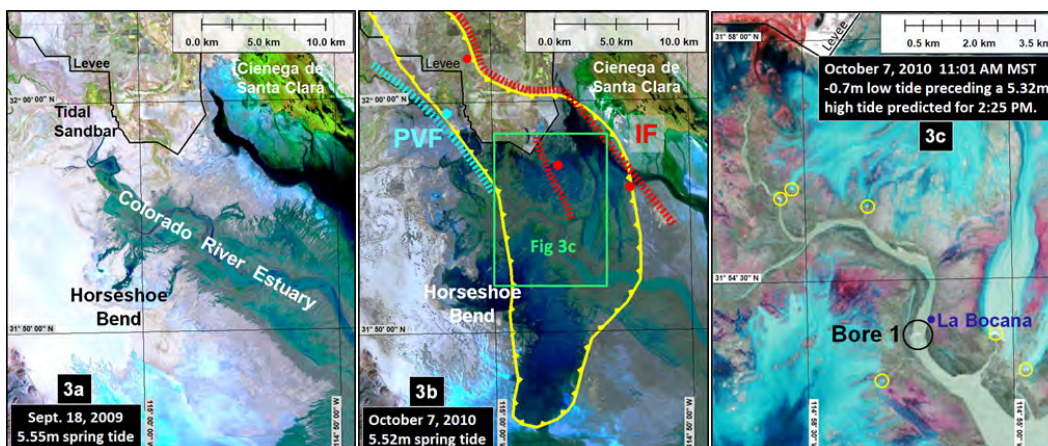


Figure 3. Changes in tidal inundation following the 2010 El Mayor-Cucapah Earthquake. Figs. 3a and 3b show the areas of tidal inundation by ~5.5m spring tides before and after the earthquake. Fig. 3a. Pre-earthquake spring tides primarily inundated areas adjacent to the main estuary channel between natural levees created by the deposition of fluvial and tidal sediment on the channel banks. Some water escaped southwest toward Horseshoe Bend or east toward the Santa Clara Slough (inundated area south of Cienega de Santa Clara) through low sections of the levees. Spring tides rarely reached the flood control levee (black line upper left). Fig 3b. The area between the Pangas Viejas Fault (PVF) and Indiviso Fault (IF) subsided up to 1m over a six month period following the earthquake. The yellow raked line shows the limits of coseismic and post seismic subsidence. Subsidence of the estuary channel's natural levees allowed most spring tides to inundate more of Horseshoe Bend than previously. Fig 3c. The area within the rectangular inset shown in 3b has been processed using false color infrared bands to accentuate water ponded on the tide flats well as whitewater rapids at headcut erosion points (small circles). A tidal bore spanning the entire 350m-wide channel (Bore 1, large circle) is moving up the channel at the head of the flood tide.

channel. The flood was mostly contained within the natural levees/berms that had developed along the channel from deposition of fluvial and tidal sediments. Overflow occurred at a few low spots, allowing some tidal water to flow southwest toward the old Horseshoe Bend meander and east toward the Santa Clara Slough (dark blue standing water south of the Cienega de Santa Clara). Spring tides rarely flooded all the way north to the flood control levee.

The previously unidentified Pangas Viejas and Indiviso faults (Figure 3b) mark the southernmost extent of the rupture zone (Chanes-Martínez, 2012; Fletcher et al., 2014). These two faults form the western and eastern margins of an extensional strike-slip duplex system that underlies the alluvial surface in the subsidence zone (Sánchez García, 2013). The zone of subsidence extends north of the flood control levee which now marks the northern limit of tidal inundation by most spring tides. Although the western part of the Horseshoe Bend meander is outside the area of seismic subsidence, the earthquake caused subsidence of the natural levees which had prevented full inundation of the abandoned meander prior to the earthquake, causing the new area of inundation to extend into Horseshoe Bend west of the subsidence zone.

As a result of the earthquake a new intertidal basin up to 1 m deep and 260³ sq km in area developed, increasing spring tide inundated area by about 190 sq km from the average pre-earthquake situation. The new intertidal basin was subject to rapid inundation and more gradual drainage during each asymmetrical spring tide cycle.

3 This includes 230 sq km of newly subsided tide flats and an additional 30 sq km of pre-existing low ground in the Horseshoe Bend which had not been subject to regular inundation prior to the 2010 earthquake.

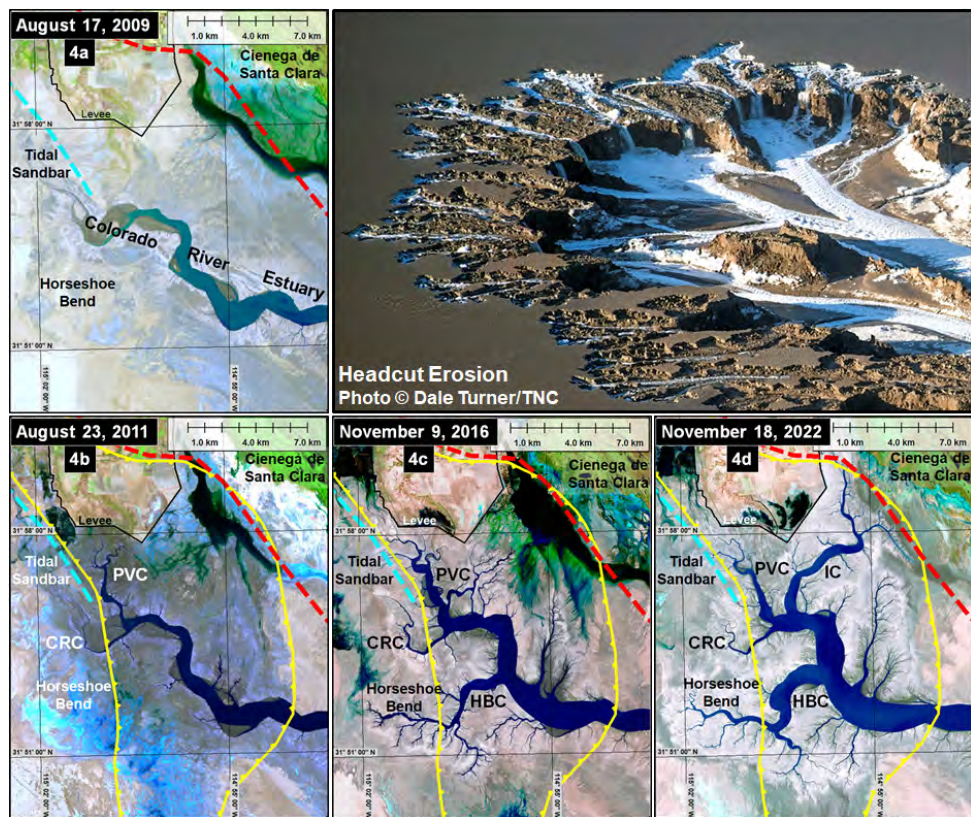


Figure 4. Headcut erosion of tidal drainage channels, 2010-2022. Red dashed line: Indiviso Fault. Aqua dashed line: Pangas Viejas Fault. Yellow raked line: Zone of earthquake subsidence. CRC: Colorado River Channel. PVC: Pangas Viejas Channel. HBC: Horseshoe Bend Channel. IC: Indiviso Channel. Images 4b, 4c, and 4d were acquired at times when the water surface in mid-estuary was estimated to be at approximately the same elevation. Fig. 4a: Pre-earthquake conditions. Fig. 4b: Sixteen months after the 2010 earthquake a new tidal drainage channel PVC has been headcut north along the east side of the Pangas Viejas Fault. The CRC upstream from the PVC is outside the subsidence zone and has not been significantly headcut. Fig. 4c: By 2016 the HBC system of drainage channels has been headcut into Horseshoe Bend and headcuts are advancing to the northeast toward the large area of impounded water west of the Indiviso Fault. Fig. 4d: The most recent major tidal channel IC now drains the low area west of the Indiviso Fault. As of 2022 a network of tidal channels insures rapid drainage of the entire tide flat surface within the subsidence zone, which now completely floods in 3-4 hours and drains in 8-9 hours during spring tides. Note the increase in width of the main estuary channel between 2011 and 2022. Figs 4a and 4b: Landsat 5 TM. Figs 4c and 4d: Sentinel 2. All satellite images processed with short wave infrared bands.

Incision of new tidal drainage channels began as headcut erosion occurred at points where water drained over existing channel banks during the long ebb tide (Figure 3c). Figure 3c has been processed using false color infrared bands to accentuate both standing water and whitewater rapids at headcutting points (small yellow circles). It also reveals a tidal bore (Bore 1, inside the larger black circle) at the head of the incoming flood. The bore extended across the entire 350 m-wide low-tide channel and must have been a substantial breaking wave to be detectable at the 30m spatial resolution of Landsat 5.

Development of tide flat drainage channels

Since there were no pre-existing drainage channels in much of the subsided area, large areas of the tide flats initially remained inundated with residual sea water for

days following spring tides, and some areas remained inundated for years until drainage channels reached them. The progress of drainage channel development is shown in Figure 4. Figure 4a shows the situation prior to the earthquake. Note the linear area of inundation nearly parallel to and just west of the (at the time unidentified) Indiviso Fault (red dashed line). This linear feature may be an indication of earlier movement of the Indiviso Fault. Prior to the 2010 earthquake it was inundated whenever the adjacent Santa Clara Slough (out of view to the southeast) was flooded, but otherwise dry.

By August 2011, 16 months after the 2010 earthquake, the first major new drainage channel (“PVC” for Pangas Viejas Channel in Figure 4b) had developed along a linear subsidence feature just east of the Pangas Viejas Fault. Drainage from this newly subsided area flowed directly into the existing Colorado River Channel (CRC), and the Pangas Viejas Channel grew quickly. Headcuts did not significantly advance up the Colorado River Channel beyond the western limit of subsidence, and the pre-existing tidal sandbar in that channel continued to aggrade.

By November 2016 another major tidal channel had been headcut into the Horseshoe Bend (“HBC”, Horseshoe Bend Channel, in Figure 4c). A third network of channels was headcutting northeastward toward the large inundated area just west of the Indiviso Fault and Cienega de Santa Clara. This area had been continuously inundated since the 2010 earthquake and remained so until a headcut channel finally reached and began to drain it in late 2017. As of late 2022 (Figure 4d) the Indiviso channel (IC) was fully developed and the entire 260 sq km subsidence zone was now well drained. Spring tides continue to inundate most of the subsidence zone during the 3–4 hour flood, and nearly all tidal waters are returned to the estuary channel during the 8–9 hour daily ebb.

Methods

Estimating bore occurrence

In order to determine which satellite imagery to examine for possible bore occurrence between 2010 and 2022, we first made an initial estimate of dates and times by querying tidal prediction data for Puerto Peñasco⁴ using parameters from Nelson (2007) and more recent field observations:

1. Minimum flood tide range at Puerto Peñasco: 5.2 m
2. Select daytime flood tides only.

3. Low tide correction factor for La Bocana (Figure 3c): Puerto Peñasco low + 4 hours

Nobeltec Tides and Currents v3.6, using United Kingdom Hydrographic Office (UKHO) data for the Puerto Peñasco harmonic station, was utilized for queries of tidal events. However, all tidal information presented in this article utilizes the times and heights as calculated by the MAR V1.0 software issued by the Centro de Investigación Científica y de Educación Superior de Ensenada, Baja California (CICESE). The two prediction databases yield similar results, but the CICESE numbers are reported here to be consistent with most other Gulf of California research.

An initial Tides and Currents query on daytime floods with a range greater than 5.2m predicted 524 events for the period April 4, 2010–December 31, 2022. These were sorted by time of predicted arrival at La Bocana. To be visible in a satellite image a bore must be present somewhere in the estuary between 11:00AM and 11:35AM MST when the images are acquired. To account for variations in bore arrival time, 449 days with predicted low tide between 10:00 AM and 12:15 PM were selected for further evaluation.

Satellite Imagery

This analysis used an existing library of Landsat and Sentinel 2 imagery maintained by the corresponding author. In conjunction with ongoing monitoring of the estuary since 2009, all Landsat and Sentinel 2 imagery covering the study area has been downloaded and processed, usually within 48 hours of acquisition by the satellite. Landsat imagery is obtained from the <https://earthexplorer.usgs.gov/> website. Sentinel 2 imagery is downloaded from Amazon Web Services (public bucket **sentinel-s2-l1c**): <https://registry.opendata.aws/sentinel-2/>. Imagery is processed using the Spectral Discovery for Landsat 8 Imagery and Spectral Discovery for Sentinel 2 Imagery programs (<https://www.geosage.com/>) to produce false color near-infrared (NIR) and Short Wave Infrared (SWIR) products as follows:

Table 1. Satellite image products

	band number, (characterized wavelength), spatial resolution		
	Landsat 5 TM	Landsat 8/9 OLI	Sentinel 2 MSI
NIR Bands:	2 (green) 30m	3 (green) 30m	B3 (green) 10m
	3 (red) 30m	4 (red) 30m	B4 (yellow) 10m
	4 (NIR) 30m	5 (NIR) 30m	B8 (NIR) 10m
		8 (Panchromatic) 15m	
SWIR Bands:	1 (blue) 30m	4 (red) 30m	B05 (red edge) 20m
	4 (NIR) 30m	5 (NIR) 30m	B8A (NIR) 20m
	5 (SWIR) 30m	6 (SWIR) 30m	B11 (SWIR) 20m
		8 (Panchromatic) 15m	B4 (yellow) 10m

⁴ Puerto Peñasco was used as the base station to maintain consistency with prior studies.

Landsat 8/9 and Sentinel 2 SWIR images are pan-sharpened using the higher resolution bands shown. For the figures in this article SWIR images are employed to emphasize water and wet features such as the estuary channels and subsidence zone. NIR images were used in the search for bores because they provide good contrast for whitewater features and the turbulent water following the bore, and because of the native 10 m spatial resolution of these bands in Sentinel 2 images.

Satellite imagery was available for 111 of the 449 days selected for evaluation. All 111 images were examined for bores, using elements of analog image interpretation. Bores were detected in 14 of the images. In some cases, multiple bores were visible in a single image as they ascended the estuary's several arms.

Field visits

Prior to the 2010 earthquake it was normally possible to drive a motor vehicle directly to the bank of the estuary channel to observe tidal bores and other characteristics of the tides (Nelson, 2007). Such easy access ended soon after the earthquake as the tidal flats subsided and became subject to regular inundation. For this reason, only three

field visits to monitor tidal conditions were completed following the earthquake.

Kayak

The corresponding author accessed the main estuary channel by kayak on March 9, 2012, to observe a bore at close range, measure the rate of vertical rise of the flood tide (up to the point when the landing spot was inundated), and measure the speed of the flood current. This mode of access also facilitated a keen appreciation of the extreme turbulence of a spring-tide flood under post-earthquake conditions.

Motor vehicle

The main channel was accessed by motor vehicle on April 28, 2013, using a causeway constructed by the State of Baja California to provide access for the Gulf Corvina fishery. This was the only motorized visit to the main channel that could be completed before the causeway was cut by the advancing Indiviso Channel in 2014. A second visit was conducted on April 19, 2015, using the surviving portion of the causeway to observe tidal conditions in the Indiviso Channel.

Table 2. Tidal Bores in the post-2010 El Mayor-Cucapah Earthquake Colorado River Estuary as detected in satellite imagery and observed during a field visit. E: Main estuary channel. PVC: Pangas Viejas Channel. CRC: Colorado River channel upstream from the subsidence zone. HBC: Horseshoe Bend Channel. IC: Indiviso Channel.

Bore Number	Date	Location		Channel	Flood tide range (m) at Puerto Peñasco (CICESE)		Time Offset from Puerto Peñasco		Sensor
		Latitude	Longitude		Time (MST)	Low Tide	Add		
1	10/7/2010	31.8951	-114.9435	E	6.05	11:01	3:47		TM
2	7/13/2011	31.9220	-114.9605	E	5.62	11:06	4:29		TM
3	3/9/2012	31.9206	-114.9481	E	6.38	12:42	4:12		Field Obs
4	5/24/2013	31.9168	-114.9515	E	6.66	11:13	4:12		OLI
5	5/24/2013	31.8857	-114.9617	HBC	6.66	11:13	4:12		OLI
6	6/12/2014	31.9206	-114.9481	E	6.32	11:10	4:07		OLI
7	8/4/2016	31.8635	-114.9049	E	5.55	11:33	2:52		MSI
8	9/18/2017	31.9463	-114.9961	PVC	5.91	11:33	4:50		MSI
9	7/12/2018	31.9220	-114.9810	PVC	6.73	11:24	4:29		MSI
10	7/12/2018	31.9144	-114.9785	CRC	6.73	11:24	4:29		MSI
11	5/6/2019	31.8660	-114.9134	E	5.75	11:36	3:09		MSI
12	8/1/2019	31.9243	-114.9492	E	6.85	11:26	3:35		MSI
13	8/14/2019	31.8662	-114.9830	HBC	5.19	11:36	4:17		MSI
14	8/14/2019	31.9229	-114.9803	PVC	5.19	11:36	4:17		MSI
15	8/14/2019	31.9162	-114.9777	CRC	5.19	11:36	4:17		MSI
16	9/28/2019	31.9395	-114.9627	IC	6.78	11:35	4:11		MSI
17	9/28/2019	31.8698	-114.9955	HBC	6.78	11:35	4:11		MSI
18	5/7/2020	31.9171	-114.9484	E	7.06	11:26	3:43		MSI
19	10/17/2020	31.9189	-114.9573	E	5.99	11:35	3:38		MSI
20	4/27/2021	31.9030	-114.9504	E	7.1	11:25	3:31		MSI
21	4/27/2021	31.9055	-114.9362	E	7.1	11:25	3:31		MSI
22	3/31/2022	31.9464	-114.9551	IC	5.73	11:35	3:47		MSI
23	5/15/2022	31.9590	-114.9311	IC	6.56	11:36	4:30		MSI
24	5/15/2022	31.9299	-114.9853	PVC	6.56	11:36	4:30		MSI
25	5/15/2022	31.9125	-114.9832	CRC	6.56	11:36	4:30		MSI
26	5/15/2022	31.8657	-114.9852	HSC	6.56	11:36	4:30		MSI
27	10/9/2022	31.9566	-114.9456	IC	5.81	11:26	3:59		MSI

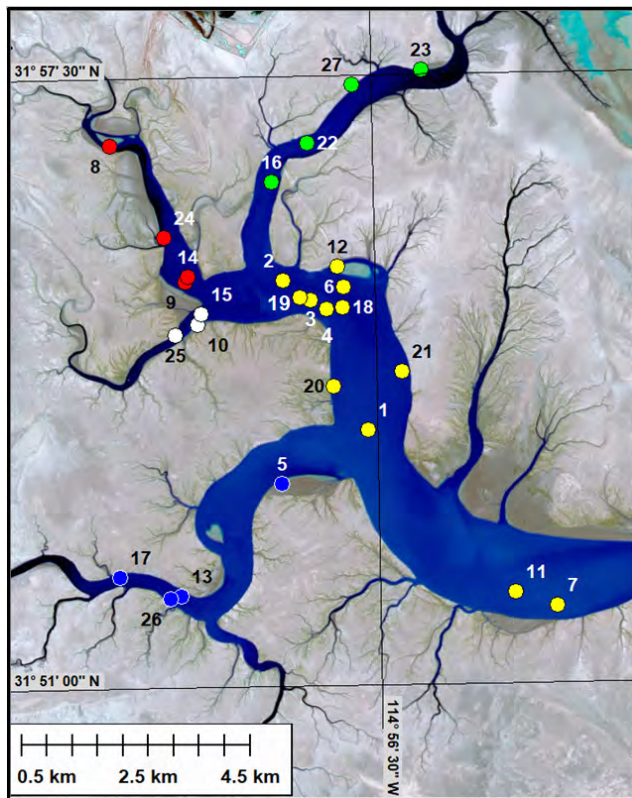


Figure 5. Map of Tidal Bores. See Table 2 for more information. All bores were detected in satellite imagery with the exception of Bore 3 which was observed in the field. Bore locations are color coded by the channel in which they were detected. Yellow: Main estuary. Red: Pangas Viejas Channel. Blue: Horseshoe Bend Channel. Green: Indiviso Channel. White: Colorado River Channel.

Results

The tidal bores

Detected tidal bores are listed chronologically by date of occurrence in Table 2. The location of each is plotted on a map in Figure 5. Satellite views of bores selected for discussion in this section are found in Figure 6.

More bores were detected in the later years of the 12 years studied because both spatial and temporal resolution of satellite imagery improved dramatically during the study period, which spanned the transition from Landsat 5 to Landsats 8/9 and Sentinel 2a/b. There were no functional Landsat satellites in 2012. Landsat 8 became operational in 2013, followed by Sentinel 2a in

2015, Sentinel 2b in 2017, and Landsat 9 in 2021, so the increased detection in later years is to be expected.

Bores 4 and 5 detected in a Landsat 8 OLI image acquired May 24, 2013 are the first for which high resolution imagery is available, and are also representative of the bores that occurred in the estuary prior to extensive development of alternate channels. Bore 4 was very similar to Bore 3 which was observed nearby on March 9, 2012. The 2012 field trip was conducted by kayak, with a 4:40 AM departure from the flood control levee to ride the ebb down the Pangas Viejas Channel to an observation point in the estuary on the east bank just upstream from the location of Bore 4. The water level in the estuary channel dropped 3 m between the 8:15 AM landing and low tide (arrival of the flood tide) at 12:42 PM. The flood approached with a roar but without a defined bore wave until it encountered a shallow bar which produced a breaking wave ~0.6m high. After passage of the bore front, the water rose 3 m in 12 minutes to inundate the observation point, and the kayaker was afloat again. The objective for the return trip was to float with the flood to determine its speed. The GPS immediately registered 7.4 knots (13.7 km/hr). The paddle was used only to maneuver away from ~1m standing wave sets which developed without warning as the water level rose over submerged bars. Similar zones of flood turbulence can be seen as white areas extending about 2 km behind Bore 4 and other bores in Figure 6. Sections of bank collapsed into the channel and numerous uprooted shrubs were seen rolling upstream in the shallows. The observer floated 9 km with the flood in just over an hour, though this included about 5 minutes waiting in an eddy for turbulence to subside. High tide back at the levee occurred at 4 PM.

The observer returned to the estuary on April 28, 2013, to record a tide change at the El Zanjon fish camp (Z1 in Figure 6), which was temporarily accessible by auto using

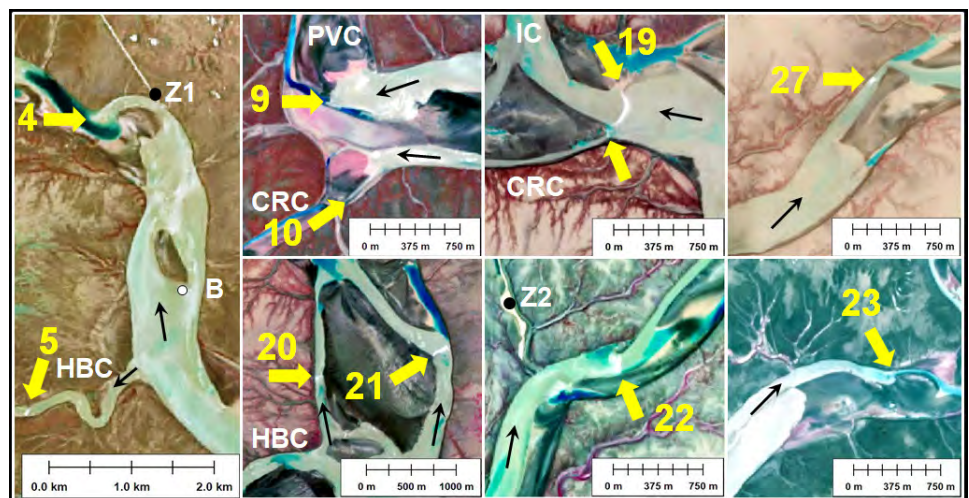


Figure 6. A selection of bores as seen in satellite imagery. See Fig. 5 for location context and Table 2 for additional information about each bore. Yellow arrows point to the bore front. Black arrows indicate the direction of flood current. B: Site of La Bocana. Z1: First location of El Zanjon. Z2: Second location of El Zanjon. CRC: Colorado River Channel. PVC: Pangas Viejas Channel. HBC: Horseshoe Bend Channel. IC: Indiviso Channel. See text for discussion.

a recently constructed elevated causeway. The 4 m-high bank at the fish camp was undergoing active erosion with large sections of collapsed bank slumped at the water's edge, though there was little sign of erosion during the gentle ebb. Despite a predicted 5.8 m tide range there was no bore although the tide turned abruptly at 1:16 PM. Small pieces of the bank began calving off immediately following the tide change. This erosion continued and intensified with the growing flood. The site of the former La Bocana fish camp (B in Figure 6) gives an idea of the extent of bank erosion underway in the estuary following the 2010 earthquake. The La Bocana site had been on the bank in 2010. By 2013 it was 250 m out in the channel. The causeway to the Z1 site was cut by the advance of the Indiviso Channel in the summer of 2013, so El Zanjón was moved to site Z2 (panel for Bore 22 in Figure 6), using the growing Indiviso Channel for fishing access.

Although a bore was not seen at Z1 on April 28, 2013, one could have formed elsewhere in the estuary on that day or on the two previous days when the flood tide range was greater. The channel at Z1 was wide and its bottom braided with bars, creating an irregular channel bed un conducive to bore wave formation. More favorable conditions, (mainly the presence of a better-defined common flood/ebb channel) could have produced a bore elsewhere. Bore pairs 9/10 and 20/21 are examples of that phenomenon. In the instance of Bores 9/10, the flood advanced over a relatively wide channel bed, probably without formation of a bore wave, but the flow was funneled into two narrow channels just as the satellite passed over. In the case of 20/21, a large bar obstructed most of the channel, causing the flood to be constricted in narrow channels on each side.

Bore 19 is second in size only to Bore 1, spanning a channel 313 m wide. It also has an unusual inverted leading edge. In a channel that is deeper in the center and shallow along the banks, a bore wave usually advances upstream faster in the deep water in mid-channel. The leading edge of Bore 19 is inverted, with the wave moving faster close to the banks. This probably indicates the presence of a shallow mid-channel bar. Note also that Bore 19 is in the process of splitting into two bore waves, with the smaller wave moving up the Colorado River Channel.

Bores 22, 23, and 27 are all advancing up the Indiviso Channel, which has recently become the focus of tidal energy. Fewer bores are advancing into the other channels for reasons that will be discussed in the following section. Bore 22 is just passing the relocated El Zanjón fish camp (Z2). Bores 23 and 27 illustrate a common pattern seen in the flood tide. The flood front, including the bore wave, surges out ahead in a narrow channel while taking longer to cover a higher mid-channel bar. An unfavorable sun angle creating a strong reflection from the water's surface makes it harder to see a distinct bore wave in the case of Bore 23, but the forces at work on the flood front are the same in both cases.

Discussion

How common are tidal bores in the blind channels of the Colorado River Estuary?

The tidal bores detected in this study represent a small subset of the bores that likely form in the estuary. Most of the bores reported here were detected during the roughly 10 minute period of the day (11:25 to 11:35AM) when Sentinel 2 satellites pass over the estuary. A query of the CICESE tidal prediction database using the criteria specified in Section 2.1 (excluding the daytime restriction) predicted acceptable conditions for bore formation on 130 occasions (64 in daylight hours, 66 at night) in 2023, with daytime bores occurring in the study area as early as 9:10 AM and as late as 1 PM. Clearly we documented only a small sample. Tidal bores are much more common in the Colorado River Estuary than opportunities to see them!

How common are tidal bores in blind tidal channels?

While most of the world's tidal bores are reported from tidal rivers, they are also known to occur in other blind (or nearly blind) channels, most notably the North Branch of the Changjiang (Yangtze) Estuary, China (Chen, 2003; Guo et al., 2022) and blind channels of the Sittaung River Estuary, Myanmar (Choi et al., 2021; Jo et al., 2022).

Tidal bores as agents of aggradation

Tidal bore waves, and the turbulence following them, mobilize sediment and contribute to bank erosion. Where has the sediment mobilized after the 2010 El Mayor-Cucapah earthquake gone? Landward movement of sediment in macrotidal estuaries with limited or no fluvial input is common worldwide (Dalrymple and Choi, 2007; Gugliotta and Saito, 2019; Nienhuis et al., 2018). Zamora et al. (2013) estimated a rate of deposition of tidal sediment of 10–21 cm/year as the tidal sandbar developed in the Colorado River Channel in the early 2000s. In the absence of a rigorous monitoring program, can we establish that channel beds and tide flat surfaces are aggrading elsewhere in the subsidence zone? Perhaps not with a great level of precision, but there are indications.

Changes in the pattern of tidal inundation and the movement of tidal bores (Figure 7) suggest that the Colorado River Channel, Pangas Viejas Channel, and Horseshoe Bend Channel are all aggrading. Bores 8 (Figure 7a) and 22 (Figure 7b) occurred on days with a similar tide range (~5.9 m vs 5.7 m), and the bores have advanced similar distances into the estuary. Caution should be used in directly comparing the water levels between images. Although the tide range was similar on both days, low tide on the 2017 date was predicted to be 0.3 m higher than on the 2022 date—so more water was likely present when the 2017 image was acquired. The significance of the comparison is that the channel bottom of the Pangas Viejas Channel is clearly higher than the channel bottom of the Indiviso Channel in 2022. The original headcutting of both channels started

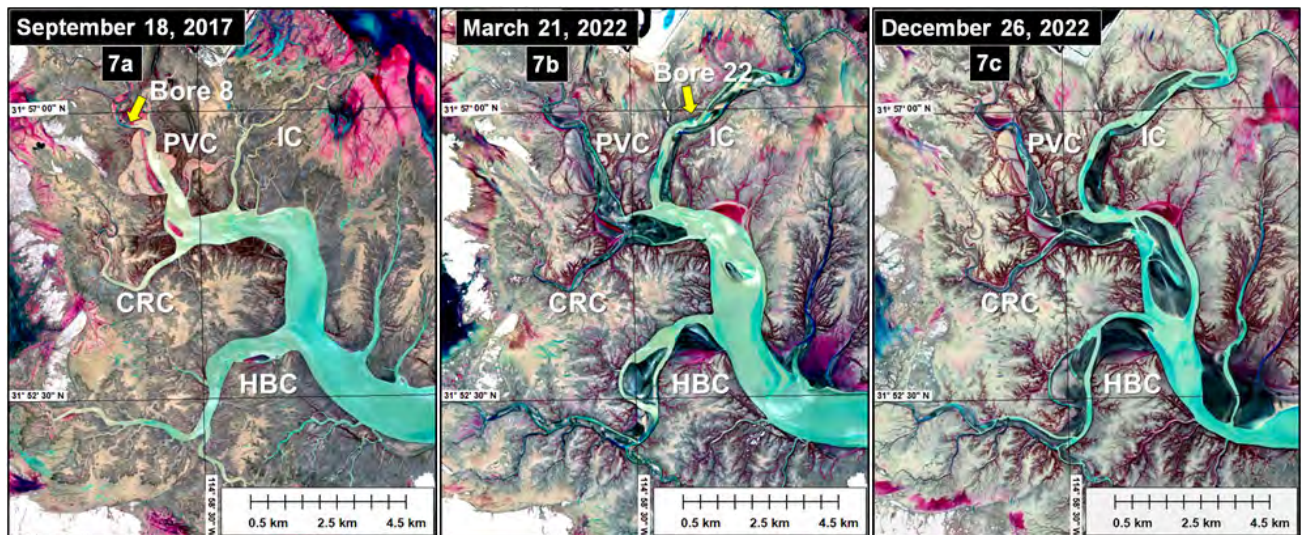


Figure 7. Aggradation of the Pangas Viejas, Colorado River, and Horseshoe Bend channels. CRC: Colorado River Channel. PVC: Pangas Viejas Channel. HBC: Horseshoe Bend Channel. IC: Indiviso Channel. Bores 8 and 22 occurred on days with a similar tidal range (~5.9m vs 5.7m). Fig. 7a: In 2017 most tidal energy was directed into the PVC, and tidal bores moved from the main estuary channel into the PVC. Fig. 7b: By 2022 most tidal energy was directed into the IC and most tidal bores moved from the main estuary into the IC. At present the PVC and HBC do not fully inundate until later in the flood, indicating that their channel bottoms have been aggraded. Since 2017 all tidal bores detected in the PVC were located near its lower connection to the estuary. The frequency of tidal bores in the HBC also seems to have diminished, although a bore did occur in 2022 on a day with a 6.6m tide swing. The tidal sandbar in the CRC continues to grow. Fig. 7c: The estuary during an ebbing spring tide revealing channel bottom conditions.

at a common base level in the estuary, so the Pangas Viejas Channel must have aggraded. Figure 7c shows the estuary on a falling spring tide, giving a clear indication of the relative levels of the channel bottoms in 2022. The Indiviso Channel is the newest channel and is less aggraded than the others, but by virtue of its lower bed elevation it is now the focus of tidal bore activity, which mobilizes sediments for upstream transport on the flood. It will most likely experience aggradation just as the other channels have.

What about the general surface of the tidal flats? Is that also aggrading? This is more difficult to establish, but there are indications that some parts of the subsided tidal flats are not being inundated as often as they were immediately after the earthquake. A case in point is an area near the flood control levee where Palmer's saltgrass (*Distichlis palmeri*) became established shortly after the area subsided following the earthquake (See Lynch et al 2023, Plant Rings of the Colorado River Delta: Clones, Ghosts, and Zombies, this volume). It did well for several years but has declined recently. A possible reason is that the area is not being inundated by the tides as often as it was immediately following the earthquake. Aggradation of the Pangas Viejas Channel which delivers flood tides to this area may reduce the frequency of inundation. Fluid mud deposits 2-3 cm thick have been noted by the authors on the surface of the tidal flats in this area following spring tide inundation. These mud drapes dry back to much thinner layers, but each contributes to gradual aggradation.

Aggradation has been documented by the authors from the area between the Colorado River and Pangas Viejas

channels where a connecting channel was dredged in 2016 in an effort to reintroduce limited fluvial flow to the lower estuary. Originally dredged to a depth of 2m, the channel had completely filled with tidal sediment by 2021.

How much of this aggradation might be attributable specifically to tidal bores? Sedimentary research has begun to examine the recognition of tidal bore signatures preserved in sedimentary successions. Tessier et al. (2017) discussed such tidal signatures and their record of the direct impact of tidal bores on the sediment bottom as well as their indirect impact in inducing very high suspended sediment concentrations. Recent studies have begun to quantify the contribution of tidal bores. Dalrymple (2021) studied the Salmon River Estuary in the Bay of Fundy and found that deposits from the small (~30 cm) tidal bores there comprise approximately 15% of the deposits in the upper-flow-regime sand flats in the inner part of the estuary. Jo et al. (2022) found that tidal bores in blind tidal channels induce less turbulent internal mixing than tidal bores in fluvial channels because of the lower intensity of the bore wave, but that they nevertheless convey a turbid plume to the tide flats in the upper intertidal zone of the Sittaung River, Myanmar. They also reported that the turbidity peak of blind channel bores coincides with the bore front, but the sedimentation rate is relatively lower than for bores in fluvial channels. This is because the peak current speed is reached about an hour after bore passage, instead of coinciding with bore passage as is normally the case with river bores. Thus, in the case of the blind channel bores currently ascending the Colorado River estuary, the intense turbulence in the hour following passage of the bore may be as important as

the bore wave itself in mobilizing sediment for landward transport.

Acknowledgements

The authors thank Lynn C. Anderson for permission to use the 1987 tidal bore photo in Figure 2 and Dale Turner and The Nature Conservancy for permission to use the photo of headcut erosion in Figure 4.

References

- ACOE U. S. Department of Defense, Army Corps of Engineers, Los Angeles District. 1982. Colorado River Basin, Hoover Dam, Review of flood control regulation, final report. Government Printing Office, Washington, D.C., USA.
- Bartsch-Winkler, S., Lynch, D.K., 1988. Catalog of worldwide tidal bore occurrences and characteristics. US Geological Survey Circular 1022. US Government Printing Office, Washington, D.C.
- Bonneton, P., Bonneton, N., Parisot, J.P., Castelle, B., 2015. Tidal bore dynamics in funnel-shaped estuaries. *Journal of Geophysical Research: Oceans*. 120 (2), 923-941. <https://doi.org/10.1002/2014JC010267>
- Chanes-Martínez, J.J. 2012. Características estructurales y sismoestratigráficas en un sector del delta del Río Colorado, noroeste de México, a partir de sísmica de reflexión. Centro de Investigación Científica y de Educación Superior de Ensenada, Departamento de la Ciencias de la Tierra, Ensenada.
- Chanson, H. 2004. Mixing and dispersion role of tidal bores, in: Mossa M., Yasuda Y., Chanson H., eds. *Fluvial, Environmental and Coastal Developments in Hydraulic Engineering*. Taylor and Francis, London, pp. 223-232.
- Chen, S. 2003. Tidal bore in the north branch of the Changjiang estuary. *Proc. Intl Conf. on Estuaries & Coasts ICEC-2003*. Zhejiang University Press, pp. 233-239.
- Choi, K., Jo, J., Kim, D., 2021. Tidal and seasonal controls on the stratigraphic architecture of blind tidal channel deposits in the fluvial-tidal transition of the macrotidal Sittaung River estuary, Myanmar. *Sediment. Geol.* 426, 106029. <https://doi.org/10.1016/j.sedgeo.2021.106029>
- Dalrymple, R.W. 2010. Tidal Depositional Systems, in: James N.P., Dalrymple R.W., eds. *Facies Models 4*. SEPM Society for Sedimentary Geology, pp. 201-231.
- Dalrymple, R.W., 2021. Sedimentation on high-energy sand flats in the Bay of Fundy: The record of tidal-bore activity and deposition from high-concentration suspensions of sand. *Sedimentology*. 68 (5), 2195-2226.
- Dalrymple, R.W., Choi, K., 2007. Morphologic and facies trends through the fluvial-marine transition in tide-dominated depositional systems: A schematic framework for environmental and sequence-stratigraphic interpretation. *Earth-Sci. Rev.* 81 (3-4), 135-174. [10.1016/j.earscirev.2006.10.002](https://doi.org/10.1016/j.earscirev.2006.10.002)
- Derby, G.H., 1852. Report of the Secretary of War communicating, in compliance with a resolution of the Senate, a reconnaissance of the Gulf of California and the Colorado river by Lieutenant Derby. Department of War, Washington, D.C.
- Fletcher, J.M., Teran, O.J., Rockwell, T.K., Oskin, M.E., Hudnut, K.W., Mueller, K.J., Spelz, R.M., Akciz, S.O., Masana, E., Faneros, G., Fielding, E.J., Leprince, S., Morelan, A.E., Stock, J., Lynch, D.K., Elliott, A.J., Gold, P., Liu-Zeng, J., González-Ortega, A., Hinojosa-Corona, A., González-García, J., 2014. Assembly of a large earthquake from a complex fault system: Surface rupture kinematics of the 4 April 2010 El Mayor-Cucapah (Mexico) Mw 7.2 earthquake. *Geosphere*. 10 (4), 797-827. [10.1130/GES00933.1](https://doi.org/10.1130/GES00933.1)
- Freeman, L.R., 1923. The Colorado River yesterday, today, and tomorrow. Dodd, Mead, and Company, Rahway, NJ.
- Gordon, J.H., 1924. Tidal bore at the mouth of the Colorado River. *Monthly Weather Review*. 52 (February 1924), 98-99.
- Graber, S.D. 2012. Perspective on the tidal bore: Background and initiation. *Proceedings of the American Society of Mechanical Engineers 2012 Fluids Engineering Summer Meeting*. Rio Grandi, Puerto Rico. pp. 211-221.
- Gugliotta, M., Saito, Y., 2019. Matching trends in channel width, sinuosity, and depth along the fluvial to marine transition zone of tide-dominated river deltas: The need for a revision of depositional and hydraulic models. *Earth-Sci. Rev.* 191, 93-113. [10.1016/j.earscirev.2019.02.002](https://doi.org/10.1016/j.earscirev.2019.02.002)
- Guo, L., Xie, W., Xu, F., Wang, X., Zhu, C., Meng, Y., Zhang, W., He, Q., 2022. A historical review of sediment export-import shift in the North Branch of Changjiang Estuary. *Earth Surface Processes and Landforms*. 47 (1), 5-16. <https://doi.org/10.1002/esp.5084>
- Henderson, R. 1922a. Seventy Drowned at La Bomba: Tide Capsizes Boat Filled with Cotton Pickers from Guymas; Only Few Survive. *Calexico Chronicle*, Calexico, California. November 20, 1922.
- Henderson, R. 1922b. Less Than Forty Are Drowned. *Engineer Tells Story of Ship Wreck*. *Calexico Chronicle*, Calexico, California. November 22, 1922.
- Huang, M.-H., Fielding, E.J., Dickinson, H., Sun, J., Gonzalez-Ortega, J.A., Freed, A.M., Bürgmann, R., 2017. Fault geometry inversion and slip distribution of the 2010 Mw 7.2 El Mayor-Cucapah earthquake from geodetic data. *Journal of Geophysical Research: Solid Earth*. 122 (1), 607-621. <https://doi.org/10.1002/2016JB012858>
- Hughes, Z.J. 2012. Tidal channels on tidal flats and marshes, in: Davis R.A., Dalrymple R.W., eds. *Principles of tidal sedimentology*. Springer, New York, pp. 269-300.
- Ives J.C., 1861. Report upon the Colorado River of the west, explored in 1857 and 1858 by Lieutenant Joseph C. Ives. Government Printing Office, Washington, D.C.
- Jo, J.H., Kim, D.H., Choi, K.S. 2022. Morphologic and hydrodynamic controls on the occurrence of tidal-bore deposits in the inshore tidal flats, Sittaung River Estuary, Myanmar (Poster). *Tidalites 2022 10th International Congress of Tidal Sedimentology*. Matera, Italy.
- Lavin, M.F., Marinone, S.G. 2003. An overview of the physical oceanography of the Gulf of California, in: Valasco Fuentes, O.U., Shenbaum J., Ochoa J., eds. *Nonlinear processes in geophysical fluid dynamics*. Springer, pp. 173-204.
- Leigh, R., 1941. *Forgotten Waters; Adventure in the Gulf of California*. J. B. Lippincott, Philadelphia.

- Lynch, D.K., 1982. Tidal bores. *Sci. Am.* 247 (4), 146-157.
- Nelson, S. 2007. In search of El Burro, the tidal bore of the Rio Colorado Delta, in: Felger R.S., Broyles B., eds. *Dry borders: Great Natural Reserves of the Sonoran Desert*. University of Utah Press, Salt Lake City, UT, pp. 519-529.
- Nelson, S.M., Fielding, E.J., Zamora-Arroyo, F., Flessa, K., 2013a. Delta Dynamics: Effects of a major earthquake, tides, and river flows on Ciénega de Santa Clara and the Colorado River Delta, Mexico. *Ecol. Eng.* 59 (2013), 144-156. <https://doi.org/10.1016/j.ecoleng.2012.09.004>
- Nelson, S.M., Kendy, E., Flessa, K.W., Rodríguez-Burgueño, J.E., Ramírez-Hernández, J., Rivas-Salcedo, T.E., 2020. Channel incision by headcut migration: Reconnection of the Colorado River to its estuary and the Gulf of California during the floods of 1979–1988. *Hydrological Processes*. 2020 (34), 4156-4174. 10.1002/hyp.13858
- Nelson, S.M., Zamora-Arroyo, F., Ramirez-Hernandez, J., Santiago-Serrano, E., 2013b. Geomorphology of a recurring tidal sandbar in the estuary of the Colorado River, Mexico: Implications for restoration. *Ecol. Eng.* 59 (2013), 121-133. <https://doi.org/10.1016/j.ecoleng.2012.12.095>
- Nienhuis, J., Hoitink, A.J.F., Törnqvist, T., 2018. Future change to tide-influenced deltas. *Geophys. Res. Lett.* 45, 3499-3507. 10.1029/2018GL077638
- Sánchez García, A.C. 2013. Rasgos estructurales en el suroeste del delta del Río Colorado : interpretación de perfiles de sísmica de reflexión. Centro de Investigación Científica y de Educación Superior de Ensenada, Tesis para obtener el grado de Maestro en Ciencias de la Tierra con orientación en Geofísica Aplicada,
- Sykes, G., 1937. *The Colorado River Delta*. American Geographical Society, New York.
- Tessier, B., Furgerot, L., Mouazé, D., 2017. Sedimentary signatures of tidal bores: a brief synthesis. *Geo-Mar. Lett.* 37, 10.1007/s00367-016-0479-x
- Thompson, R.W., 1968. Tidal flat sedimentation on the Colorado River Delta, northwestern Gulf of California. *Bull. Geol. Soc. Am. Memoir* 107, 1-133.
- Waters, F., 1946. *The Colorado*. Rinehart & Company, New York.
- Wells, J.T. 1995. Tide-Dominated Estuaries and Tidal Rivers, in: Perillo G.M.E., ed. *Geomorphology and Sedimentology of Estuaries*. Elsevier, Amsterdam, pp. 179–205.
- Zamora, H.A., Nelson, S.M., Flessa, K.W., Nomura, R., 2013. Post-dam sediment dynamics and processes in the Colorado River estuary: Implications for habitat restoration. *Ecol. Eng.* 59 (2013), 134-143. <https://doi.org/10.1016/j.ecoleng.2012.11.012>

Curtis Howe Springer and Zzyzx

Larry M. Vredenburg
lvrednb@gmail.com

Introduction

Soda Springs is a wonder! Abundant potable water flows out of the ground without ceasing in the middle of the Mojave Desert. There is a reason the world's largest thermometer is in Baker, about 9 miles away – this place is *hot*, being just some 40 miles from Death Valley. Soda Springs was a life saver. Native Americans lived here, as did soldiers during the 1860s and a few miners and prospectors from time to time. It was a critical stopping point on the Mojave Road beginning around 1859. If you are attracted to the vast, empty vistas of the Mojave Desert, this is your place. This place also attracted Curtis Howe Springer. He established a “Haven of Rest” here, though it wasn't his first. His stated purpose for Zzyzx was to give people a place to relax and unwind. As an unapologetic teetotaler, Springer made Zzyzx the perfect refuge from that addiction.

Curtis Howe Springer before Zzyzx

Curtis Howe Springer, founder of Zzyzx, was born December 2, 1896, in Wheeling, West Virginia. As a teenager he successfully ran a portion of the family's chicken farm. He sold this business prior to heading off to World War I in September 1918. Also, during this period of his life, he built several houses which provided him with significant income. After returning home from Europe, he attended Wesleyan College at Buckhannon, West Virginia, and later Moody Bible Institute. During the early 1920s he preached and sang in and around his hometown and later toured around the country, sponsored at times by the National Reform Association. By the late 1920s he set out on his own speaking tours. Springer was a gifted speaker; his lectures drew large crowds. In 1929 he began running display advertisements in newspapers promoting his free lectures, typically held at the YMCA. One such ad that appeared October 2, 1929, in the Davenport Iowa “Daily Times” read in part:

“Curtis H. Springer, Dean, Greer College. Money For You. Develop Your Power. Be Healthy, Happy, Successful. A series of Free Lectures is offered to the public under the auspices of the Extension Department of Greer College. Thousands have paid to hear the lecture, but you can hear them free, through the courtesy of the Davenport Psychology Class. . .”

Soon after this he presented himself in his advertisements as “Dr.” or “Professor” Springer, and later added ND, MD, DO, and PhD to his name. In 1934

he began selling medicinal products such as Re-Hib and Antediluvian Tea as well as food products. After investigating Springer in 1935, the American Medical Association discovered Antediluvian Tea, which was advertised to cure constipation, was simply a mixture of laxative herbs, while Re-Hib, an antacid, was little more than sodium bicarbonate. In their report they noted Springer had no connection with Greer College, which taught automobile mechanics. Also, he didn't have any of the degrees he purported to have. He and his family lived in Chicago for a couple of years in the mid-1930s. In March 1934 the Chicago *Daily Worker* stated that Springer was a “quack doctor and racketeer wanted by the police.”

Springer's free lectures were held throughout the eastern United States, according to his ads, while in St. Petersburg, Florida over 8,000 people attended his final message. Besides lecturing, he was on radio throughout the region and eventually the entire world.

In late 1932 Springer purchased 3,000 acres at Maple Glen about 5 miles southwest of Mt. Davis, the highest point in Pennsylvania. This property became the “Haven of Rest” health resort. He spent thousands of dollars improving an old farm, constructing buildings, a swimming pool, a 116-acre reservoir, and planting trees. About 50 men were employed on the project. He also built a large rabbitry, the meat of which was sold in Pittsburgh. Guests could stay at no charge, and he offered free college to youngsters who were willing to work on his rabbit farm.

Apparently, his sale of medicinal products and food supplements, along with donations, failed to keep up with expenses. In early 1937 Sheriff's Sale notices began to be run in newspapers alerting the Springers that their resort would soon be sold to cover unpaid taxes. But, even after losing his resort, the Springers were anything but poor; in 1938 they took a trip through the eastern states in their \$50,000 travel trailer that had been built by Edsel Ford as a concept vehicle for the 1934 Chicago World's Fair. Shortly afterward they left Pennsylvania and struck out for California. He pulled into Port Arthur, Texas in April 1939 to begin a two-week lecture series. By 1940 he had purchased a home in the Hollywood Dell area of Los Angeles for \$10,000. He was still broadcasting radio shows, travelling to lectures, and selling his wares. In April 1941 he ran an ad in the Modesto Bee announcing a free lecture. In this ad he is stated that he had a PhD and was “Former Dean of Greer College.” A few months later he found himself in jail in Tacoma, Washington for selling drugs without a license.

During the transition to the west coast, the Federal Trade Commission hadn't forgot about him. On

November 15, 1940, he was ordered to cease and desist false advertising, false or misleading qualities or properties of his products, and from using the word “doctor.” Of course, that never happened!

Zzyzx

In 1944 we find Springer at Soda Springs. Located in the middle of the Mojave Desert, Soda Springs had been an important water stop on the Mojave Road and a small army outpost established there in 1860 was known as Hancock’s Redoubt. The army built another post here in 1867, often referred to as Soda Station. During the 1880s local prospectors called the place Shenandoah Camp. The Tonopah and Tidewater Railroad laid tracks through here in the spring of 1906, establishing a short siding. A year later, the Pacific Coast Soda Company began construction of solar evaporation ponds, a narrow-gauge railroad, and a plant to process the salt crust mined from the surface of the lakebed (Wilkerson and Vredenburg, this volume). The operation was a failure and was scrapped around 1910. In 1940 the T & T rails were taken up.

Springer sold his home and on September 13, 1944, moved his family to Soda Springs where they first lived



Figure 1. Zzyzx Sign formerly along I-40 at Zzyzx Road. Photo by Dennis Casebier, Dec. 31, 1981. photo courtesy of the Mojave Desert Heritage and Cultural Association.

in tents. Less than a month later, on October 9, 1944, Springer and others filed placer mining claims on 12,800 acres or 20 square miles on Soda Lake for his “Mineral Salts Project.” He named his new “Haven of Rest”—“Zzyzx Mineral Springs and Health Resort.” According to Springer’s testimony in the hearing transcripts, the name Zzyzx is pronounced “ZiZex.” He created it to be the last word in the English language. At the resort a modern pool was built, and provisions were made for mud baths. There were accommodations for 100 guests, as well as a kitchen, storage buildings, dining hall, offices, and a church. There was also a broadcast studio and air strip. All of this cost some 2 million dollars. Much of the

construction work was done by men from Los Angeles rescue missions who had come to Zzyzx to “dry out.” These men were paid a small wage. Springer’s radio programs continued and hundreds of thousands of guests visited over the years. He never charged for a bed or a meal; guests would donate as they saw fit. As a side venture Springer was still selling his food supplements and “patent medicines.”

Curtis Springer’s unauthorized Zzyzx community was



Figure 2. View of Zzyzx in 1967. Springer had a fleet of buses that would bring guests to Zzyzx from the Los Angeles area. Photo by Dennis Casebier, courtesy of the Mojave Desert Heritage and Cultural Association.

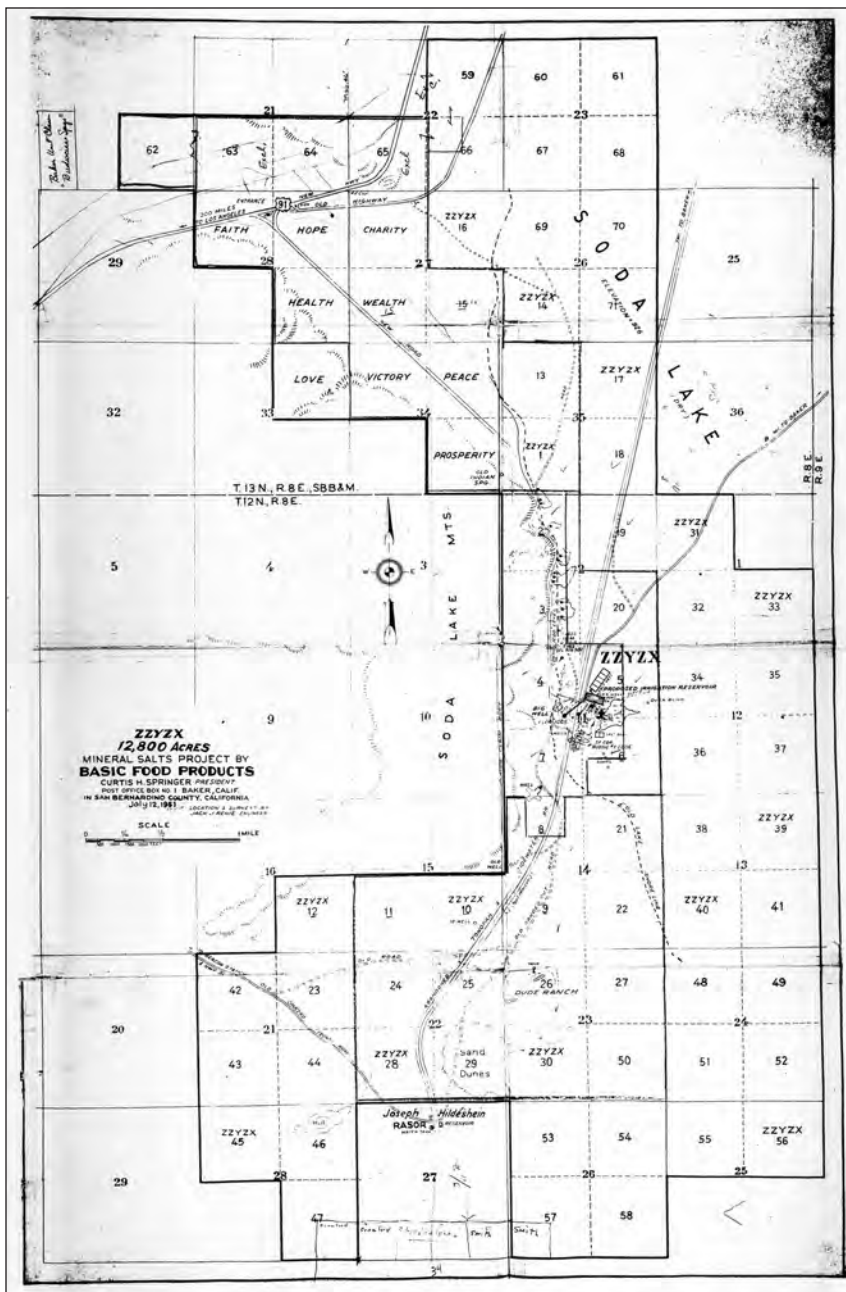


Figure 3. Map titled: Zzyzx, 18,000 Acres. Mineral Salts Project by Basic Food Products, Curtis H. Springer, President. July 12, 1951.

brought to the public's attention in an extensive article that began on page 1 of part 2 of the Friday, July 14, 1967, Los Angeles Times. The article accurately represents the BLM's involvement with Springer up to that time. After this appeared, the Times repeatedly ran articles about Springer.

The mining law requires claims to have a valid discovery. "To constitute a valid discovery there must be shown to exist within the limits of the mining claim a valuable mineral deposit, which is subject to location under the mining laws, and which would warrant a prudent man in the further expenditure of his labor and means, with a reasonable prospect of success in developing a paying mine." His claims failed these tests

– neither a deposit subject to location nor a valuable mineral deposit existed. In summary, a mining claim isn't a claim unless it can pass these two tests.

The main problem with Springer's "Mineral Salts Program" was that sodium minerals were removed from the mining law by the Mineral Leasing Act of 1920. To develop sodium minerals on Federal land you need a lease, they can not be "claimed" with a mining claim.

During the mining claim contest hearing Springer testified that two of his products were derived from Soda Lake: ZY-Mud "Minerals from the Mojave for facials" and Zzyzx Foot Crystals "for poor tired feet."

He also testified that: "After every rainfall (there are sometimes several a year) the water on the lake bed draws saline minerals up from the clay bed of the lake. When the water is evaporated by the heat of the sun, the minerals crystalize and are left as incrustations on top of the clay bed (Ex. I). The lake bed is approximately 7 miles wide and close to 14 miles long. The crystals on the surface of the lake bed are gathered, crushed into a fine powder, and after perfume is added to improve the fragrance, placed in small cans for distribution. Also, the crystals are secured by running the water from mineral springs (on Claims 2, 3, 4, 5, 6 and 7 as shown on Ex. L) into large vats where again solar heat is used to evaporate the water which in turn causes the minerals to crystalize."

Furthermore, he stated:

"The crystals generally are within the top six inches of the lakebed. Below the top six inches is the clay that is ground, perfumed, and placed in cans and distributed for use as a facial mud pack under the name ZY Mud or Mojave Mud."

Although Springer had many testimonials from satisfied users, a spectrographic analysis failed to reveal that these samples of mud contained anything out of the ordinary. Common clay, or mud, is defined as a common

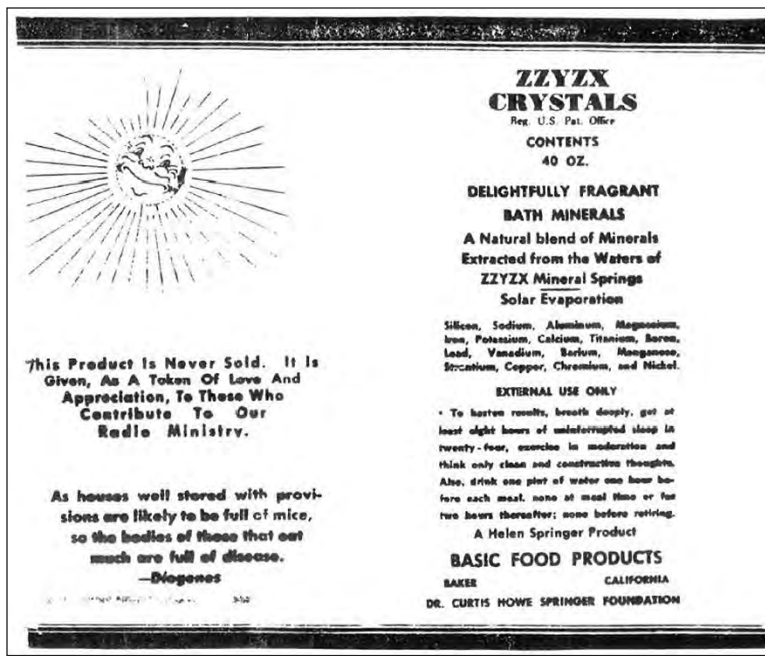


Figure 4. Zzyzx Crystals advertisement from Mining Claim Contest file R1888.

variety mineral and is not locatable under the mining law. It is defined as a Salable Mineral.

Springer also referred to gold and silver as being found on the Buddie No. 1 lode mining claim.

After examining Springer's mining claims Edward F. Cruskie, the Bureau of Land Management Mining Engineer assigned to evaluate these claims concluded:

"There is no apparent significant mineralization, veins or structures, in the rock in place portions of these claims that could have contributed any gold or other placer values to the predominant covering of the lake silt beds. The claims are essentially non mineral in character."

Springer certainly wasn't the first or only person to construct a home or business on a mining claim without authorization. On July 23, 1955, Congress passed Public Law 167 to help address this problem. This law reads in part:

"Any mining claim hereafter located under the mining laws of the United States shall not be used, prior to issuance of patent therefor, for any purposes other than prospecting, mining or processing operations and uses reasonably incident thereto."

Springer realized early on that the presence of his health resort on public land without authorization was risky. The Bureau of Land Management (BLM) was alerted to the possible occupancy trespass at Zzyzx in 1952 by the IRS. On July 12, 1951, Springer and his wife Helen filed for separate 320-acre parcels under the Desert Land Act. Both applications were rejected, and the cases were closed on September 25, 1957. Immediately following this, on

November 4, 1957, he applied for a Recreation and Public Purposes (R&PP) Act lease. This law allows private or public entities to lease land from the government for a variety of uses. This application was rejected on September 4, 1964. He also filed for a R&PP lease on June 17, 1958, which was rejected on the same day as the previous application.

The proceeding summary was based on many hundreds of pages contained in two case files. United States of America, Contestant v. Curtis H. Springer, etc., et al., Contestees, Contest Nos. R-1888 and R-1907. Contest R-1888 involved the one lode mining claim the Buddie No. 1. Contest R-1907 involved the placer mining claims: ZZYZX Numbers 2, 3, 4, 5, 6, 7, 18, 18, and 20 located in T12N R8E Sec. 2, 11 and T13N R8E Sec. 35 SE¼ SBM. The placer claims encompassed 1,440 acres. The contests were filed by the Bureau of Land Management on November 6, 1968.



Figure 5. Curtis Howe Springer. Date unknown, photo courtesy of the Mojave Desert Heritage and Cultural Association.

<u>"Order from this List and Allow Two to Four Weeks for Delivery by Parcel Post</u>	<u>Quantity</u>	<u>Retail Price</u>	<u>Suggested Contribution</u>
ANTEDILUVIAN HERB TEA (Botanical Laxative)	24 ozs	\$15.00	\$10.00 3 for \$25.00
DELICIOUS MANNA (Vegetarian Food Supplement)	24 ozs	15.00	10.00 3 for 25.00
NERVE CELL FOOD (N.C.F.)	24 ozs	15.00	10.00 3 for 25.00
ANTHRON (My Mother's Favorite Food)	24 ozs	25.00	15.00 2 for 25.00
"YUTH" (A Food For The Young at Heart)	24 ozs	15.00	10.00 3 for 25.00
HOLLYWOOD "PEP COCKTAIL" (PICKUP)	24 ozs	15.00	10.00 3 for 25.00
"RE-HIB" (Potential Iron Bearing Foods)	24 ozs	15.00	10.00 3 for 25.00
PRISTINE (Vegetarian, Potential Protein Foods)	24 ozs	15.00	10.00 3 for 25.00
CAL PLUS (Potential Calcium Bearing Foods)	24 ozs	15.00	10.00 3 for 25.00
BAN-O-WHEY (Appetite Discourager)	24 ozs	15.00	10.00 3 for 25.00
NEPTUNES (Potential Iodine Bearing Foods)	24 ozs	15.00	10.00 3 for 25.00
TROPICOES (Dehydrated Foods Of The Tropics)	24 ozs	15.00	10.00 3 for 25.00
LAMOURI (Vegetarian, Potential Vitamin C Foods)	24 ozs	15.00	10.00 3 for 25.00
F-W-O (Foods Delightfully Pleasing to Women)	24 ozs	15.00	10.00 3 for 25.00
NORM (A Basic Food Supplement)	24 ozs	25.00	15.00 2 for 25.00
ZY-MUD (Minerals from the Mojave for Facials)	30 ozs	15.00	10.00 3 for 25.00
ZZYXX FOOT CRYSTALS (For Poor Tired Feet)	40 ozs	15.00	10.00 3 for 25.00
B-PLUS (A Food Supplement for the Whole Family)	24 ozs	15.00	10.00 3 for 25.00
O-M-R (An Anti-Acid Containing Food Value)	24 ozs	15.00	10.00 3 for 25.00
COTOLOYDS (DELICIOUS FOOD Supplement)	24 ozs	15.00	10.00 3 for 25.00
ALLEROIDS (Natural Source Containing Vitamin A)200 cap	15.00	10.00 3 for 25.00
EMBROIDS (Natural Source Containing Vitamine E)300 cap	15.00	10.00 3 for 25.00
IMPERIALS (German Formulae - Pain Relieving)200 tab	5.00	4.00 3 for 10.00
ORGANIC RETURN (Containing Foods from the Sea)	2 prod	15.00	10.00 3 for 25.00
DANGO (To Assist in Conditions of Dandruff)	2 prod	15.00	10.00 3 for 25.00
MO-HAIR (A Plan to Assist Live Hairs to Grow)	3 prod	15.00	10.00 3 for 25.00
COSMO (Suggested by an Indian for Lovely Skin)	3 prod	15.00	10.00 3 for 25.00
HEMORRHOID RELIEF (A System to Assist Nature)	3 prod	25.00	15.00 3 for 25.00
SHANGRALAE (Suggested by an Asian Missionary)	4 prod	20.00	15.00 2 for 25.00

Figure 6. Zzyzx Order Form from Mining Claim Contest file R1888.

The mining claims were declared null and void on November 14, 1972, by the Interior Board of Land Appeals (IBLA) for failure to show discovery of a valuable mineral deposit on any of the claims. Following the IBLA decision the case was heard by the District Court. On March 6, 1973, the court permanently enjoined Springer and the other appellants from trespassing on or occupying the federal land at issue. Following this decision Springer appealed to the 9th Circuit Court of Appeals which upheld the District Court decision. In 1974, the US Supreme Court refused to review the lower court decisions.

Charges were brought against Springer by the California State Food and Drug Commission. In 1970 he was found guilty of making "false and misleading

statements" about some of his products. The terms of his probation forbid him from producing, advertising, distributing, or soliciting contributions for health food products. Another term ordered him to dissolve all of his Zzyzx enterprises. He violated the terms of his probation and in January 1973 was sentenced to six months in jail. Springer was 77 years old at the time.

On April 11, 1974, the Springers were evicted from Zzyzx. They were given 36 hours to remove their property and were escorted off the property by armed deputies. The BLM now had a "white elephant" on their hands. They had no plan for the facility and no budget. Before long vandals began to destroy the buildings. BLM was considering destroying the buildings as well, but at this point a group of colleges and universities from the California State system stepped forward and expressed interest in making use of the site.

The Desert Studies Center was established in 1976 under a cooperative management agreement with the Bureau of Land Management. The Center is operated for the CSU by the California Desert Studies Consortium, an organization of seven southern California CSU campuses: Dominguez Hills, Fullerton, Long Beach, Los Angeles, Northridge, Pomona, and San Bernardino. With the passage of the California Desert Protection Act of 1994, the Desert Studies Center was placed into the Mojave National Preserve and established the Desert Studies Center as a partnership between the National Park Service and the California State University in perpetuity.

Springer died in Las Vegas, Nevada on August 19, 1985, at age 88, and was buried in the Riverside National Cemetery, Riverside, California on April 26, 1991.

Acknowledgements

On a personal note: This paper has been fascinating to research. It is a very cursory biography of Curtis Howe Springer, and it couldn't have been accomplished without the vast collections of newspapers available online and help from some friends.

First, I want to thank and acknowledge Dennis Casebier for asking me to request the Springer Case Files from the National Records Center back in the 1990s and planting a seed of interest about Springer and Zzyzx. I would like to thank the Mojave Desert Heritage and Cultural Association, located in Goffs, California for the use of the Curtis H. Springer photo, and for the use of

archival information. I thank Darelyn Casebier for the review of this paper, and David M. Miller for reviewing the paper and challenging me to expand my original concept.

References

A note on references: I consulted numerous newspaper articles for the preparation of this paper. The list is too long to document here. However, I can provide them on request.

- Bureau of Investigation: "Curtis Howe Springer, A Quack and his Nostrums," *Journal of the American Medical Association*. 105 (11): 900. September 14, 1935
https://archive.org/details/sim_jama_1935-09-14_105_11 (accessed 26 Feb 2023)
- Casebier, D. G., 1976, *The Mojave Road* (Tales of the Mojave Road Publishing Company: Norco, California), 191 pp.
- Casebier, D. G., 1983, *Guide to the Mojave Road* (Tales of the Mojave Road Publishing Company: Norco, California), 283 pp.
- Contest of Mining Claim R 1888, Buddie No. 1 – Lode Mining Claim, Federal Record Center, San Bruno Accession No. 049-94-0009, Container No. U11124
- Contest of Mining Claim R 1907, Zzyzx Numbers 2, 3, 4, 5, 6, 7, 18, 19, 20 [Placer] Mining Claims, Federal Record Center, San Bruno Accession No. 049-94-0009, Container No. U11124
- Desert Studies Center, <http://biology.fullerton.edu/dsc/school/symposium.html> (accessed 26 Feb 2023)
- Duffield-Stoll, A. Q., 1994, *Zzyzx: History of an Oasis. San Bernardino County, California*, California Desert Studies Consortium (Santa Susanna Press, University Library, California State Library, Northridge. 71 pp.
- Hillinger, C., (July 14, 1967), "Ready to Argue from A to Zzyzx, 'Squatter' Owes Rent, U.S. Says," *Los Angeles Times*, Friday, Part II p. 1, 6.
- National Archives of the United States, Federal Record Nov. 15, 1940, Vol. 5, No. 223, p. 4481-4481 <https://www.govinfo.gov/content/pkg/FR-1940-11-15/pdf/FR-1940-11-15.pdf> (accessed 26 Feb 2023)
- Roberts, Stephen V., (July 19, 1970), "Improbable Name, But... Zzyzx is a Booming Health Spa". *Daytona Beach Morning Journal*. p. 8B. <https://news.google.com/newspapers?id=p4gfAAAAIIBAJ&pg=788,4132398&dq=zzyzx&hl=en> (accessed 26 Feb 2023)
- Wikipedia, "Curtis Howe Springer," https://en.wikipedia.org/wiki/Curtis_Howe_Springer (accessed 26 Feb 2023)
- Wikipedia, "Zzyzx," https://en.wikipedia.org/wiki/Zzyzx,_California (accessed 26 Feb 2023)
- Wikipedia, "Desert Studies Center," https://en.wikipedia.org/wiki/Desert_Studies_Center (accessed 26 Feb 2023)
- Wilkerson, G. and Vredenburg, L.M., 2023, Mines of the Mojave: the 2023 Desert Symposium field trip road log; in Miller, D.M., and Rowland, S.M., eds., *Mines of the Mojave: Desert Symposium Proceedings* (this volume)

Abstracts from proceedings: the 2023 Desert Symposium

Lithium enrichment in claystones of the mid-Miocene Barstow Formation, Mojave Desert, California

Thomas R. Benson^{1,2}

¹Lithium Americas Corp.; ²Lamont-Doherty Earth Observatory, Columbia University, thomasrbenson@gmail.com

The Miocene Barstow Formation of the central Mojave Desert in southern California is famous for its well-characterized eponymous Barstovian mammalian fossils in fluviolacustrine sediments of the Mud Hills ~15 km north of Barstow. Outcrops of time-equivalent (~19-14 Ma) sedimentary rock throughout the northwestern portion of the Barstow–Bristol trough are correlated to the Barstow Formation by various researchers (e.g., Dibblee, 1964; 1967; 1968; Singleton and Gans, 2008; Reynolds and Miller, 2010), though most of these occurrences likely represent spatially distinct depocenters. Recent reconnaissance exploration work by Lithium Americas Corp. on outcrops of “Barstow Formation” indicates that claystone-dominated intervals of the Barstow Formation can contain elevated lithium (Li) enrichment up to 2,700 ppm Li (whole-rock basis). The measured concentrations are on par with average Measured and Indicated Resource grades (~1,000 – 2,000 ppm Li) at other lacustrine-type deposits in the Basin and Range Province (e.g., Thacker Pass, Clayton Valley, Big Sandy).

Here, new regional whole-rock trace-element ICP-OES data is presented from > 400 outcrop samples of sedimentary rocks classified as “Barstow Formation” in the central Mojave Desert. Nearly all analyzed samples contain Li concentrations higher than average sedimentary rock (17-46 ppm; Rankama and Sahama, 1950). The most enriched samples (>2,000 ppm Li) occur in two distinct 40–100-meter intervals dominated by extremely fine-grained claystone lithologies. Moderate but still economic concentrations (~1,000–2,000 ppm Li) occur in siltstone and sandstone lithologies with minor to moderate clay-size-fraction components. In both Li-rich sections, the clays are dominantly Mg-smectites like those found at Thacker Pass (Morissette, 2012; Castor and Henry, 2020; Benson et al., in prep.) based on XRD and SEM analysis and extremely high whole-rock Mg concentrations (> 8 wt. % Mg). Though the clays from both Li-rich sections are similar in composition, the geological and environmental processes leading to precipitation of Mg-smectite (e.g., Tosca and Masterson, 2014) in the paleo Barstow basin were widespread and longstanding, as the economic intervals are separated by ~25 km and ~3 million years. This suggests that additional

outcropping and/or buried “Barstow” sediments may also contain economic Li concentrations. Ongoing geological mapping and tephrochronology (Eden et al., this vol.) combined with stable isotopic analysis of key sections aims to reconstruct Barstovian basinal evolution to help further define the locations and mechanisms of Li enrichment.

Formation of gas-escape sedimentary structures in ephemeral ponds (Ubehebe Crater, Death Valley NP): relevance to Mars

R. Bonaccorsi,^{1,2} D. Willson,^{2,3} L. Baker,⁴ and C.P. McKay²

¹SETI Institute, Mountain View, CA 94043; ²NASA Ames Research Center, Moffett Field, CA 94035; ³KISS Institute for Practical Robotics, OK; ⁴Dept. of Geological Sciences, University of Idaho, Moscow, ID 83844

We describe the formation of microbially-induced sedimentary gas-escape structures under extreme evaporation conditions (~2 cm/day) of a ca. 2-week ephemeral pond at the bottom playa of the 237 m-deep Ubehebe Crater (UC) (37°0'35" N, 117°27'01" W; ~752 m-elevation) in Death Valley National Park, California. The ~2 mm-sized bubble casts in the dry smectite-rich surface are strikingly similar to the sedimentary structures, referred to as Hollow nodules, imaged by Mars Science Laboratory Curiosity in the < 3.7 Ga Gale Crater's smectite-rich mudstone, at the Yellowknife Bay site (sol 159).

On Earth, these sedimentary structures form along the muddy shoreline of shallow ephemeral playa lakes and ponds with ongoing rapid desiccation in hyper-arid poly-extreme environments such as the Mars-like Death Valley and Atacama Desert (Chile). In Death Valley, the short-lived 5–20 cm-deep freshwater pond formed after two preceding monsoonal rain events. The gas bubbles formed at the sediment-water interface due to the cryptic and short-lived terrestrial microbial mats that the desiccating UC mud preserved against surface erosion. In a plausible literature-based model, the gas-escape forming smectite-rich mud is the most biologically active layer with bacteria plausibly supported by redox reactions involving iron sulfides (FeS₂, FeS) from HS⁻ and Fe²⁺ in reduced sediments, sulfates, iron-bearing minerals, and biological sulfur from decaying aquatic cyanobacterial biomass.

On Mars, gas escape structures preserved in mudstone deposits might suggest ancient microbial activity in Martian lake sediment and be relevant to future astrobiology life-detection missions to the Red Planet.

Bagdad-Chase mine, San Bernardino County, California

Tara Bonas¹ and Jake Anderson²

¹ *California State University, Bakersfield, tbonas@csb.edu;* ²

The Bagdad Chase Mining Company, LLC

The Bagdad-Chase mine is located 7 miles south of Ludlow, California and 0.2 miles south-southeast of the former town of Stedman in the northern Bullion Mountains. It was discovered in the 1880s by John Suter roadmaster for the Atlantic and Pacific subsidiary of the Santa Fe Railway. The subsequent ownership and production techniques are shown in Table 1.

The Bagdad-Chase and other mines were served by a railroad, known as the Ludlow and Southern, which ran 7.5 miles south from Ludlow to Rochester. It was constructed between 1899 and 1901 and operated until the mid-1920s. Between 1904 and 1910 the Bagdad-Chase was

Table 1

Years	Company	Mining and beneficiation methods
2020 to Present	Owned by The Bagdad Chase Mining Company, LLC (Private Entity)	Exploration and permitting
1990–2020	Owned by Bagdad Chase Mining Company California	Exploration and permitting
1978	Mine Closed	Care and maintenance
1978	Owned by Bagdad Chase Inc. California	Open Pit
1978	Owned by Clark Mining and Exploration, California	Open Pit
1943–1977	Owned by John Hobbs	Underground to 1954, then open pit
1940–1943	Owned by Bagdad Chase Ltd., California	Underground
1938–1939	Operated by D'Aix Syndicate, California	Underground
1910–1916	Operated by Pacific Mines Corporation., California	Underground
1904–1919	Owned by the Bagdad Chase Mining Company, California.	Underground. Fifty 1,000-pound stamps with five re-grinders; a cyanide plant with a capacity of 200 short tons of ore per day.

the largest single source of gold in the county and yielded a significant amount of silver, as well. The mine went bankrupt in 1916 and starting in the early 1930s, Bagdad-Chase was leased to several different parties who operated the project periodically. The Bagdad-Chase was one of only four gold mines in California to be authorized to remain in production during World War II; the ore's silica content made it useful as a flux in smelting. Although not very profitable, the mine operated continuously from 1940 to 1954. Around 1972 Bagdad Chase, Inc. reportedly began open-pit operations at Stedman, which continued through 1975. In 1987, Bentley Resources, Vancouver, B. C., announced plans for extensive exploration and drilling around the Bagdad-Chase, to bring the Bagdad-Chase operations back into production, and to pour the first gold ore bar in the second quarter of 1988. Operation plans called for an annual production of 20,000 troy oz Au from three open pits: Bagdad, Middle Mine, and Roosevelt.

These plans never materialized. Currently a new mining plan by a private entity called The Bagdad Chase Mining Company, LLC is being reviewed by San Bernardino County.

This area consists of volcanic flows and pyroclastic deposits of Miocene age, which are located primarily in the northwestern part of the district. There are also several Tertiary intrusive rocks forming andesitic plugs and a stock. A stock located in the southwestern part of the area is of notable importance as it may have provided the mineralizing solutions. The pyroclastic and flow deposits have been intensely altered by hydrothermal activity, while the andesitic plugs show no hydrothermal alteration. Mineralization in the mine is believed to be related to the dextral strike-slip of the Ludlow and the Bullion Range Mine faults and their associated antithetic faults. The deposit consists of poly metallic copper-gold and lead-zinc-silver mineral assemblages. The ore is a hydrothermal quartz-hematite breccia that is composed of argillically altered and leached rhyodacite fragments that are set in a fine-grained matrix of hydrothermal quartz and specular hematite.

Extensional deformation occurred both after and during the Miocene basalt to rhyolite volcanism. In the late Cenozoic, three structurally different deformation events affected the central Mojave area. Around 24 to 21 Ma, the Mojave extensional belt opened in a N-S direction. After extension, E-W striking dextral shearing occurred around 21 to 18 Ma at the trans Mojave-Sierra shear zone. From 13 to 0 Ma the eastern California shear zone has been experiencing right-lateral shearing, with dominantly strike-slip faults in the Mojave. The southern Bagdad-Chase mine lies on the Bagdad-Chase fault lineament. This is a zone of anastomosing faults that connect unnamed prospects and the Old Pete mine on the north end with the Ambush Canon mine on its south end. Ore bodies are developed at fault intersections, where the zone exhibits dilation and fault pairing.

The area of focus is the mineralized breccia zone that strikes east and dips gently north. The breccias consist of fragments of andesite porphyry cemented by silica containing iron oxides. The main value of these breccias was gold, which probably occurred as finely divided material in the silica. Secondary copper in the form of malachite and chrysocolla occurs commonly in these breccia zones as either replacements of the fragments or the silica cement and/or as fillings in cavities. There is evidence of supergene enrichment of copper oxide throughout the upper rhyodacite.

Potassium-rich, magmatic-hydrothermal fluids spread upward along fractures and laterally along the developing fault zones of various types. A zone of potassic alteration formed along faults and fracture zones (incipient breccia pipes). Hydrothermal fluids, accumulating in a magma chamber, were subsequently forced out in several pulses, and rose along the faults and fractures. As the fluids neared the surface, a pressure and/or temperature

differential between the magmatic fluids and the wallrock caused the wallrock to brecciate by thermal and/or hydraulic fracturing. Brecciation was initially in the form of breccia pipes that developed in permeable, fractured rock within the lower rhyodacite. As the fluids reached the faulted host rock, they traveled laterally along it, brecciating the footwall to form a hydrothermal breccia blanket (or sill). Hydrothermal breccia fragments mixed with material from the base of the hanging wall indicate that some movement along the fault occurred after emplacement of the hydrothermal breccia sill. A primary geochemical dispersion halo, roughly coincident with the zone of potassic alteration, developed in the footwall adjacent to the hydrothermal breccia sill. Alternatively, the geochemical halo formed around the breccia sill in both the footwall and hanging wall rhyodacite, and subsequently a portion of the hanging wall that was not K-altered or mineralized was structurally juxtaposed upon the mineralized column. The mine has 950 thousand short tons of reserves. The average grade is 0.147 oz Au/short ton and 0.35% Cu.

Origin of borate deposits in the Furnace Creek Formation, Death Valley, CA

J.P. Calzia

U.S. Geological Survey, Menlo Park, CA 94025

The Late Miocene–Pliocene Furnace Creek Formation in Death Valley, CA, hosts numerous borate prospect pits as well as the Monte Blanco and Boraxo mines from Zabriskie Point to Ryan. Most of these pits and deposits consist of colemanite ($\text{CaB}_3\text{O}_4(\text{OH})_3 \cdot \text{H}_2\text{O}$) and are unzoned; the Monte Blanco deposit is zoned from a ulexite ($\text{NaCaB}_5\text{O}_6(\text{OH})_6 \cdot 5\text{H}_2\text{O}$) and proberite ($\text{NaCaB}_5\text{O}_7(\text{OH})_4 \cdot 3\text{H}_2\text{O}$) core to a colemanite rim. Colemanite and ulexite have a narrow range of $\delta^{11}\text{B}$ of -1 to -4‰; proberite $\delta^{11}\text{B}$ is ca 5‰.

All these deposits occur within the lower lacustrine member of the Furnace Creek Formation and are spatially associated with ca. 5.9–5.7 Ma basalt flows and intrusions. The borate deposits occur in laminated mudstone interbedded with lenticular stacks of porous brecciated limestone up to 30 m high; these limestone stacks have a texture and fabric(s) similar to tufa mounds deposited at the bottom of lakes. Near Monte Blanco, fractures in altered basalt breccia filled with ulexite and colemanite represent subaqueous eruptions with fragments spread over adjacent lake floor; basalt debris locally mixed with the borate deposits suggest the basalt and borate deposits may be synchronous.

The source of B in these deposits is debatable. Experimental studies suggest $\text{B}(\text{OH})_3$ is the dominant boron species at 25°C and pH < 8.8. At higher temperatures and above this pH, $\text{B}(\text{OH})_4^-$ becomes the dominant boron species. $\delta^{11}\text{B}$ values suggest all three borate phases have a similar source. Pleistocene tuffs in Death Valley contain <3 ppm B, local groundwater contains <1 ppm B, Tertiary basalt <10 ppm B, and sediments derived from

Precambrian schist or shale 15–300 ppm B. Given that lake sediments in the Furnace Creek Formation are locally derived, these data suggest boron is leached from the lake sediments and concentrated by hydrothermal fluids formed by heated connate water in the lake sediments. The heat source for this hydrothermal system was the 5.9 – 5.7 Ma basalt.

Paul VanderEike and the California Federation of Mineralogical Societies

Stephen Collett

Kern County Mineral Society, Bakersfield, starmstr1@bak.rr.com

Paul VanderEike was born in Wisconsin in 1871. He moved to Bakersfield in 1911 to teach science at Kern County Union High School (now Bakersfield High School). In 1913 he was appointed the first dean of the Community College (now Bakersfield High School), located on the KCUHS campus.

VanderEike continued as Science Department chair and in various administrative positions until retiring in 1950. At that time, he was Assistant Superintendent of Kern County Union High School District.

By 1935, Mr. VanderEike had generated enough interest in recreational rockhounding to be a founder, along with T. A. Little of Shafter, of the **Kern County Mineral Society**. The following year he participated in the founding of the **California Federation of Mineralogical Societies**, hosting their first convention in Bakersfield in January of 1937. Until his retirement, Mr. VanderEike was intimately involved in the activities of the growing Federation, overseeing publication of the Federation's newsletter, "Mineral Notes and News". This presentation will illustrate the growth and development of the Federation and its newsletter.

Freshwater turtles in the Mojave Desert: what could go wrong?

Kristy Cummings,¹ Jeffrey E. Lovich,¹ Shellie R. Puffer,¹ and Sara Greely^{2,3}

¹U. S. Geological Survey, Southwest Biological Science Center, 2255 North Gemini Dr., Flagstaff, AZ 86001, USA, kcummings@usgs.gov; ²The Living Desert Zoo, 47900 Portola Avenue, Palm Desert, CA 92260, USA; ³Current address: 37872 Huddersfield St., Indio, CA 92203, USA.

The southwestern pond turtle (*Actinemys pallida*) has occupied the Mojave Desert in California since the Miocene. *A. pallida* is mostly aquatic, except for basking, egg laying, and occasional terrestrial movements and over-wintering. Using terrestrial habitat exposes aquatic turtles to increased risk of injury or mortality from predation and other environmental hazards (e.g., human activities like road injuries). We collected injury data from turtles at three study sites along the Mojave River (one site in the upper river and two sites each in the lower river) in San Bernardino County, California between May 1998–October 1999 and again from April 2016–September 2019.

Turtles were visually examined for shell or body damage. A total of 84 *A. pallida* were captured between all sites and all years. Sixty-eight percent (n=26) of captured turtles at the two lower Mojave sites combined had shell damage and 78 percent (n=36) of turtles captured at the upper Mojave river site alone also displayed shell damage. A total of 74 percent (n = 62) turtles had shell damage at all sites combined. Evidence of shell disease was not observed. There was no statistical significance in the proportion of injured and non-injured turtles between the sexes for either the two lower river sites combined or the upper river site. Mean carapace length was not significantly different between injured and non-injured turtles for these same sites. Injuries occurred in the majority of captured turtles at all sites and may be an indicator of the extent of threats facing these turtles but is a poor indicator of predator pressure.

New surficial geologic mapping of Leuhman Ridge and the surrounding area, northeastern Edwards Air Force Base, Kern and San Bernardino Counties, California in support of Quaternary fault and hydrologic evaluations

Andrew J. Cyr and David M. Miller
*Geology, Minerals, Energy, and Geophysics Science Center,
 U.S. Geological Survey, Moffett Field, California*

Communities and military installations in the arid Mojave Desert depend on groundwater for their water supplies. Faults can alter groundwater flow paths, creating either conduits or impediments to flow, by affecting the physical properties of the geologic materials they cut. As part of a larger USGS effort to study controls on groundwater movement in the northeast part of Edwards Air Force Base (EAFB) in the western Mojave Desert, we produced a new, detailed (1:18,000 scale) geologic map of surficial deposits and bedrock to refine the locations and characteristics of the previously mapped Spring and Leuhman faults.

The northeast part of EAFB is located in the northern Antelope Valley, a generally low relief, internally drained basin between the Transverse Ranges to the south and the Tehachapi and southern Sierra Nevada to the north. The topography in the area is dominated by the northeast-trending, linear Leuhman Ridge. The western piedmont of Leuhman Ridge slopes down to the west towards Rogers Dry Lake bed and the larger valley that was previously occupied by paleo Lake Thompson; both of these provide a source of sand and finer grained sediments that comprise common eolian and eolian-affected alluvial deposits within the mapping area. The eastern piedmont of Leuhman Ridge slopes down to the northeast into an alluvial valley between Leuhman Ridge and an adjacent pediment on the west and south, and the Kramer Hills on the north.

The Spring and Leuhman faults are located in this eastern and central part of the map area. These two faults are part of the little-studied Mojave strike-slip province,

a region of Pleistocene and older (>12 ka) deformation between the Garlock and San Andreas Fault Systems to the west and the younger strike-slip and transpressional faults of the Eastern California Shear Zone (ECSZ) in the central and eastern Mojave Desert. Previous mapping shows that the Spring fault juxtaposes Cretaceous granite against Quaternary alluvial deposits along the southwestern side of the Kramer Hills. The subparallel Leuhman fault, between ~0.5 and 2 km to the southwest, is mapped as inferred beneath Quaternary alluvial and eolian deposits. This previous work has moderately constrained the location of the Spring fault. The age of both faults is poorly constrained to <1.6 Ma.

Our new mapping confirms that the previously mapped Spring fault is a Quaternary-active right-lateral fault. Our observations demonstrate that displacement on it has cut latest Pleistocene to early Holocene alluvial fan deposits along the southwest side of the Kramer Hills and that, based on poorly constrained offset of Cretaceous granodiorite, it could have as much as 1.7 to 2.2 km minimum of total offset. We did not find any convincing evidence to support the existence of the sub-parallel Leuhman fault within the map area. However, we identified four additional probable faults, indicated by a combination of geomorphic lineaments and brecciated rock, which were previously unmapped. Pleistocene and Holocene eolian deposits are widespread, including sand sheets, dunes, and admixtures into alluvial fan deposits. New luminescence geochronology indicates these were deposited between 8.32 ± 0.71 and 38.9 ± 2.9 ka. In general, our field observations indicate that Quaternary alluvial fan and eolian deposits are thin. Monitoring-well data show groundwater levels consistent with flow beneath the Quaternary deposits within Cretaceous units. The presence of Pleistocene-aged groundwater discharge deposits adjacent to, and cut by, the Spring fault indicates that shallow groundwater flow may have been affected by fault rock properties since at least the Pleistocene. Together, these two observations indicate that secondary bedrock porosity and permeability, defined by degree of weathering, fault-related fracturing, rock fracture density, and the degree to which those fractures are filled by fine-grained material, are the important factors for the location and flow patterns of groundwater.

Finally, the Paleontological Resources Preservation Act final regulations—what changed in the 66 months that passed since the draft rule was published, and why

Chris Dalu
*Bureau of Land Management, 1303 South U.S. Highway 95,
 Needles, CA 92363. cdalu@blm.gov*

In the 2020 *Desert Symposium Field Guide and Proceedings*, I provided information about the 2009 Paleontological Resources Preservation Act (PRPA, or Act), including the historical context and various parties associated with its development, its structural

and procedural relationship to the Archaeological Resources Protection Act (ARPA), comparison of agency implementation and the status of promulgating the regulations. Based on what was known at the time, it was anticipated that the Department of Interior (DOI) would publish the final regulations soon after the 2020 elections and would contain minimal changes to the draft rule published in 2016, so, it seemed a good opportunity to inform through the Symposium. When the final regulations were published in August 2022, it became apparent that there was a need to provide a follow-up to the information presented in 2020.

The focus here is to inform readers of the substantive differences between the 2016 draft rule and the final regulations, provide the impetus that led to the change, and briefly assess the degree to which the PRPA and regulations meet the intent of the seven principles that were introduced in the Secretary of Interior's 2000 report, *Assessment of Fossil Management on Federal and Indian Lands*. The report was a highly collaborative effort among eight consulting agencies and the public, and it is definitely considered the foundational document that led to the PRPA.

The PRPA applies to four bureaus within the DOI as well as the Forest Service, which published their final regulations in May 2015. The final DOI regulations that implement the 2009 PRPA were promulgated on August 2, 2022. This date marks the end of a 66-month rulemaking process, and the end of a 23-year effort that spanned the law's first draft to the final regulations. Throughout each stage of the process, there was an admirable amount of collaboration among various agencies, professional and amateur paleontologists, rockhounds, curation and repository professionals, and members of the public. The DOI issued its draft rule in 2016, and during the two-month comment period, received 1,611 comments, of which sixty percent (60 %) were related to casual collecting, twelve percent (12 %) associated with permitting, eight percent (8%) on management, five percent (5%) on curation, and fifteen percent (15%) spread out among various other aspects of the Act. Incorporating DOIs final rule into the Code of Federal Regulations resulted in the following:

- created a new part (Part 49) in Title 43 – 43 CFR 49 – Paleontological Resources Preservation.
- revised the authority citation in Title 43, Part 8360 – Visitor Services, and amended §8365.1-5 – Property and Resources by revising paragraph (b), which authorizes casual collecting of common invertebrates on all BLM land unless prohibited by another authority and posted.
- revised the authority citation in Title 50, Part 27 – Prohibited Acts, and amended §27.63 by adding paragraph (c), which specifies the requirement of a permit to collect paleontological resources from national wildlife refuges.

For reference, a listing of substantive changes to the final rule is provided at the end of this abstract. The changes made by DOI to the final rule were both substantive and non-substantive. The non-substantive changes included minor stylistic, formatting and structural adjustments to improve readability and clarity. The primary impetus for substantive changes included responding to public comments and concerns on matters of clarity and policy, as well as additional review by the bureaus. Key objectives that guided the revisions to the draft rule included clarification, flexibility, balance, recognition and discretion, within the required framework of compliance. In cases when a draft rule was considered by the public to be overly rigid or represented a one-size-fits-all approach, adjustments were made to increase flexibility and provide a better balance between enumerated criteria and discretion. For example, in response to comments regarding the role of repositories in the permitting process, the final regulation maximized the flexibility for repositories, permittees, and the bureaus by separating the repository approval process from the permitting decision process and allowing the development of project-specific and collection-specific approaches. When the public expressed concerns that land managers had too much discretion and a lack of expertise over a matter, the final rule required the land manager to consult with experts as part of the process in formulating their decisions. As an example, the public expressed concerns that land managers lacked the expertise to determine what non-vertebrates are rare, and the final regulation included the requirement for the land manager to consult with knowledgeable paleontologists in making the determination.

In response to many comments that suggested less stringent qualification requirements to acquire a permit should be considered, the bureaus acknowledged that many amateurs and avocational paleontologist possess a deep knowledge of resources and so removed the requirement of an advanced degree, while also clarifying that a number of factors would be taken into account, in relation to the complexity of the project. The final regulations also included a provision to allow individuals who do not meet baseline requirements to work under an issued permit when supervised by a permittee. Beyond being responsive to public comments, there is another overarching reason for the bureau's flexibility, which is to increase public involvement in paleontological fieldwork performed under partnerships or with the assistance of volunteers.

Public comments also brought to the attention of bureaus, cases when the regulations limited an activity, but no such limitation was included in the Act. For instance, the draft rule disallowed casual collection (as defined in PRPA) within National Monuments and National Conservation Areas, but in response to comments from the public that pointed out PRPA did not identify these limitations, the final regulation did not

include National Monuments and Conservation Areas in the listing of areas where casual collection could not occur.

While some changes in the final regulations were limited to one specific topic or comment, there are cases in which provisions were made that addressed numerous comments and concerns. Such is the case with the final regulations including a provision that would allow a person to return fossils collected or obtained in violation of the Act and regulations without penalty if the Federal land manager deems it appropriate. This provision addressed a direct comment making that specific request, a comment that was concerned that a child who picks up a fossil could be in violation, and several comments of concern that bureaus could criminally penalize adults who accidentally violate the regulations.

As previously noted, 60% of the comments to the 2016 draft rule were related to casual collecting. The PRPA made substantive changes in the overall policies of the BLM, BOR and USFS as it relates to casual collecting. Prior to the PRPA, casual collecting was not formally authorized on these public lands and was always subject to discretion of the land manager. Beyond this, there were many cases when land managers considered casual collection in a manner that equated it with casual use, which is not defined consistently throughout federal regulations. The PRPA, through congressional intent, formally authorized casual collecting on BLM, BOR and USFS managed lands, and further clarified a “casual collecting exception” under Sec. 6304 - Permit Requirements, stating casual collecting is authorized without a permit on public lands managed by the BLM, BOR and USFS, as long as collection is consistent with the laws governing the management of those lands. The PRPA definition of “casual collecting” is vague, as it states:

Casual collecting means the collecting without a permit of a reasonable amount of common invertebrate or plant paleontological resources for non-commercial personal use, either by surface collection or the use of non-powered hand tools, resulting in only negligible disturbance to the Earth’s surface or paleontological or other resources. As used in this paragraph, the terms “reasonable amount”, “common invertebrate and plant paleontological resources” and “negligible disturbance” shall be determined by the Secretary.

Prior to PRPA, and usually applied to the collection of rocks and gemstones, the BLM defined casual collection similar to the above, but replaced “reasonable amount” with 25 pounds or less/day/person. The problem with this definition is that negligible disturbance is an extremely relative term in the desert because sediments and rock can easily be backfilled, and natural wind or rain could make it appear as if very little disturbance occurred. Another concern with this definition is that in many cases, a

person collecting rocks, minerals, and invertebrate fossils may not have the ability to identify when they are actually disturbing an archaeological site, a rare and endangered plant, or a Mojave Fringe Toed lizard resting in the sands just below the surface.

The 2016 DOI draft rule seems to have recognized this concern, because it specified the following definitions associated with casual:

1. Reasonable amount is defined as 25 pounds/day/person, with up to 100 pounds per year.
2. Negligible disturbance is defined as little or no change to the surface of the land, surface disturbance cannot exceed one square yard per individual collector. For multiple collectors, each square yard of disturbance must be separated by no less than 10 feet. All areas of disturbance must be backfilled, so the disturbance is unnoticeable.
3. Common invertebrate or plant fossil – the draft rule clarified that a collector should be sure that the invertebrate or plant fossil is common, and in the absence of being sure, should not collect it.

The combination of these three clarifications of definitions made for a reasonable policy in which all public land is open for casual collecting unless otherwise closed and posted in accordance with law. However, the final regulations removed all of these specifications, with the exception of the 25 pounds/day/person (with no annual limit). While it is understood that one aim of the final regulations is to avoid penalizing casual collecting and avoid unreasonable constraints, it’s not serving anyone’s purpose in the event that casual collecting would inadvertently be impacting resources that a casual collector would not recognize.

The Secretary of Interior’s 2000 report, *Assessment of Fossil Management on Federal and Indian Lands* is considered a foundation document to PRPA, because the PRPA was drafted shortly after the report was released, and many of the basic premises within the PRPA, are clearly derived from that report. This includes acknowledging the contributions of amateurs (Principal #7), recognizing fossils as a part of American heritage (Principal #1), realizing rarity of vertebrate fossils and the importance of professional involvement (Principal #2), acknowledging differences between common and uncommon invertebrates and plant fossils (Principal #3), ongoing public education (Principal #6, #7), the importance of a consistent permitting system (Principal #6), curation that ensures collections are available for research and education (Principal #6), and increasing penalties for theft (Principal #4).

Principal #5 is the one principal that is currently not met by the PRPA, and unfortunately, the same was true when they wrote the report. Principal #5 is associated with the development of a strong, adequately staffed and funded paleontological program, and working proactively to conduct new surveys to provide a clear understanding

of resources on Federal land. It is only with such an understanding that paleontological resources can be effectively managed and a stewardship program can be supported. Most staff at BLM offices have few records available to inform them about existing fossil localities. The BLM has taken to relying heavily on PFYC (potential fossil yield classification) models that have mostly been generated based on rock units, with little or no locality data.

Funding, staffing, proactive surveying, and geospatial databases with locality information are necessities. There is a desire to get the public more involved, yet in cases when the public identifies significant resources, there is a lack of funding to adequately address them. The greatest challenge to the success of the PRPA is funding it in a manner that increases our understanding of resources under our jurisdiction.

Title 43: Description of changes

Subpart A: Changed heading from “Managing, Protecting, and Preserving Paleontological Resources” to “Preserving, Managing, and Protecting Paleontological Resources.”

- § 49.1: Replaced “fossils” with “paleontological resources” here and throughout the final rule to clarify that the rule applies to paleontological resources, which are a subset of fossils.
- § 49.5: Replaced the term “authorized officer” with “Federal land manager” for clarification and consistency with other laws and regulations.
- § 49.5: Replaced the term “curatorial services” with “curation.” DOI reverted to the language used by USDA at 36 CFR 291.5 in order to remain consistent with the Forest Service, existing DOI policy at 411 DM, and with the Act. Previous versions, including the proposed rule, stated the same information, but DOI found that the USDA version of the definition provided the clearest definition of curation.
- § 49.5: Clarified definitions of “collection,” “consumptive analysis,” “day,” “fossilized,” and “nature.”
- § 49.5: Added definitions of “deposit,” “preparation,” and “working collection.”
- § 49.15: Added language to clarify that on lands administered by BLM or Reclamation, certain fossilized mineral materials, including petrified wood, and conodonts (microscopic remains of a Paleozoic-era eel-like animal) are not subject to these regulations.
- § 49.25: Streamlined and simplified the process of determining when specific locality information may be disclosed by eliminating the requirement for the Federal land manager to enter into written agreements with each party seeking disclosure, authorizing the Federal land manager to define bureau confidentiality requirements consistent with the regulation; and clarifying that the disclosure of information in furtherance of the Act does not constitute an official public disclosure under the Freedom of Information Act.
- Subpart B:** Corrected section-numbering sequence throughout this subpart. In the proposed rule, these sections were numbered §§ 49.50 through 49.95. In the final, they are numbered §§ 49.100 through 49.145. Subsequent citations in this table refer to the corrected numbers.
- § 49.100: Clarified that a permit may be required for paleontological research or consulting activities and eliminated the requirement for a permit for disturbance because the term “disturbance” was unclear in this context.

- § 49.105(b): Clarified that a person not meeting the criteria to receive a permit can perform work under an issued permit when appropriately supervised by a permittee.
- § 49.110: Eliminated the requirement contained in the proposed regulation that would have required permit applicants to possess a graduate degree.
- § 49.115: Simplified permit application requirements by using concise language, and by not requiring that permit applicants include written verification of collection acceptance from a repository in their permit applications. The verification from the repository is a condition of permit approval, not the permit application.
- § 49.120: Removed the repository approval process from the permit approval process, in order to speed up and simplify the permit decision. Under the final regulation, repository approval may happen at any time.
- § 49.125(a)(1): Clarified that both permittees and approved repositories named in the permit are subject to the Act and regulations’ confidentiality requirements, and that they may disclose information if the Federal land manager determines that the disclosure is consistent with applicable bureau policy.
- § 49.125(a)(2) : Removed a permittee reporting requirement regarding persons conducting activities under a permit (proposed § 49.75(a)(2)) and replaced it with the requirement to maintain a safe and secure worksite.
- § 49.125(a)(8): Added requirement for permittees to safeguard collections and related data until the collection is deposited in the approved repository named in the permit.
- § 49.125(a)(10): Clarified that a permittee cannot also act as the repository official who signs the receipt for collections.
- § 49.125(a)(11): Added requirement that copy of the permit and other associated records must accompany the collection during transport and be provided to the approved repository named in the permit.
- § 49.125(a)(13): Clarified that permittees are responsible for the costs of the permitted activity, including initial curation costs. Proposed rule stated that permittees are responsible for all curation costs.
- § 49.125(e): Added permit modification, suspension, and revocation to the possible consequences of permittee non-compliance with the terms of a permit.
- § 49.130: Added a provision that bureaus may modify permits when there is a potential violation of a term or condition.
- § 49.140: Clarified the permit-related decisions by NPS may be reconsidered, rather than appealed, to be consistent with other NPS permitting practices.
- § 49.200(a): Clarified that, under this regulation, repositories are approved to receive a collection, not generally approved for everything.
- § 49.200(c): Added authorization for Federal land managers to move paleontological resource collections that do not further paleontological knowledge, public education, or management of paleontological resources into working collections.
- § 49.205: Deleted the language requiring repository approval during the permit approval process, in order to provide more flexibility and speed up permit decisions. Also, simplified the requirements for approval of a proposed repository. Also, amended the process for Federal land managers to follow in the event of a repository’s lack of compliance with the approval criteria.
- § 49.210: Eliminated entire section that was in the proposed rule regarding the process for depositing a collection at an approved repository because of public comment and because it was redundant with § 49.125(a)(10). This section now addresses terms and conditions of agreements between the bureaus and repositories, which were formerly addressed by § 49.215.
- § 49.210(b)(5): Now clarifies that determinations related to disclosure of specific locality information pursuant to § 49.25 are made by the Federal land manager.

- § 49.210(b)(7): Now clarifies that agreements between bureaus and approved repositories must address loans to other entities.
- § 49.210(b)(10): Now contains detail about the provision of publications or reports to the bureaus.
- § 49.210(b)(12): Added affirmative requirement that repository employees must work to preserve and protect specimens in their care using best professional practices.
- § 49.215: With the elimination of one of the sections from the proposed rule (§ 49.210), the bureaus were able to move all subsequent sections up in this final rule. Thus, this section was, in the proposed rule, § 49.220.
- § 49.215(a): Streamlined this language from the proposed rule to make it shorter, simpler, and less redundant with the definitions section.
- § 49.215(b): Included language to clarify that the Federal land manager may remove specimens from museum collections and assign them to working collections. This will reduce burdens on repositories
- § 49.215(c): Added clarifying language regarding the fees that repositories may charge to recover their costs.
- § 49.300(b): Added option for a person to return paleontological resources that were collected or obtained in violation of the Act without penalty to the Federal land manager if deemed appropriate by the Federal land manager
- § 49.400: Streamlined the language regarding the effective date of this criminal penalties subpart and added minor clarifying edits to enhance wording consistency between this section and subpart G.
- § 49.500–49.535: Minor clarifying edits such as reorganization of a sentence, making headings lower-case, elimination of redundant clauses and sentences, and simplification of language.
- § 49.540: Added new paragraphs (c) and (d) for improved consistency between this subpart’s hearing provisions and existing DOI regulations pertaining to hearings.
- § 49.575(a): Added “prepare” and “curate” to the list of actions that can be funded by collected civil penalties. These are subsets of the terms “protect,” “restore,” and “repair.” These latter terms appeared in the proposed regulation and appear in the Act, but the final regulation includes “prepare” and “curate” as well, for the sake of clarity.
- Subpart G:** Throughout this subpart, added language to clarify that this subpart defines scientific value, commercial value, and the cost of response, restoration and repair only for determining civil and criminal penalties, not for any other purpose.
- § 49.600: Clarifies that scientific value is determined for the calculation of criminal and civil penalties, and clarifies the various components for determining this value.
- § 49.605: Clarifies that commercial value is determined for the calculation of criminal and civil penalties, and clarifies the various components for determining this value.
- § 49.610: Clarifies that cost of response, restoration, and repair is determined for the calculation of criminal and civil penalties, and clarifies the various components for determining this value. Adds preparation and stabilization to the calculation of this cost.
- § 49.700: Removes the reference to “stolen Federal property” because it is unnecessary for purposes of this section.
- § 49.805(a): Removed list of specific types of BLM-administered lands, such as national monuments, national conservation areas, outstanding natural areas, or forest reserves that BLM had proposed for closure to casual collection by regulation. All BLM- managed public lands are open to casual collection unless specifically closed by statute or through the process at § 49.40 of these regulations.
- § 49.810(a)(1): Added “non-vertebrate paleontological resources” as a shorthand for “invertebrate or plant paleontological resources” for simplicity and streamlining.

- § 49.810(a)(2): Removed limitation that a person may collect only 100 pounds of common plant and invertebrate paleontological resources per year. Also allows collectors to remove a slab or cobble of rock that exceeds 25 pounds in order to preserve the integrity of an embedded specimen.
- § 49.810(a)(3): Removed the language that was in the proposed rule regarding the size of and distance between disturbed areas as a component of the definition of negligible disturbance.
- § 49.810(a)(5): Removed reference to the size of hand tools to be more consistent with the Act, which focused on the non-powered aspect of the hand tools rather than their size.
- § 49.810(c): Established that Federal land managers will consult with knowledgeable paleontologists to determine which plant and in-vertebrate paleontological resources are not common

Tephrochronology of the Miocene Barstow Formation, western Mojave, CA

Ryan Eden, Phil Gans, and John Cottle
Dept. of Earth Science, UC Santa Barbara

Records of Miocene volcanism, sedimentation, and deformation are preserved in widely scattered exposures across the Mojave province of southeastern CA. The middle Miocene Barstow Formation (BF) in the Mud Hills north of Barstow, CA, is a notable example with its ~1 km-thick fluvio-lacustrine section of sandstone, mudstones, minor carbonate and conglomerate and intercalated tephra horizons. The BF was mapped and described in some detail by Dibblee (1967) and has been interpreted to represent late-stage infilling of an extensional basin, subsequently associated with detachment faulting of the Central Mojave Core Complex (e.g., Fillmore and Walker, 1996; Ingersoll et al., 1996). It is best known for its rich vertebrate fossil record—the type Barstovian Land Mammal assemblages—whose ages were partially calibrated by ⁴⁰Ar/³⁹Ar and U-Pb geochronology (McFadden et al, 1990; Woodburne et al, 1990; Miller et al; 2022). Despite extensive previous work on the BF, its full depositional history, stratigraphic architecture, and the paleogeographic/tectonic setting of the basin in which it accumulated remain incompletely understood. Abrupt lateral facies changes within known BF exposures and conflicting ages from previously correlated sections, combined with extensive deformational overprinting by dextral strike-slip faults, normal faults, and folds have all hindered the development of a comprehensive geologic model for the BF. Recent discovery of highly elevated lithium concentrations in claystone horizons of the BF (Benson, this volume) motivate a renewed focus on this important succession of rocks.

We have embarked on a comprehensive detailed geologic mapping, structural analysis, and radiometric dating campaign to better reconstruct the original architecture and evolution of the Barstow basin. Our approach is to subdivide and carefully map as many different lithostratigraphic members within the formation as possible, and to use the abundant tephra horizons to delineate chronostratigraphic markers throughout the BF. Tephra samples collected from different stratigraphic

levels and from exposures that span the entire width of the Mud Hills are being dated by U-Pb geochronology on zircon using the LA-ICPMS facility at UCSB. Water laid tuffs such as occur in the BF are notorious for having variable amounts of older xenocrystic contamination introduced by winds or streams and subsequently mixed with the juvenile material. Our dating approach has the advantage of allowing us to quickly and precisely date a large number of zircons (50–100) from each sample and confidently identify the youngest concordant population of zircons, thus providing a reliable (maximum) age for each tephra. Integration of this geochronologic work with careful petrographic studies of the tephra, CL imaging and careful selection of zircons to be dated helps assess the degree of sedimentary reworking and allows us to focus our U-Pb analyses on the population of small euhedral prismatic zircons that are most likely to represent the juvenile population. We find that primary fallout tephra—evidenced by preservation of delicate glass shards (or the zeolitized outlines of same) and minimal internal stratification—contain only a small percentage of older xenocrystic zircons and consistently yield a dominant population of concordant young zircons whose weighted mean age provides a reliable estimate of the eruptive/depositional age. Reworked tephra, evidenced by significant rounding of juvenile glass fragments, a high percentage of accidental detritus, and internal stratification and laminations, often yield multiple age populations of Miocene and Mesozoic basement zircons, but can still yield a reliable depositional (or maximum) age from the youngest population of concordant zircons—an age that can be tested based on its local stratigraphic position.

We present new U-Pb zircon ages from preliminary work on tephra within the BF in the Rainbow Basin section. A tephra > 150 m below the Skyline Tuff yields an age of 15.6 ± 0.1 Ma ($n=9$) and may correlate with the previously dated Oreodont Tuff (15.8 ± 0.2 Ma; McFadden et al, 1990). The Skyline Tuff has always been a problematic unit to date. This prominent 1–2 m thick marker bed consists of a lower, very fine-grained “porcelain” ash layer virtually devoid of crystals, and an upper interval of sandy mudflows and laminated sandstone consisting mainly of reworked older volcanic and basement detritus. The eruption that produced this deposit was apparently nearly aphyric, but we were able to identify a (sparse) juvenile zircon population yielding a weighted mean age of 14.75 ± 0.15 Ma ($n=6$). The Dated Tuff is only 15 m above the Skyline Tuff and yielded a straightforward age of 14.7 ± 0.1 Ma ($n=38$), in excellent agreement with the previously reported age of 14.7 ± 0.8 reported by McFadden et al (1990). Two thin tephra separated by 8 m of section in the core of the Barstow syncline adjacent to the Rainbow Basin loop road are ~ 50 m above the Skyline Tuff and yielded ages of 14.4 ± 0.1 Ma ($n=4$) and 14.3 ± 0.1 Ma ($n=30$), in correct stratigraphic order. We anticipate having many more ages to present at

the symposium in April, but these preliminary results are highly encouraging.

Geologic framework of the Rio Tinto boron deposit, Mojave Desert, California

Phillip B. Gans

University of California, Santa Barbara

The Rio Tinto borax mine near Boron, CA in the northwestern Mojave Desert supplies most of the United States’ boron. Despite its economic importance, questions remain regarding its origin, including: (1) What was the ultimate source of boron and the character of the mineralizing hydrothermal system? and (2) What were the structural, stratigraphic, and/or magmatic conditions that resulted in this exceptionally large concentration of nearly pure borates? New geologic mapping of bedrock exposures surrounding the mine and examination of selected drill cores and surface exposures within the Kramer Pit, in concert with previously published $^{40}\text{Ar}/^{39}\text{Ar}$ whole rock ages and new U-Pb zircon ages from lava and tephra horizons within the host Miocene sections, shed important new light on the stratigraphic and structural framework of the deposit and offer new insights into the origins of borate mineralization.

The Miocene stratigraphy near Boron, previously assigned to the Tropico Group by Dibblee (1967), consistently dips southward in the vicinity of the mine and is up to 1 km thick but displays abrupt lateral lithologic and thickness variations. A composite section pieced together from surface and subsurface exposures includes, in ascending order, the following chrono/lithostratigraphic units. Note that ages on the mafic rocks previously reported by Gans (2022) have been adjusted upward 1.3% in accord with the revised age for the Fish Canyon Tuff flux monitor.

- (a) Discontinuous lenses of arkose derived from underlying basement (0–30 m).
- (b) An interval of white (tuffaceous) volcanoclastic sediments, plutonic sandstone, limestone, and thin pyroclastic flows, one of which is 21.3 ± 0.4 Ma (0–100 m).
- (d) Several lavas of 20.8 ± 0.3 Ma coarse-grained (diabasic) plagioclase-olivine-clinopyroxene basalt lavas, including the “type” Saddleback Basalt (Tsb) at Saddleback Mountain (0–50 m).
- (d) Plutonic sandstone and conglomerate above Tsb that thickens southward to > 300 m. U-Pb zircon ages on tephra at its base and top are 20.6 ± 0.1 and 20.1 ± 0.1 Ma, respectively.
- (e) The 19.7 to 20.0 (± 0.2) Ma Stonehouse Olivine Andesite (Tsoa)—a group of extensive trachytic andesite lavas with olivine microphenocrysts that emanated from cinder cones north of the mine and flowed southward, forming a persistent E-W band up to 300 m thick.

- (f) Mixed sandstone, siltstone, and minor claystone up to 100 m thick that lie above Tsoa.
- (g) The 19.5 ± 0.2 Ma Boron Basaltic Andesite (Tbba)—plag-olv phyric lavas and compositionally identical sills that are only exposed in the Kramer Pit, where they directly underlie the main ore horizons and are up to 50 m thick.
- (h) The “Kramer beds” of green lacustrine claystone and siltstone, up to 100 m thick, that host the main borate ore horizon. Mineralization is zoned inward from a lower and upper barren zone into colemanite-, ulexite-, and borax-dominated intervals. Ash layers at the base and top of the mineralized section have yielded ages of 19.5 ± 0.1 and 19.1 ± 0.04 Ma.
- (i) A thick section of tan arkosic sandstone and pebble conglomerate (up to 350 m thick) conformably overlies the lacustrine beds, and includes a 19.1 ± 0.2 Ma ash bed at its base.

Thus, this exceptionally well-dated section spans ~ 2.5 Ma of early Miocene history and records both lacustrine and alluvial/fluvial sedimentation as well as three distinct episodes of local mafic volcanic activity. Importantly, units (d) through (i) all thicken dramatically toward the south from the hills north of the mine, where Tsoa locally rests directly on Mesozoic basement, toward the Kramer Pit, where the section is > 1 km thick and only the arkose was originally exposed at the surface. On the southern wall of the mine, all units are faulted against Mesozoic plutonic rocks along the E-W striking, N-dipping West Boron Fault. The simplest interpretation is that the Miocene section in the Boron mine accumulated in an extensional half graben in the hanging wall of the West Boron Fault—a fault that was apparently active from ~20.5 to ≤ 19.0 Ma. Lacustrine facies sedimentation and borate mineralization were both localized in the deepest part of this basin close to the bounding fault and are tightly bracketed between 19.5 and 19.1 Ma.

The existing paradigm for borate mineralization at the Boron mine is that boron- and Na-rich hydrothermal fluids were emanating from sub-lacustrine hot springs and precipitating as pure borates on a shallow lake bottom, possibly enhanced by periodic evaporative processes (e.g. Barnard and Kistler, 1965). Problems with this interpretation include the lack of any identified hot spring vents or borate tufa mounds, the lack of other expected precipitate or evaporite minerals, and the abundance of clear replacement textures—e.g. clusters, veins, and isolated pockets of borate minerals that replace thinly laminated mudstones. Indeed, the overall character of the borates with concentrically zoned mineralogy, metasomatic fronts, and well preserved delicate internal host rock stratification are all reminiscent of stratiform replacement deposits. It is also noteworthy that borate mineralization is closely associated (both spatially and temporally) with the emplacement of Tbba sills into the wet lake claystones directly beneath the borate ores.

I speculate that borate mineralization was driven by hydrothermal activity caused by these intrusions, and that boron leached from deeper levels was deposited into overlying sediments during early diagenesis of the claystones primarily by replacement processes.

Wetland dynamics at the Salton Sea

Krishangi Groover¹ and Alexandra Lutz²

¹University of Nevada Reno; ²Desert Research Institute

Declining water levels in the Salton Sea of southern California have resulted in the formation of unmanaged wetlands maintained by agricultural drains along the freshly exposed playa. Nutrient-rich agricultural runoff has caused explosive growth in many of these wetlands, which has resulted in the colonization of many endangered species such as Yuma Ridgway's rail and desert pupfish. Federal- and state-managed wetland habitat on nearby wildlife refuges, using relatively clean Colorado River water, maintains habitat productivity by controlled burning or through mowing. Wetland burning, in particular, appears to result in an increase in vegetation density and strength during wetland recovery. Colorado River water has low levels of dissolved selenium, which evaporatively concentrates and can be present at high concentrations in agricultural drains. Selenium bioaccumulates in wildlife and is known to cause teratogenesis and mortalities in avian species, a phenomenon that has been historically observed in piscivorous birds at the Salton Sea. Drought and additional water diversions from the Colorado River to maintain water levels in Lake Mead have increased focus on the sources of water used for wetland habitat at the Salton Sea. Colorado River water purchased for use in federally owned habitat is expensive, particularly in comparison to agricultural drain water which would be available for low to no cost. In this study, we will be examining the impact of wetland burning on selenium geochemistry in selected cattail wetlands. Remote sensing applications will be used to enhance observations of wetland recovery, and examine potential interferences caused by local geology.

The cosmogenic origin of boron

Ted A. Hadley

Swarf Systems, 907 Anaconda Way, Sunnyvale, CA 94087,
theadley01@yahoo.com

Much research has been performed on the geologic origin of secondary borate deposits in Death Valley. Although many of the publications and presentations adequately describe the geologic processes which concentrate the borate minerals into mineable deposits, none address the problem of where the boron came from and how it found its way into the desert terrains. Here the author introduces the phenomenon of cosmic ray spallation. Very high energy cosmic rays (>1GeV) collide with the nuclei of elements and cause fragments to break off (“spall”).

Occasionally, the result of one or more of these collisions results in a boron nucleus. The boron atom reacts with oxygen in the environment, forming boric acid anhydride, BO_3 ,³ which is soluble in water and finds its way to the oceans, which act as a reservoir for the boron. The boron-enriched seawater is dragged into the lithosphere at subduction zones and incorporated into igneous rocks being formed. The boron ends up as substitutions in the structures of silicate minerals and as primary borate minerals (those which have BO_3 in their structure), the most common silicate mineral being tourmaline. Weathering releases the boron that may accumulate in the playas of closed basins in arid environments. Further oxidation of the boron creates the many different borate salts seen in secondary borate minerals such as the ores colemanite, kernite, ulexite, etc. Lithium and beryllium are shown to be created by the same process, occur in the same types of rocks, and accumulate in playas in a similar manner.

The ecological impacts of solar energy development in the southwestern U.S.

Claire Karban,¹ Jeffrey E. Lovich,¹ Seth M. Munson,¹ Josh R. Ennen,² Steven M. Grodsky³

¹U.S. Geological Survey, Southwest Biological Science Center; ²Renewable Energy Wildlife Institute; ³U.S. Geological Survey, New York Cooperative Fish and Wildlife Research Unit, Department of Natural Resources and the Environment, Cornell University, Ithaca, NY 14853

To meet renewable energy targets, solar energy development is expanding rapidly throughout the United States. In 2023, the U.S. plans to add nearly 30 gigawatts of utility-scale solar energy capacity—the most of any year to date. Although solar energy can reduce carbon emissions relative to more traditional forms of energy, it has an intensive land use, requiring approximately 1.8 times as much land as surface-mined coal, and 15.8 times as much land as natural gas, for the same energy-generating capacity. Much of the solar energy capacity is being developed in the southwestern U.S., where there is large solar irradiance across the Mojave, Sonoran, and Chihuahuan deserts and the Colorado Plateau. However, these deserts are sensitive to land use disturbance, and the environmental consequences associated with solar energy land conversion are predominantly unknown or only beginning to be understood.

To fill this knowledge gap, we present a novel framework for predicting the impacts of solar energy development to plants and wildlife by linking disturbance types associated with solar facility construction and operation to the morphological, physiological, life history, and behavioral traits of species and guilds. In the absence of empirical research on the impacts of solar development on the many organisms affected, this framework provides new insights to fill the current gap in our understanding of the impacts of rapidly expanding solar energy

development and contributes a predictive framework for evaluating impacts to species and guilds.

Anthropogenic impacts on Bonanza Spring: Clipper Mountains, Mojave Desert

Miles Kenney PhD PG

Kenney GeoScience, miles.kenney@yahoo.com

Bonanza Spring is a gravity-fault spring at the geomorphic base of the southwestern Clipper Mountains, California at an elevation of 2100 feet, and is considered to exhibit the highest spring flow rate (~10 gallons per minute) of any spring in the southeastern California Mojave Desert. An erosional pediment surface cut into Miocene bedrock occurs at the surface or under only 1 to possibly 3 feet of alluvium south of Bonanza Spring downslope for approximately 2 miles. Spring waters flow perched on this bedrock pediment surface, which exhibits very low permeability due to near-surface secondary carbonate fracture/joint infilling. Groundwater is also believed to flow below the surface pediment surface as “perched” flow. Surface flow commonly extends southward at least ~0.5 mile, but during wet periods can reach 0.7 mile. Saturated thin alluvial sediments commonly extend approximately 1 mile south of Bonanza Spring where waters likely “sink” to greater depths when encountering southward dipping porous Miocene volcanic and sedimentary rocks and thickening Holocene fluvial deposits.

The Clipper Mountains exhibit a weak domal shape likely resulting from the development of an approximately southwest–northeast trending anticline. Northward dipping Miocene volcanic rocks overlying Pre-Cambrian and Jurassic age bedrock occur in the north and northeast portion of the range, and southwest to south dipping Miocene interbedded volcanic and sedimentary rocks occur in the pediment surface region immediately south and southwest of Bonanza Spring. In the western Clipper Mountains, a hypabyssal igneous suite that intruded as northwest trending, near vertically “dipping” tabular bodies is referred to as the Western Clipper Mountains igneous intrusive suite (WCMIS). A very similar igneous suite occurs in the Marble Mountains to the west.

The WCMIS experienced rotational block deformation demonstrated by a high density (10s to 100s foot scale spacing) of northwest and southwest striking conjugate fault and joints. Most faults are near vertical and exhibit less than 10 feet of apparent lateral or dip-slip separation. Northeast striking faults commonly exhibit apparent left-lateral separation of the northwest trending members of the WCMIS. Some relatively more major faults occur in the system that likely had 100-ft or more total displacement. These fault zones are over 20 to 50 feet wide and exhibit numerous smaller scales faults and fault gouge of crushed rock and secondary clays. Bonanza Spring occurs at the intersection of two relatively major northwest and northeast striking fault zones. Formational units at the spring are members of

the WCMIS and southward dipping Miocene cobble to boulder fanglomerates.

Bonanza Spring occurs geomorphically at the base of a ~30-acre regionally unusual cusped shaped valley (half-bowl) micro-watershed. The micro-watershed exhibits 500-ft relief (2600' highest—2100' lowest-Bonanza Spring), within which all drainages flow southward to converge at Bonanza Spring. High-rate precipitation events dramatically increase flow rates at and immediately south of Bonanza Spring within upper Bonanza Wash. The southwestern and southeastern boundaries of the cusped valley geomorphically and structurally occur along the northwest- and northeast striking relatively major fault zones that intersect at the Bonanza Spring. This is due to faster erosion rates along the fault zones and within hydro-chemical alteration of rocks north of the bounding faults within the cusped valley. The cusped valley walls exhibit youthful erosional geomorphology that, along with its circular cusped shape, suggest that it may be a head-scarp to a landslide. Mass wasting “rotational” type slides are common in the desert where springs occur. However, no landslide deposits have been identified in the cusped valley.

Bonanza Spring has existed for hundreds of thousands of years. Evidence for this includes abundant secondary mineralization and chemical weathering (colorization-mottling of the rocks, dissolution of plagioclase phenocrysts) within nearly all bedrock in the cusped valley associated with flowing and alternating groundwater levels. Additional evidence includes an abandoned ancient south flowing channel swale southwest of and approximately 15 feet higher than Bonanza Spring. The channel is about 20 to 30 feet wide and exhibits a thick section of travertine.

The geomorphology of the Bonanza Spring, its associated cusped valley, and Bonanza Wash immediately south of the spring have been strongly altered by anthropogenic surface grading, placement of artificial fill, and tunnelling during the 1900s. These activities altered surface runoff rates, increased erosion, and may be the cause for strong surface flow to this day. Most of surface earthwork and tunnelling was conducted around 1915.

An approximately 50-foot long horizontal tunnel located ~500 feet northwest of and 35-feet higher than Bonanza Spring was excavated historically with the likely intention of pooling groundwater within the tunnel to be piped to the Danby railroad station. This tunnel exposes the northwest-striking relatively major fault zone that intersects to the SE at Bonanza Spring. A smaller scale fault that strikes northeast intersects at the location of the tunnel opening, providing supportive evidence that local faults are groundwater barriers. In addition, the moisture content of the rocks in the tunnel across the fault exhibit greater moisture on the cusped side (northeast side of the fault) relative to the SW side.

A second horizontal tunnel (length unknown) occurs approximately 600 feet northeast of Bonanza Spring. Its

purpose is unknown, but it occurs in an area of relatively abundant secondary fracture-filled mineralization that presumably occurred during the Miocene. A third horizontal tunnel at Bonanza Spring extends a minimum of 30 feet north of the spring outlet. This tunnel was identified when the roof collapsed in 2020 and its features are documented in Kenney (2020). At Bonanza Spring and the opening of the tunnel, an approximately 100 ft long southward trending trench was excavated that removed surficial alluvium and extended into bedrock. Evidence for this is the entrenched geomorphology of the spring water flow area (heavily vegetated) and a spoil pile along the western side of the trench composed mostly of bedrock (i.e., Miocene age).

Surficial grading was conducted throughout the lower to mid-elevations of the cusped valley and mostly above Bonanza Spring in the early 1900s. The areal extent of the grading is approximately 4.5 acres and consists of roads and placement of fill. Approximately 2 to possibly 10 feet of fill was placed above and east of the water source tunnel north of Bonanza Spring. A fill pile approximately 15-feet tall creates a small hill in the middle of Bonanza Wash around which the shallow spring surface water flows. The fill, composed of mostly alluvial sediments rather than bedrock, was removed from Bonanza Wash near and south of the spring. This greatly assisted in creating spring water surface flow.

The surficial grading has increased flood runoff rates and has thus increased erosion rates in the cusped valley. The increased erosion rates created or exacerbated the development of a 20- to 30-foot high cliff exposing older alluvium located ~100-feet east of Bonanza Spring and has not allowed for significant deposition in the trench. Immediately south of Bonanza Spring, and along the riparian reach of Bonanza Wash south of the spring, wash deposits may have been removed as a result of the increased erosion. This assists in maintaining a thin layer of alluvium in the wash, and thus allows for surface flow to persist. It is possible that Bonanza Spring surface flow would not continue in modern times if it were not assisted by the tunnel and trench construction at the mouth of the spring, removal of youthful alluvial sediments in Bonanza Wash south of the spring, and increased erosion rates due to grading.

Pleistocene porcupine (*Erethizontidae*) records in arid southwestern North America and comparisons with their modern distribution in southern California and Arizona

Jeffrey E. Lovich¹ and George T. Jefferson²

¹*U.S. Geological Survey, Southwest Biological Science Center, 2255 North Gemini Drive, MS-9394, Flagstaff, AZ 86001. jeffrey_lovich@usgs.gov.* ²*Department of Parks and Recreation, Colorado Desert District, Stout Research Center, Borrego Springs, California 92004. george.jefferson@parks.ca.gov*

The North American porcupine (*Erethizon dorsatum*) is widely distributed throughout most of North America from northern México to the Arctic Ocean, with the notable exception of the southeastern portion of the United States. Within their huge range they occupy an exceptionally diverse array of ecosystems, including some in the arid Desert Southwest region where modern records are generally sparse. They occupied this vast range following the arrival of their ancestors from South America as recently as 2–3 million years ago after the closing of the Isthmus of Panama and the ensuing Great American Biotic Exchange. The paleogeographic range in the Desert Southwest is not unlike the modern distribution of *Erethizon*, with some exceptions. For example, although there are early Pleistocene records of *Erethizon* for southern California, no late Pleistocene records (Rancholabrean NALMA) for *Erethizon* are known for Imperial, Inyo, Riverside, or San Bernardino counties in southern California. This is surprising given modern records of *Erethizon* from southern California. In addition, there are no late Pleistocene records of *Erethizon* for northwestern Sonora, Mexico despite modern records. The lack of any late Pleistocene, Rancholabrean NALMA records of porcupines in the Mojave Desert or the northwestern Sonora Desert region is curious, given scattered modern records in those deserts and the presence of porcupines at this time in Arizona, Nevada, and New Mexico. Pleistocene habitats for porcupines were similar to those occupied today, just at different elevations due to differing climates. Modern preferred habitats in the Desert Southwest include forested high elevation mountains, including pinyon/juniper belts, and occasionally in riparian corridors in desert environments. The overall rarity of porcupines today in arid parts of the Desert Southwest is likely due to the combination of increasing aridity in the region during the Holocene, past persecution by humans, and increasing predator populations.

Phil Swing and the path to Hoover Dam: a river, a canal, an empire

Brian McNeece
bmcneece@gmail.com

During much of 1905–1907, the Colorado River rushed into the Imperial Valley, destroying about 30,000 acres of farmland and creating the modern Salton Sea. In President Teddy Roosevelt's 1907 message to Congress, he promised the residents of the booming Imperial Valley that they would be protected from future floods. But these were empty promises. Young Philip David Swing arrived that year, a young attorney ready to make his name. As the protégé of John Eshleman, Swing would soon help Imperial County separate from San Diego County. In 1911, Swing and Eshleman created the legal foundation for the formation of the Imperial Irrigation District. Swing held the offices of IID legal counsel, district attorney, and judge. In 1919, people of the valley, understanding they

had to fend for themselves, sent Phil Swing to Washington to secure bonds for an “All-American Canal” to get their irrigation system out of Mexico, and for a high dam to protect the valley from flooding in the spring and lack of supply in the winter. Congress balked, but Swing went on to become a 6-term U.S. congressman, representing seven California counties. He was the principal author of the Swing–Johnson Bill, which he submitted four times. When Calvin Coolidge signed the Boulder Canyon Project Act in 1928, the largest public works project in the world began. Boulder Dam (later named Hoover Dam) was completed in 1935, and the All-American Canal was finished in 1942. With Phil Swing as lead advocate for a high dam and a hydroelectric plant built with government funds, he set the wheels in motion for the subsequent explosive development of the American west.

The Vanderbilt mine, San Bernardino County, California

Leonardo Menchaca
California State University, Bakersfield, lmenchaca5@csu.edu

The Vanderbilt mine is located partly on private land in San Bernardino County, two miles west of the California-Nevada state line in the New York Mountains and four miles southeast of the Ivanpah Valley within the Mojave National Preserve. The Vanderbilt mine is in the New York (Vanderbilt) gold mining district, within the Mojave Desert geomorphic province of California. Discovered in the late 1870s, it was one of the earliest and most substantial gold mines of the eastern Mojave Desert. During its peak production in 1896, a 10-foot-wide vein was developed by methods of underground mining. The mine was closed 1937 and was evaluated for redevelopment by the Homestake Mining Company in the 1980s. Host rocks are comprised of Precambrian gneiss, schistose granite, and metavolcanic hornblende schist. The mine is associated with a group of northwest-striking faults. Two mineralized fault zones strike N. 55–63° W and dip 65–80° NE. Many branch veins and or cross veins are between the two main veins. Mineralized fault zones are accompanied by heavily argillic altered, gray dike rocks which are highly fractured. Ore shoots occur along dike-schist contacts and as lenticular bodies within the fractured dikes. Gold is associated with pyrite, while sulfide ore consists of quartz with major pyrite and minor chalcopyrite, galena, sphalerite, marcasite, and cubanite. Also included are traces of arsenopyrite, magnetite, tennantite, tetrahedrite, bornite, and pyrrotite. Several of the underground mine structures are 10–15 feet in height and width and extend to depths of 100–900 meters. The workings were once accessible via a decline but the decline has now caved. Processing included crushing and milling the ore with gravity separation of coarse gold, and treatment of tailings by vat cyanide methods. During production, ore grade usually consisted of 3.74 oz/ton Ag and 0.62 oz/ton Au. These grades would be mineable at

today's commodity prices if sufficient ore reserves could be identified.

Structural framework for the Mountain Pass rare earth metals mine, Clark Mountain Range, California

David M. Miller and Joseph L. Wooden
U.S. Geological Survey, retired; dmiller@usgs.gov

Mesoproterozoic (~1.4 Ga) carbonatite and related ultrapotassic intrusions of the Mountain Pass (MP) district have exceptionally high concentrations of light rare earth elements (LREE). The MP carbonatite, averaging ~9 wt% rare-earth oxides, is a vital mineral resource. The MP district has been studied extensively since its discovery in the 1950s, with a focus on a pervasively altered area ~3 by 10 km within which numerous dikes and small intrusive bodies ("stocks") of Mesoproterozoic rocks are known. These studies led to a model for intrusion along preexisting fabric in the host rocks. Several stocks were argued to have been faulted, with offset parts not present and total offset on faults undetermined but assumed to be several kilometers.

Our studies of the host rocks at MP and elsewhere in the mountains surrounding Ivanpah Valley include geologic mapping, geochronological studies, and geochemical reconnaissance. These studies reveal the following: (1) a 1.78-1.65 Ga granulite-facies gneiss complex that is widespread in the Ivanpah and New York Mountains hosts the MP intrusions; (2) the gneiss complex can be divided into belts of migmatized rock with dominant rock types such as paragneisses, mafic orthogneiss, tonalite and trondhjemite, and granite and granodiorite plutonic belts; (3) rocks throughout the gneiss complex are folded and injected; and (4) pervasive amphibolite dikes are present. Throughout the complex, faults with offsets typically less than 1 km cut the gneiss. Two mylonitic zones, each about one kilometer thick, cross the gneiss complex, postdating the youngest ~1.65 Ga gneiss. These mylonites, along with several thinner zones, are at slightly lower metamorphic grade than the gneiss.

Ultrapotassic dikes and associated veins, like those at MP, are found across this same Ivanpah Valley region, as much as 30 km from MP, although the majority are close to the MP district where all stocks are mapped. In contrast, potassic alteration (finitization) associated with 1.4-Ga carbonatite and ultrapotassic rocks is restricted to an area 3 x 10 km wide, limited largely by the North and South faults, and by the Wheaton Wash fault to the east. Ultrapotassic and carbonate-shonkinite dikes regionally strike east-west, but in the heavily finitized MP district their strikes swing to north-northwest, apparently parallel to gneissic foliation. However, the dikes generally dip more steeply (80-90°) than do the gneisses (~60°).

We conclude that the widespread intrusion of geochemically unusual, highly LREE-enriched melts at 1.4 Ga indicates that melting of metasomatized mantle was regional in scope, as previously pointed out by Castor.

The pattern appears to be a bulls-eye centered on MP, although part of the pattern is covered by Mesozoic thrust plates. Although most 1.4 Ga stocks of MP are hosted within a belt of Paleoproterozoic granodiorite gneisses, it is likely that the ultrapotassic intrusions ascended nearly vertically and were not guided by either structures or the compositional homogeneity of the host gneiss. In contrast, the carbonatite body is approximately concordant with gneissic foliation. Despite this emplacement orientation it must have ascended across tens of kilometers of complex crust and its ascent probably was guided by the earlier ascent of the ultrapotassic stocks and dikes. The pattern of intrusions is most readily reconciled with a model of melt generation across a broad (10-20 km diameter) area of mantle, with melts concentrated in the MP district area.

Our mapping shows that the MP district has no faults that have significantly displaced the ore body or any other 1.4 Ga stocks because the host Paleoproterozoic gneiss is not significantly offset. We interpret the stocks that are apparently truncated by faults as having intruded along pre-existing faults, along which small offsets later occurred. These faults have lower greenschist facies mineral assemblages and must significantly postdate the metamorphism of the high grade gneiss. However, previously unrecognized thrust faults structurally below the Cretaceous frontal thrust (west of the carbonatite body) cut the Paleoproterozoic gneiss complex, and potentially could have affected the ore body at depth.

Early Miocene volcanism, sedimentation, and faulting in the western Lava Hills, California

Alexander S. Noorzad, Cole B. Jacobs, Phillip B. Gans, and Andrew Kylander-Clark
University of California, Santa Barbara

The Lava Hills are located in the eastern Mojave Desert region southeast of Ludlow, CA and expose a thick succession of early Miocene sedimentary and volcanic rocks overlying or faulted against Mesozoic plutonic rocks. Previous work by D. Miller (1993) laid out the general geologic framework, reported several early Miocene K-Ar dates, and summarized the Cenozoic stratigraphy of the broader Lava Hills-southern Bristol Mountains region. This study builds on that previous work and investigates the Miocene structure and stratigraphy of the western part of the Lava Hills through detailed (1:5000) geologic mapping, structural and stratigraphic analysis, and LA-ICPMS U-Pb zircon geochronology.

The exposed Miocene section consists of a southwest dipping ~500 m thick succession of volcanoclastic breccias, sandstone, and discontinuous dacite lavas that are faulted against Mesozoic plutonic rocks to the southwest and rest conformably on aphyric andesite and other lavas to the northeast. The dominant sedimentary rock types throughout the section are 0.5 to 3 m-thick tabular massive beds of volcanoclastic breccia, separated by thin discontinuous intervals of plane-laminated sandstone, commonly displaying conspicuous normal grading.

Additional lithofacies include what appear to be primary unwelded pumiceous pyroclastic flows and rare ash fall tuffs, but the vast majority of the section appears to be sedimentary and water-laid. The breccias range from clast-supported rock-avalanche deposits with clasts up to 1 m in diameter, to matrix-supported debris flow deposits, to faintly stratified hyperconcentrated flows. Clast composition ranges from monolithologic brick-red porphyritic crystal-rich dacite, to more heterolithic assemblages of different dacite compositions and phenocryst assemblages as well as sparse andesite clasts. The entire sedimentary section is dominated by volcanic (especially dacite) detritus, with virtually no basement derived clasts. Lavas of aphyric andesite, a hornblende-rich andesite, and a quartz-rich dacite underlie the section and form a northwest trending ridge along the northeastern boundary of the mapped area. Additional sedimentary and volcanic units occur even further down section to the northeast but have not yet been mapped or examined in any detail. Capping the section is a plagioclase-biotite dacite lava dome.

LA-ICPMS U-Pb single zircon dates were obtained from several lavas near the base of the section, two ash fall tuffs and a possible primary ash flow within the section, and the dacite lava at the top of the section. These yielded virtually indistinguishable ages ranging from 22.52 ± 0.07 to 22.91 ± 0.08 , and are generally in correct stratigraphic order. These new ages improve on the existing K-Ar geochronology and indicate that the sedimentary succession accumulated rapidly in less than 0.5 Ma at an average rate of ~ 1 mm/yr.

The Miocene section strikes southeast and consistently dips to the southwest, with dips generally increasing up-section from ~ 25 to 65° . The Miocene section is cut off along its southwestern boundary by a major fault that trends WNW to NW and appears to dip steeply NE. The principal fault plane is not exposed but measurements on subsidiary fault planes within this zone yield an average orientation of $\sim 337/73^\circ$, and display slickenlines that range from pure dip slip (normal) to oblique (right lateral-normal). Smaller scale faults are present throughout the study area, most with a few meters to a few 10s of meters of displacement and display either normal or right lateral displacement.

The rapid accumulation of a thick section of juvenile volcanoclastic debris and the presence of lavas at several stratigraphic levels suggest that sedimentation was coeval with active volcanism between 22.9 and 22.5 Ma. The simplest interpretation is that the Lava Hills sedimentary succession represents a series of debris flows (lahars), rock avalanches, and fluvial deposits that accumulated in the lowlands adjacent to and sourced from highlands of an active dacite dome field. Though it is tempting to view the section as an extensional basin fill (half graben) that accumulated synchronous with slip on the major normal fault to the SW, there is little evidence to support this—especially in light of the increase in dips up section.

A more likely interpretation is that normal faulting and tilting of the Lava Hills section occurred after 22.5 Ma during NE-SW directed regional extension, and that the steepening of dips in the vicinity of the major fault on its SW margin is a consequence of later reactivation of this fault by dextral shearing with a component of transpression—younger deformation associated with the Eastern California Shear Zone. Future work will expand our mapping and structural/stratigraphic studies to the northern and eastern portions of the Lava Hills and hopefully paint a more complete picture of Miocene volcanism, sedimentation, and deformation in this part of the Mojave Desert.

Telegraph mine, Halloran Springs District, San Bernardino County, California

Michelle Nop

California State University, Bakersfield, mnop1@csub.edu

The Telegraph Au-Cu mine is 16.3 miles east of Baker, California on the south flank of the Halloran Hills and south of highway I-15. Spanish era arrastras in the area suggest that mining was occurring in the area circa 1650 CE. In 1930, A.A. Brown and Ralph Brown of Salina, Utah discovered a quartz vein of high-grade gold ore. The area was mined from 1932 until 1948, yielding a total of \$100,000 of gold or approximately 2860 ounces of gold at the prevailing gold price of \$35 during that period. The mine was subsequently explored with financial assistance through the federal government's Defense Mineral Exploration Act program during the 1950s. Development drilling by Cascade Energy and Minerals Corporation of Salt Lake City, Utah was performed in 1984. The drilling identified an extension of the Telegraph vein system along strike that is favorable for hydrothermal deposit formation for a distance of several thousand feet. A heap leach test plant was constructed to process low grade materials. Heap leach pads from this era are still visible.

The Telegraph mine is within an area of low relief underlain principally by Cretaceous Teutonia adamellite. The adamellite intrudes or includes Proterozoic metasediments. An aplite dike about one to two feet thick lies along the footwall of the mineralized vein. The original development worked a vein 3 to 8 feet wide and several hundred feet long. That vein strikes N. 38° E. and dips 30° to 50° NW with an average thickness of eight feet. When last operating, the Telegraph deposit consisted of two five feet thick parallel vein-stockworks of intensely silicified adamellite. The stockworks consist of systems of closely spaced 1/4" to 1/2" thick quartz veins in sheeted, porous adamellite containing large and abundant cavities that are partly or wholly filled with iron oxides. The quartz veins are brecciated, cemented, and encrusted with calcium carbonate and silica, indicating multiple vents of shearing and associated mineralization. Feeble pyritization (hematite after pyrite), chalcopyrite, manganese oxide, and traces of bornite and malachite absorbed in kaolin are present, along with bornite and

free gold and silver. The intervening ground between the two silicified zones is approximately 10 to 20 feet wide and weakly but consistently pyritized. Silicified materials in the hanging wall and foot wall have minimum thicknesses of 30 feet and are intensely kaolinized or chloritized. The vein is accessed and excavated by three inclined shafts. Two of the three inclined shafts are more than 100 feet deep and are joined by several hundred feet of level workings. The ores were treated through a flotation plant on the property and the yielded concentrates were reported to carry \$300–400 (1932–1948) Au/ton, or about 1 oz Au per ton of concentrate. The Telegraph mine area has a large area of potential reserves at today's commodity prices. Any development is likely to be curtailed because of its presence within the Mojave National Preserve.

Isotopic constraints on the origin of the igneous hosts of the Mountain Pass REE deposit, San Bernardino County, California

O. Tapani Rämö¹ and James P. Calzia²

¹University of Helsinki, Geosciences, Helsinki, Finland;

²US Geological Survey, Menlo Park, CA, United States

The Mountain Pass rare earth element deposit, San Bernardino County, California is hosted by a ~1.4 Ga ultrapotassic (UP) silicate and carbonatitic igneous suite that intrudes Paleoproterozoic high-grade gneiss, amphibolite, and pegmatite at the southern end of the Clark Mountains. Stocks of UP rocks range from phlogopite melasyenite (or shonkinite) through amphibole-biotite syenite and leucosyenite to alkali granite. The main mass of carbonatite (Sulfide Queen) is a tabular, moderately dipping multiple intrusion and consists of a heterogeneous assemblage of bastnaesite-, barite-, parisite- and monazite-bearing calciocarbonatites and magnesiocarbonatites (Castor, 2008). Published U-Th-Pb mineral geochronology (Poletti et al., 2016; Watts et al., 2022) implies protracted magmatism with a peak at 1415–1410 Ma (main volume of UP rocks) and subsequent but partly coeval emplacement of carbonatite at ~1380 Ma. Accessory zircon bears evidence for contamination of the UP melts by Paleo-Mesoproterozoic crustal rocks (Watts et al., 2022). Very high contents of incompatible elements in the UP and carbonatitic melts have, however, made certain elemental systems (e.g., LREE, Sr) inert to the effects of crustal contamination. Whole-rock Sm-Nd and Rb-Sr isotope compositions thus offer a robust window to the mantle sources and evolution of the UP and carbonatitic melts. The UP rocks of Mountain Pass (our data; Poletti et al., 2016) have epsilon-Nd (1410 Ma) values of -4.2 ± 0.6 (1SD, n=10) and show no change across a wide fractionation window [molar MgO/(MgO+FeO_{tot}) of ~0.8 to ~0.2]. The carbonatites (our data; Poletti et al., 2016; Verplack et al., 2016) have epsilon-Nd (1380 Ma) values of -3.0 ± 0.4 (1SD, n=10) and show no dependence on the lithologic variation observed (magnesiocarbonatite through calciocarbonatite). Initial ⁸⁷Sr/⁸⁶Sr ratios (our data; Verplack et al., 2016) of the carbonatites (~0.705

to 0.706) are less radiogenic than those of the UP rocks (~0.708 to 0.709). The discernible difference in the Nd-Sr isotope composition of the UP and carbonatitic rocks of Mountain Pass implies compositional variation in the source (metasomatized subcontinental lithospheric mantle) beneath exposed Mojavia and that the alkali and carbonate melts may have formed in separate melting events.

Evidence of Miocene earthquakes recorded in sedimentary structures within the Horse Spring Formation, southern Nevada, including paleoliquefaction evidence of a very large earthquake on the Las Vegas Valley shear zone or Lake Mead fault system at approximately 13.7 Ma

Stephen M. Rowland¹ and Jerry King²

¹Department of Geoscience, University of Nevada Las Vegas, Las Vegas, Nevada 89154-4010 and Las Vegas Natural History Museum, 900 Las Vegas Blvd N., Las Vegas Nevada 89101; steve.rowland@unlv.edu; ²King Engineering, 916 Crescent Moon Drive, North Las Vegas, NV 89031

Paleoliquefaction features and intrastratal folds and faults document the occurrence of seismicity during deposition of the Miocene Horse Spring Formation in southern Nevada. One of the paleoliquefaction structures is a very large, cylindrical injection pipe, ~5 m long and ~1 m in diameter, which is among the largest such structures known. This feature is the lithified feeder conduit of a “sand boil” or “sand blow” (although composed of silt in this case) which formed on Earth's surface at the time of the earthquake. The upper end of this cylinder is a flat surface, so the silt that was deposited on the earth's surface was later eroded away. Based on previous dating of strata within the Horse Spring Formation, this structure dates to ~13.7 Ma. It records the liquefaction of sediment due to seismic shaking and the resulting forceful injection of liquefied silt through five meters of overlying strata.

A high-magnitude earthquake on a nearby fault must have triggered this liquefaction event. Such large earthquakes do not characteristically occur on continental normal faults. We infer that this earthquake occurred on either (a) the Las Vegas Valley shear zone, a dextral, strike-slip fault that extends for roughly 100 km in the southern Walker Lane fault system, or (b) the Lake Mead fault system, a much less extensive system of sinistral strike-slip faults.

We suggest that because of its greater length the Las Vegas Valley shear zone is the more likely source of this earthquake. This ~13.7 Ma earthquake may represent the early development of the Walker Lane-Eastern California shear zone and the initiation of a new phase of major plate-boundary interactions between the Pacific and North American plates.

The Frenchman Mountain Dolostone: a new Cambrian formation in southern Nevada and the Grand Canyon

Stephen M. Rowland,^{1,2} Slava Korolev,¹ and James W. Hagadorn³

¹Department of Geoscience, University of Nevada Las Vegas, Las Vegas, NV 89154; ²Las Vegas Natural History Museum, Las Vegas, NV 89101; ³Department of Earth Sciences, Denver Museum of Nature and Science, Denver, CO 80238.

In 1945, a prominent Grand Canyon geologist named Edwin McKee called attention to an interval of dolostone that is approximately 100 m thick in central Grand Canyon, and which lies stratigraphically above the Muav Formation. McKee made a point of not formally naming this interval, in part because it does not contain datable fossils, so he was unable to determine its age with confidence. McKee simply referred to this interval as “undifferentiated dolomites.” For 78 years this stratigraphic interval, which occurs throughout the Grand Canyon and across the Lake Mead region, has remained unnamed. Grand Canyon stratigraphic columns typically lump this interval with the Muav Formation.

Following a detailed study of McKee’s “undifferentiated dolomites,” including analyses of thickness trends, carbonate facies, depositional environments, and carbon-isotope chemostratigraphy, we are able to establish the age range and paleoenvironmental context of this rock interval. Its westernmost exposure is on Frenchman Mountain, adjacent to Las Vegas. Farther west it transitions into the Banded Mountain Member of the Bonanza King Formation. The Frenchman Mountain exposure is especially important because, contrary to exposures in the Grand Canyon, there it is overlain by trilobite-bearing beds of the Nopah Formation, so the age of the top of the interval is tightly constrained as being Furongian (formerly “Upper Cambrian”). At 371 meters, the unit is also thickest at Frenchman Mountain. In the western Grand Canyon, at Quartermaster Canyon (below the Grand Canyon Skywalk) the unit is 117 meters thick; it thins eastward to just 8 meters in the easternmost Grand Canyon. We are naming this previously unnamed interval the Frenchman Mountain Dolostone.

Even though biostratigraphically useful fossils are not present, chemostratigraphic analysis has allowed us to correlate the Frenchman Mountain Dolostone regionally and globally. We have determined that this interval spans approximately 7.2 million years of Cambrian time, from the middle of the Miaolingian Series (formerly “Middle Cambrian”) to the lower portion of the Furongian Series (formerly “Upper Cambrian”). The Frenchman Mountain Dolostone is the uppermost unit of the Tonto Group (Tapeats Ss, Bright Angel Fm., Muav, Fm., Frenchman Mtn. Dol.) which records the flooding of the continent Laurentia in the Sauk Transgression, following the break-up of Supercontinent Rodinia. The Frenchman Mountain Dolostone formed in intertidal and shallow subtidal settings on a flat-topped carbonate platform.

A vascular flora of the Sacatar Trail Wilderness

Kimberly Schaefer

California Botanic Garden & Claremont Graduate University; recipient of the 2022 Robert E. Reynolds Student Research Award; kschaefer@calbg.org

The Sacatar Trail Wilderness (STW) occupies a unique ecological transition zone in the southeast Sierra Nevada at the interface of the Mojave Desert, Great Basin Floristic Province, and highly diverse California Floristic Province. This 88 mi² area encompasses a significant elevational gradient from 3,500 to nearly 9,000 feet, and supports a diverse array of vegetation communities, from creosote scrub to montane meadows. The absence of weather stations within the STW make it difficult to understand the precise microclimates its plants are subject to, especially considering that conditions vary within such a wide elevational range. This region of the eastern Sierra on the western edge of the Mojave Desert, if more thoroughly studied, could potentially serve as a setting for future research on plant migration in response to climate change. The STW is also a “botanical black-hole,” an area with little to no documentation of the plants that occur there. Historically, the most notable collector in the area was botanist Ernest C. Twisselmann, who made 36 collections from 1958 to 1971. The STW’s habitat heterogeneity coupled with insufficient documentation suggests possibilities for discovering new rare plant occurrences, and even new (undescribed) species.

Research objectives are (1) to produce a comprehensive inventory and annotated species checklist to document all vascular plants within the STW, (2) to generate more precise weather data from the site, and (3) to characterize the vegetation communities through quantitative surveys.

Thirteen trips were made to the study site between March and September 2022, with an estimated fifteen additional trips to be made in 2023 to collect voucher specimens of all vascular plant taxa present. To supplement the limited climate information available for the STW, 12 iButton temperature data loggers have been installed along the study site’s elevational gradient at 1,000-foot intervals. The data logging points will be further analyzed with 10-meter radius surveys in order to characterize vegetation types with elevation. Historic collections from the site will be examined and identifications verified. All collections data, including those from historic collections, will be assimilated into an annotated species checklist. Specimen vouchers collected as part of this research will be deposited in RSA, UCR, and CAS herbaria and corresponding data shared with the Consortium of California Herbaria (CCH2) database portal.

During the first field season 827 collections were made, representing 67 different plant families. I have documented range extensions including the southernmost record of yellow-flowered wild buckwheat (*Eriogonum microtheca* var. *ambiguum*), and the first ever record of California milkweed (*Asclepias californica*) in Inyo

County. I've located several rare taxa, including a new occurrence of Charlotte's phacelia (*Phacelia nashiana*), which the California Native Plant Society classifies as a rank 1B.2 threatened species. Aside from exciting plant observations, I have confirmed through multiple sightings that this area is inhabited by the rare and threatened Mojave desert tortoise at the very northwest reaches of its range. The STW is proving to be a unique and ecologically important place that is in need of floristic research.

Ediacaran test tubes: constraining the taxonomy of Ediacaran nonmineralized tubular taxa to elucidate Earth's earliest experiments in multicellularity

Rachel Surprenant

Department of Earth and Planetary Sciences, Univ. California, Riverside

The Ediacara Biota (574-539 Ma) represents the first complex, community-forming animals on Earth and are preserved in fossil Lagerstätten around the globe. Some of these sites are found within the Mojave Desert, which in stark contrast to today's desert ecosystems was the home to diverse marine ecosystems in deep time. Within the fossiliferous Ediacaran rocks of the Mojave Desert, of which many are found in the lower Wood Canyon and Deep Spring formations of the Nopah and Resting Spring ranges, the most common organisms are the morphogroup tubular organisms which are defined by their macroscopic, simple, hollow, and elongate forms. This reflects a broader trend in the global Ediacaran fossil record wherein tubular bodies are the most common morphology adopted by early animals.

Taxonomically described tubes in Ediacaran rocks of the Mojave Region represent mineralized forms such as *Cloudina hartmannae*, but this research aimed to recover nonmineralized tubular taxa that have been informally described in previous publications. However, extensive investigation of the Deep Spring and lower Wood Canyon formations did not recover nonmineralized tubes; instead it uncovered a different, but equally important aspect of the fossil record of Ediacaran nonmineralized tubes: morphotypic convergence of sedimentary structures, trace fossils and tubular body fossils. Morphologically and taphonomically geared investigation of these pseudo-tubes provides criteria for differentiating between sedimentary structures such as microbial mat cracks, planar trace fossils, and soft bodied tubular fossils.

Data collected on the morphology and taphonomy of these disparate structures provide several criteria for the identification of simple, elongate structures in siliciclastic rocks as definitive tubular body fossils. These criteria for tubular body fossils, which are not present in morphologically similar sedimentary structures and trace fossils, include: 1) evidence of soft-tissue deformation (i.e., wrinkling, folding, twisting, ripping), 2) presence of discrete taphomorphs including internal molds and composite external molds, 3) absence of sediment levees and curled sediment around the structure's margins, 4)

constriction of the structure at curving points but no discontinuity in the margin of the structure along its length, 5) evidence of overlapping, not cross-cutting, relationships between overlain specimens, 6) alignment of multiple specimens with current direction, and 7) underprinting of underlying topography, such as microbial mat textures, in composite external molds.

These criteria provide a taphonomic framework which will facilitate the reexamination of simple, elongate structures that are tenuously defined as tubular body fossils in the Ediacaran siliciclastic record, thusly preventing the conflation of pseudo-tubes with tubular body fossils in future investigations and correcting similarly misguided interpretations put forth in past investigations. As such, the results of this research provide broadly useful strategies for refining understanding of the most common morphotype in the earliest animal communities both within the Mojave region and in the Ediacaran rock record globally.

The Morning Star mine, San Bernardino County, California

Ryan Tengelsen

California State University Bakersfield, rtengelsen@csub.edu

The Morning Star mine is a 1000-acre mine in the Ivanpah Mountains, north of Kewanee camp in San Bernardino County and 65 miles southwest of Las Vegas in the Mojave National Preserve. It was first opened in 1907 and was an episodic gold producer until the Vanderbilt Gold Corporation procured the property in 1964. The Vanderbilt Gold Corporation operated the mine until about 1982 when the price of gold dropped, forcing the mine to close. In 1983 testing with cyanide carbon-in-leaching commenced at the mine. Full-scale leaching began in October 1987. The mine would continue to operate until it closed permanently in 1993. The claims were not patented and today the mine area is managed by the National Park Service. The mine is hosted by the large Jurassic Ivanpah Granite pluton that is cut by dacite dikes. The major tectonic and ore-localizing feature in the area is a thrust fault striking north 20 degrees west and dipping 32 degrees to the southwest. The host rock of the mine was intruded by the dikes. Mining relics include a water-filled deep and steep-sided mining pit and leaching piles. Stratification in the heap leach piles reflects variations in the heap leach technology. Early heaps from the main ore body were amalgamated with cement. It was later learned that this was not economically advantageous, so later heaps were constructed using untreated ores. Ore minerals at the Morning Star are gold and silver with secondary sulfides and oxides of copper, zinc, and lead. The ore yields about 25% gold and 75% silver; historic production was from \$2 to \$15 per ton in gold, averaging a grade of \$4 to \$6 per ton. The remaining unmined portions of the deposit contain minable precious and base metals at current commodity prices.

Bureau of Land Management's mineral investigation of Viceroy Gold Corporation's mineral patent applications at the Castle Mountain mine during the period from 1992 through 2001

Robert Waiwood

Professional Geologist, robwaiwood@aol.com

In 1985, Viceroy Gold Corporation (VGC) became the operator of the Castle Mountain project area, and after extensive exploration and development drilling, conducted open pit-cyanide heap leaching operations in 1991 to 2003. The mine is located in eastern San Bernardino county and lies within the Castle Mountains near the Nevada-California state line. The project area is located 16 air miles southwest from Searchlight, Nevada. In 1989, VGC filed an application to patent 21 lode mining claims aggregating 298 acres centered around their open pit operations and in 1992 filed two notices to apply for patent of 291 mill site locations, each 5-acres in size and aggregating approximately 1,439 acres. Mill sites were used in support of non-mining operations at the mine. While work on the mineral patent cases began by the Bureau of Land Management (BLM) field office in 1993, it was not until May 30, 1995, that the Secretary of the Interior signed the First Half of the Final Certificate showing that all filing requirements were met by VGC, and payment was submitted by VGC for patent. The case was assigned to the BLM California Desert District office to assess and evaluate the bona fides of each claim and mill site in the patent applications under current direction and policy. BLM investigates mining claims and mill sites to ensure that "...valid claims may be recognized, invalid ones eliminated, and the rights of the public preserved..." (*Cameron v. United States*, 252 US 450 (1920)).

The Castle Mountains are a small range at the northern end of the Lanfair Valley in California and extend north into Nevada. Most rock in the general area is Precambrian gneissic basement and local Paleozoic marine sediments intruded by Cretaceous quartz monzonite, typically overlain by Miocene age rhyolite, andesite, and basalt. VGC's Castle Mountain project is within the Hart mining district of California, its mining history dating back to the late 1880s. As indicated by exploration drilling and old workings, gold mineralization is widespread over an area of at least two square miles with a vertical range of more than 1,500 feet. Mineralization can be classified as volcanic-hosted epithermal, with gold the major metal present. Controls for gold mineralization are related to porosity and permeability of the rocks, occurring in major structures such as shear zones and sheared contacts of lava dome structures. These zones of intensely fractured rock produced a widespread series of stockwork veins.

Mining starts with the deposit being drilled and blasted. Holes are surveyed and sampled for gold content, and blasted rock is loaded into haul trucks and delivered to the primary crusher or waste depending on blast hole grade. Following 3-stage crushing to 80 percent

passing 3/8 inch, the ore is sent by an overland conveyor to the heap leach pad where it is stacked in 20-ft lifts. At the leach site, weak solution of sodium cyanide is applied to the heap by a drip-irrigation system. Gold-bearing cyanide solution is percolated through the heap "lifts", where the solution dissolves gold and silver and is collected by gravity and piped to carbon columns for recovery of the gold and silver. The precious metals are then stripped from the carbon, recovered onto steel wool in electrowinning cells, and smelted to produce a doré bullion averaging 80% gold and 20% silver. During later operations, a gravity and vat-leach circuit was added to recover gold that was too coarse to be leached effectively in the heap-leach circuit.

BLM's examination process began by collecting all available information about the project. This includes information on the geology, mineralization, location of lode mining claims and mill site locations, and salient improvements on the property. All lode mining claims, mill site locations, geology and mineralization, drill and sample data, and the public land survey system were converted to a common coordinate system (Universal Transverse Mercator (UTM)) using various surveying methods. Selected core, blast hole and exploration drill hole cuttings were sampled as well as samples from the heads and tails of the carbon system. All samples were analyzed and compared with VGC's data to verify integrity of exploration drill data and that the processing and blasthole samples supported the stated recovery. During operations, actual gold and silver recovered exceeded the forecast recovery by about 6 percent. Drill hole assay data were processed by BLM using various estimation methods to develop grade blocks. Grade blocks used in mine modeling and resource calculations consisted of cube-shaped blocks 20 feet on a side and grading above the mine cut-off grade of 0.015 ounces per ton (opt). The block model was then employed using ESRI ArcInfo by taking the final pit contour data provided by VGC and merging these data with pre-development contour data layers to create grade level polygons. Lode mining claim boundaries were superimposed on each 20-foot pit level polygon and clipped to provide the ounces of gold that can be produced at each level by each mining claim. An economic evaluation of the property was made from costing data of all elements of mining and processing from the period 1991 to 2003 when reclamation would be completed. From BLM's estimation model approximately 43,624,000 tons of resources would be mined in 10 years, with an average grade of 0.039 opt. Approximately 2,954,000 tons would be directed to the mill-gravity circuit. At the end of operations, BLM estimated that a break-even operating cost of \$6.62 per ton of ore mined would be realized (using a "0" net present value in the cash flow analysis). This is below or within the range for similar operations in the southwestern United States. VGC's actual mine and processing operating cash costs in 2000 were \$6.28 per ton of ore mined, below the break-even

cost supporting a discovery of a valuable mineral deposit, the requirement for a valid lode mining claim.

Major uses of the mill sites included crushing, grinding, and conveying facilities; heap-leach pads and leach collection ponds; mill-gravity circuit; waste dumps; plant service buildings and ancillary facilities; security and wildlife fencing; and water and monitoring wells. Digital orthophoto quadrangle (DOQ) files were obtained for the area from the U.S. Geological Survey to determine the use and occupancy of each mill site at the time the image was acquired. Approved mine plan maps showing the surveyed location of facilities were also registered using global positioning surveys of public land survey monuments, physical features such as road intersections, VGC survey reference and witness stations. With the mill sites registered to the UTM coordinate system, all outlines of surface use after the date of the DOQ were traced in the field using GPS tracking surveys. In addition, drill hole data for the mill site areas were examined to determine if any area was considered mineral in character. These data were merged with the areas of approved surface use and mineral character to determine which 2-1/2 acre subdivision of each mill site could be recommended for patent or contest action.

Twelve lode mining claims were supported by the statutory requirement that each claim have a discovery of a valuable mineral deposit within each boundary. In addition, 269 mill sites were found to be supported in whole or in part by appropriate use and occupation and determined not mineral in character. Overall patent was granted to VGC in 2007 to approximately 207 acres of lode mining claims and approximately 830 acres of mill sites. Six lode mining claims aggregating 36.7 acres were not supported by a discovery of a valuable mineral deposit and subsequently recommended for contest action. Portions of 4 mill sites were recommended for patent but were located within the Mojave National Preserve. Twenty-eight mill sites were withdrawn from the applications. Subsequent to issuance of patent, operations had ceased and the property was reclaimed as directed in compliance with VGC's reclamation plan. VGC received an award from the California Department of Conservation for its outstanding reclamation efforts. When gold prices escalated beginning in 2012 the property was re-evaluated, and a new mining and reclamation plan was submitted for approval. In 2017, the Castle Mountain project was re-opened by a new operator. Independent evaluations of the property in 2022 indicate resources at 150.6 million tons of proven reserves at a grade of 0.017 ounce per ton.

Stromatolites in spring-fed streams of Death Valley National Park: past, present, and future

Kenneth L. Wright Jr., Torrey Nyborg, Kevin E. Nick
Department of Earth and Biological Sciences, Loma Linda University, Loma Linda, CA 92350

Stromatolites are laminated biosedimentary structures generated by colonies of photosynthetic cyanobacteria in aquatic environments. They are abundant in the fossil record in general, and Death Valley National Park specifically has a rich record. Stromatolites were among the first life forms on Earth, dating back more than three billion years, and played an enormous role in elevating the level of free oxygen in the atmosphere. However, living examples are very rarely found in modern environments. Death Valley National Park preserves several areas where modern stromatolites grow and thrive, providing a rare opportunity to investigate one of Earth's oldest life forms.

Stromatolites with incipient mineralization thrive in several spring-fed streams of Death Valley National Park, forming carpets, terraces, and domical buildups. By comparing environmental conditions among streams with dense stromatolite growth to those where stromatolites are rare or absent, factors controlling stromatolite growth and survival in the harsh environments of Death Valley may be inferred. This information can be used to help monitor and protect one of Death Valley's more unique and enigmatic organisms, as well as having potential application in the search for life on Mars.

One of the most prolific stromatolite habitats in Death Valley lies next to one of its most prolific mines. Generating almost \$1 million in gold between 1907 and 1912, the Keane Wonder mine was the second largest gold producer in Death Valley. Spring-fed streams that once powered the stamp mill traverse the travertine terraces west of the mine. Flowing at least since the Pleistocene, these streams are rich with stromatolites and microbial mats. A 10m long branch of one of the more accessible and prolific streams was selected as a baseline for this study. Multiple overlapping, georeferenced images of the section (taken with GoPro Hero 10 on a handheld monopod) were used to generate a digital elevation model (DEM) via OpenDroneMap software. Further analysis gave qualitative measures of stream gradient and stromatolite growth density. Water chemistry data, including dissolved ion concentrations, pH, and temperature were then added to the DEM. Relationships between the physical and chemical conditions and stromatolite density and morphology were evaluated and compared among stromatolite-bearing and stromatolite-free spring-fed streams in Death Valley National Park.

Several associations between stromatolite characteristics and environmental parameters were apparent in the Keane Wonder Spring stream. All water samples are alkaline (8.3–9.2) and are sodium chloride sulfate-dominated. 1) Stromatolites are generally absent in shaded areas or where abundant green algae occur. 2) Shallow stream sections with higher flow velocity are preferentially inhabited by small (1–10 mm diameter) mat- or terrace-forming, laterally linked hemispherical heads. 3) Larger (10–50 cm) domical heads are the predominant morphology in splash zones of waterfalls and cascades. 4) Stromatolite density is inversely related to calcium

ion concentration. However, these associations are not perfectly correlated at all localities, despite the similarities in water chemistry.

Stromatolites in the spring-fed streams of Death Valley are composed of cyanobacteria in the genus *Rivularia*, which, like several other taxa of cyanobacteria, have adapted to life under intense solar radiation by generating their own sunscreen, the ultra-violet blocking alkaloid molecule scytonemin. Our future research on Death Valley stromatolites will focus on uncovering their past. Using scytonemin as a biomarker we will attempt to identify lithified stromatolites and microbial mats in the laminated sediments of abandoned ponds and stream channels dating back to the Miocene.

The ability to positively identify ancient stromatolites and deduce their preferred habitats in the extreme temperature and insolation of Death Valley will contribute to our understanding of stromatolites through time and space, highlighting the most favorable conditions for stromatolite development at locations decidedly unfavorable to most lifeforms.

Billie borate mine, Inyo County, California

Gregg Wilkerson

California State University Bakersfield

The Billie mine is located in the Furnace Creek borate area within Death Valley National Monument, Inyo County, California. It consists of a main shaft that is about 1½ miles northwest of the historic town of Ryan and about 12 miles southeast of Furnace Creek Ranch. The portal to a decline that accesses the mine is located about 1500 feet away from the ore body because of environmental restrictions imposed by Public Law 94-429. Mining activity in the vicinity of the Billie mine began at the Boraxo deposit in 1915, which was claimed as the Clara lode by Pacific Coast Borax Company. Legal problems over title plagued the mine until 1960 when the Kern County Land Company purchased the deposit and sank the 120-foot main shaft. They produced a few thousand tons of colemanite. The mine was re-opened by Tenneco Oil company in 1970 as a small open pit named the Boraxo pit that was mined to a depth of 400 feet. Colemanite was trucked to a washing-calcining plant north of Death Valley Junction. Ulexite-probertite was trucked to a grinding facility on the railroad at Dunn Siding, California. In 1974, Tenneco was the largest producer of colemanite and ulexite-probertite in the United States. In late 1976 the United States Congress passed Public Law 94-429 which effected a four-year moratorium on further surface disturbance within Death Valley National Monument for the purposes of mineral extraction, with minor exceptions. The Billie mine was purchased by American Borate Company (ABC). Although ABC owned other mineable deposits within the monument, the passage of this law along with other considerations caused ABC to proceed with the Billie mine as its most environmentally and economically

feasible project. In 1991 the project was permitted and mined until it closed in 2005.

The Billie and most other borate deposits in the Furnace Creek borate area are part of the Black Mountains tectonic block. This block is characterized by numerous exposures of Tertiary rocks along an elongate belt that includes borate deposits sub-parallel to the Furnace Creek fault zone. This suggests the presence of a structurally controlled Tertiary basin or line of basins. Most faults within the block strike northwest, sub-parallel to the major bounding faults. Most faults are normal, although lateral movement is probably significant on some. The Ryan, Sigma, Billie, Boraxo, and Inyo deposits occur along a highly faulted anticline which is truncated by the Grand View fault northwest of the Boraxo pit. Folding was probably in response to episodic compression and drag along the Furnace Creek and Grand View fault zones in post-Furnace Creek Formation time. The Billie borate deposit is a lens of zoned ulexite ($\text{NaCaB}_5\text{O}_6(\text{OH})_6 \cdot 5\text{H}_2\text{O}$), probertite ($\text{NaCa}[\text{B}_5\text{O}_7(\text{OH})_4] \cdot 3\text{H}_2\text{O}$), and colemanite ($\text{Ca}_2\text{B}_6\text{O}_{11} \cdot 5\text{H}_2\text{O}$) or ($\text{CaB}_3\text{O}_4(\text{OH})_3 \cdot \text{H}_2\text{O}$) that is intercalated with and surrounded by limey lacustrine mudstones and shales of the middle to late Pliocene Furnace Creek Formation. The entire Billie deposit is sub-surface and has an average stratigraphic thickness of 150 to 175 feet. It is 3,700 feet long in a N50°W direction and has an average width of 700 feet. The ore body dips 20° to 30° southeast. The shallowest ore is 150 feet from the surface and the down-dip ore extends to 1,300 feet deep. In-place demonstrated reserves of the Billie borate deposit are about 3,000,000 short tons of 27% B₂O₃ sodium-calcium (ulexite-probertite) ore and about 12,000,000 short tons of 21% calcium borate (colemanite). Ulexite, the primary borate mineral, is preserved in centrally located deep pods surrounded by secondary probertite, which forms when ulexite is dewatered and recrystallized under lithostatic load and increased temperature upon downwarping and burial of the Pliocene sediments. When calcium rich groundwaters encounter sodium-calcium borate zones, the alteration product is a thick colemanite (calcium borate) envelope, which forms around the ulexite or probertite core. Colemanite and ulexite-probertite contacts in the Billie are usually abrupt solution contacts that sometimes contain water, but the central ulexite-probertite zones are dry and less disturbed than the colemanite margins. In summary, the Billie Borate deposit remains a significant potential source of borate minerals. It formed through lateral secretion of fluids leached from Pliocene lake beds which were concentrated by hydrothermally heated connate water. Heating was associated with nearby 5.9–5.7 Ma intrusive feeders for basalt flows. The deposit is classified by the U.S. Geological Survey as lacustrine borate USGS Model 35b.3.

Briggs mine, Inyo County, California

Gregg Wilkerson

California State University, Bakersfield, gwilkerson1@csu.edu

The Briggs mine is located 4.3 miles WNW of Manly Peak along the base and west flank of the Panamint Range, southeastern California. The mine lies in the area north to Manly Falls at the mouth of Redlands Canyon. The mine is developed on unpatented mining claims on land administered by the U.S. Bureau of Land Management. Gold was first discovered to the north of the current Briggs mine in the 1890s. The first recorded exploration at Briggs was in the 1930s. Harry Briggs conducted exploration, underground development, and minor production until modern exploration began in the early 1970s. Various companies examined the Briggs area from the 1970s through mid-1980s and conducted surface mapping, sampling, and several shallow drill programs. Addwest Gold Inc. was the first company to discover a larger low-grade gold mineralized zone at Briggs in the late-1980s and began development drilling of the project in 1988. Canyon Resources Corporation continued the development work after acquiring Addwest in 1989. The mine went through several changes in design and mining ceased in 2004 due to changes in reclamation requirements while heap leaching continued. The mine was closed due to low gold prices in 2012. Gold prices exceeded \$1,500/oz in 2015 and that led to several drilling programs through 2022 that identified additional reserves.

The geology of the Panamint Range near the Briggs mine consists of crystalline basement rocks overlain by Neoproterozoic strata, all intruded by Mesozoic granitic rocks. Mesozoic thrust faults and folds formed at the time that granitic to dioritic intrusions were emplaced. Base metal and minor gold-silver-bearing veins are associated with the intrusive bodies north and east of Briggs. These rocks were affected by Cenozoic extensional tectonics including high-angle normal faults and related low-angle detachment faults. The gold occurrences at the Briggs mine area are strongly controlled by several parallel vertical to near-vertical faults, including the regionally persistent Goldtooth fault, and detachment faults. The vertical faults have acted as the feeder conduits to the disseminated Briggs mineralization and to the mineralization that made its way into the permeable plumbing zones represented by silicification and breccia associated with the low-angle faults. Mineralization is characterized by the introduction of 0.5 percent to 2 percent pyrite, both as disseminations and as concentrations along the high-angle fault zones. The gold system is considered mesothermal in nature, showing no significant change in gangue mineralogy or trace element geochemistry over the over 2,000 vertical feet mined and/or explored. Gold mineralization occurred during the mid- to late Miocene, contemporaneous with extensional tectonics and detachment faulting; at the Briggs mine low-angle faults steepen at the valley margin

and appear to transform into range-front faults. The mesothermal nature of the deposits suggests that they formed prior to or during the onset of detachment and that the deposits have been tectonically raised to their present elevation since their formation. This could be due to wrench faulting along the Panamint Range front. At current gold prices there are sufficient proven reserves at the Briggs mine for continued production for several years. The rate of production is projected to be at a rate of 40,000 oz Au per year.

Bristol Lake salt plant, Amboy Crater area, San Bernardino County, California

Gregg Wilkerson

California State University, Bakersfield, gwilkerson1@csu.edu

The Bristol Lake salt plant (formerly California Salt, Leslie Chloride plant) is southeast of Amboy Crater volcanic flows in Bristol Dry Lake. The playa surface consists of tan to dark brown clay containing scattered gypsum crystals along the lake margins. The clay surface is very rough with puffy hummocks, which is characteristic of high salt content in the clay that commonly produces a "salt bloom" due to capillary action. In places on Bristol there is a very thin crust of salt. This has been deposited by the evaporation of surface runoff water which in wet years may stand to a depth of several feet. Gypsum occurs in a belt around the north and west sides of Bristol dry Lake. Bristol basin is filled with over 1000 feet of alternating beds of salt, clay, and silt. Core data indicate the salt is associated with beds of green clay. This relationship indicates that a fairly persistent body of water existed during deposition of the green clay before it desiccated enough to form calcium and sodium chlorides with associated salines in brine derived from a bed of rock salt.

Deflation has removed sediment from the surface of the dry lake. This deflation and a veneer of eolian sand along the west side of the playa gives the impression that the basalt overlies the lake clay. The basalt has a ^{36}Cl age of 79 ± 5 ka. Alluvial material around the sides of the playa overlies and extends in places onto the dry lake (especially southeast of Saltus). The lake deposits are Pleistocene to Holocene in age.

Of present commercial interest is an extensive horizontal rock salt layer as much as 7 feet thick, which is covered by 3 to 7 feet of overburden. It is believed possible to mine the rock salt profitably over an area of 5 square miles in the northwestern part of the lake where the salt layer exceeds 3 feet in thickness. Bordering this area on the south is a depression, known as Salt Lake, where mud is covered with a thin crust of rock salt. Recovery of calcium chloride from the brines of Salt Lake has produced common salt (NaCl) as a byproduct. Gypsum, although occasionally found in layers at depth, is most abundant in deposits at or near the surface. The largest gypsum concentration lies along the northwest border of the lake near the margin of the lava flows where

gypsiferous layers, 8 feet or more in thickness, have been encountered. Celestite (SrSO₄) in nodular, potato-like masses, occurs in mud close to or on the lake surface, and is particularly abundant along the south side of the lake. These masses appear to be chemical precipitates, perhaps segregated by shallow ground water conditions. Permeating the sediments and salt bodies of Bristol Lake are brines which, from place to place, differ somewhat in their concentration and chemical composition. At several localities, particularly at Salt Lake and the bordering salt excavations, the brines are rich in calcium chloride, an unusual constituent for desert saline deposits. Brine samples taken from a 1005-foot drill hole contain approximately the same proportion of calcium chloride as is found in the brine from surface excavations. The chlorine probably is of volcanic origin derived from the Amboy Crater basalt lava. The brine in the crystal body of Bristol Lake is collected by a series of drainage canals that are dug through the uppermost layer of salt. Solar evaporation of the brine precipitates sodium chloride and concentrates calcium chloride in the liquor. The liquor is converted to flake calcium chloride which has a CaCl₂ content of 73 to 75 per cent. In the preparation of this material the 40% liquor is further evaporated by heating it to approximately 350° F in a boiler fired with oil burners; and the hot, saturated solution is chilled on a revolving, water cooled drum. Following drying, the flakes are packed in moisture-proof paper bags. The mine is essentially a renewable resource and production is likely for many years to come.

Geology and history Cerro Gordo Mining District, Inyo County, California

Gregg Wilkerson

California State University Bakersfield, gwilkerson1@csub.edu

The Cerro Gordo Mining District on the western slope of the Inyo Mountains, southern California, lies about seven road miles east of Keeler and thirty miles south of Independence. It was the first major silver strike in the Owens Valley area. Cerro Gordo's major development took place in the early 1870s, primarily by Mortimer Belshaw and Victor Beaudry. While there were a number of mines and prospects within the Cerro Gordo District, almost 90% of the production came from independent mines and workings localized in an area of less than 1 square mile high on and just below the summit of, Cerro Gordo Peak and which later became collectively known as the Cerro Gordo mines. These mines were important in the history of Owens Valley, Los Angeles, and the port of San Pedro. Access to the mines was difficult. Roads to Cerro Gordo were improved to service the Salt Tram construction and operation. That tram connected Saline Valley with Swansea at the northeast shore of Owens Lake. Two tramways were constructed at Cerro Gordo to convey ores and materials to and from Keeler on the valley floor. In its early history, smelting was done at Cerro Gordo townsite and at Swansea. Later, a smelter was

built to process the ores in Keeler. Steamboats were used to transport silver bars from Keeler on Owens Lake to Olancho where a railroad was built to connect deliveries to Mojave and Los Angeles. From Olancho the steamboats went to the Cottonwood charcoal kilns and returned with charcoal for the Swansea and Keeler smelters.

The Cerro Gordo District mineralization is controlled by lithology, normal faults, and igneous intrusives. Replacement lead and silver deposits are concentrated in chimney-like replacement bodies and fractures in a zone associated with the Cerro Gordo fault and associated faults and fractures. In later years, smithsonite has been mined as commercial zinc ore, largely from one large deposit in the vicinity of the Union Chimney lead-silver ore body. The majority of the district's production has come from ore bodies within Devonian marble of the Lost Burro Formation. The ores at Cerro Gordo are very rich with concentrations up to 12% lead. These contact metamorphic replacement deposits formed when Mesozoic granites invaded the Paleozoic carbonates. The Cerro Gordo District was California's preeminent silver and lead producing area during the decade following the Civil War. Total recorded production was on the order of 4.4 million ounces silver and 37,000 tons of lead. Zinc production, which commenced in 1911, totaled approximately 12,000 tons. Gold and copper production, important byproducts from the siliceous quartz vein ores, totaled about 2,000 ounces and 300 tons respectively. Undeveloped reserves at the now-abandoned mine are not known.

Fort Cady borate solution mine, San Bernardino County, California

Gregg Wilkerson

California State University Bakersfield, gwilkerson1@csub.edu

The Fort Cady borate deposit is located in San Bernardino County near Pisgah Crater, approximately 40 miles east of Barstow and 17 miles east of Newberry Springs, California. The site is about two and one-half miles south of Interstate 40 and the Southern Pacific Railway Pisgah siding. It is 1.2 to 1.6 miles east of the Hector mine. Initial discovery of the Fort Cady borate deposit occurred in 1964 when the Congdon Exploration Company found several zones of colemanite, a calcium borate mineral, between the depths of 1,330 and 1,570 feet below the surface in Section 26, TSN, RSE. In September 1977, Duval Corporation initiated land acquisition and exploration activities near Hector, California, and by March 1981 had completed 33 exploration holes in an approximately 800-foot drilling grid configuration on the project site. As a result of that drilling program, it was estimated that a borate ore body of sufficient size and grade existed to warrant further investigation. In 1981, Duval Corporation began conventional underground mine planning. Duval developed, tested, and patented a unique in-situ solution mining and solar evaporation process for colemanite. In this process, colemanite is converted to boric acid and

calcium chloride while still underground. Because of the depth of the ore body, it appeared that underground mining methods would not be technically or economically feasible for use in its recovery. However, subsequent studies and tests indicated that in-situ technology could be a feasible method to employ in mining the Fort Cady colemanite ore body, and a pilot mining and processing operation was initiated in order to explore this possibility. Mountain States Mineral Enterprises of Tucson, Arizona, purchased the property in 1986. In May 1990, Corona Corporation was in the process of transferring ownership of Fort Cady Minerals to Avalon Corporation, a NYSE-listed oil and gas company. At that time, 35% of detailed construction engineering work was completed and mining and reclamation plans were about to be submitted for permitting. Project management was awarded to Kilbourne International Construction for an 82,000 ton/year plant that would cover an area of 155 ha. This is the largest known colemanite deposit in the United States. It was scheduled for opening in 1990. Permitting was delayed for a number of years due to concerns about water use, brine processing, and disposal. In 1994 the Fort Cady Mining Company was formed. The project later was purchased by American Pacific Minerals which received a permit to operate in 2022. Construction of a processing plant and drilling of production wells was continuing in February 2023.

The project area is located in the Barstow trough. The deposits are in a fault block between two faults to the northeast the Pisgah Fault. Strata ranging in age from probable Miocene through Recent are exposed at the surface. Fine-grained lacustrine sediments and tuffs, which are possibly Barstovian (19.3-13.4 Ma) in age, rest on undated andesite. The borate-bearing strata may be equivalent to the Barstow Formation. Younger alluvium occurs in washes and overlies the older lacustrine sediments. Recent olivine basalt flows from Pisgah Crater occur in the central and eastern portions of the project area, and along the northern boundary of the western portion of the project area. The Pisgah Fault is one of the many throughgoing northwest-striking strike slip faults which are found in the region and exhibits substantial vertical separation in the project area, with borate beds on the eastern side of the fault upthrown at least 700 feet relative to beds on the western side of the fault. Two faults farther east are in the project area, and strike north. They also exhibit about 700 feet of east side upward separation on borate beds. The block of fine-grained lacustrine sediment between the two faults has been tilted down to the east. The lacustrine sediment in the tilted block appears to be floored by an undated andesitic lava flow. Other researchers have suggested that this andesite is related to the Red Mountain andesite in the Newberry Mountains. Boring logs have consistently demonstrated the presence of a clay layer beneath the evaporite and mudstone body that surrounds and encloses the ore body. The lower clay layer appears to be underlain by volcanic

sand and andesitic volcanic rock. Exploratory drilling in the project area indicates that the ore body is 1,000 feet below ground surface. It is elongate in shape and trends northwesterly, roughly parallel to the Pisgah Fault. This geometry and stratigraphy are similar to the nearby Hector lithium clay deposit. The ore body consists of variable amounts of calcium borate (colemanite) within the mudstone matrix. X-ray diffraction analysis of the ore minerals indicates the presence of the evaporite minerals anhydrite, colemanite, celestite, and calcite. The mineralogy of the detrital sediment included quartz, illite, feldspars, and clinoptilolite, a zeolite mineral. The deposit has the following ore reserve data: Reserves 147,435,000 tons, Grade: 6.4% B₂O₃, Product: 9,393,000 tons B₂O₃.

Hectorite from Hector, San Bernardino County, California

Gregg Wilkerson

California State University Bakersfield, gwilkerson1@csub.edu

The Hector lithium clay (hectorite) deposits are located in the Mojave Desert northwest of Pisgah Crater, approximately 34 miles east of Barstow, California near U.S. I-40 and historic Route 66. There are two groups of claims in the Hector area: the South group, three miles south of Hector Station on the Southern Pacific Railroad; and the North group, six miles northwest of the South group. The southern group is being systematically mined and is the focus of this abstract. Clay mining began at Hector in 1953 by the Inerto Company. Today the mine is owned and operated by the Elementis company. The clays occur in lacustrine deposits beneath lithified gravel or Pisgah Crater olivine basalt and above a layer of Red Mountain andesite. Erosion has reduced the lacustrine section, which may have been 500 feet thick. The fresh ore is clay that is whitish to grayish in color and in some ore pockets has a very waxy appearance. However, the clay occurring in the South group is unique in that it is a high magnesia and relatively lithium-rich montmorillonite clay. The substitution of magnesium for the normal aluminum in the clay structure results in formation of an unusual bentonite (hectorite) with special and valuable characteristics. It instantaneously forms a "house of cards" structure after agitation, and also "dries" instantaneously upon contact with anything. It is mixed with pigments to make high-speed inks for the printing of newspapers. It can survive stomach acids and the small intestine and so is used in specialty drugs, taken as pills for treatment of lower bowel conditions. Recently it has been considered as a source of Li for batteries. Pure hectorite sells for \$6,000 a ton.

Hectorite occurs near the northwest-striking Pisgah fault zone. This fault zone can be traced for about five miles. The North group is on the west side of the surface trace of Pisgah fault and the South group is on the east side. The hectorite occurs in the Cenozoic ash beds deposited upon pre-Barstovian (19.3–13.4 ma) andesite. They may correlate with the Barstow Formation. The

hectorite orebodies are located on a subsidiary fault that is parallel to and 2,000 feet to the northeast of the Pisgah fault. It is possible that hot springs emanating along this subsidiary fault deposited travertine in a Barstovian lake in which sand, marl, and silicic pyroclastics also were being deposited. The tuff lying on the travertine benches was altered to saponite by solutions containing lithium and fluorine in the last stages of hot spring activity, with the magnesium being extracted from the lake water. Analcime, representing alteration of the tuff when the springs were inactive, is found below and above the hectorite bed. Clinoptilolite is present directly associated with the hot spring bench. The hectorite is structurally controlled by a fault. Area fault correlations (for faults younger than the fault that supplied Li to form the hectorite deposit) suggest that there is a component of right-lateral displacements on the faults. The South and North groups appear to be offset equivalents, indicating a right-lateral separation of 5.8 miles since deposit formation. Sediment deposition associated with the older fault zone may have restricted the flow of the lithium rich water from the hot springs, limiting formation of hectorite to the area now being mined. I propose that a Miocene fault was the conduit for the hot spring fluids responsible for converting the volcanic ash to hectorite via introduction of Li-rich solutions and replacement of Mg with Li. Lesser cross faults and bedding shears locally control deformation of the clay beds. The Hector deposits have similarities to the Franklin Wells hectorite deposit in the Amargosa Valley.

War Eagle mine, San Bernardino County, California

Gregg Wilkerson
gwilkerson1@csu.edu

The War Eagle mine is located on the U.S. Marine Corps Twentynine Palms Training Center on the southeast flank of Lead Mountain. It lies about 10 miles south of old highway 66 at Bagdad, about 5 miles east-southeast of the Quaternary Lead Mountain volcanic center, and about 10 miles southwest of Amboy Crater. The area is off limits to the public and is subject to military operations using live ordinance. Current entry is both illegal and dangerous because of unexploded ordinance. The mine was discovered in 1850 by a Mormon party and located by a Mr. Stephenson. Early mining in 1885 by Mr. Stephenson obtained \$400 out of 50 tons of ore. The mine was later developed in 1905–1908 and was operated by the Bagdad-Chase Company from 1912 to 1920. At that time lead content was 8.0 percent and silver content was 7 ounces per ton. Mr. K.E. Bensusan indicated the average value of seven samples was \$26.00 per ton in lead and silver in 1949. The mine closed in 1949 but was actively maintained by Mr. Wolterdorf and Associates, who shipped product gleaned from mine dumps until it was taken over by the Department of the Navy in 1952. After 14 years of court actions, the Navy purchased the claims. By 1965 all structures had been destroyed by practice bombing and

artillery fire. The headframe and hoist had taken a direct hit and had been blown 700 feet down the shaft to the bottom of the mine.

The War Eagle exploits a barite-sulfide vein in host rocks of Tertiary rhyodacite flows and intrusives. To the west of the mine are younger basalt flows of Lead Mountain. About 0.7 mile to the northeast, Lead Mountain is bounded by the Quaternary Ludlow fault zone. A high angle secondary fault related to this fault zone terminates the west end of the War Eagle vein. The regional structure is dominated by the Barstow-Bristol trough. The vein consists of a brecciated and mineralized fault zone with frequent apophyses into adjacent fractures. It cuts a dense rhyodacite flow over the entire length of its surface exposure, about 1,200 feet. Superficially the vein at the surface is very similar to the reddish-brown silver-barite veins of the Calico District. The high ridge just north of the west end of the vein is capped by a volcanic flow which overlies moderately dipping altered tuffs. The tuffs extend almost down to the vein in this area. Opposite the vein on the west side of the secondary fault lies a mass of volcanic breccia containing a variety of volcanic debris, including abundant pumice fragments. At the surface, the War Eagle vein does not come into contact with either of these more permeable rocks in the vicinity of the mine. Based on regional stratigraphy, there is a good chance that the rhyodacite flow is underlain by more permeable host rocks which could give rise to a much larger ore accumulation than has thus far been exposed in the mine. The vein is traced 500 feet west and 700 feet east of the main shaft. Vein width was controlled by a change in dip of the vein from about 37° to 42° where it thickened to 15 feet. Vein character is influenced by host rocks on both hanging and footwalls. Two orebodies are recognized, one a fissure vein and the other a breccia. The ore occurs along fault fractures with thicknesses varying from a mere seam to 30 feet. Irregular lenses of high-grade ore were encountered. Values were high in Ag in the form of chlorargyrite-bromargyrite with some galena. The mineral assemblages at the War Eagle suggest a deep magmatic source. Supergene minerals are superimposed on hypogene minerals. The mine contains additional reserves of argentiferous galena on the 700-foot level with potential for additional ore at depth and at each end of the workings. The barite-sulfide vein system has anomalous amounts of gallium, vanadium, palladium, and other rare elements. The main dump contained about 6,500 tons of waste in 1965, and a composite sample suggested it contains approximately 4.2 ounces (130 gm) of gallium per ton. At 90% recovery this would yield more than 24,000 ounces (750 kg) from the dump. Palladium is associated primarily with copper minerals (chrysocolla).

The Brubaker–Mann Quarries, San Bernardino County, California

Gregg Wilkerson and Alyssa Kaess

California State University, Bakersfield, gwilkerson1@csub.edu

The Mojave Desert has beautiful colorful hills and mountains. Some of these colored rocks are of commercial grade for dimension stone, landscaping, and roofing granules. A long-time producer of these minerals in the Mojave Desert is the Brubaker–Mann Company, located near Barstow. They have produced from the following quarries:

Quarry Name and land status	Section, Township, Range,	Latitude	Longitude	Geology from maps by Dibblee
C Beige Quarry. BLM	Sec 30, T.10N, R.01E, SBM	34.9308	-116.9189	Andesite to dacite porphyry, (Tap)
D Bentonite Quarry. BLM	Sec 06, T.09N, R.01E, SBM	34.8993	-116.9265	Tuff, tuff breccia (Tt) and tan felsite (Ttf)
E Gold, Brown and Lilac Quarry. Private	Sec. 01, T.09N, R.01W, SBM	34.8945	-116.9421	Tan felsite (Ttf) and lacustrine limestone (Tls)
F Bark Brown Quarry. Private	Sec. 01, T.09N, R.01W, SBM	34.9001	-116.9358	Lacustrine limestone (Tls)
G Birdseye Quarry and Processing Plant Private	Sec. 04, T.09N, R.01W, SBM	34.9054	-116.9882	Andesite to dacite intrusive (Tai)
H Desert Pink Quarry. Private	Sec. 33, T.10N, R.01W, SBM	34.9201	-116.9967	Andesite to dacite intrusive (Tai)
I Shadow Mountain Quarry. Private	Sec. 29, T.08N, R.06W, SBM	34.7490	-117.5256	
J Wine Red Quarry. Private	Sec. 04, T.08N, R.03E, SBM	34.8121	-116.6646	Multicolored Miocene andesite (Ta)
K1 Green Mountain Private	Sec. 34, T.12N, R.05E, SBM	35.0928	-116.4411	Cambrian or older gneiss or gneissoid quartz diorite (gn)
K2 Green Island Private	Sec. 34, T.12N, R.05E, SBM	35.0878	-116.4428	Cambrian or older gneiss or gneissoid quartz diorite (gn)
L Near Stoddard Well Private	Sec. 09, T.07N, R.02W, SBM	34.6692	-117.0954	Roof pendant contact between Carboniferous (?) limestone (ml) and Cretaceous biotite quartz monzonite (bqm)

The rock products from these quarries are developed by drilling, blasting, and excavating. Excavations are conducted using bulldozers and front-end loaders. The mined materials are hauled by contract carriers to the Brubaker–Mann plant. There they are crushed to various sizes or sorted by hand for smaller boulders or by front-end loaders for larger ones. Materials are sold by weight and size.

Brubaker–Mann opened in 1950 and has been owned and operated by the Mann family ever since (Brubaker-Mann website, 2022). Bill Mann wrote a series of popular books and guides focused in and around the Mojave Desert.

Robert E. Reynolds Desert Symposium Student Research Award



Bob Reynolds at the Blue Bell mine, Soda Mountains.

This award to honor and acknowledge Bob Reynolds' decades of service to desert sciences, from directing large fossil excavations and exploring for minerals to mentoring numerous students and apprentices. For these and other achievements, Bob received the 2019 Morris Skinner Prize from the Society of Vertebrate Paleontology. In addition, Bob has been central to holding the annual Desert Symposium for over 30 years, in many cases singlehandedly soliciting contributors, organizing the meeting, and running the field trip. Bob's leadership and service are honored with this award by promoting student research projects.

Information on applying for and donating to the award is available at <http://desertsymposium.org>. Donors will be identified in the annual volume published by the Desert Symposium. Desert Symposium Inc. is a non-profit 501(c)3 organization. Contributions are tax-deductible as allowed by law.

The latest Reynolds Student Research Award recipient:

Krishangi Groover, University of Nevada Reno
"Selenium oxidation and partitioning in a cattail wetland following a controlled burn event"



The 1989 MDQRC field trip.

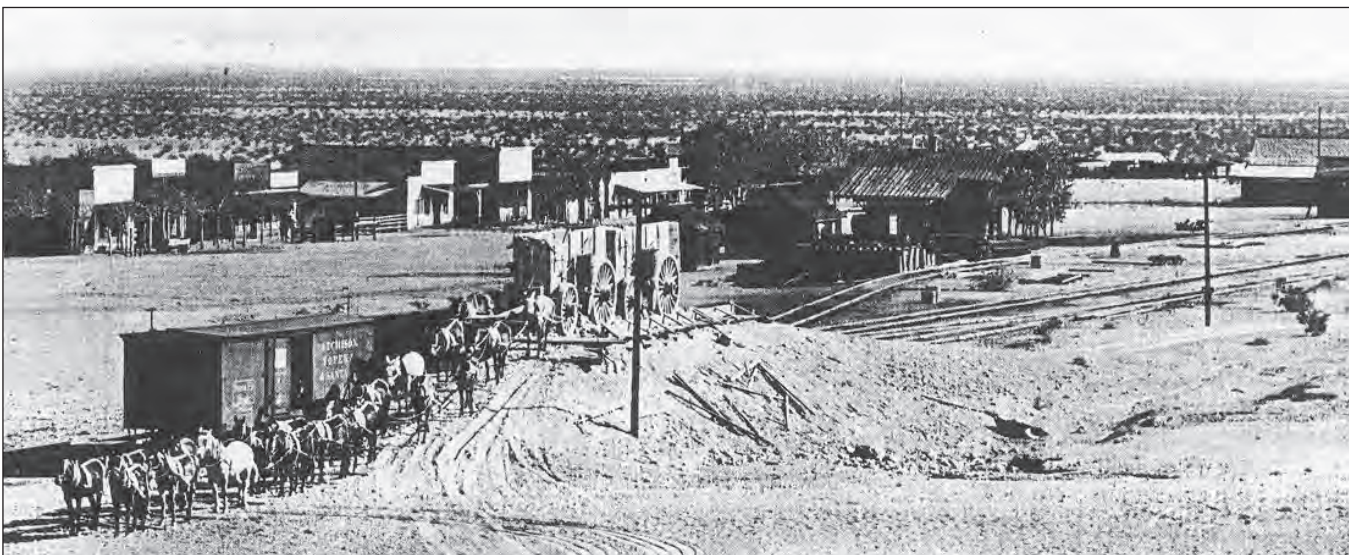




Above, The Bartlett #1 shaft with head frame, ore chute system, and storage bunker, at the town of Borate, Calico Mountains, pre-1897. White concentrate sits on a storage platform in the lower right of the photograph. F. M. "Borax" Smith's house is on the horizon, atop the hill. *Smitheram collection.*



Left, workers loading high grade borax ore, pre-1898, at the ore storage bunker below the Bartlett shaft at Borate. *Smitheram collection.*



Below, view northeast toward Santa Fe Avenue in Daggett, 1895. Borax freight wagons from the Calicos pulled onto a hill to load ore into railroad cars bound for a processing plant at Alameda, northern California. *Smitheram collection.*